Stem Cells International

Stem Cells and Ion Channels

Guest Editors: Stefan Liebau, Alexander Kleger, Michael Levin, and Shan Ping Yu

Stem Cells and Ion Channels

Stem Cells International

Stem Cells and Ion Channels

Guest Editors: Stefan Liebau, Alexander Kleger, Michael Levin, and Shan Ping Yu

Editorial Board

Contents

Hindawi Publishing Corporation
Stem Cells International
Volume 2013, Article ID 238635, 3 pages
http://dx.doi.org/10.1155/2013/238635

Editorial

Stem Cells and Ion Channels

Stefan Liebau,[1] Alexander Kleger,[1] Michael Levin,[2] and Shan Ping Yu[3]

[1] *University of Ulm, 89081 Ulm, Germany*
[2] *Tufts University, Medford, MA 02155-4243, USA*
[3] *Emory University School of Medicine, Atlanta, GA 30322, USA*

Correspondence should be addressed to Stefan Liebau; stefan.liebau@uni-ulm.de

Received 9 May 2013; Accepted 9 May 2013

Once the zygote has formed by the fusion of the sperm cell with the oocyte, the early embryo quickly races through development, thereby gaining and losing several stages and types of stem cells. Only stem cells until the morula stage (~16–32 cell stage) are called totipotent which means the ability to form a complete, new organism. In contrast, the famous embryonic stem cell derived from the inner cell mass (embryoblast, ICM) exhibits pluripotency, resembling the differentiation capacity to form all cells of the organism, besides the extraembryonic structures when transplanted. These characteristics can also be found in the set-aside germline stem cells. Subsequently, after the formation of the three germ layers during gastrulation, germ layer stem cells are responsible for the generation of cells from the respective germ layer until gaining full functionality in the mature tissue network. The mature organism is full of various adult stem cells, also referred to as tissue-specific stem cells, which are mostly responsible for the cell turnover and regeneration in tissues.

Ion channels are represented by numerous families of pore forming structures which allow for the exchange of ions between the intra- and extracellular spaces or between the cytoplasm and organelles. These channel molecules vary, among others, in their ion specificity and conductance, their gating mechanisms, their subunit conformation, their downstream signaling including modulation of/by interacting molecules, or their expression profiles. Although ion channels have been thoroughly investigated in mature tissues and cells, their roles during development have remained elusive. Nevertheless, during recent years, it has become more and more evident that ion channels are involved in various cellular mechanisms during development, including germ layer generation, cell fate determination, migration, and stem cell differentiation. Moreover, the voltage gradients produced by several families of ion channels serve as instructive cues for positional information and organ identity during morphogenesis having been implicated in left-right asymmetry, craniofacial patterning, eye induction, and other roles in a range of model systems. Interestingly, not only the "simple" conductance of ions through biological membranes, but also the modulation of downstream signaling cascades linking bioelectrical events to changes in cell behavior is part of ion channel activity. Of note, many of these ion channel-mediated mechanisms are conserved throughout phylogenesis.

To this end, we have selected a series of beautiful studies, which have investigated the role of ion channels within the development and stem cell differentiation. This includes not only relevant developmental model organism such as the *Xenopus laevis*, *Macrostomum lignano*, or the zebrafish, but also the whole spectrum of different stem cell populations being relevant to study differentiation.

D. Simanov and colleagues describe and discuss the role of ion channels during regeneration in the nonvertebrate flatworm *Macrostomum lignano*. They establish this animal as a versatile model organism for addressing these topics. They discuss biological and experimental properties of *M. lignano*, provide an overview of the recently developed experimental tools for this animal model, and demonstrate how manipulation of membrane potential influences regeneration in *M. lignano*. The authors show that modulation of ion channels in the worm greatly influences the regeneration of tissues and development of head-associated structures.

These findings implicate that distinct ion channels and ion current adjustments are involved in the developmental events of invertebrates, making them an interesting model to study ion channel-mediated mechanisms throughout regeneration.

Going further in phylogenic evolution, V. P. Pai et al. provide evidence that ion channel-driven resting potential differences in key cell groups underlie consistent left-right patterning of neural tissues and organs in the developing *Xenopus larvae*. They show that the striking hyperpolarization of transmembrane potential demarcating eye induction usually occurs in the right eye field first. This asymmetry is randomized by perturbing pathways that regulate left-right patterning of the heart and visceral organs, suggesting that eye asymmetry is linked to mechanisms establishing primary laterality. Bilateral misexpression of a depolarizing channel mRNA affects primarily the right eye, revealing an additional functional asymmetry in the control of eye patterning. Further, they describe that the ATP-sensitive K^+ channel subunit transcript, SUR1, asymmetrically expressed in the eye primordia is a good candidate for the observed physiological asymmetries.

M. Keßler et al. provide an overview of the current knowledge from the zebrafish about ion channels and heart development. In that model, it has been observed that certain channel proteins such as scn5Laa and scn5Lab (representing the mammalian gene SCN5A), encoding a voltage-gated sodium channel, are not only present in the functional myocardium, but also are expressed in the developing heart during early embryonic stages. Indeed, the respective genes in mice or fish recapitulate these expression data as both in mammals and fish specific knock-down experiments lead to developmental defects of the heart. Interestingly, experiments indicate that the voltage-gated sodium channel exerts influence on cardiac development independent of ion flux. Furthermore, calcium channels which comprise different pore forming subunits are responsible for proper heart development as the pore-forming α1C subunit as well as the modulatory cytoplasmic β2.1 subunit specifically influences heart development in zebrafish. Finally, the authors discuss other ion channels and exchangers that are also involved in heart development such as the Sodium-Calcium-Exchanger, Ca^{2+}-ATPase, Na^+/K^+-ATPase, and potassium channels.

The review of S. A. Becchetti Pillozzi et al. overviews the knowledge about the cell physiology of ion channels, especially of hematopoietic stem cells and one of their subpopulations, the mesenchymal stem cells (MSCs). It is already known that stem cells express a variety of ion channels, implicated in numerous cellular processes. This includes, for example, volume and resting potential oscillations accompanying the cell cycle. Other ion channel types control cell anchorage with the stromal matrix and cell migration as well as release of paracrine growth factors. Nevertheless, analyses of ion channel expression in MSCs seem to be highly varying. This may be an indication for several different populations in the cultures or cells at different cellular stages, respectively.

M. Yamashita summarizes the mechanisms by which calcium ion fluctuations modulate the characteristics and behavior of neuroepithelial neural stem cells. In this respect, several channel proteins involving calcium channels, ligand-gated ion channels, and sodium and potassium channels mediate an ion equilibrium of the membrane and even the nuclear envelope. Calcium is thereby able to influence electric coupling of neighbored cells and is involved in the cell cycle by influencing DNA-synthesis during the S-phase.

The influence and role of large pore channels on neural stem cells (NSCs) and progenitor cells (NPCs) of the subventricular zone of the brain are summarized by L. E. Wicki-Stordeur and L. A. Swayne. They bring together knowledge about the interplay and individual functions of certain connexins, aquaporins, and pannexins in this cell system. Interestingly, these large pore channels do not only allow the passage of ions, but also mediate the highly controlled movement of small molecules. This, in turn, influences numerous cellular mechanisms such as adult neurogenesis. These pore-protein complexes, their regulation, and functions seem to be intimately connected and mediate cytoskeletal interactions, Ca^{2+} signaling, transcriptional regulation, ATP flux, and cell-cell communication between ventricular zone NSC/NPCs.

J. Aprea and F. Caligari summarize the current knowledge on the role of ion channels and pumps in the context of mammalian corticogenesis with particular emphasis on their contribution to the switch of neural stem cells from proliferation to differentiation and generation of more committed progenitors and neurons, whose lineage during brain development has been recently elucidated. They conclude that although several studies have, for example, depicted an influence of the membrane potential and ion currents on neural stem/progenitor cell proliferation, it is remaining elusive at what degree these *in vitro* findings may be translated to the *in vivo* situation.

The review article of M. Müller et al. sheds light on the various cardiac, developmental defects, which are mediated by the dysfunction or loss of distinct ion channels and finally lead to the distinct forms of long QT syndrome. During many years, numerous genetic defects have been investigated with the help of mouse models. Since the initial report on the generation of induced pluripotent stem cells that can be gathered from almost every individual, a human *in vitro* "model" has emerged. Therefore, this review highlights the respective stem-cell-based studies which investigate the underlying pathomechanisms and frequently show a predicted cellular behavior mimicking long QT syndrome.

Using human-induced pluripotent stem cells, L. Linta et al. compare a large number of ion channels and their subtypes which undergo differential expression starting from the initially used somatic cell further to the reprogrammed iPS cell and finally to the differentiated progeny, neurons and cardiomyocytes. This transcriptome array-based study depicts most of the commonly known ion channel families and subunits to draw a starting line for the study of ion channels in, for example, stem cells. Of note, numerous ion channel subtypes are highly upregulated after the process of reprogramming leaving iPS cells with a large number of expressed ion channels, at least on mRNA levels.

A. Illing et al. give insights into the differentially regulated expression patterns of an ion channel family known for its

influence on stem cell differentiation towards the cardiac lineage. Here, they show the regulation of SK channel expression (small/intermediate conductance, calcium-activated potassium channels) during endodermal differentiation of human iPS cells. The authors not only provide a very robust protocol for the differentiation of human iPS cells into definitive endoderm cells, but also show that SK channels are highly regulated during this process.

Together, these papers give an overview of an important emerging field. The synthesis of information on the genetics of individual channels with endogenous roles in cell regulation and the developmental biophysics that highlights the importance of resting potential for directing cell behavior, have exciting implications for basic biology and biomedicine of stem cell function.

Stefan Liebau
Alexander Kleger
Michael Levin
Shan Ping Yu

Hindawi Publishing Corporation
Stem Cells International
Volume 2013, Article ID 496501, 7 pages
http://dx.doi.org/10.1155/2013/496501

Review Article

Modelling Human Channelopathies Using Induced Pluripotent Stem Cells: A Comprehensive Review

Martin Müller,[1] Thomas Seufferlein,[1] Anett Illing,[1] and Jörg Homann[2]

[1] *Department of Internal Medicine I, University Hospital of Ulm, Albert-Einstein Allee 23, 89081 Ulm, Germany*
[2] *Department of Internal Medicine II, University Hospital of Ulm, Albert-Einstein Allee 23, 89081 Ulm, Germany*

Correspondence should be addressed to Martin Müller; martin.mueller42@gmx.de

Received 1 February 2013; Accepted 16 April 2013

Academic Editor: Stefan Liebau

The generation of induced pluripotent stem cells (iPS cells) has pioneered the field of regenerative medicine and developmental biology. They can be generated by overexpression of a defined set of transcription factors in somatic cells derived from easily accessible tissues such as skin or plucked hair or even human urine. In case of applying this tool to patients who are classified into a disease group, it enables the generation of a disease- and patient-specific research platform. iPS cells have proven a significant tool to elucidate pathophysiological mechanisms in various diseases such as diabetes, blood disorders, defined neurological disorders, and genetic liver disease. One of the first successfully modelled human diseases was long QT syndrome, an inherited cardiac channelopathy which causes potentially fatal cardiac arrhythmia. This review summarizes the efforts of reprogramming various types of long QT syndrome and discusses the potential underlying mechanisms and their application.

1. Introduction

"Inherited long QT syndrome" comprises a group of channelopathies that cause a delayed repolarization of the heart leading to an increased risk of malignant ventricular tachycardias, in particular *torsade de pointes,* that imply the risk of a fatal cardiac arrest. Several attempts have been made to estimate the prevalence of long QT syndromes in the past, while older studies quantify the prevalence between 1:20000 and 1:5000. The latest analysis by Schwartz et al. provides evidence for a higher prevalence close to 1:2000 in a Caucasian population [1]. It is assumed that up to 30% of sudden unexpected deaths in infants are caused by different forms of long QT syndromes (LQTS). These data also implicate that most cases of the LQTSs are diagnosed when they become clinically apparent in an individual or his/her family. Subclinical forms of LQT syndrome can become apparent under the influence of various drugs with QT elongation capability [2].

Ion channels represent a large group of pore proteins regulating ion efflux from the inner cell to the extracellular compartment or vice versa, thereby inducing changes in the membrane potential. Activity is mainly regulated either by voltage or by certain ligands. Thereby, a variety of ion currents are regulated in various tissues. Sodium, potassium, and calcium channels are the primary representatives of ion channel families in the human heart. A complex interplay of certain ion fluxes in a defined sequence operates the cardiac action potential. Thus, it is not surprising that slight mutations can disturb the ion pore structure, leading to changes in the currents' biophysical properties. Severe arrhythmia and eventually sudden cardiac death are the worst consequences. Those mutations causing human disease are so-called cardiac channelopathies. Different channelopathies are forming a basis of QT interval elongation, thereby increasing the susceptibility of electrophysiological deregulation of cardiomyocytes, particularly by decreasing the cardiomyocytes' ability of accurately timed repolarization. The myocardial action potential can be divided into 4 phases as follows (Figure 1): the primary depolarization in ventricular cardiomyocytes is characterized by a rapid increase of membrane conductance by Na^+ channel ($hNa_v1.5$ channel, encoded by the SCN5A gene) opening (phase1), followed by a light decrease of depolarization by subsequent opening of a special type of transient outward K^+ channel (K_{to}), which causes a short-lived, hyperpolarizing outward K^+ current (I_{Kto}). In a second

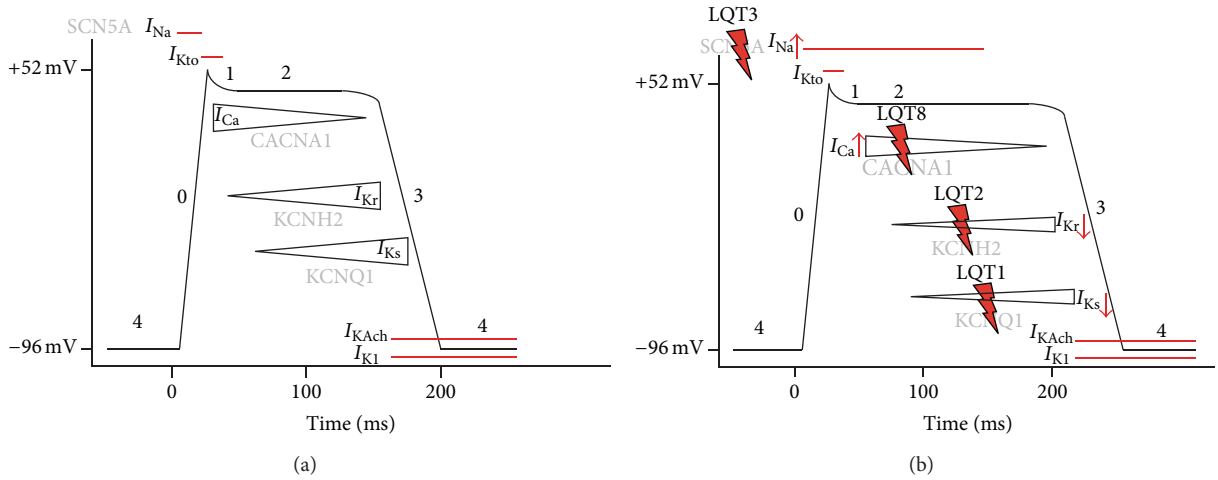

FIGURE 1: Schematic delineation of the cardiac action potential—resting "4," upstroke "0," early repolarization "1," plateau "2," and final repolarization "3." Inward currents: I_{Na} and I_{Ca}. Delayed rectifier currents: I_{Kr}, I_{Ks}. Inward rectifier currents: I_{K1}, I_{KAch}. Adapted from [3]: (a) normal cardiac action potential. Different currents are allocated to their chronology in the AP course. Ion channel genes are written semitransparent. (b) Different LQTSs are shown in relation to their distinct ion current causative for the indicated syndrome. Overactivation/reduction of different currents leads to a significant elongation of the action potential.

phase, rapid repolarization is—in contrast to for example, neurons—impeded by a slow calcium influx ($I_{Ca,L}$). Finally, repolarization is reached after closure of Ca^{2+} channels and when K^+ (and therefore I_K) increases, along with the inactivation of Ca^{2+} channels. Delayed rectifier K^+ currents I_{Kur}, I_{Kr}, and I_{Ks} are slowly activating outward currents that play major roles in the control of repolarization. The deactivation of these channels is sufficiently slow so that they contribute outward current throughout phase 3 repolarization. Phase 4, or the resting potential, is stable at ≈−96 mV in normal working myocardial cells and held up mainly by two inward rectifier channels I_{KAch} and I_{K1}.

Mutations in long QT syndromes are consistently resulting in a relative increase of depolarizing currents against repolarizing ones (Figure 1). This results in two arrhythmia-promoting situations: (i) channels that remain depolarized for extended periods lead to increased refractory period, thus leading to areas of functional blocking which act as a reentry spot for ectopic excitation; (ii) as the elongation of action potential differs between epicardial (outer) and more endocardial (inner) cardiomyocytes, this may also promote the generation of functional reentry circles [2]. To date, 13 types of long QT syndromes are distinguished. Long QT syndromes are inherited either autosomal dominant or recessive with the recessive ones mostly having a more severe phenotype. Nonetheless, the penetrance in most long QT syndromes differs; as a consequence, there are individuals with mutations without any clinical appearance [4].

Upon expression of a defined set of transcription factors in somatic cells, iPS cells can be generated from virtually every type of tissue. The first human iPSCs were generated independently in 2007 by the Yamanaka [5] and the Thomson Laboratory [6]. Their unique features of unlimited self-renewal and nonrestricted differentiation power define a landmark in the context of understanding human development and disease [7–9]. More precisely, in case of applying this tool to patients who are classified into a disease group, it enables the generation of disease-specific iPS cells. iPS cells have proven a significant tool to elucidate pathophysiological mechanisms in various diseases such as diabetes, blood disorders, defined neurological disorders, and genetic liver disease [10–12]. iPS cells enable the dissection of monogenic human disease [13] mechanisms as well as mechanisms of genetically complex human disorders such as schizophrenia [14]. This opens promising perspectives both for the screening of innovative "druggable" targets [15] and *ex vivo* gene targeting therapies [13]. Moreover, a series of studies have successfully dissected a wide range of morphological and electric cardiac disease using patient-specific iPS cells as a model system [16–20]. In 2008, Mauritz et al. were the first to measure an AP from hiPSCs [21], followed by the first disease-specific study modelling LEOPARD syndrome [22]. Here, we summarize the current effort to model "electrical human cardiac disease" caused by channelopathies finally leading to LQT-syndromes: LQT1, LQT2, LQT3, and LQT8 (Table 1).

2. Modelling LQ Type 1 Syndrome

2.1. Pathophysiology. The highest incidence of all LQT syndromes is accredited to LQT1. It is characterized by clinical symptoms like adrenergic-induced *torsade de pointes* tachycardia, syncope, and effectiveness of β-adrenergic antagonistic "β-blocker" treatment. LQT1 accounts for about 50 percent of all genotyped patients with LQTs. Gene mutations in both KCNQ1 and KCNE1 lead to LQTS1. Thus, the myocardial sensitivity to catecholamine stimulation is increased by I_{Ks} reduction. As I_{Kr} (rapid component of the delayed rectifier current) can maintain normal duration of action potentials, LQT1 is often concealed. In those patients, the intake of I_{Kr} blocking drugs or hypokalaemia can lead to a burst of *torsade de pointes* by triggering a QT prolongation [4, 23]. I_{Ks} reduction leads to transmural dispersion of

Table 1: Current iPS cell-based models for long QT syndromes.

LQTS subtype	Gene mutation	Protein	iPSC-C model
LQTS1	KCNQ1	Alpha-subunit of the delayed rectifier (slow) potassium channel (I_{ks})	Moretti et al., 2010 [25]
LQTS2	HERG	Alpha-subunit of the delayed rectifier (rapid) potassium channel (I_{kr})	Itzhaki et al., 2011 [15], Matsa et al., 2011 [26], Lahti et al., 2012 [27]
LQTS3	SNC5A	Alpha-subunit of the cardiac sodium channel	Malan et al., 2011 [28], Davis et al., 2012 [17]
LQTS8	CACNA1c	Alpha-1c-subunit of the L-type calcium channel	Yazawa et al., 2011 [20]

repolarization in the left ventricular wall; this dispersion may even be amplified by adrenergic stimulation as the resulting shortening of the action potential is emphasized in the epicardium and decreased in the midmyocardium [24]. This explains effectiveness of β-adrenergic blockade in LQT1.

2.2. The Model. Moretti et al. were the first group to publish a hiPSC model for LQTS. Moretti and her coworkers used fibroblast-derived iPSCs from two asymptomatic patients (father and son) with a KCNQ1-G569A mutation and cells from healthy controls. Differentiation of iPSCs was performed after embryoid body formation and consequent selection of areas of spontaneous contraction (indicative of cardiac differentiation). Finally, several different types of action potentials (atrial, nodal, and ventricular) were distinguished. Delayed rectifier currents were measured in specific ventricular-like cells: the cardiomyocytes (CM) derived from patient-specific LQT1 iPS cells showed reduced I_{Ks} peak and tail current densities, whereas I_{Kr} conductance appeared to be regular. APs of both atrial-like and ventricular-like hiPSC-CMs were significantly prolonged within in the LQT1 patient group compared to control cells. Only pacemaker-like cells showed no significant differences in AP periods. In 6 out of 9 LQT1-iPSC-CMs early afterdepolarisation (EAD)—as a proarrhythmogenic predicate—could be triggered by treatment with isoproterenol. No EADs could be triggered in WT-iPSC derived cardiomyocytes. The proarrhythmic effect of isoproterenol could be antagonized by admittance of β-blockers [25]. Thus, basic features of adult LQT-CMs could be reproduced.

3. Human iPS Cells Generated from Long QT Type 2 Syndrome

3.1. Pathophysiology. Next to LQTS1, LQTS2 represents the second most frequent genotype of LQTSs. About 40% of LQTS patients show aberrations in LQT2-associated gene locus for KCNH2 encoding the α-subunit of the I_{Kr} channel, linked to chromosome 7 [29]. Reduction of I_{Kr} slows and decelerates repolarization and, again, increases transmural dispersion by prolonging the action potential preferentially in the midmyocardium. A characteristic property of LQT2 is a faculty of arrhythmia induction by acute sympathetic activation like loud noise, anger, or other forms of emotional stress. These stimuli can acutely prolong the action potential and finally cause an enhancement of transmural repolarization heterogeneity. As bradycardia can also reduce I_{Kr} and, thus, lead to a delay of repolarization, arrhythmias can be triggered by both catecholaminergic-induced tachycardias and bradycardias. β-blockers can reduce the overall amount of cardiac events in LQT2 patients but they induce more cardiac events compared to the LQT1 collective [30–33]. On the other hand, LQT2 can be treated with controlled potassium supply as this leads to a reduction of QT dispersion and shortened QT intervals in those patients.

3.2. The Model. First to report an iPSC-model of LQT2 were Itzhaki et al. in 2011 [15]. A patient- and disease-specific human iPSC line was generated from an individual with an A614 missense mutation in the KCN2 gene leading to LQT2, and cardiomyocytes were subsequently generated from those cells. Similar to the work previously published by Moretti et al. [25], three types of action potential morphologies were recorded from control- and LQTS iPSC-CMs: atrial-, nodal-, and ventricular-like, characterized by AP morphology. LQT2-derived cardiomyocytes showed marked prolongation of the action potential duration (APD). This prolongation persisted at different rates with external electrical stimulation. The LQT2 phenotype could even be recapitulated in control iPSC lines by pharmacologic inactivation of the I_{Kr} current with a specific blocker (E-4031). Single-cell voltage clamp studies identified the presence of an E4031-sensitive current (I_{Kr}) in control human iPSC-CMs. Peak amplitudes of the I_{Kr} activation currents in LQTS cardiomyocytes were found to be significantly lower than in control cells. Even at multicellular level, the hiPSC-CMs produced a significant longer APD when compared to control cells. EADs could be found in both the atrial-like and ventricular-like LQT2 iPSC-CMs. APD prolongation could even be increased by E-4031 and cisapride in these cells. Moreover, Itzhaki et al. used their LQT2 iPSC-CMs as a platform for drug screens with a Ca^{2+} blocker (nifedipine), a K_{ATP}-channel opener (pinacidil), and a Na^{+-} channel blocker (ranolazine). While nifedipine and pinacidil led to a significant shortening of the APD and could completely abolish triggered arrhythmias in LQT2 iPSC-CMs on multicell level, ranolazine reduced triggered arrhythmias but had no influence on APD, probably because of its nonspecific blocking effect on various ion channels [15]. Matsa et al. generated hiPSC-CMs from both symptomatic and asymptomatic patients with a G1681 mutation in KCNH2 and put more emphasis on iPS-based disease modelling as a drug screen platform. The LQT patients in this work (mother: asymptomatic, QTc interval 445 ms; daughter: symptomatic, QTc interval 571 ms) showed contrarious phenotypes despite

the same mutation. In the symptomatic patient, syncope-like events took place after arousal from sleep, as typical for LQT2. hiPSC-CMs originated from skin fibroblasts. Interestingly, APDs from the mother's hiPSC-CMs were shorter than the daughter's thus reflecting the *in vivo* penetrance. Application of a sympathetic stimulus with isoprenaline led to electrophysiological abnormalities, for example, EADs, in 25% of the LQT2-hiPSC-CMs. These arrhythmias could be antagonized by β-blockers [26]. Lahti et al. used skin biopsy-derived iPSCs of an asymptomatic individual with a missense mutation in KCNH2 causing arginine-to-tryptophan substitution at position 176 (R176, hERG-FinB). CM differentiation was performed with WT-hiPSC-CMs, LQT2-hiPSC-CMs, and hES-CMs. Again, APs were divided into "atrial-like" and "ventricular-like." Only ventricular-like APs showed a significant elongation, especially at low frequencies. EADs were observed in 1 out of 20 LQT2-hiPSC-CMs and were never observed in WT- hiPSC-CMs. Blocking of I_{Kr} channels with E4031 lead to an increase in EADs in both LQT2 and wild-type-derived cell lines, but this effect turned out to be more emphasized in LQT2-hiPSC-CMs [27].

4. A Long QT Type 3 Syndrome Model

4.1. Pathophysiology. LQT3 has a vastly lower incidence than LQT1/2, it is evident in about 7-8% of genotyped patients with LQTS [34]. Patients with LQT3 suffer from fatal cardiac events typically at night without excitation or arousal. Interestingly, only infrequently preliminary sympathetic stimulation can be found before cardiac events [35]. Surface ECG in LQT3 shows a flat, long ST segment with a late appearance of a narrow-peaked T wave [4, 36]. SCN5A mutations lead to gain of function of Na^+ channel activity. Briefly, late sustained Na^+ currents, slowed rate of inactivation, faster recovery from inactivation, and abnormal interaction with the channel's β-subunit define the mode of action in LQT3 syndrome [36]. Thereby, the plateau phase of the action potential is prolonged, producing long ST segments and later appearance of T wave in the ECG. Compared to patients with LQT1/2, β-blocker treatment is less effective in LQT3, for example, as that might prolong action potentials due to bradycardia [37]. On the other hand, Na^+ channel blockers like mexiletine and flecainide can shorten the action potential both *in vitro* and *in vivo* [38]. Mexiletine leads to a shortened QT interval, a normalization of the T wave, and can even prevent *torsade de pointes* in short-time course. Atrioventricular block can also be improved. The effect of flecainide seems to be more mutation specific and it can induce Brugada type ECG changes. Once diagnosed, patients require implantation of a cardioverter defibrillator (ICD) because of the high incidence of malignant arrhythmias. Moreover, the pacemaker-function of the ICD helps to prevent arrhythmia-inducing bradycardias.

4.2. The Models. Generation of LQT3-miPSC-CMs was first performed in 2011 by Malan et al. [28], this work is based on murine cells with deletion of the amino acids lysine-proline-glutamine in the intracellular loop between domains III and IV of the cardiac Na^+ channel (SCN5). Patch clamp measurements of LQT3-miPSC-CMs showed faster recovery from inactivation and larger late currents than observed in controls. Duration of AP was prolonged; also EADs could be provoked at low pacing rates.

Davis et al. generated iPSC lines from mice carrying the Scn5a (1798insD/+) (SCN5a-het) mutation [17]. In humans, the underlying mutation causes an overlap syndrome with clinical features of both LQT3 and Brugada syndrome. This work addresses the question whether relatively immature iPSCs-derived CMs can truly model gain- and loss-of-function genetic disorder affecting the Na^+-current (I_{Na}) in the face of their immaturity. Patch-clamp experiments showed that the SCN5-het cardiomyocytes had a significant decrease in I_{Na} density and a larger persistent I_{Na} compared with SCN5a-WT cells. AP measurements indicated longer APD in SCN5-het-derived CMs. Interestingly, these characteristics recapitulated the findings of isolated cardiomyocytes from adult mice. Patch-clamp measurements on the derivative cardiomyocytes revealed changes similar to those in the mouse iPSC-derived cardiomyocytes [17].

5. LQT8 (Timothy Syndrome)

LQT8, also named Timothy syndrome, was first described by Marks et al. and Reichenbach et al. [39, 40]. Compared to the named above types of LQTS, this syndrome manifests with major phenotypic abnormalities in multiple-organ systems, including skin, eyes, teeth, immune system, and brain. The majority of affected children die at an average age of 2.5 years. All affected individuals have severe prolongation of QT intervals, syndactyly, and abnormal teeth. Cardiac arrhythmias are the most serious aspect of this disorder: patients show QT prolongation, 2:1 atrioventricular block, T wave alteration, and life-threatening polymorphic ventricular tachycardias. In 2004, Splawski et al. [41] could specify the phenotypic characterization of the Timothy syndrome and finally attribute its variegated clinical attributes to a *de novo* missense mutation in the $Ca_V1.2$ L-type calcium channel gene: Analysis of the affected patients $Ca_V1.2$ splice variant revealed a G121A transition in exon 8A. The $Ca_V1.2$ gene is expressed in multiple tissues. The disease-associated mutation causes abnormal Ca^{2+} currents. The mutated Ca^{2+} channel loses its voltage-dependent inactivation leading to sustained $I_{Ca,L}$ action potential prolongation and Ca^{2+} overload. The consequence is a spontaneous Ca^{2+} release from the sarcoplasmatic reticulum and thus is a promotion of early delayed afterdepolarizations. It has been shown in single cases that treatment with Ca^{2+}-channel blockers like verapamil can reduce the risk of arrhythmias.

5.1. The Model. In 2011, Yazawa et al. have generated hiPSC-CMs from two Patients suffering from LQT8/Timothy syndrome due to an amino acid substitution in exon 8a of *CACNA1C*, the gene encoding $Ca_V1.2$. The APs from iPSC-derived ventricular cells were three times longer than in controls, and EBs from those cells contracted only at 30 bpm (controls 60 bpm). Electrophysiological recordings and Ca^{2+} imaging studies of these ventricular-like cells showed irregular contraction, excessive Ca^{2+} influx as a source of prolonged

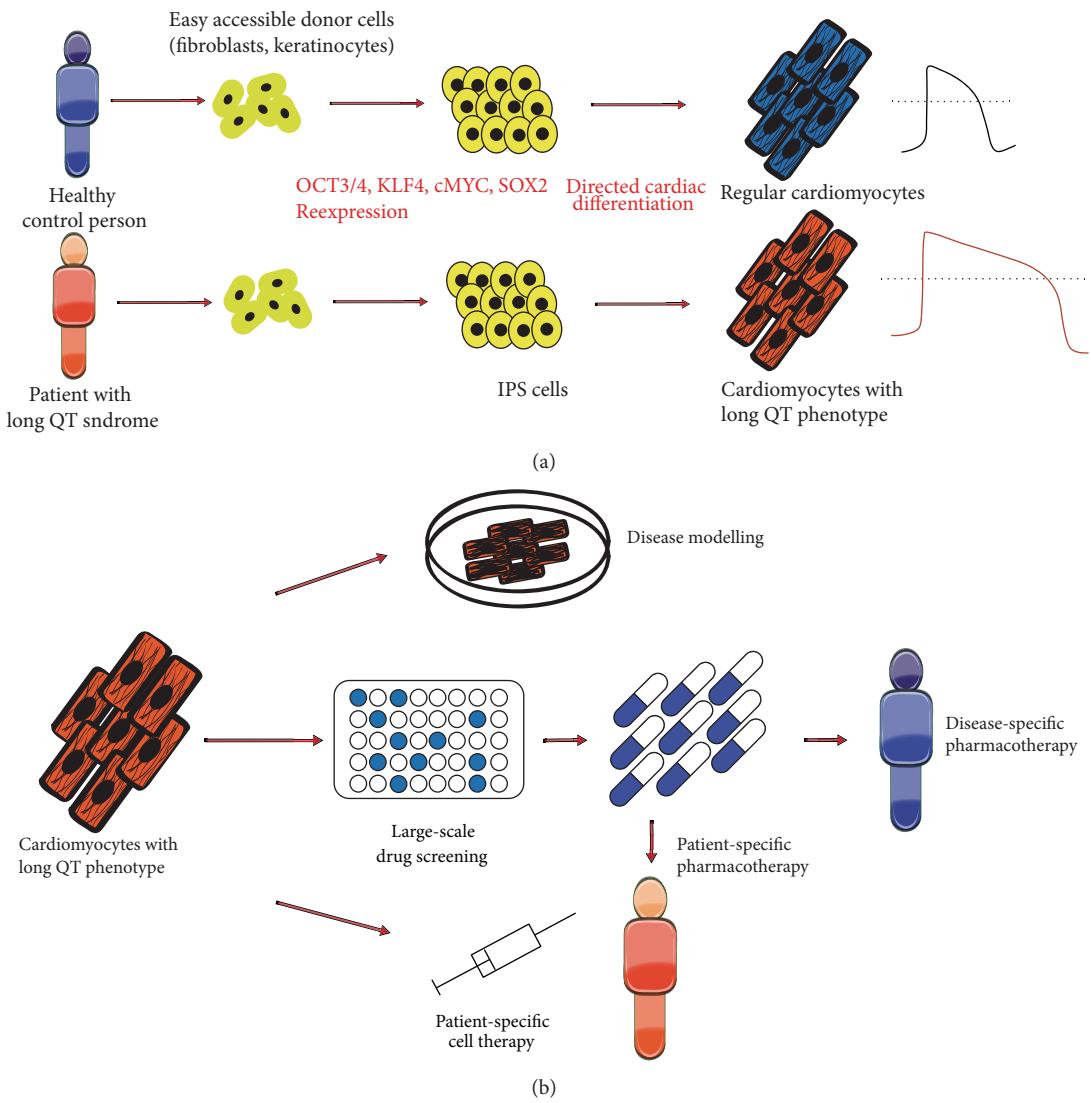

Figure 2: (a) Schematic presentation of iPSC-derived cardiomyocytes' retrieval. Based on easy accessible donor cells, like, for example, fibroblasts and consequent overexpression of different pluripotency factors, reprogrammed donor cells fall into a state of pluripotency (iPS-Cells). By various forms of directed cardiac differentiation, cardiomyocyte-like cells show essential characteristics of adult cardiomyocytes, maintaining their LQT-/non-LQT-phenotype. (b) Possible applications for iPSC-derived cardiomyocytes: (i) disease modelling for better understanding of genetic and epigenetic causation of LQTS; (ii) large-scale drug screening for both patient-specific and nonspecific pharmacotherapy; (iii) circumventing transplantation-associated immunogenicity by patient-specific cell therapy.

action potentials, irregular electrical activity, and abnormal calcium: LQT8-iPSC-CMs showed a delay in inactivation of $I_{Ca,L}$. The great impact of this work is outlined by the rescue experiments. Briefly, roscovitine, a compound that increases the voltage-dependent inactivation of $Ca_V1.2$, restored the electrical and Ca^{2+} signalling properties of cardiomyocytes from Timothy syndrome patients [20, 42].

6. Conclusion

Several limitations of iPS-derived CMs have to be overcome. To date, most models mentioned previously lead to an "immature" electrophysiological phenotype, reminding more of fetal than adult CMs. As in most iPS cell-based disease models, further limitations come due to deficient purity of the cell populations. To date, these are not exceeding 50% purity of CMs. Beyond that, iPC-derived "CMs" comprise mixed cardiac subpopulations with various AP characteristics.

Nevertheless, human disease-specific iPS cells can be used to model different types of long QT syndrome. Not only the generated cardiomyocytes recapitulated human disease phenotype but also allowed the development of potential rescue strategies. In fact, this points to major application of human disease-specific iPS cells, namely, the opportunity of drug development in a disease-specific setting. Thereby, a variety of human diseases have been successfully studied while the vast majority of rescuing strategies were based on an educated guess. In the future, large-scale screening

approaches using small molecule, shRNA, or cDNA libraries will shed a deep light on the pathophysiology of human disease and allow the development of specific drugs (Figure 2).

Abbreviations

AP:	Action potential
APD:	Action potential duration
CM:	Cardiomyocyte
EB:	Embryoid body
EAD:	Early afterdepolarization
ECG:	Electrocardiogram
hESC:	Human embryonic stem cell
hiPSC:	Human-induced pluripotent stem cell
ICD:	Implantable cardioverter defibrillator
miPSC:	Murine-induced pluripotent stem cells
LQT(S):	Long QT (syndrome)
QT-Interval:	Time between start and end of cardiac ventricular electrical depolarization.

References

[1] P. J. Schwartz, M. Stramba-Badiale, L. Crotti et al., "Prevalence of the congenital long-QT syndrome," *Circulation*, vol. 120, no. 18, pp. 1761–1767, 2009.

[2] C. A. Martin, G. D. Matthews, and C. L. Huang, "Sudden cardiac death and inherited channelopathy: the basic electrophysiology of the myocyte and myocardium in ion channel disease," *Heart*, vol. 98, no. 7, pp. 536–543, 2012.

[3] A. O. Grant, "Cardiac ion channels," *Circulation*, vol. 2, no. 2, pp. 185–194, 2009.

[4] H. Morita, J. Wu, and D. P. Zipes, "The QT syndromes: long and short," *The Lancet*, vol. 372, no. 9640, pp. 750–763, 2008.

[5] K. Takahashi, K. Tanabe, M. Ohnuki et al., "Induction of pluripotent stem cells from adult human fibroblasts by defined factors," *Cell*, vol. 131, no. 5, pp. 861–872, 2007.

[6] J. Yu, M. A. Vodyanik, K. Smuga-Otto et al., "Induced pluripotent stem cell lines derived from human somatic cells," *Science*, vol. 318, no. 5858, pp. 1917–1920, 2007.

[7] S. Liebau, P. U. Mahaddalkar, H. A. Kestler, A. Illing, T. Seufferlein, and A. Kleger, "A hierarchy in reprogramming capacity in different tissue microenvironments: what we know and what we need to know," *Stem Cells and Development*, vol. 22, no. 5, pp. 695–706, 2013.

[8] L. Linta, M. Stockmann, T. M. Boeckers, A. Kleger, and S. Liebau, "The potential of iPS cells in synucleinopathy research," *Stem Cells and Development*, vol. 2012, Article ID 629230, 6 pages, 2012.

[9] A. Kleger, P. U. Mahaddalkar, S. F. Katz, A. Lechel, J. Y. Joo, K. Loya et al., "Increased reprogramming capacity of mouse liver progenitor cells, compared with differentiated liver cells, requires the BAF complex," *Gastroenterology*, vol. 142, no. 4, pp. 907–917, 2012.

[10] R. Maehr, S. Chen, M. Snitow et al., "Generation of pluripotent stem cells from patients with type 1 diabetes," *Proceedings of the National Academy of Sciences of the United States of America*, vol. 106, no. 37, pp. 15768–15773, 2009.

[11] A. Raya, I. Rodríguez-Piz, G. Guenechea et al., "Disease-corrected haematopoietic progenitors from Fanconi anaemia induced pluripotent stem cells," *Nature*, vol. 460, no. 7251, pp. 53–59, 2009.

[12] S. T. Rashid, S. Corbineau, N. Hannan et al., "Modeling inherited metabolic disorders of the liver using human induced pluripotent stem cells," *Journal of Clinical Investigation*, vol. 120, no. 9, pp. 3127–3136, 2010.

[13] G. H. Liu, B. Z. Barkho, S. Ruiz et al., "Recapitulation of premature ageing with iPSCs from Hutchinson-Gilford progeria syndrome," *Nature*, vol. 472, no. 7342, pp. 221–227, 2011.

[14] K. J. Brennand, A. Simone, J. Jou, C. Gelboin-Burkhart, N. Tran, S. Sangar et al., "Modelling schizophrenia using human induced pluripotent stem cells," *Nature*, vol. 473, pp. 221–225, 2011.

[15] I. Itzhaki, L. Maizels, I. Huber, L. Zwi-Dantsis, O. Caspi, A. Winterstern et al., "Modelling the long QT syndrome with induced pluripotent stem cells," *Nature*, vol. 471, no. 7337, pp. 225–229, 2011.

[16] X. Ge, Y. Ren, O. Bartulos, M. Y. Lee, Z. Yue, K. Y. Kim et al., "Modeling supravalvular aortic stenosis syndrome with human induced pluripotent stem cells," *Circulation*, vol. 126, no. 14, pp. 1695–1704, 2012.

[17] R. P. Davis, S. Casini, C. W. van den Berg, M. Hoekstra, C. A. Remme, C. Dambrot et al., "Cardiomyocytes derived from pluripotent stem cells recapitulate electrophysiological characteristics of an overlap syndrome of cardiac sodium channel disease," *Circulation*, vol. 125, no. 25, pp. 3079–3091, 2012.

[18] N. Sun, M. Yazawa, J. Liu, L. Han, V. Sanchez-Freire, O. J. Abilez et al., "Patient-specific induced pluripotent stem cells as a model for familial dilated cardiomyopathy," *Science Translational Medicine*, vol. 4, no. 130, Article ID 130ra47, 2012.

[19] C. B. Jung, A. Moretti, M. Mederos y Schnitzler, L. Iop, U. Storch, M. Bellin et al., "Dantrolene rescues arrhythmogenic RYR2 defect in a patient-specific stem cell model of catecholaminergic polymorphic ventricular tachycardia," *EMBO Molecular Medicine*, vol. 4, no. 3, pp. 180–191, 2012.

[20] M. Yazawa, B. Hsueh, X. Jia et al., "Using induced pluripotent stem cells to investigate cardiac phenotypes in Timothy syndrome," *Nature*, vol. 471, no. 7337, pp. 230–236, 2011.

[21] C. Mauritz, K. Schwanke, M. Reppel et al., "Generation of functional murine cardiac myocytes from induced pluripotent stem cells," *Circulation*, vol. 118, no. 5, pp. 507–517, 2008.

[22] X. Carvajal-Vergara, A. Sevilla, S. L. Dsouza et al., "Patient-specific induced pluripotent stem-cell-derived models of LEOPARD syndrome," *Nature*, vol. 465, no. 7299, pp. 808–812, 2010.

[23] C. Donger, I. Denjoy, M. Berthet et al., "KVLQT1 C-terminal missense mutation causes a forme fruste long-QT syndrome," *Circulation*, vol. 96, no. 9, pp. 2778–2781, 1997.

[24] W. Shimizu and C. Antzelevitch, "Differential effects of beta-adrenergic agonists and antagonist in LQT1, LQT2 and LQT3 models of the long QT syndrome," *Journal of the American College of Cardiology*, vol. 35, no. 3, pp. 778–786, 2000.

[25] A. Moretti, M. Bellin, A. Welling, C. B. Jung, J. T. Lam, L. Bott-Flugel et al., "Patient-specific induced pluripotent stem-cell models for long-QT syndrome," *The New England Journal of Medicine*, vol. 363, no. 15, pp. 1397–1409, 2010.

[26] E. Matsa, D. Rajamohan, E. Dick et al., "Drug evaluation in cardiomyocytes derived from human induced pluripotent stem cells carrying a long QT syndrome type 2 mutation," *European Heart Journal*, vol. 32, no. 8, pp. 952–962, 2011.

[27] A. L. Lahti, V. J. Kujala, H. Chapman, A. P. Koivisto, M. Pekkanen-Mattila, E. Kerkela et al., "Model for long QT syndrome type 2 using human iPS cells demonstrates arrhythmogenic characteristics in cell culture," *Disease Models and Mechanisms*, vol. 5, no. 2, pp. 220–230, 2012.

[28] D. Malan, S. Friedrichs, B. K. Fleischmann, and P. Sasse, "Cardiomyocytes obtained from induced pluripotent stem cells with long-QT syndrome 3 recapitulate typical disease-specific features in vitro," *Circulation Research*, vol. 109, no. 8, pp. 841–847, 2011.

[29] M. E. Curran, I. Splawski, K. W. Timothy, G. M. Vincent, E. D. Green, and M. T. Keating, "A molecular basis for cardiac arrhythmia: HERG mutations cause long QT syndrome," *Cell*, vol. 80, no. 5, pp. 795–803, 1995.

[30] S. G. Priori, C. Napolitano, P. J. Schwartz et al., "Association of long QT syndrome loci and cardiac events among patients treated with β-blockers," *Journal of the American Medical Association*, vol. 292, no. 11, pp. 1341–1344, 2004.

[31] P. J. Schwartz, S. G. Priori, C. Spazzolini et al., "Genotype-phenotype correlation in the long-QT syndrome: gene-specific triggers for life-threatening arrhythmias," *Circulation*, vol. 103, no. 1, pp. 89–95, 2001.

[32] T. Noda, W. Shimizu, K. Satomi et al., "Classification and mechanism of Torsade de Pointes initiation in patients with congenital long QT syndrome," *European Heart Journal*, vol. 25, no. 23, pp. 2149–2154, 2004.

[33] T. Noda, H. Takaki, T. Kurita et al., "Gene-specific response of dynamic ventricular repolarization to sympathetic stimulation in LQT1, LQT2 and LQT3 forms of congenital long QT syndrome," *European Heart Journal*, vol. 23, no. 12, pp. 975–983, 2002.

[34] J. N. Johnson, D. J. Tester, J. Perry, B. A. Salisbury, C. R. Reed, and M. J. Ackerman, "Prevalence of early-onset atrial fibrillation in congenital long QT syndrome," *Heart Rhythm*, vol. 5, no. 5, pp. 704–709, 2008.

[35] N. Hofman, A. A. M. Wilde, S. Kääb et al., "Diagnostic criteria for congenital long QT syndrome in the era of molecular genetics: do we need a scoring system?" *European Heart Journal*, vol. 28, no. 5, pp. 575–580, 2007.

[36] L. Zhang, D. W. Benson, M. Tristani-Firouzi et al., "Electrocardiographic features in Andersen-Tawil syndrome patients with KCNJ2 mutations: characteristic T-U-wave patterns predict the KCNJ2 genotype," *Circulation*, vol. 111, no. 21, pp. 2720–2726, 2005.

[37] A. J. Moss, W. Zareba, W. J. Hall et al., "Effectiveness and limitations of β-blocker therapy in congenital long- QT syndrome," *Circulation*, vol. 101, no. 6, pp. 616–623, 2000.

[38] S. G. Priori, C. Napolitano, P. J. Schwartz, R. Bloise, L. Crotti, and E. Ronchetti, "The elusive link between LQT3 and brugada syndrome: the role of flecainide challenge," *Circulation*, vol. 102, no. 9, pp. 945–947, 2000.

[39] M. L. Marks, S. L. Whisler, C. Clericuzio, and M. Keating, "A new form of long QT syndrome associated with syndactyly," *Journal of the American College of Cardiology*, vol. 25, no. 1, pp. 59–64, 1995.

[40] H. Reichenbach, E. M. Meister, and H. Theile, "The heart-hand syndrome: a new variant of disorders of heart conduction and syndactylia including osseous changes in hands and feet," *Kinderarztliche Praxis*, vol. 60, no. 2, pp. 54–56, 1992.

[41] I. Splawski, K. W. Timothy, L. M. Sharpe et al., "CaV1.2 calcium channel dysfunction causes a multisystem disorder including arrhythmia and autism," *Cell*, vol. 119, no. 1, pp. 19–31, 2004.

[42] M. Yazawa and R. E. Dolmetsch, "Modeling timothy syndrome with iPS cells," *Journal of Cardiovascular Translational Research*, vol. 6, no. 1, pp. 1–9, 2013.

Hindawi Publishing Corporation
Stem Cells International
Volume 2013, Article ID 360573, 13 pages
http://dx.doi.org/10.1155/2013/360573

Research Article

Definitive Endoderm Formation from Plucked Human Hair-Derived Induced Pluripotent Stem Cells and SK Channel Regulation

Anett Illing,[1] Marianne Stockmann,[1] Narasimha Swamy Telugu,[1] Leonhard Linta,[2] Ronan Russell,[1] Martin Müller,[1] Thomas Seufferlein,[1] Stefan Liebau,[2] and Alexander Kleger[1]

[1] *Department of Internal Medicine I, University of Ulm, Albert-Einstein Allee 23, 89081 Ulm, Germany*
[2] *Institute for Anatomy and Cell Biology, University of Ulm, Albert-Einstein Allee 11, 89081 Ulm, Germany*

Correspondence should be addressed to Stefan Liebau; stefan.liebau@uni-ulm.de and Alexander Kleger; alexander.kleger@uni-ulm.de

Received 18 January 2013; Accepted 13 March 2013

Academic Editor: Michael Levin

Pluripotent stem cells present an extraordinary powerful tool to investigate embryonic development in humans. Essentially, they provide a unique platform for dissecting the distinct mechanisms underlying pluripotency and subsequent lineage commitment. Modest information currently exists about the expression and the role of ion channels during human embryogenesis, organ development, and cell fate determination. Of note, small and intermediate conductance, calcium-activated potassium channels have been reported to modify stem cell behaviour and differentiation. These channels are broadly expressed throughout human tissues and are involved in various cellular processes, such as the after-hyperpolarization in excitable cells, and also in differentiation processes. To this end, human induced pluripotent stem cells (hiPSCs) generated from plucked human hair keratinocytes have been exploited *in vitro* to recapitulate endoderm formation and, concomitantly, used to map the expression of the SK channel (SKCa) subtypes over time. Thus, we report the successful generation of definitive endoderm from hiPSCs of ectodermal origin using a highly reproducible and robust differentiation system. Furthermore, we provide the first evidence that SKCas subtypes are dynamically regulated in the transition from a pluripotent stem cell to a more lineage restricted, endodermal progeny.

1. Introduction

Mammalian development is a tightly regulated process, with considerable biochemical and physiological changes occurring from the time of fertilization to the onset of gastrulation and further differentiation towards fully formed organisms. However, understanding early fate decision events, such as segregation of the three germ layers, is a prerequisite for regenerative medicine [1–5]. The advent of induced pluripotent stem cells and their unique features of unlimited self-renewal and nonrestricted differentiation capacity marked a milestone in the battle to dissect such processes—directly in the context of human development [6–8]. Given the incredible accordance of embryonic development *in vivo* and its respective model system *in vitro*, it is not surprising that most of the currently available pluripotent stem cell differentiation protocols make use of physiological, stage-specific signalling clues in order to recapitulate development of all three germ layers: ectoderm, mesoderm, and endoderm. Further differentiation towards more specialized cell types has also been achieved, for example, formation of primitive gut tube endoderm (SOX17/Hnf1b positive [9, 10]), pancreatic progenitor cells (Pdx1/Cpa1 positive [11, 12]), and hepatic progenitor cells (AFP/HNF4a positive [13]) from definitive endoderm progenitor cells. Nevertheless, the precise mechanisms governing such complex processes are

not completely understood. Another limitation exists in achieving highly homogenous, reproducible cell type-specific yields. As a result, the current use of hiPSCs for disease modelling where the aim is to use *in vitro* differentiated patient-specific pluripotent stem cells to replace the patients' damaged cells is massively hindered. In consequence, critically defined, efficient, and robust differentiation protocols are highly anticipated.

Endoderm comprises the innermost of the primary germ layers of an animal embryo and has a primary role to provide the epithelial lining of two major tubes within the body. The first tube, which extends the entire length of the body, is known as the digestive tube and undergoes budding during embryogenesis to form the liver, gallbladder, and pancreas. The second tube, the respiratory tube, forms an outgrowth of the digestive tube and gives rise to the lungs. Notably, two distinct sets of endoderm can be distinguished in the developing embryo: visceral endoderm arising directly from the inner cell mass and definitive endoderm (DE) derived from mesendoderm within the anterior primitive streak in close proximity to the cardiovascular progenitors [1, 14–16]. The visceral endoderm forms the epithelial lining of the yolk sac [17] while the DE is responsible for the internal (mucosal) lining of the embryonic gut and is governed by the expression of key transcription factors such as SOX17 [18], Foxa2, or Hex1 [19].

To date, a large group of proteins has been broadly neglected concerning its role during developmental processes, namely, ion channels. In addition to the modulation of the membrane potential in various tissues and cell populations, ion channels were identified to be involved in a number of biological processes, such as proliferation, cell differentiation, and cell morphogenesis. Since these mechanisms are apparently abundant in the transition of stem or progenitor cell populations to more defined cells types of different origin and potency, a role for ion channels in developmental processes can be hypothesized [20–23]. In particular, the adsorptive tissues derived from the DE are often rich in ion channels and defects in these channels are responsible for some harmful diseases. One prominent example is cystic fibrosis (CF), a common, autosomal recessive disorder due to mutations in a chloride channel known as the CFTR. Located on the plasma membrane of many epithelial cells, this simple mutation gives rise to abnormalities of salt and fluid transport in many endodermal derived tissues including lung, pancreas, and liver [24]. However the contribution of other ion channel families to diseases within the foregut has been poorly studied.

Indeed, in pluripotent stem cells, activation of small and intermediate conductance calcium activated potassium channels (SK channels; SKCas) triggers the MAPK/ERK pathway following RAS/RAF activation finally, giving rise to cytoskeletal rearrangement, cardiogenesis, and cardiac subtype specification [2, 3, 5, 25]. The group consists of four members, namely, SK1 (KCa 2.1, KCNN1), SK2 (KCa 2.2, KCNN2), SK3 (KCa 2.3, KCNN3), and SK4 (KCa 3.1, KCNN4). The functional form of the ion pore is mediated by the combination of the 4 subunits, respectively. Additionally, widely distributed functional splice variants of SKCas have been found throughout the organism in several tissues [26–28]. Functional SKCas are not only constructed as homo- but also as hetero-tetrameric channel proteins, most probably serving a cellular and functional specificity [26, 29]. The pore is opened following subtle elevation of intracellular calcium levels. Calmodulin, attached in a Ca^{2+}-dependent manner to the C-terminal of the channel subunits, specifically binds Ca^{2+}-ions and mediates a conformational change of the channel protein, leading to the opening of the pore [30, 31]. Calcium is the only known physiological activator of SKCas and channel opening occurs within a few milliseconds [31]. SK1-3 are highly expressed in the nervous system where they modify the membrane potential; that is, they crucially contribute to the after-hyperpolarization and therefore regulate the firing pattern, frequency, and length of action potentials in different neuronal networks [32–35]. On the other hand, SKCas play important roles in multiple other cellular functions, namely in cerebral and peripheral blood vessel smooth muscle, the functional myocardium, or neural progenitor cells [21, 36, 37].

In the current study, we highlight a robust and efficient differentiation protocol to drive plucked human hair-derived hiPSCs towards definitive endoderm. Furthermore, we analyse changes in protein and mRNA expression in the SKCa family of ion channels in the transition from a pluripotent cell state to a definitive endodermal committed cell type.

2. Materials and Methods

2.1. Keratinocyte Culture from Plucked Human Hair. Outgrowth of keratinocytes from plucked human hair was induced as described previously [25, 38]. Keratinocytes were split on 20 μg/mL collagen IV-coated dishes and cultured in EpiLife medium with HKGS supplement (both Invitrogen, USA). The use of human material in this study has been approved by the ethical committee of the Ulm University (Nr. 0148/2009) and in compliance with the guidelines of the Federal Government of Germany and the Declaration of Helsinki concerning Ethical Principles for Medical Research Involving Human Subjects.

2.2. Rat Embryonic Fibroblasts (REFs) Culture. REFs were isolated from day E14 Sprague Dawley rat embryos as described previously [38] and cultured in DMEM supplemented with 15% FCS, 2 mM GlutaMAX, 100 μM nonessential amino acids, and 1% Antibiotic-Antimycotic (all Invitrogen). Cells were passaged using 0.125% trypsin digestion when reaching confluence for up to 5 passages. All animal experiments were performed in compliance with the guidelines for the welfare of experimental animals issued by the Federal Government of Germany, the National Institutes of Health, and the Max Planck Society (Nr. O.103).

2.3. Lentivirus Generation. Lentivirus containing a polycistronic expression cassette encoding OCT4, SOX2, KlF4, and cMYC was produced as described previously [3, 25, 38].

2.4. Reprogramming Keratinocytes. Keratinocytes at 75% confluence were infected with 5×10^5 proviral genome copies in EpiLife medium supplemented with 8 μg/mL polybrene on two subsequent days. On the third day, keratinocytes were transferred onto irradiated REF feeder cells (2.5×10^5 cells per well irradiated with 30 Gy). Cells were cultured in hiPSCs medium in a 5% O_2 incubator and medium was changed daily. After 3–5 days small colonies appeared, showing a typical hiPSCs like morphology. Around 14 days later, hiPSC colonies had the appropriate size for mechanically passaging and were transferred onto irradiated MEFs or onto Matrigel-coated (BD, USA) dishes for further passaging.

2.5. hiPSC Culture. hiPSCs were initially cultured on feeder cells in Knockout DMEM (Invitrogen) supplemented with 20% Knockout Serum Replacement (Invitrogen), 2 mM GlutaMAX (Invitrogen), 100 μM nonessential amino acids (Invitrogen), 1% Antibiotic-Antimycotic (Invitrogen), 100 μM β-mercaptoethanol (Millipore, USA), 50 μg/mL ascorbic acid, and 10 ng/mL FGF2 (both PeproTech, USA) in a 5% CO_2 incubator.

For later passages, hiPSCs were mechanically picked and transferred onto Matrigel-coated dishes (BD) and kept in FTDA medium that contains DMEM/F12-GlutaMax (Invitrogen), 1 × ITS (Insulin-Transferrin-Selenium, Invitrogen), 0.1% HSA (Biological Industries, Israel), 1 × Lipid mix (Invitrogen), 1 × Penicillin-Streptomycin (Millipore), 10 ng/mL FGF2 (PeproTech), 0.5 ng/mL TGF-β1 (PeproTech), 50 nM Dorsomorphin (Sigma, Germany), and 5 ng/mL Activin A (PeproTech) [39]. hiPSCs were cultured in a 5% O_2 incubator and medium was changed daily. For splitting cells, hiPSCs colonies were incubated with Dispase (StemCell Technologies, France) for 5–7 min at 37° and subsequently detached using a cell scraper. After brief centrifugation, cells were resuspended in FTDA medium and transferred onto Matrigel-coated dishes. Excision of the viral cassette was achieved by incubation with recombinant TAT-Cre protein (1.5 μM for 5 h).

2.6. Monolayer-Based hiPSC Differentiation towards Definitive Endoderm. For DE differentiation, hiPSCs were plated onto Matrigel-coated dishes and cultured in FDTA medium supplemented with 10 μM Rock-inhibitor Y-276342 (Ascent, UK) for 24 hours. When the cells reached about 75% confluence, medium was changed to RPMI 1640 medium (Invitrogen) containing 2% FBS (Lonza, CH) with 500 nM IDE1 (R&D systems, USA), 3 μM CHIR99021 (Axonemedchem), 5 μM LY294002 (Sigma, Germany), and 10 ng/mL BMP4 (PeproTech) for 24 hours. Then, medium was changed to RPMI 1640 medium containing 2% FBS and supplemented with 500 nM IDE1 and 5 μL LY294002 for two days. From day 3 on, cells were cultured in RPMI 1640 supplemented with 500 nm IDE1, 5 μM LY294002, and 50 ng/mL FGF2. The respective figure contains an experimental outline illustrating detailed culture conditions and treatment regimens [40–45] (Figure 2(a)).

2.7. Immunocytochemistry. Immunofluorescence has been previously described [5]. Nuclei were stained with DAPI. Primary antibodies were used as follows: SK1/2 (both 1 : 100, Sigma), SK3 (1 : 100, Alomone Labs, Israel), SK4 (1 : 100, Cell Applications, USA), SOX17 (1 : 500, R&D systems), and FOXA2 (1 : 100, Santa Cruz, USA). hiPSC lines were characterized using the StemLite Pluripotency Antibody Kit (Cell Signaling, USA). Fluorescence labelled secondary antibodies were Alexa Fluor 488 and Alexa Fluor 568 (both Invitrogen). Images were captured using an upright fluorescence microscope (Axioskop 2, Zeiss, Oberkochen, Germany) equipped with a Zeiss CCD camera and analysed using Axiovision software (Zeiss) [46].

2.8. Quantitative One-Step Real Time. RT-PCR (qPCR) Analysis was performed as previously described. Briefly, one-step real-time qPCR was carried out with the LightCycler System (Roche, Mannheim, Germany) using the QuantiTect SYBR Green RT-PCR kit (Qiagen, Hilden, Germany). Relative transcript expression was expressed as the ratio of target gene concentration to the housekeeping gene hydroxymethylbilane synthase (*HMBS*) [47, 48].

2.9. FACS Analysis . For flow cytometry cells were harvested with TrypLE (Invitrogen) for 7 min at 37°C to obtain single-cells suspension. Next, cells were washed twice with PBS, blocked with 5% HSA-solution (in PBS) to avoid unspecific binding of the antibodies to the Fc-receptor. Cells were washed again with PBS and incubated for 40 min at 4°C with CXCR4-PE (Invitrogen), subsequently c-Kit-APC (Invitrogen) was added for additional 10 min at 4◦C in FACS buffer (2% FCS in PBS), according to the manufacturer's instructions. Cells were washed with FACS buffer, 50 ng/mL DAPI was added, to exclude dead cells from analysis, and the samples were directly analysed on a LSRII flow cytometer (BD).

For intracellular SOX17 staining cells were washed twice with PBS, blocked with 5% HSA-solution (in PBS) to avoid unspecific binding of the antibodies to the Fc-receptor. Cells were washed again with PBS and the pellet was resuspended in 4% PFA and incubated for 15 min at 37°C for fixation. Subsequently the cell pellet was resuspended in 0.5% Saponin in FACS buffer (saponin buffer) and incubated for 30 min on ice. Cells were pelleted and stained with SOX17 (1 : 100, R&D systems) at 4°C for one hour. Cells were washed with saponin buffer and afterwards incubated for 30 min at 4°C with anti-goat Alexa Fluor 647. Finally cells were washed with FACS buffer and directly analysed on an LSRII flow cytometer (BD).

2.10. Statistical Analysis. If not stated otherwise, error bars indicate standard deviations. Calculations were done with GraphPad Prism 5 (GraphPad Software, Inc., San Diego, http://www.graphpad.com/).

3. Results

3.1. Reprogramming Human Hair-Derived Keratinocytes to hiPSCs. For the depicted studies we utilized keratinocyte

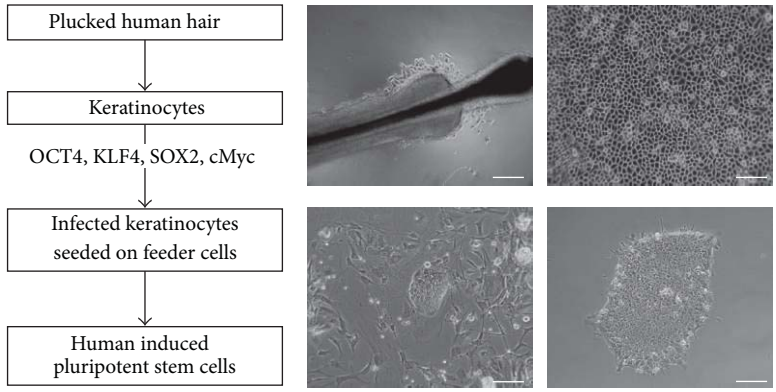

(a)

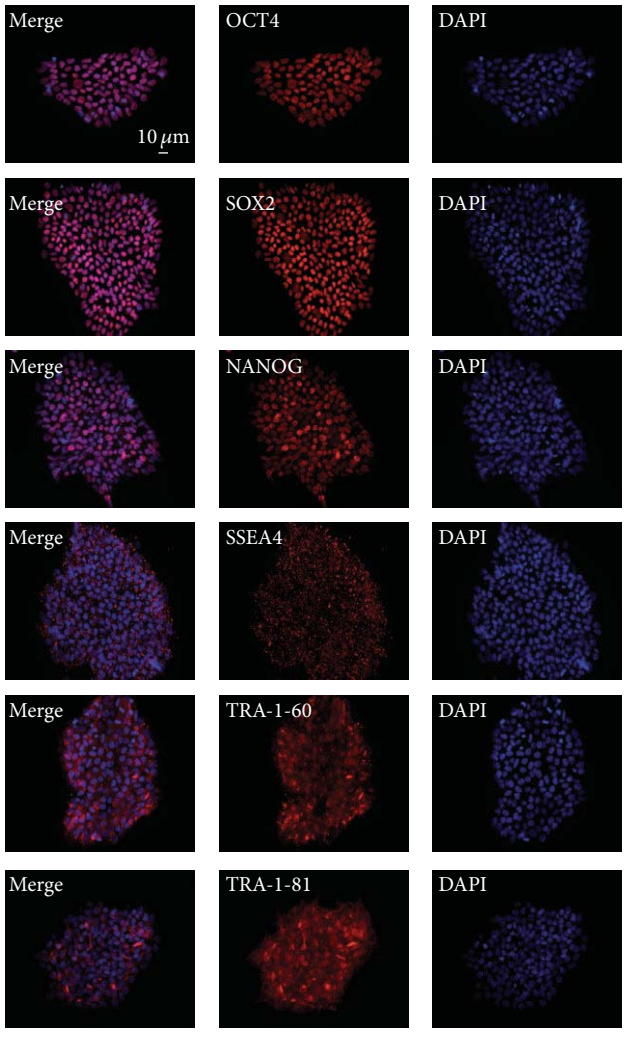

(b)

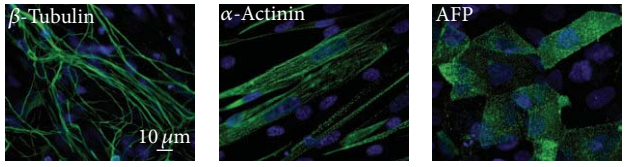

(c)

Figure 1: Continued.

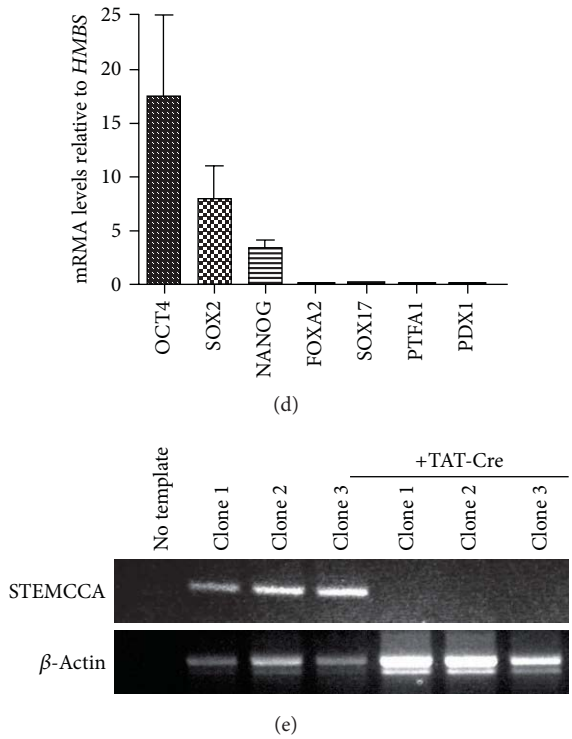

Figure 1: Generation of human induced pluripotent stem cells. (a) Scheme of reprogramming keratinocytes from human plucked hair into induced pluripotent stem cells (hiPSCs). Bright field microscopy images from outgrowing keratinocytes, in detail, the outer root sheath of a plucked human hair. Keratinocytes were infected with a lentiviral construct containing the reprogramming factors OCT4, SOX2, KlF4, and cMyc on two subsequent days. On the following day keratinocytes were transferred onto a monolayer of irradiated REFs (rat embryonic fibroblasts) and after some days small hiPSC colonies could be detected. For later passaging hiPSCs were cultured, under feeder-free conditions, on Matrigel-coated dishes in FTDA medium. Scale bars are 20 μm. (b) hiPSCs express the nuclear factors OCT4, SOX2, and NANOG as well as the pluripotent surface markers SSEA4, TRA-1-60, and TRA-1-81 (*all red*). Scale bars as indicated. (c) hiPSCs used in the present study are capable of differentiating into cells of all 3-germ layers represented by β-tubulin (beta-tubulin 3 in green, neurons—ectoderm), α-actinin (alpha-actinin in green, myocytes—mesoderm), and AFP (alpha-fetoprotein in green, liver cells—endoderm). Nuclei are stained with DAPI in blue. (d) Transcript levels of pluripotent markers such as *OCT4*, *SOX2,* and *NANOG* were highly expressed whereas markers for definitive endoderm (*SOX17* and *FOXA2*) and markers for pancreatic progenitor cells (*PTFA1* and *PDX1*) were not expressed at all. (e) Polymerase chain reaction to detect the STEMCCA cassette in iPS cell subclones before and after treatment with recombinant Cre protein (actin band ~480 bp, STEMCCA band ~400 bp).

cultures from plucked human hair of healthy individuals (Figure 1(a)). With the use of a lentiviral, multicistronic four-factor reprogramming system, keratinocytes were successfully reprogrammed to human induced pluripotent stem cells displaying embryonic stem cell like morphology (Figure 1(a)) as well as hallmarks of pluripotency tested via immunohistochemistry and qRT-PCR for the expression of embryonic stem cell markers. Several lines of more than 5 individuals (data not shown or reported in [3, 25, 38]) were tested for their proliferation and differentiation capacity and subsequently two lines were selected, named "hiPSC_1 and hiPSC_2." Both lines were additionally tested for the protein expression of OCT4, SOX2, NANOG, SSEA4, TRA1-60, and TRA1-81 (Figure 1(b)) and mRNA levels of three pluripotency markers (*OCT4*, *SOX2*, *NANOG*). At the pluripotent stage definitive endoderm makers (*FOXA2*, *SOX17*) and markers for pancreatic progenitors (*PTFA1*, *PDX1*) were negative (Figure 1(d)). Additionally, all lines were capable of differentiating into cells of all 3 germ-layers, as shown by β-3-tubulin (neurons—ectoderm), α-actinin (muscle cells—mesoderm), and α-fetoprotein (liver cells—endoderm) (Figure 1(c)). One line was further treated with recombinant Cre protein to excise the reprogramming STEMCCA cassette being flanked with loxp sites. To test for successful excision, PCR amplification of the STEMCCA cassette was performed in cre- and nontreated iPS cell clones from this respective line showing the band only in controls (Figure 1(e)). Taken together, our established hiPSC lines display an embryonic stem cell like phenotype, proven by morphology and expression of pluripotency markers as well as absent mRNA for endodermal markers.

3.2. Human Induced Pluripotent Stem Cells Can Be Differentiated to Cells Representing the Definitive Endoderm. To test the differentiation potential of our established hiPSC lines into definitive endoderm (DE), previously published protocols were combined in terms of a small molecule-driven

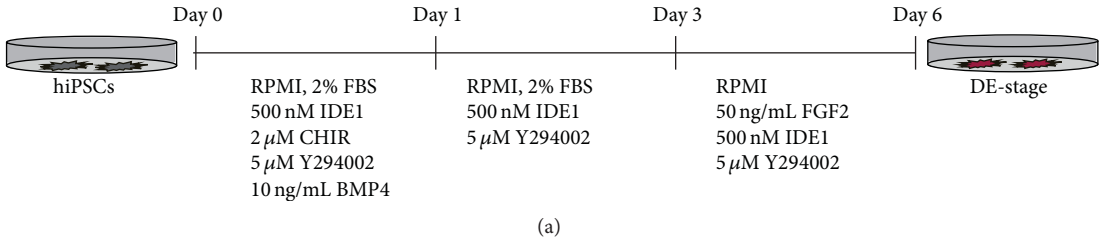

(a)

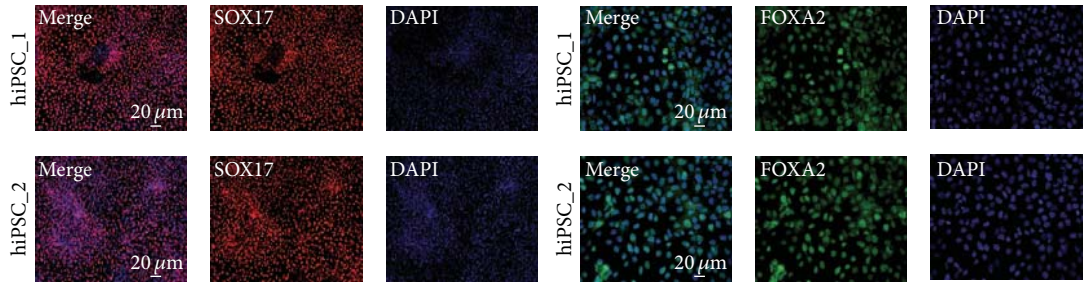

(b)

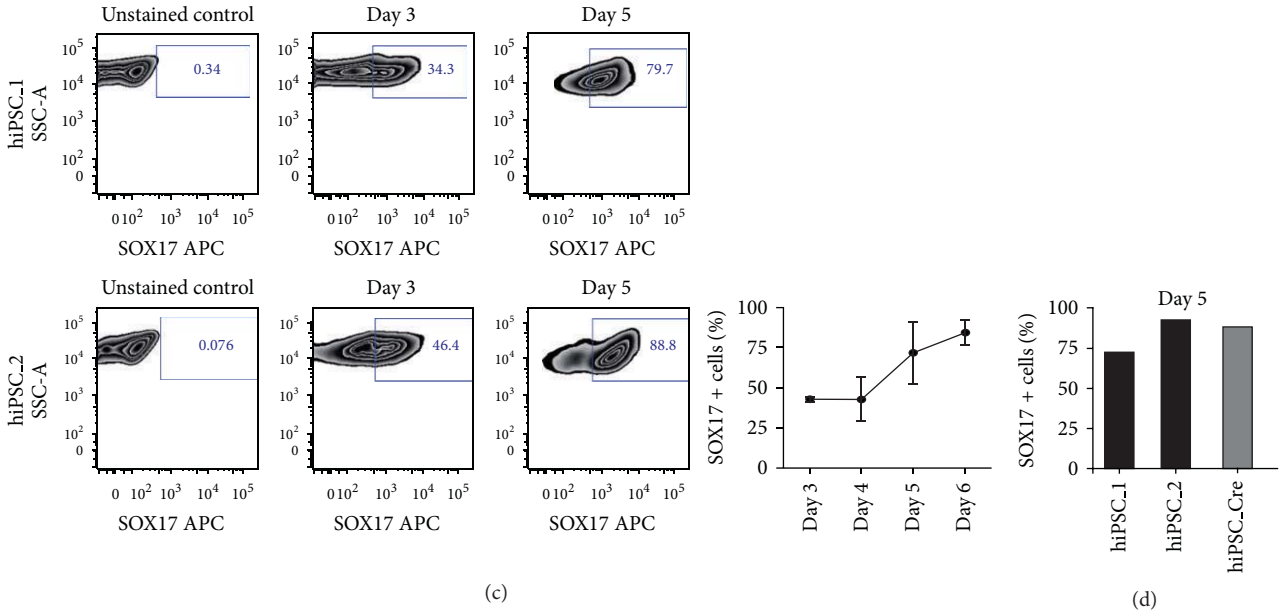

(c)

(d)

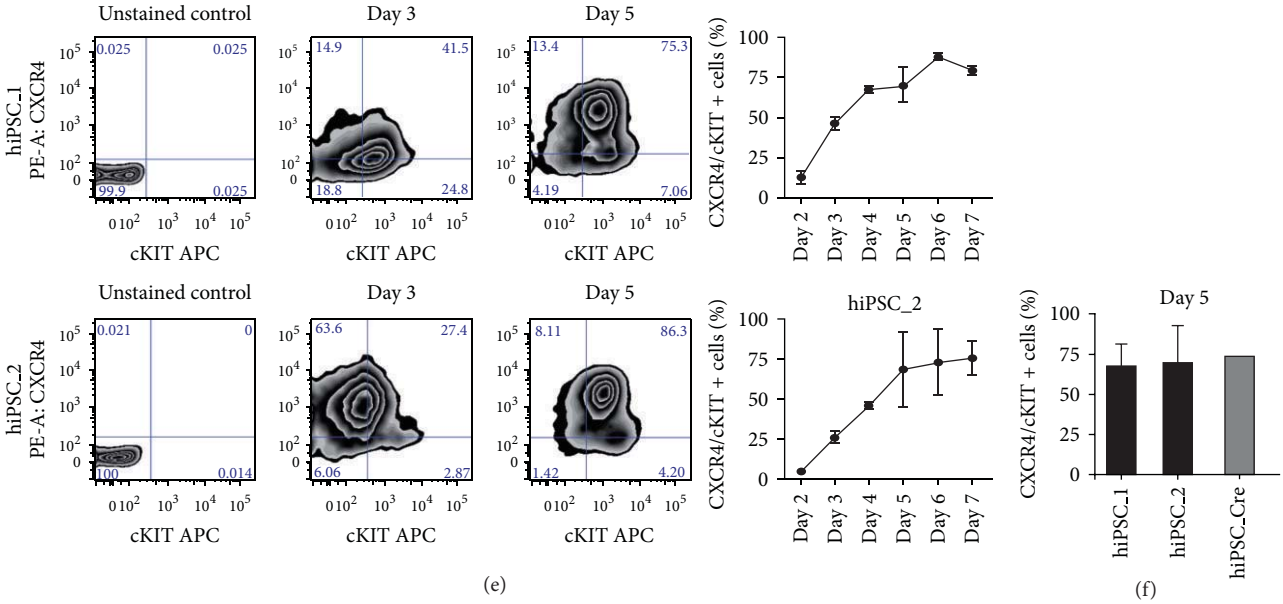

(e)

(f)

Figure 2: Continued.

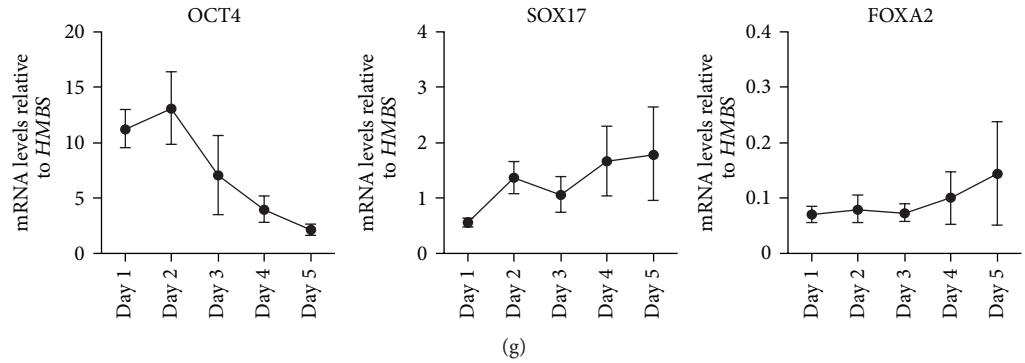

Figure 2: Differentiation of hiPSCs into DE (definitive endoderm) cells. (a) Scheme of monolayer differentiation of hiPSCs into DE cells. (b) Immunocytochemistry shows that hiPSCs-derived DE cells express the early endodermal markers SOX 17 (*red*) or FOXA2 (*green*). Scale bars as indicated. (c) FACS analysis reveals that after 3 days of differentiation approximately 45% of the cells have become SOX17 positive. After 6 days of differentiation about 80% of the cells express SOX17. This data was consistent within two different hiPSC lines. (d) (e) Number of CXCR4/cKIT double-positive cells after 3 days and 5 days of differentiation, respectively. After 5 to 6 days of differentiation both hiPSCs lines express the highest amount of CXCR4/cKIT double-positive cells in the region of 75–80%. (f) Virus-containing hiPSCs (hiPSC_1/hiPSC_2) did not show differences in the number of CXCR4/cKIT double-positive cells compared to virus-free iPSCs (hiPSC_Cre). (g) Continuous loss of *OCT4* mRNA levels during DE differentiation. In contrast, transcript levels of early endodermal genes such as *SOX17* and *FOXA2* steadily increased and reached highest levels after 5 days of differentiation. Expression levels are shown relative to the housekeeping gene *HMBS* ($n = 4$, two different hiPSCs lines).

approach [43–45]. Small molecule-based assays are less biased by batch-to-batch variations and are usually more cost effective. Upon extensive testing of different combinations, our protocol led to the following replacements of established growth factors being known to drive definitive endoderm differentiation: CHIR90021 replaced Wnt3a [40], IDE1 replaced Activin A [41], and LY294002 inhibited the AKT signalling pathway to abolish pluripotency [42]. Figure 2(a) represents a detailed scheme of the differentiation conditions used for the formation of DE from day 0 (undifferentiated pluripotent hiPSCs) to day 6 (definitive endodermal cells). *In vitro* differentiated hiPSCs became positive for endodermal markers, confirmed by positive immunostaining of cells on day 5 for FOXA2 and SOX17 (Figure 2(b)). To analyse and characterize the SOX17 expression more objectively, we quantified SOX17 expression via intracellular FACS analysis in a time course from day 3 to day 6 of the applied protocol. Figure 2(c) shows representative FACS plots from both lines, representing SOX17 positive cells on day 3 and day 5. We did not observe differences in the differentiation capacity of virus-free hiPSCs after excision of the reprogramming cassette in comparison to virus-containing cells, making further analyses of silencing of exogenous factors unnecessary (Figure 2(d)). In summary, SOX17 expression is increasing from approximately 45% at day 3 to nearly 80% of SOX17 positive cells on day 6. Recent publications depict CXCR4 and c-KIT positive cells as definitive endoderm progenitors, that give rise to self-renewing endodermal progenitor cells (EPCs) [49]. To confirm our protocol, we did time course analysis by flow cytometry for CXCR4 and c-KIT positive cells during differentiation. Figure 2(e) shows representative FACS plots of CXCR4 and c-KIT positive cells of the two hiPSC lines on day 3 and 5. Two independent experiments for each line were summarized and shown from day 2 to 7 of endodermal differentiation. From day 2 on, the double positive population (CXCR4 and c-KIT) is steadily increasing in both lines. The maximum is reached with almost 90% double positive cells for hiPSC_1 and almost 80% for hiPSC_2 (Figure 2(d)). Again there was no relevant difference upon excision of the reprogramming cassette (Figure 2(f)).

To further confirm the definitive endodermal identity of the differentiated lines, we measured mRNA levels using qRT-PCR analysis for *OCT4*, *SOX17,* and *FOXA2*. From day 1 to day 5 mRNA levels for the pluripotency marker OCT4 decrease continuously (Figure 2(g), summarized for hiPSC 1 and hiPSC 2). *SOX17* and *FOXA2* levels were tested in the two established hiPSC lines during differentiation and displayed increasing mRNA levels from day 1 to day 5 (Figure 2(g)). This data clearly indicates that the investigated hiPSC lines can be differentiated into DE, loosing markers of pluripotency and up regulating the expression of endodermal markers during endoderm formation.

3.3. Expression of Calcium-Activated Potassium Channels (SKCas) during DE Differentiation. Next, we had a closer look on the expression of the different SKCas subtypes during DE differentiation. hiPSCs were differentiated into DE cells and expression of SKCa was investigated after 5 days of differentiation. On day 5 SOX17 is strongly expressed indicating the differentiation into DE cells (Figure 3(a)). To analyse the expression of the SKCas, DE cells were stained for the different SKCa subtypes. Immunofluorescence analyses show a quite strong and stable expression of SK1, SK2, and SK3 whereas SK4 seems to be expressed at a lower level (Figure 3(b)). SK1, 2, and 4 are localized in the cytoplasm and the cell membrane. However, SK3 is not only localized at the cell membrane but also as PUNCTUA

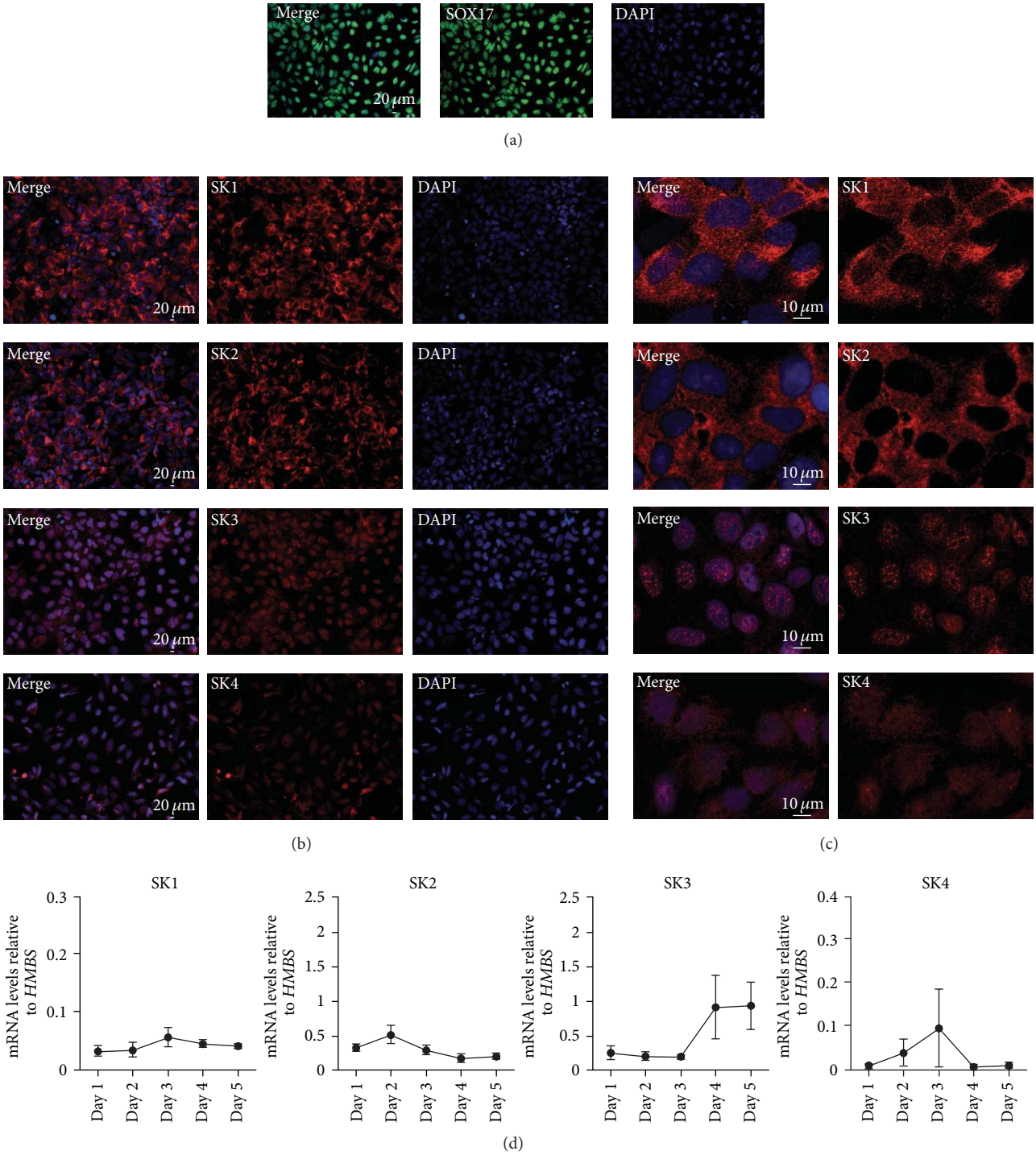

Figure 3: Expression of Calcium-activated Potassium channels during formation of definitive endoderm. (a) Expression of SOX17 (*green*) after 5 days of DE differentiation. (b) Immunofluorescence analysis of SKCa proteins in DE cells. Indicated SKCa subtype (*red)*. Scale bars as indicated. (c) Higher magnifications of indicated SKCa subtype (*red)*. Scale bars as indicated. (d) Transcript levels of SK1 and SK2 remained relatively low during the DE differentiation. In contrast, mRNA levels of SK3 increased after 4 days of differentiation. SK4 mRNA levels slightly increased during the first days of differentiation and peaked on day 3 followed by a sharp decrease until day 5. Expression levels are shown relative to the housekeeping gene *HMBS* ($n = 4$, two different hiPSCs lines).

in the nuclei (Figure 3(c)). This is a finding that needs to be analysed in further studies. Double immunofluorescence staining for SOX17 and respective channel proteins are shown in Supplementary Figure 1 available online at http://dx.doi.org/10.1155/2013/360573.

mRNA expression analysis via quantitative RT-PCR (qRT-PCR) shows a relative constant expression of SK1 and SK2 during DE differentiation (Figure 3(d)). In contrast, transcript levels of SK3 obviously increased after 4 days of differentiation (Figure 3(d)). SK4 mRNAs levels marginally increased during the first days of differentiation and peaked on day 3, followed by a sharp decline up to day 5 (Figure 3(d)). To note, all four SKCa subtypes are expressed during DE differentiation. SK1 and SK2 are constantly expressed whereas SK3 seems to be up regulated during ongoing DE differentiation. The transcript levels of the different SKCa subtypes on day 5 reflect our observations of the immunofluorescence analysis. In sum, all 4 SK subtypes are differentially expressed during DE differentiation of human induced pluripotent stem cells with a yet undescribed localization of SK3 in the nucleus.

4. Discussion

In the current study, we provide proof of the concept that plucked human hair-derived iPSCs are highly potent in their capacity to commit not only towards mesoderm [3] and neuroectoderm [25] but also towards the endodermal germ layer, particularly definitive endoderm. To this end, a newly adopted protocol based on previously published studies was applied and resulting cells were extensively characterized by gene expression analysis, immunofluorescence microscopy, and FACS-staining for intracellular and surface markers defining the definitive endoderm signature.

As induced pluripotent cells are currently considered to resemble human embryonic stem cells, a state-of-the-art assay for hiPSC generation is required. Such an assay requires the following prerequisites: (i) noninvasive harvest of the cell type of origin, (ii) broad applicability in terms of guided differentiation to all three germ layers, (iii) useful for large-scale hiPSC biobanking, (iv) highly efficient, and (v) fast reprogramming to the hiPSC stage. Keratinocytes from the outer root sheath of plucked human hair represent such a cell source and thus points towards the generation of patient-specific human induced pluripotent stem cells as a new paradigm for modelling human disease and for individualizing drug testing. Previously, we have further optimized this method in terms of efficiency and speed by using rat embryonic fibroblasts as a feeder layer for keratinocyte reprogramming [38]. The arising hiPSCs fulfilled all the prerequisites of pluripotency including teratoma formation and spontaneous three-germ layer differentiation.

In further studies, we have applied plucked hair-derived hiPSCs to guide differentiation towards motoneurons [25] and cardiac pacemaker cells [3], both representing highly specified cell types from either ectodermal or mesodermal origin. However, their differentiation capacity to give rise to definitive and primitive gut tube endoderm remained elusive. While forming, definitive endoderm is incorporated by morphogenetic movements into a primitive gut tube stage. This in turn is patterned into foregut, midgut, and hindgut to form the functional epithelial compartment of multiple internal organs: liver, intestines, lungs, and the pancreas [50]. Nowadays, virtually every cell population arising from the primitive gut tube has been generated using guided differentiation of pluripotent cells towards liver, intestines, lungs, and the pancreas [51–53]. Thus, the induction of DE cells marks a prerequisite for the entire process of pluripotent stem cell differentiation into, for example, pancreatic or hepatic progenitor cells [54, 55]. Several protocols have been developed and modified to increase the efficiency of DE commitment. All these protocols are strongly dependent on high doses of TGFβ signalling mediated by Activin A as the major driving force of the process. However, large-scale differentiation experiments should be cost effective, thus, making a small molecule-based assay more desirable. To this end, we combined several previously described strategies. First, we replaced Activin A by IDE1, a compound having shown to display similar but also superior characteristics compared to Nodal or Activin A [41]. Similarly, we substituted Wnt3a by the small molecule CHIR90021 that inhibits GSK 3 kinase to mimic Wnt signalling [40]. The third small molecule LY294002 inhibited the AKT signalling pathway, by repressing PI3K, to promote the exit from pluripotency [42]. In consequence, a robust and reproducible assay was developed which shows to be effective in several human plucked hair-derived iPSCs. As the formation of definitive endoderm is a prerequisite to obtain, for example, relevant numbers of pancreatic β-cells, our data in combination with the presented reprogramming strategy are highly relevant for human disease modelling approaches.

However, several studies have suggested that β-cells generated from human pluripotent stem cells lack adult, and at the most reach, fetal maturity as particularly expressed by their polyhormonality. This observation reinforces the notion that establishing culture conditions that promote appropriate maturation represents a significant obstacle for the generation of functional β-cells *in vitro* [56]. A recent landmark paper identified self-renewing definitive endodermal progenitor cells as a potential cell source to bypass this limitation. β-cells generated from these cells showed features of adult maturity as even shown by functional assays [57]. Given the fact that all published protocols so far lack this feature, the quality of the definitive endodermal intermediate seems to have an impact on the final maturity. The generation of definitive endodermal progenitor cells was characterized by high positivity for c-KIT and CXCR4 [57]. Thus, we included in our current DE analysis an FACS-based tool and indeed succeeded in obtaining a pattern likely to allow the isolation of this distinct cell type. The similar differentiation capacity of all our analysed plucked human hair-derived iPSCs is relevant to the field of disease modelling, using patient-specific material. Plucked hair keratinocytes are more or less the only cell type, which matches the above criteria. Nevertheless, a potential ectodermally biased epigenetic memory could limit their utility [58]. Our finding abolishes such a bias at least based on the number of different cell lines and the reproducible endodermal commitment pattern.

The development of *in vitro* models underlying embryonic development is a prerequisite to build new knowledge and to develop new strategies targeting various genetic diseases. The development and investigation of endoderm-derived cells are such as pancreatic cells, are of high importance for the field of developmental biology and clinical implications. Induced pluripotent stem cells (iPSCs) with their unique features of unlimited self-renewal and non-restricted differentiation capacity are a highly promising tool for regenerative medicine as well as for studies on developmental biology. iPSCs have been generated from a variety of different cells types originating from all three-germ layers [38, 58, 59]. Finally, this setup has been used to determine the expression pattern of a certain ion channel family which has been previously shown to be differentially regulated in embryonic stem cells and involved in differentiation processes, namely, small and intermediate conductance calcium-activated potassium channels [2, 3, 5, 60]. Thus, our study gives novel insights into guided pluripotent stem cell differentiation towards definitive endoderm and a potentially involved protein family.

SKCas either exhibit small (SK1, KCa2.1, Kcnn1; SK2, KCa2.2, Kcnn2; and SK3, KCa2.3, Kcnn3) or intermediate (SK4, IK, KCa3.1, and Kcnn4) unitary conductance for K^+ ions. Important roles in multiple cellular functions, for example, cell cycle regulation in cancer cells [20, 61], smooth muscle relaxation [23, 62], mesenchymal stem cell proliferation [22], and cytoskeleton reorganization in neural progenitors [21] have been reported. SKCas are widely expressed throughout all different tissues. While SK1 is exclusively expressed in the central nervous system, SK2 is more widely expressed in different organs arising from different germ layers such as brain, liver, or heart. SK3 is the most widespread expressed isoform with a predominant expression pattern in the central nervous system but also in smooth muscle rich tissue. SK4 can be detected in inflammatory cell-rich, surface-rich, and secretory tissues such as the pancreas [63]. In the pancreas, for example, SK4 regulates glucose homeostasis and enzyme secretion of acinar cells [64, 65]. Moreover, SKCas are overexpressed in a variety of cancers, including pancreatic cancer [20] and, for example, SK3 was shown to be involved in cancer cell migration [66]. Nevertheless, the role of SKCas in developmental processes remains enigmatic though it is well accepted that cell differentiation and maturation affect the expression patterns of ion channels. Our group has shed for the first time light on their role in differentiating pluripotent stem cells derived from mouse and men [2, 3, 5, 25]. A potential role of SKCas was already suggested by their differentially regulated expression pattern. In fact, it temporally coincides with the commitment of the cardiovascular progenitor showing an expression peak of the respective isoform around day 5 [5]. In consequence, we aimed to address the expression pattern of SKCas in the developing endoderm using plucked human hair-derived iPSCs as a bona fide modelling system. Interestingly, the differential regulation of most SKCa isoforms was relatively modest. Albeit SK2 and SK4 show a slight expression peak around day 2/3, the only regulated isoform seems to be SK3 showing a continuously increasing expression with ongoing DE formation. Interestingly, reports showing SK3 expression in DE-derived organs are restricted to a handful of studies showing SK3 expression in epithelial cancer cells and a liver-specific splice variant [67, 68]. Further studies including gain and loss of function approaches within the same assay have to clarify the respective functions of SKCa isoforms with DE formation and later maturation processes towards liver and pancreas.

To summarize, we present an efficient, novel, and robust DE formation assay being suitable for ectoderm-derived plucked human hair iPSCs. Given the prerequisites for reprogramming fulfilled by plucked human hair, a robust DE assay for this particular iPSCs type is highly relevant for disease modelling approaches. Subsequently, we have identified dynamic expression of the SKCa family of proteins during DE formation.

Conflict of Interests

The authors declare no conflict of interests.

Authors' Contribution

Anett Illing and Marianne Stockmann contributed equally.

Acknowledgments

The authors thank Stefanie Fischer, Ralf Köhntop, and Sabine Seltenheim for the excellent technical assistance enabling research to be conducted in our laboratories. The authors thank all members of the Kleger and Liebau lab for discussing and critically reading the paper. The research that enabled this paper was funded by a Fellowship by the Medical Faculty of Ulm University (Bausteinprogramm, L. SBR.0011) and by the Deutsche Forschungsgemeinschaft (KL 2544/1-1, SL BO1718/4-1), the German Foundation for Heart Research (F/34/11; to AK and SL), Boehringer-Ingelheim BIU (N5 to SL; C1 to AK), the virtual Helmholtz-Institute (VH-VI-510 to SL), and the Else-Kröner-Fresenius-Stiftung (2011_ A200; to AK and SL). AK is indebted to the Baden-Württemberg Stiftung for the financial support of this research project by the Eliteprogramme for Postdocs. The authors apologize to authors whose work has not been covered or directly cited due to space limitations.

References

[1] A. M. Zorn and J. M. Wells, "Vertebrate endoderm development and organ formation," *Annual Review of Cell and Developmental Biology*, vol. 25, pp. 221–251, 2009.

[2] A. Kleger and S. Liebau, "Calcium-activated potassium channels, cardiogenesis of pluripotent stem cells, and enrichment of pacemaker-like cells," *Trends in Cardiovascular Medicine*, vol. 21, no. 3, pp. 74–83, 2011.

[3] M. Muller, M. Stockmann, D. Malan et al., "Ca^{2+} activated K channels-new tools to induce cardiac commitment from pluripotent stem cells in mice and men," *Stem Cell Reviews and Reports*, vol. 8, no. 3, pp. 720–740, 2012.

[4] A. Kleger, C. Loebnitz, G. V. Pusapati et al., "Protein kinase D2 is an essential regulator of murine myoblast differentiation," *PLoS One*, vol. 6, no. 1, Article ID e14599, 2011.

[5] A. Kleger, T. Seufferlein, D. Malan et al., "Modulation of calcium-activated potassium channels induces cardiogenesis of pluripotent stem cells and enrichment of pacemaker-like cells," *Circulation*, vol. 122, no. 18, pp. 1823–1836, 2010.

[6] S. Liebau, P. U. Mahaddalkar, H. A. Kestler, A. Illing, T. Seufferlein, and A. Kleger, "A hierarchy in reprogramming capacity in different tissue microenvironments: what we know and what we need to know," *Stem Cells and Development*, vol. 22, no. 5, pp. 695–706, 2013.

[7] L. Linta, M. Stockmann, T. M. Boeckers, A. Kleger, and S. Liebau, "The potential of iPS cells in synucleinopathy research," *Stem Cells International*, vol. 2012, Article ID 629230, 6 pages, 2012.

[8] A. Kleger, P. U. Mahaddalkar, S. F. Katz et al., "Increased reprogramming capacity of mouse liver progenitor cells, compared with differentiated liver cells, requires the BAF complex," *Gastroenterology*, vol. 142, no. 4, pp. 907–917, 2012.

[9] S. Chen, M. Borowiak, J. L. Fox et al., "A small molecule that directs differentiation of human ESCs into the pancreatic lineage," *Nature Chemical Biology*, vol. 5, no. 4, pp. 258–265, 2009.

[10] K. A. D'Amour, A. G. Bang, S. Eliazer et al., "Production of pancreatic hormone-expressing endocrine cells from human embryonic stem cells," *Nature Biotechnology*, vol. 24, no. 11, pp. 1392–1401, 2006.

[11] N. Shiraki, T. Yoshida, K. Araki et al., "Guided differentiation of embryonic stem cells into Pdx1-expressing regional-specific definitive endoderm," *Stem Cells*, vol. 26, no. 4, pp. 874–885, 2008.

[12] Q. Zhou, A. C. Law, J. Rajagopal, W. J. Anderson, P. A. Gray, and D. A. Melton, "A multipotent progenitor domain guides pancreatic organogenesis," *Developmental Cell*, vol. 13, no. 1, pp. 103–114, 2007.

[13] T. Touboul, N. R. Hannan, S. Corbineau et al., "Generation of functional hepatocytes from human embryonic stem cells under chemically defined conditions that recapitulate liver development," *Hepatology*, vol. 51, no. 5, pp. 1754–1765, 2010.

[14] S. J. Arnold and E. J. Robertson, "Making a commitment: cell lineage allocation and axis patterning in the early mouse embryo," *Nature Reviews Molecular Cell Biology*, vol. 10, no. 2, pp. 91–103, 2009.

[15] K. A. Lawson, J. J. Meneses, and R. A. Pedersen, "Clonal analysis of epiblast fate during germ layer formation in the mouse embryo," *Development*, vol. 113, no. 3, pp. 891–911, 1991.

[16] A. Rodaway and R. Patient, "Mesendoderm: an ancient germ layer?" *Cell*, vol. 105, no. 2, pp. 169–172, 2001.

[17] Y. Kadokawa, Y. Kato, and G. Eguchi, "Cell lineage analysis of the primitive and visceral endoderm of mouse embryos cultured in vitro," *Cell Differentiation*, vol. 21, no. 1, pp. 69–76, 1987.

[18] M. Kanai-Azuma, Y. Kanai, J. M. Gad et al., "Depletion of definitive gut endoderm in Sox17-null mutant mice," *Development*, vol. 129, no. 10, pp. 2367–2379, 2002.

[19] A. H. Hart, L. Hartley, K. Sourris et al., "Mixl1 is required for axial mesendoderm morphogenesis and patterning in the murine embryo," *Development*, vol. 129, no. 15, pp. 3597–3608, 2002.

[20] H. Jäger, T. Dreker, A. Buck, K. Giehl, T. Gress, and S. Grissmer, "Blockage of intermediate-conductance Ca^{2+}-activated K^+ channels inhibit human pancreatic cancer cell growth in vitro," *Molecular Pharmacology*, vol. 65, no. 3, pp. 630–638, 2004.

[21] S. Liebau, B. Vaida, C. Proepper et al., "Formation of cellular projections in neural progenitor cells depends on SK3 channel activity," *Journal of Neurochemistry*, vol. 101, no. 5, pp. 1338–1350, 2007.

[22] S. P. Wang, J. A. Wang, R. H. Luo, W. Y. Cui, and H. Wang, "Potassium channel currents in rat mesenchymal stem cells and their possible roles in cell proliferation," *Clinical and Experimental Pharmacology and Physiology*, vol. 35, no. 9, pp. 1077–1084, 2008.

[23] D. L. Tharp, B. R. Wamhoff, J. R. Turk, and D. K. Bowles, "Upregulation of intermediate-conductance Ca^{2+}-activated K^+ channel (IKCa1) mediates phenotypic modulation of coronary smooth muscle," *American Journal of Physiology*, vol. 291, no. 5, pp. H2493–H2503, 2006.

[24] A. P. Wong, C. E. Bear, S. Chin et al., "Directed differentiation of human pluripotent stem cells into mature airway epithelia expressing functional CFTR protein," *Nature Biotechnology*, vol. 30, no. 9, pp. 876–882, 2012.

[25] M. Stockmann, L. Linta, K. J. Fohr et al., "Developmental and functional nature of human iPSC derived motoneurons," *Stem Cell Reviews*, 2011.

[26] B. E. Shmukler, C. T. Bond, S. Wilhelm et al., "Structure and complex transcription pattern of the mouse SK1 KCa channel gene, KCNN1," *Biochimica et Biophysica Acta*, vol. 1518, no. 1-2, pp. 36–46, 2001.

[27] T. Strassmaier, C. T. Bond, C. A. Sailer, H. G. Knaus, J. Maylie, and J. P. Adelman, "A novel isoform of SK2 assembles with other SK subunits in mouse brain," *Journal of Biological Chemistry*, vol. 280, no. 22, pp. 21231–21236, 2005.

[28] H. Tomita, V. G. Shakkottai, G. A. Gutman et al., "Novel truncated isoform of SK3 potassium channel is a potent dominant-negative regulator of SK currents: implications in schizophrenia," *Molecular Psychiatry*, vol. 8, no. 5, pp. 524–535, 2003.

[29] D. Tuteja, S. Rafizadeh, V. Timofeyev et al., "Cardiac small conductance Ca^{2+}-activated K^+ channel subunits form heteromultimers via the coiled-coil domains in the C termini of the channels," *Circulation Research*, vol. 107, no. 7, pp. 851–859, 2010.

[30] M. A. Schumacher, A. F. Rivard, H. P. Bächinger, and J. P. Adelman, "Structure of the gating domain of a Ca^{2+}-activated K^+ channel complexed with Ca^{2+}/calmodulin," *Nature*, vol. 410, no. 6832, pp. 1120–1124, 2001.

[31] X. M. Xia, B. Fakler, A. Rivard et al., "Mechanism of calcium gating in small-conductance calcium-activated potassium channels," *Nature*, vol. 395, no. 6701, pp. 503–507, 1998.

[32] P. Sah and E. M. McLachlan, "Potassium currents contributing to action potential repolarization and the afterhyperpolarization in rat vagal motoneurons," *Journal of Neurophysiology*, vol. 68, no. 5, pp. 1834–1841, 1992.

[33] M. Stocker, "Ca^{2+}-activated K^+ channels: molecular determinants and function of the SK family," *Nature Reviews Neuroscience*, vol. 5, no. 10, pp. 758–770, 2004.

[34] N. Rouchet, O. Waroux, C. Lamy et al., "SK channel blockade promotes burst firing in dorsal raphe serotonergic neurons," *European Journal of Neuroscience*, vol. 28, no. 6, pp. 1108–1115, 2008.

[35] O. Waroux, L. Massotte, L. Alleva et al., "SK channels control the firing pattern of midbrain dopaminergic neurons in vivo,"

European Journal of Neuroscience, vol. 22, no. 12, pp. 3111–3121, 2005.

[36] M. P. Davies, R. H. An, P. Doevendans, S. Kubalak, K. R. Chien, and R. S. Kass, "Developmental changes in ionic channel activity in the embryonic murine heart," *Circulation Research*, vol. 78, no. 1, pp. 15–25, 1996.

[37] L. Lu, Q. Zhang, V. Timofeyev et al., "Molecular coupling of a Ca^{2+}-activated K^+ channel to L-type Ca^{2+} channels via α-actinin2," *Circulation Research*, vol. 100, no. 1, pp. 112–120, 2007.

[38] L. Linta, M. Stockmann, K. N. Kleinhans et al., "Rat embryonic fibroblasts improve reprogramming of human keratinocytes into induced pluripotent stem cells," *Stem Cells and Development*, vol. 21, no. 6, pp. 965–976, 2012.

[39] S. Frank, M. Zhang, H. R. Scholer, and B. Greber, "Small molecule-assisted, line-independent maintenance of human pluripotent stem cells in defined conditions," *PLoS One*, vol. 7, Article ID e41958, 2012.

[40] Y. Kunisada, N. Tsubooka-Yamazoe, M. Shoji, and M. Hosoya, "Small molecules induce efficient differentiation into insulin-producing cells from human induced pluripotent stem cells," *Stem Cell Research*, vol. 8, pp. 274–284, 2012.

[41] M. Borowiak, R. Maehr, S. Chen et al., "Small molecules efficiently direct endodermal differentiation of mouse and human embryonic stem cells," *Cell Stem Cell*, vol. 4, no. 4, pp. 348–358, 2009.

[42] C. H. Cho, N. R. Hannan, F. M. Docherty et al., "Inhibition of activin/nodal signalling is necessary for pancreatic differentiation of human pluripotent stem cells," *Diabetologia*, vol. 55, no. 12, pp. 3284–3295, 2012.

[43] M. Hosoya, Y. Kunisada, A. Kurisaki, and M. Asashima, "Induction of differentiation of undifferentiated cells into pancreatic beta cells in vertebrates," *The International Journal of Developmental Biology*, vol. 56, no. 5, pp. 313–323, 2012.

[44] Y. Kunisada, N. Tsubooka-Yamazoe, M. Shoji, and M. Hosoya, "Small molecules induce efficient differentiation into insulin-producing cells from human induced pluripotent stem cells," *Stem Cell Research*, vol. 8, no. 2, pp. 274–284, 2012.

[45] Y. Kunisada, M. Shoji, and M. Hosoya, "A gene expression-based screening system for compounds influencing differentiation of mouse embryonic stem cells," *Journal of Biomolecular Screening*, vol. 17, no. 2, pp. 140–151, 2012.

[46] N. Azoitei, G. V. Pusapati, A. Kleger et al., "Protein kinase D2 is a crucial regulator of tumour cell—endothelial cell communication in gastrointestinal tumours," *Gut*, vol. 59, no. 10, pp. 1316–1330, 2010.

[47] A. Kleger, T. Busch, S. Liebau et al., "The bioactive lipid sphingosylphosphorylcholine induces differentiation of mouse embryonic stem cells and human promyelocytic leukaemia cells," *Cellular Signalling*, vol. 19, no. 2, pp. 367–377, 2007.

[48] A. Kleger, S. Liebau, Q. Lin, G. von Wichert, and T. Seufferlein, "The impact of bioactive lipids on cardiovascular development," *Stem Cells International*, vol. 2011, Article ID 916180, 13 pages, 2011.

[49] X. Cheng, L. Ying, L. Lu et al., "Self-renewing endodermal progenitor lines generated from human pluripotent stem cells," *Cell Stem Cell*, vol. 10, no. 4, pp. 371–384, 2012.

[50] A. E. Chen, M. Borowiak, R. I. Sherwood, A. Kweudjeu, and D. A. Melton, "Functional evaluation of ES cell-derived endodermal populations reveals differences between Nodal and Activin A-guided differentiation," *Development*, vol. 140, no. 3, pp. 675–686, 2013.

[51] M. D. Green, A. Chen, M. C. Nostro et al., "Generation of anterior foregut endoderm from human embryonic and induced pluripotent stem cells," *Nature Biotechnology*, vol. 29, no. 3, pp. 267–273, 2011.

[52] M. C. Nostro, F. Sarangi, S. Ogawa et al., "Stage-specific signaling through TGFβ family members and WNT regulates patterning and pancreatic specification of human pluripotent stem cells," *Development*, vol. 138, no. 5, pp. 861–871, 2011.

[53] J. R. Spence, C. N. Mayhew, S. A. Rankin et al., "Directed differentiation of human pluripotent stem cells into intestinal tissue in vitro," *Nature*, vol. 470, no. 7332, pp. 105–109, 2011.

[54] F. Li, Z. He, Y. Li et al., "Combined activin A/LiCl/Noggin treatment improves production of mouse embryonic stem cell-derived definitive endoderm cells," *Journal of Cellular Biochemistry*, vol. 112, no. 4, pp. 1022–1034, 2011.

[55] P. Wang, R. T. Rodriguez, J. Wang, A. Ghodasara, and S. K. Kim, "Targeting SOX17 in human embryonic stem cells creates unique strategies for isolating and analyzing developing endoderm," *Cell Stem Cell*, vol. 8, no. 3, pp. 335–346, 2011.

[56] S. J. Micallef, X. Li, J. V. Schiesser et al., "INS(GFP/w) human embryonic stem cells facilitate isolation of in vitro derived insulin-producing cells," *Diabetologia*, vol. 55, no. 3, pp. 694–706, 2012.

[57] X. Cheng, L. Ying, L. Lu et al., "Self-renewing endodermal progenitor lines generated from human pluripotent stem cells," *Cell Stem Cell*, vol. 10, no. 4, pp. 371–384, 2012.

[58] O. Bar-Nur, H. A. Russ, S. Efrat, and N. Benvenisty, "Epigenetic memory and preferential lineage-specific differentiation in induced pluripotent stem cells derived from human pancreatic islet beta cells," *Cell Stem Cell*, vol. 9, no. 1, pp. 17–23, 2011.

[59] M. Kajiwara, T. Aoi, K. Okita et al., "Donor-dependent variations in hepatic differentiation from human-induced pluripotent stem cells," *Proceedings of the National Academy of Sciences of the United States of America*, vol. 109, no. 31, pp. 12538–12543, 2012.

[60] S. Liebau, M. Tischendorf, D. Ansorge et al., "An inducible expression system of the calcium-activated potassium channel 4 to study the differential impact on embryonic stem cells," *Stem Cells International*, vol. 2011, Article ID 456815, 12 pages, 2011.

[61] O. Gavrilova-Ruch, K. Schönherr, G. Gessner et al., "Effects of imipramine on ion channels and proliferation of IGR1 melanoma cells," *Journal of Membrane Biology*, vol. 188, no. 2, pp. 137–149, 2002.

[62] S. Ro, W. J. Hatton, S. D. Koh, and B. Horowitz, "Molecular properties of small-conductance Ca^{2+}-activated K^+ channels expressed in murine colonic smooth muscle," *American Journal of Physiology*, vol. 281, no. 4, pp. G964–G973, 2001.

[63] M. X. Chen, S. A. Gorman, B. Benson et al., "Small and intermediate conductance Ca^{2+}-activated K^+ channels confer distinctive patterns of distribution in human tissues and differential cellular localisation in the colon and corpus cavernosum," *Naunyn-Schmiedeberg's Archives of Pharmacology*, vol. 369, no. 6, pp. 602–615, 2004.

[64] S. Ohya, T. Fujimori, T. Kimura, H. Yamamura, and Y. Imaizumi, "Novel spliced variants of large-conductance Ca^{2+}-activated K^+-channel β2-subunit in human and rodent pancreas," *Journal of Pharmacological Sciences*, vol. 114, no. 2, pp. 198–205, 2010.

[65] G. Drews, "Physiological significance of SK4 channels in pancreatic β-cell oscillations," *Islets*, vol. 1, no. 2, pp. 148–150, 2009.

[66] M. Potier, V. Joulin, S. Roger et al., "Identification of SK3 channel as a new mediator of breast cancer cell migration,"

Molecular Cancer Therapeutics, vol. 5, no. 11, pp. 2946–2953, 2006.

[67] M. L. Palmer, K. R. Schiller, and S. M. O'Grady, "Apical SK potassium channels and Ca^{2+}-dependent anion secretion in endometrial epithelial cells," *Journal of Physiology*, vol. 586, no. 3, pp. 717–726, 2008.

[68] E. T. Barfod, A. L. Moore, and S. D. Lidofsky, "Cloning and functional expression of a liver isoform of the small conductance Ca^{2+}-activated K^+ channel SK3," *American Journal of Physiology*, vol. 280, no. 4, pp. C836–C842, 2001.

Hindawi Publishing Corporation
Stem Cells International
Volume 2013, Article ID 784629, 25 pages
http://dx.doi.org/10.1155/2013/784629

Research Article

Microarray-Based Comparisons of Ion Channel Expression Patterns: Human Keratinocytes to Reprogrammed hiPSCs to Differentiated Neuronal and Cardiac Progeny

Leonhard Linta,[1] Marianne Stockmann,[1] Qiong Lin,[2] André Lechel,[3] Christian Proepper,[1] Tobias M. Boeckers,[1] Alexander Kleger,[3] and Stefan Liebau[1]

[1] *Institute for Anatomy Cell Biology, Ulm University, Albert-Einstein Allee 11, 89081 Ulm, Germany*
[2] *Institute for Biomedical Engineering, Department of Cell Biology, RWTH Aachen, Pauwelstrasse 30, 52074 Aachen, Germany*
[3] *Department of Internal Medicine I, Ulm University, Albert-Einstein Allee 11, 89081 Ulm, Germany*

Correspondence should be addressed to Alexander Kleger; alexander.kleger@uni-ulm.de and Stefan Liebau; stefan.liebau@uni-ulm.de

Received 31 January 2013; Accepted 6 March 2013

Academic Editor: Michael Levin

Ion channels are involved in a large variety of cellular processes including stem cell differentiation. Numerous families of ion channels are present in the organism which can be distinguished by means of, for example, ion selectivity, gating mechanism, composition, or cell biological function. To characterize the distinct expression of this group of ion channels we have compared the mRNA expression levels of ion channel genes between human keratinocyte-derived induced pluripotent stem cells (hiPSCs) and their somatic cell source, keratinocytes from plucked human hair. This comparison revealed that 26% of the analyzed probes showed an upregulation of ion channels in hiPSCs while just 6% were downregulated. Additionally, iPSCs express a much higher number of ion channels compared to keratinocytes. Further, to narrow down specificity of ion channel expression in iPS cells we compared their expression patterns with differentiated progeny, namely, neurons and cardiomyocytes derived from iPS cells. To conclude, hiPSCs exhibit a very considerable and diverse ion channel expression pattern. Their detailed analysis could give an insight into their contribution to many cellular processes and even disease mechanisms.

1. Introduction

Ion channels are comprised of a large variety of differing families of pore proteins. Initially, ion channels were mostly known for their role in the nervous system where they play a crucial role in the signal transmission over neurites and synapses. But in fact they are involved in numerous other cellular processes including cell size regulation, muscle contractions, immune system activation [1], or hormone release [2]. Distinct ion channels are furthermore recognized to be of high importance for excitable cells of the heart: cardiomyocytes of the working myocardium as well as cells of the cardiac conduction system. In the heart, specific ion channels are responsible, for example, for the regulated generation of action potentials and for cardiac muscle contraction strength and time [3]. Additionally, ion channels play an important role in several differentiation and maturation processes [4–6]. The presented study aims to take a closer look at ion channel expression in human-induced pluripotent stem cells (hiPSCs) to give a start point for further analyses of their distinct roles at an early developmental cell state and differentiation processes.

hiPSCs are generated from somatic cells by timed overexpression of specific transcription factors and strongly resemble pluripotent embryonic stem cells [7, 8]. Pluripotency is amongst others defined by the ability to differentiate into cells of all three germ layers and unlimited symmetrical cell division. This cell system is widely utilized for studies investigating developmental processes or disease mechanisms [9, 10]. Although it has become clear that differentiation processes influence ion channel expression [11], the distinct role of ion channels during these processes is so far only poorly

understood. Nevertheless, it became evident that certain ion channels play a pivotal role in stem cell biology, including cell fate determination, cell cycle regulation, or cytoskeletal reorganization [6, 12–15].

The possibilities of iPSCs include the generation of individual or patient-specific-pluripotent cells, which can be subsequently differentiated into the affected cell types. This is already utilized to study pathomechanisms in a variety of tissues and cell types [9, 16–18]. The so-called channelopathies which are based on mutations in ion channels are the cause of developmental disorders and are the subject of various studies [19, 20]. To elucidate the role of ion channels in cell differentiation, maturation or their role in pathomechanisms a well-founded knowledge of ion channel distribution in pluripotent cells, representing one of the earliest stages of development, is indispensable. In that respect, we compared the expression levels of several ion channels in human keratinocytes with their reprogrammed progeny, hiPSCs. Keratinocytes derived from plucked human hair [21, 22] represent one of the most promising cell sources for the generation of the investigated hiPSCs [23]. We have elucidated ion channel regulation for various channel families and their subtypes. Additionally, we compared the expression levels of ion channel families and subtypes, found to be regulated during reprogramming, with iPSC-differentiated progeny, namely, neurons and cardiomyocytes. These comparisons could be a start point to evaluate the contribution and function of different ion channels, for example, for self-renewal and differentiation processes in stem cells.

2. Material and Methods

2.1. Ethical Statement and Donor Information. After informed consent was given by the donors (ethical agreement by the University of Ulm, number 88/12) hair with intact hair roots was gathered by plucking from the scalp after desinfection. We used hair from healthy volunteers (age between 24 to 45 and both male and female gender).

2.2. hiPSC Generation and Cell Culture. Keratinocytes were obtained from plucked human scalp hair as already described [22]. Keratinocytes were propagated in EpiLife medium with HKGS supplement (both Invitrogen, Carlsbad, CA, USA). hiPSCs were generated from keratinocytes by lentiviral transduction of four reprogramming factors (Oct4, Sox2, Klf4, and cMyc) as described earlier [23]. After the reprogramming on rat embryonic fibroblasts they were maintained feeder-free on Matrigel (BD Biosciences, Franklin Lakes, NJ, USA) coated dishes in mTeSR1 medium (Stemcell Technologies, Vancouver, CA, USA).

2.3. Gene Expression Microarrays. Gene expression microarrays were performed for 6 keratinocyte samples and 9 hiPSC samples with the Agilent Whole Human Genome Microarray Kit (4x44k microarray kit G4112F, Agilent Technologies, Santa Clara, CA, USA). 500 ng of total RNA was used to produce Cy3-CTP-labeled cRNA with the Agilent Low RNA Input Liner Amplification Kit. The cRNA was purified and 1,65 μg per array was hybridized for 17 h at 65°C and 10 r.p.m. Afterwards, the arrays were washed with Agilent Gene Expression Wash Buffers one and two and finally with acetonitrile for 1 min. The slides were scanned using Scan Control 7.0 software with a resolution of 5 μm. Scan data was extracted with the Feature Extraction 9.1 software. Expression levels were background adjusted and quantile normalized with the GeneSpring GX 12 software. Differential expression between keratinocytes and hiPSCs was analyzed using student's t-test. A fold change > 2 and a P value < 0.05 was considered significant and highlighted bold (upregulation) or italic (downregulation) in the results table. For comparisons of iPSCs with iPSC-derived neurons published data from GSE34879 (GSM856936, GSM856937, GSM856915, GSM856916) and for cardiomyocytes GSE17579 (GSM438022, GSM438026, GSM438034, GSM438021, GSM438032, GSM438036) were used (both from NCBI Gene Expression Omnibus, http://www.ncbi.nlm.nih.gov/geo/). Fold change is shown if >2.

3. Results

3.1. Differential Expression of Ion Channels in hiPSCs Compared to Keratinocytes. We first compared the expression of various ion channel families from keratinocytes to hiPSCs and from hiPSCs to cardiomyocytes and neurons, respectively. From the 387 probes (Table 1) binding in ion channel genes from parental keratinocytes to hiPSCs, 101 (26%) showed a significant increase in expression (fold change > 2, $P < 0.05$; labeled in bold) while 23 (6%) showed a significant decrease (fold change > −2, $P < 0.05$; labeled in italic). In a second step differentially regulated ion channels from hiPSCs to hiPSC-derived neurons were investigated and we found 29 ion channel transcripts to be upregulated (fold change > 2; labeled in bold) while 6 showed a significant decrease (fold change > −2; labeled in italic). For cardiomyocytes, mRNA levels of only 7 ion channel members were upregulated (fold change > 2; labeled in bold) and 10 mRNA levels showed a significant decrease (fold change > −2; labeled in italic).

3.2. Voltage-Gated Calcium Channels. Voltage-gated calcium channels are crucially involved in the Ca^{2+}-influx thereby playing an important role in calcium signaling of virtually all cells. High-voltage-gated calcium channels include the neural N-type channel, the poorly defined brain-specific R-type channel, the closely related P/Q-type channel, and the dihydropyridine-sensitive L-type channels responsible for excitation-contraction coupling of skeletal, smooth, and cardiac muscles as well as for hormone secretion in endocrine cells (reviewed in [24]). While mainly permeable for calcium ions they also show a low permeability for sodium ions. Upon depolarization of the cell they mediate a calcium influx into the cell. The channels consist of the main alpha subunit as well as regulatory beta, alpha 2/delta, and gamma subunits. The α_1 subunit forms the ion conducting pore while the associated subunits have several functions including modulation of gating [25]. *CACNA1A* mutations are for example involved in ataxia [26]. We have analyzed their expression with 42 probes.

Table 1: The expression levels for ion channel genes were compared in hiPSCs (9 samples) and keratinocytes (6 samples) via microarray. Gene names, accession numbers, and gene symbols are shown together with the corresponding fold change and P values. Significant changes (defined as fold change > 2, $P < 0.05$) are labeled in bold for upregulation or italic for downregulation. Accession numbers refer to the NCBI or Ensembl (numbers starting with ENST) databases. Analyses of hiPSC-derived neurons or hiPSC-derived cardiomyocytes were performed using published data sets from GSE34879 (neurons) and GSE17579 (cardiomyocytes). These data sets already contain both iPSCs and differentiated progeny. Fold changes > 2 (marked bold) and < −2 (marked italic) are shown in the respective columns.

(a) Voltage-gated calcium channels

Gene name	Accession number	Gene symbol	P	Fold change Ker → hiPSC	Fold change hiPSC → Neuron	Fold change hiPSC → CM
Calcium channel, voltage-dependent, P/Q type, alpha 1A subunit, transcript variant 1	NM_000068	CACNA1A	2.26E − 01	−1.32		
Calcium channel, voltage-dependent, N type, alpha 1B subunit	NM_000718	CACNA1B	7.27E − 01	−1.10		
Calcium channel, voltage-dependent, N type, alpha 1B subunit [Source: HGNC Symbol; Acc: 1389]	ENST00000277550	CACNA1B	7.15E − 01	−1.14		
Calcium channel, voltage-dependent, N type, alpha 1B subunit	NM_000718	CACNA1B	**6.32E − 09**	**6.82**		
Calcium channel, voltage-dependent, N type, alpha 1B subunit [Source: HGNC Symbol; Acc: 1389]	ENST00000277551	CACNA1B	3.32E − 02	−1.57		
Calcium channel, voltage-dependent, L type, alpha 1C subunit, transcript variant 18	NM_000719	CACNA1C	6.77E − 02	−1.37		
Calcium channel, voltage-dependent, L type, alpha 1C subunit, transcript variant 18	NM_000719	CACNA1C	**5.72E − 03**	**2.37**		**2.94**
Calcium channel, voltage-dependent, L type, alpha 1D subunit, transcript variant 1	NM_000720	CACNA1D	3.83E − 01	1.58		
Calcium channel, voltage-dependent, R type, alpha 1E subunit, transcript variant 3	NM_000721	CACNA1E	*3.10 E−02*	*−4.48*	**2.08**	
Calcium channel, voltage-dependent, R type, alpha 1E subunit [Source: HGNC Symbol; Acc: 1392]	ENST00000524607	CACNA1E	8.83E − 01	1.05		
Calcium channel, voltage-dependent, L type, alpha 1F subunit	NM_005183	CACNA1F	8.92E − 01	1.02		
Calcium channel, voltage-dependent, T type, alpha 1G subunit, transcript variant 15	NM_198397	CACNA1G	6.42E − 01	−1.12	**4.60**	
Calcium channel, voltage-dependent, T type, alpha 1G subunit, transcript variant 1	NM_018896	CACNA1G	**5.37E − 07**	**6.96**		
Calcium channel, voltage-dependent, T type, alpha 1H subunit, transcript variant 1	NM_021098	CACNA1H	**7.38E − 10**	**6.78**		
Calcium channel, voltage-dependent, T type, alpha 1I subunit, transcript variant 1	NM_021096	CACNA1I	**2.22E − 11**	**37.25**		
Calcium channel, voltage-dependent, T type, alpha 1I subunit, transcript variant 1	NM_021096	CACNA1I	7.56E − 02	−1.56		
Calcium channel, voltage-dependent, L type, alpha 1S subunit	NM_000069	CACNA1S	5.22E − 02	−1.97		
Calcium channel, voltage-dependent, alpha 2/delta subunit 1	NM_000722	CACNA2D1	**1.38E − 09**	**9.65**		
Calcium channel, voltage-dependent, alpha 2/delta subunit 2, transcript variant 1	NM_001005505	CACNA2D2	**3.30E − 10**	**62.50**	**2.02**	
Calcium channel, voltage-dependent, alpha 2/delta subunit 3	NM_018398	CACNA2D3	**5.14E − 05**	**5.42**	**2.55**	

(a) Continued.

Gene name	Accession number	Gene symbol	P	Fold change Ker → hiPSC	Fold change hiPSC → Neuron	Fold change hiPSC → CM
Calcium channel, voltage-dependent, alpha 2/delta subunit 3	AF516696	CACNA2D3	**4.68E − 11**	**33.67**		
Calcium channel, voltage-dependent, alpha 2/delta subunit 4	NM_172364	CACNA2D4	2.95E − 01	−1.41		
Calcium channel, voltage-dependent, beta 1 subunit, transcript variant 3	NM_199248	CACNB1	4.31E − 01	−1.14		
Calcium channel, voltage-dependent, beta 1 subunit, transcript variant 1	NM_000723	CACNB1	8.02E − 01	−1.02		
Calcium channel, voltage-dependent, beta 1 subunit, transcript variant 1	NM_000723	CACNB1	6.22E − 01	1.04		
cDNA FLJ45229 fis, clone BRCAN2020972,	AK128769	CACNB2	9.78E − 01	1.02		
Calcium channel, voltage-dependent, beta 2 subunit, transcript variant 1	NM_000724	CACNB2	**4.71E − 02**	**3.45**		
Calcium channel, voltage-dependent, beta 3 subunit, transcript variant 1	NM_000725	CACNB3	3.55E − 02	−1.93	**9.56**	
Calcium channel, voltage-dependent, beta 3 subunit, transcript variant 1	NM_000725	CACNB3	6.61E − 01	1.09		
Calcium channel, voltage-dependent, beta 4 subunit, transcript variant 1	NM_001005747	CACNB4	**1.33E − 03**	**4.43**		
Calcium channel, voltage-dependent, gamma subunit 1	NM_000727	CACNG1	9.46E − 01	1.02		
Calcium channel, voltage-dependent, gamma subunit 2	NM_006078	CACNG2	4.19E − 01	−1.29		
Calcium channel, voltage-dependent, gamma subunit 2	NM_006078	CACNG2	7.91E − 01	1.09		
Calcium channel, voltage-dependent, gamma subunit 3	NM_006539	CACNG3	2.21E − 01	−1.95		
Calcium channel, voltage-dependent, gamma subunit 4	NM_014405	CACNG4	4.93E − 01	1.14		
Calcium channel, voltage-dependent, gamma subunit 5	NM_145811	CACNG5	7.49E − 01	−1.13		
Calcium channel, voltage-dependent, gamma subunit 5 [Source: HGNC Symbol; Acc: 1409]	ENST00000169565	CACNG5	2.19E − 01	−1.56		
Calcium channel, voltage-dependent, gamma subunit 6, transcript variant 1	NM_145814	CACNG6	**5.56E − 11**	**46.40**		
Calcium channel, voltage-dependent, gamma subunit 7	NM_031896	CACNG7	**3.54E − 13**	**1439.36**	**3.37**	
Calcium channel, voltage-dependent, gamma subunit 7	NM_031896	CACNG7	1.82E − 01	1.26		
Calcium channel, voltage-dependent, gamma subunit 8	NM_031895	CACNG8	2.01E − 01	1.43		
Calcium channel, voltage-dependent, gamma subunit 8	NM_031895	CACNG8	**1.18E − 09**	**9.70**		

(b) Sperm-associated cation channels

Gene name	Accession number	Gene symbol	P	Fold change Ker → hiPSC	Fold change hiPSC → Neuron	Fold change hiPSC → CM
Cation channel, sperm associated 1	NM_053054	CATSPER1	3.26E − 01	1.51		
Cation channel, sperm associated 2, transcript variant 2	NM_172095	CATSPER2	*1.32 E−04*	*−2.78*		

(b) Continued.

Gene name	Accession number	Gene symbol	P	Fold change Ker → hiPSC	Fold change hiPSC → Neuron	Fold change hiPSC → CM
Cation channel, sperm associated 2, transcript variant 4	NM_172097	CATSPER2	$3.12E-02$	−1.78		
Cation channel, sperm associated 3	NM_178019	CATSPER3	$1.50E-03$	1.93		
Cation channel, sperm associated 4	NM_198137	CATSPER4	$2.51E-01$	1.48		
Cation channel, sperm-associated, beta	NM_024764	CATSPERB	$4.38E-01$	−1.25		
Cation channel, sperm-associated, gamma	NM_021185	CATSPERG	$3.56E-01$	1.34		

(c) Nicotinic acetylcholine receptors

Gene name	Accession number	Gene symbol	P	Fold change Ker → hiPSC	Fold change hiPSC → Neuron	Fold change hiPSC → CM
Cholinergic receptor, nicotinic, alpha 1 (muscle), transcript variant 1	NM_001039523	CHRNA1	$8.06E-01$	−1.10		
Cholinergic receptor, nicotinic, alpha 1 (muscle), (cDNA clone IMAGE: 4124038), with apparent retained intron	BC006314	CHRNA1	$4.64E-01$	1.47		
Cholinergic receptor, nicotinic, alpha 2 (neuronal)	NM_000742	CHRNA2	$6.05E-01$	−1.30		
Cholinergic receptor, nicotinic, alpha 3, transcript variant 1	NM_000743	CHRNA3	**1.84E − 10**	**34.22**		
Cholinergic receptor, nicotinic, alpha 4	NM_000744	CHRNA4	$6.79E-01$	1.15		
Cholinergic receptor, nicotinic, alpha 4 (neuronal), exon 1	X89741	CHRNA4	*2.79 E−02*	*−2.53*		
Cholinergic receptor, nicotinic, alpha 5	NM_000745	CHRNA5	**4.03E − 05**	**3.41**		
Cholinergic receptor, nicotinic, alpha 6, transcript variant 1	NM_004198	CHRNA6	$2.23E-01$	−1.27	**2.21**	
Cholinergic receptor, nicotinic, alpha 7, transcript variant 1	NM_000746	CHRNA7	$4.61E-04$	1.86		
Cholinergic receptor, nicotinic, alpha 7, transcript variant 2	NM_001190455	CHRNA7	$1.56E-11$	13.24		
Cholinergic receptor, nicotinic, alpha 9	NM_017581	CHRNA9	**6.30E − 06**	**6.15**		
Cholinergic receptor, nicotinic, alpha 10	NM_020402	CHRNA10	$1.57E-02$	1.57		
Cholinergic receptor, nicotinic, beta 1 (muscle)	NM_000747	CHRNB1	*8.07 E−04*	*−2.47*		
Cholinergic receptor, nicotinic, beta 1 (muscle)	NM_000747	CHRNB1	$8.87E-03$	−1.92		
Cholinergic receptor, nicotinic, beta 2 (neuronal)	NM_000748	CHRNB2	*6.03 E−04*	*−3.01*		
Cholinergic receptor, nicotinic, beta 2 (neuronal) [Source: HGNC Symbol; Acc: 1962]	ENST00000368476	CHRNB2	**2.98E − 09**	**32.05**		
Cholinergic receptor, nicotinic, beta 3	NM_000749	CHRNB3	$5.91E-01$	1.12		
Cholinergic receptor, nicotinic, beta 4	NM_000750	CHRNB4	**1.76E − 02**	**4.20**		
Cholinergic receptor, nicotinic, delta	NM_000751	CHRND	$9.84E-01$	1.01		
Cholinergic receptor, nicotinic, epsilon	NM_000080	CHRNE	$3.66E-01$	−1.20		
Cholinergic receptor, nicotinic, gamma	NM_005199	CHRNG	$6.70E-01$	1.14		

(d) Cyclic nucleotide-gated channels

Gene name	Accession number	Gene symbol	P	Fold change Ker → hiPSC	Fold change hiPSC → Neuron	Fold change hiPSC → CM
Cyclic nucleotide-gated channel alpha 1, transcript variant 2	NM_000087	CNGA1	$7.14E-01$	1.15		

(d) Continued.

Gene name	Accession number	Gene symbol	P	Fold change Ker → hiPSC	Fold change hiPSC → Neuron	Fold change hiPSC → CM
Cyclic nucleotide-gated channel alpha 1, transcript variant 2	NM_000087	CNGA1	**1.18E − 02**	**2.00**		
Cyclic nucleotide-gated channel alpha 3, transcript variant 1	NM_001298	CNGA3	2.00E − 01	1.21		
Cyclic nucleotide-gated channel alpha 4	NM_001037329	CNGA4	2.78E − 01	1.82		
Cyclic nucleotide-gated channel beta 1, transcript variant 1	NM_001297	CNGB1	*9.22 E−03*	*−2.05*		
Cyclic nucleotide-gated channel beta 1, transcript variant 1	NM_001297	CNGB1	6.36E − 01	−1.13		
Cyclic nucleotide-gated channel beta 3	NM_019098	CNGB3	2.93E − 01	1.78		

(e) GABA receptors

Gene name	Accession number	Gene symbol	P	Fold change Ker → hiPSC	Fold change hiPSC → Neuron	Fold change hiPSC → CM
Gamma-aminobutyric acid (GABA) A receptor, alpha 1, transcript variant 1	NM_000806	GABRA1	1.26E − 01	1.41		
Gamma-aminobutyric acid (GABA) A receptor, alpha 1, transcript variant 1	NM_000806	GABRA1	8.87E − 01	1.05		
Gamma-aminobutyric acid (GABA) A receptor, alpha 2, transcript variant 1	NM_000807	GABRA2	9.70E − 02	1.70		
Gamma-aminobutyric acid (GABA) A receptor, alpha 2, transcript variant 1	NM_000807	GABRA2	4.49E − 01	1.48		
Gamma-aminobutyric acid (GABA) A receptor, alpha 3	NM_000808	GABRA3	2.10E − 01	1.43		
Gamma-aminobutyric acid (GABA) A receptor, alpha 4, transcript variant 1	NM_000809	GABRA4	3.76E − 01	1.43		
Gamma-aminobutyric acid (GABA) A receptor, alpha 4, transcript variant 1	NM_000809	GABRA4	8.30E − 01	1.05		
Gamma-aminobutyric acid (GABA) A receptor, alpha 5, transcript variant 1	NM_000810	GABRA5	**1.09E − 08**	**14.41**		
Gamma-aminobutyric acid (GABA) A receptor, alpha 6	NM_000811	GABRA6	1.69E − 01	1.23		
Gamma-aminobutyric acid (GABA) A receptor, beta 1	NM_000812	GABRB1	1.14E − 01	1.43		
Gamma-aminobutyric acid (GABA) A receptor, beta 2, transcript variant 2	NM_000813	GABRB2	1.27E − 02	1.94		
Gamma-aminobutyric acid (GABA) A receptor, beta 3, transcript variant 1	NM_000814	GABRB3	**6.70E − 10**	**85.93**		*−4.49*
Gamma-aminobutyric acid (GABA) A receptor, beta 3, transcript variant 1	NM_000814	GABRB3	**1.15E − 09**	**115.69**		
Gamma-aminobutyric acid (GABA) A receptor, delta	NM_000815	GABRD	6.26E − 02	3.02		
Gamma-aminobutyric acid (GABA) A receptor, epsilon	NM_004961	GABRE	*5.83 E−05*	*−5.47*		
Gamma-aminobutyric acid (GABA) A receptor, Gamma 1	NM_173536	GABRG1	1.78E − 01	1.24		
Gamma-aminobutyric acid (GABA) A receptor, Gamma 1	NM_173536	GABRG1	**1.70E − 02**	**2.19**		
Gamma-aminobutyric acid (GABA) A receptor, Gamma 2, transcript variant 1	NM_198904	GABRG2	6.02E − 01	1.14		

(e) Continued.

Gene name	Accession number	Gene symbol	P	Fold change Ker → hiPSC	Fold change hiPSC → Neuron	Fold change hiPSC → CM
Gamma-aminobutyric acid (GABA) A receptor, Gamma 2, transcript variant 2	NM_000816	GABRG2	$5.28E-02$	1.72		
Gamma-aminobutyric acid (GABA) A receptor, Gamma 2, transcript variant 2	NM_000816	GABRG2	**9.47E − 09**	**8.41**		
Gamma-aminobutyric acid (GABA) A receptor, Gamma 3	NM_033223	GABRG3	$1.99E-01$	2.00		
Gamma-aminobutyric acid (GABA) A receptor, Gamma 3	NM_033223	GABRG3	$1.04E-01$	1.61		
Gamma-aminobutyric acid (GABA) A receptor, pi	NM_014211	GABRP	$6.62E-01$	−1.12		**17.25**
Gamma-aminobutyric acid (GABA) receptor, theta	NM_018558	GABRQ	$1.60E-01$	1.56		
Gamma-aminobutyric acid (GABA) receptor, theta	NM_018558	GABRQ	$4.76E-01$	−1.27		
Gamma-aminobutyric acid (GABA) receptor, theta [Source: HGNC Symbol; Acc: 14454]	ENST00000370306	GABRQ	**8.22E − 09**	**52.17**		
Gamma-aminobutyric acid (GABA) receptor, rho 1	NM_002042	GABRR1	$8.94E-01$	−1.04		
Gamma-aminobutyric acid (GABA) receptor, rho 2	NM_002043	GABRR2	$2.83E-01$	1.54		
Gamma-aminobutyric acid (GABA) receptor, rho 3	NM_001105580	GABRR3	$3.05E-01$	−1.34		

(f) Glycine receptors

Gene name	Accession number	Gene symbol	P	Fold change Ker → hiPSC	Fold change hiPSC → Neuron	Fold change hiPSC → CM
Glycine receptor, alpha 1, transcript variant 2	NM_000171	GLRA1	$5.47E-01$	−1.29		
Glycine receptor, alpha 2, transcript variant 1	NM_002063	GLRA2	$1.17E-01$	1.42	**11.41**	
Glycine receptor, alpha 3, transcript variant 1	NM_006529	GLRA3	$5.16E-01$	−1.26		
Glycine receptor, alpha 3 [Source: HGNC Symbol; Acc: 4328]	ENST00000274093	GLRA3	$8.33E-02$	1.64		
Glycine receptor, alpha 3, transcript variant 1	NM_006529	GLRA3	$1.46E-01$	1.41		
Glycine receptor, alpha 4, transcript variant 1	NM_001024452	GLRA4	$7.75E-01$	1.17		
Glycine receptor, beta, transcript variant 1	NM_000824	GLRB	$6.38E-02$	−1.69	**6.61**	

(g) Ionotropic glutamate receptors

Gene name	Accession number	Gene symbol	P	Fold change Ker → hiPSC	Fold change hiPSC → Neuron	Fold change hiPSC → CM
Glutamate receptor, ionotropic, AMPA 1, transcript variant 1	NM_000827	GRIA1	$7.65E-01$	−1.20	**2.06**	
Glutamate receptor, ionotropic, AMPA 2, transcript variant 1	NM_000826	GRIA2	$2.87E-01$	−1.87	**21.26**	
Glutamate receptor, ionotropic, AMPA 2, transcript variant 1	NM_000826	GRIA2	$2.72E-01$	1.33		
Glutamate receptor, ionotropic, AMPA 2, transcript variant 1	NM_000826	GRIA2	$6.54E-01$	1.22		

(g) Continued.

Gene name	Accession number	Gene symbol	P	Fold change Ker → hiPSC	Fold change hiPSC → Neuron	Fold change hiPSC → CM
Glutamate receptor, ionotropic, AMPA 3, transcript variant 2	NM_000828	GRIA3	$5.05E-01$	1.26		
Glutamate receptor, ionotropic, AMPA 3 [Source: HGNC Symbol; Acc: 4573]	ENST00000371264	GRIA3	$1.14E-01$	1.50		
Glutamate receptor, ionotropic, AMPA 3, transcript variant 2	NM_000828	GRIA3	$9.05E-01$	−1.05		
Glutamate receptor, ionotropic, AMPA 4, transcript variant 1	NM_000829	GRIA4	$2.30E-02$	1.80	**3.73**	
Glutamate receptor, ionotropic, delta 1	NM_017551	GRID1	$1.82E-01$	1.50		
Glutamate receptor, ionotropic, delta 1	NM_017551	GRID1	**5.08E − 05**	**3.63**		
Glutamate receptor, ionotropic, delta 2	NM_001510	GRID2	$7.64E-01$	−1.11		
Glutamate receptor, ionotropic, delta 2	NM_001510	GRID2	**5.55E − 09**	**55.66**		
Glutamate receptor, ionotropic, kainate 1, transcript variant 1	NM_000830	GRIK1	$1.64E-01$	1.29	**2.58**	
Glutamate receptor, ionotropic, kainate 2, transcript variant 3	NM_001166247	GRIK2	$1.42E-01$	1.56	**2.53**	
Glutamate receptor, ionotropic, kainate 2, transcript variant 1	NM_021956	GRIK2	$1.14E-01$	−2.01		
Glutamate receptor, ionotropic, kainate 2, transcript variant 2	NM_175768	GRIK2	$7.80E-01$	1.08		
Glutamate receptor, ionotropic, kainate 3	NM_000831	GRIK3	$1.58E-01$	1.64		
Glutamate receptor, ionotropic, kainate 3	NM_000831	GRIK3	**6.15E − 10**	**22.64**		
Glutamate receptor, ionotropic, kainate 4 [Source: HGNC Symbol; Acc: 4582]	ENST00000527524	GRIK4	**1.77E − 11**	**18.10**		
Glutamate receptor, ionotropic, kainate 4	NM_014619	GRIK4	$5.73E-02$	2.54		
Glutamate receptor, ionotropic, kainate 5	NM_002088	GRIK5	$2.65E-03$	1.79		*−2.41*
Glutamate receptor, ionotropic, N-methyl D-aspartate 1, transcript variant NR1-3	NM_007327	GRIN1	*1.93 E−02*	*−3.02*	**2.69**	
Glutamate receptor, ionotropic, N-methyl D-aspartate 1, transcript variant NR1-3	NM_007327	GRIN1	$6.01E-02$	−2.45		
Glutamate receptor, ionotropic, N-methyl D-aspartate 1, transcript variant NR1-3	NM_007327	GRIN1	$3.86E-01$	−1.65		
Glutamate receptor, ionotropic, N-methyl D-aspartate 2A, transcript variant 2	NM_000833	GRIN2A	$6.54E-01$	1.18		
Glutamate receptor, ionotropic, N-methyl D-aspartate 2A, transcript variant 2	NM_000833	GRIN2A	$9.21E-01$	−1.02		
Glutamate receptor, ionotropic, N-methyl D-aspartate 2A, transcript variant 1	NM_001134407	GRIN2A	**3.32E − 10**	**29.85**		
Glutamate receptor, ionotropic, N-methyl D-aspartate 2A, transcript variant 2	NM_000833	GRIN2A	$2.63E-01$	1.55		
Glutamate receptor, ionotropic, N-methyl D-aspartate 2B	NM_000834	GRIN2B	$6.64E-01$	−1.26		
Glutamate receptor, ionotropic, N-methyl D-aspartate 2C	NM_000835	GRIN2C	$8.01E-01$	−1.08		
Glutamate receptor, ionotropic, N-methyl D-aspartate 2C	NM_000835	GRIN2C	$5.01E-01$	1.13		
Glutamate receptor, ionotropic, N-methyl D-aspartate 2D	NM_000836	GRIN2D	$4.69E-02$	−1.82		
Glutamate receptor, ionotropic, N-methyl-D-aspartate 3A	NM_133445	GRIN3A	$3.28E-01$	−1.41		

(g) Continued.

Gene name	Accession number	Gene symbol	P	Fold change Ker → hiPSC	Fold change hiPSC → Neuron	Fold change hiPSC → CM
Glutamate receptor, ionotropic, N-methyl-D-aspartate 3B	NM_138690	GRIN3B	$9.36E-01$	−1.02		
Glutamate receptor, ionotropic, N-methyl D-aspartate-associated protein 1 (glutamate binding), transcript variant 1	NM_000837	GRINA	*3.68 E−04*	*−2.05*	**2.05**	
NMDA receptor glutamate-binding chain (hnrgw), partial	U44954	GRINA	$3.06E-04$	−1.81		

(h) Hyperpolarization-activated cyclic nucleotide-gated channels

Gene name	Accession number	Gene symbol	P	Fold change Ker → hiPSC	Fold change hiPSC → Neuron	Fold change hiPSC → CM
Hyperpolarization-activated cyclic nucleotide-gated potassium channel 1	NM_021072	HCN1	**3.47E − 11**	**52.85**		
Hyperpolarization-activated cyclic nucleotide-gated potassium channel 1	NM_021072	HCN1	**1.01E − 08**	**9.91**		
Hyperpolarization-activated cyclic nucleotide-gated potassium channel 2	NM_001194	HCN2	$5.36E-02$	−1.63		
Hyperpolarization-activated cyclic nucleotide-gated potassium channel 3	NM_020897	HCN3	**1.98E − 02**	**2.12**	**6.56**	
Hyperpolarization-activated cyclic nucleotide-gated potassium channel 4	NM_005477	HCN4	$1.01E-01$	−1.66		

(i) Serotonin receptors

Gene name	Accession number	Gene symbol	P	Fold change Ker → hiPSC	Fold change hiPSC → Neuron	Fold change hiPSC → CM
5-hydroxytryptamine (serotonin) receptor 3A, transcript variant 1	NM_213621	HTR3A	**1.99E − 03**	**2.77**	*−2.20*	
5-hydroxytryptamine (serotonin) receptor 3A, transcript variant 1	NM_213621	HTR3A	**2.63E − 11**	**11.11**		
5-hydroxytryptamine (serotonin) receptor 3B	NM_006028	HTR3B	$1.99E-01$	−1.54		
5-hydroxytryptamine (serotonin) receptor 3, family member C	NM_130770	HTR3C	$4.81E-01$	1.34		
5-hydroxytryptamine (serotonin) receptor 3 family member D, transcript variant 2	NM_182537	HTR3D	$4.75E-01$	−1.37		
5-hydroxytryptamine (serotonin) receptor 3, family member E	NM_182589	HTR3E	$1.52E-01$	−1.44		

(j) Voltage-gated potassium channels

Gene name	Accession number	Gene symbol	P	Fold change Ker → hiPSC	Fold change hiPSC → Neuron	Fold change hiPSC → CM
Potassium voltage-gated channel, shaker-related subfamily, member 1 (episodic ataxia with myokymia)	NM_000217	KCNA1	$1.64E-01$	2.00		
Potassium voltage-gated channel, shaker-related subfamily, member 1 (episodic ataxia with myokymia)	NM_000217	KCNA1	$1.31E-01$	1.87		
Potassium voltage-gated channel, shaker-related subfamily, member 2, transcript variant 2	NM_001204269	KCNA2	$8.55E-02$	1.33		

(j) Continued.

Gene name	Accession number	Gene symbol	P	Fold change Ker → hiPSC	Fold change hiPSC → Neuron	Fold change hiPSC → CM
Potassium voltage-gated channel, shaker-related subfamily, member 2, transcript variant 1	NM_004974	KCNA2	$8.33E-01$	1.06		
Potassium voltage-gated channel, shaker-related subfamily, member 3	NM_002232	KCNA3	$2.43E-01$	1.76		
Potassium voltage-gated channel, shaker-related subfamily, member 4	NM_002233	KCNA4	$5.75E-01$	1.11		
Potassium voltage-gated channel, shaker-related subfamily, member 5	NM_002234	KCNA5	**1.76E − 04**	**4.11**		**5.63**
Potassium voltage-gated channel, shaker-related subfamily, member 6	NM_002235	KCNA6	$7.20E-02$	2.28		
Potassium voltage-gated channel, shaker-related subfamily, member 7	NM_031886	KCNA7	**8.53E − 03**	**3.67**		
Potassium voltage-gated channel, shaker-related subfamily, member 7	NM_031886	KCNA7	$1.04E-01$	2.39		
Potassium voltage-gated channel, shaker-related subfamily, member 10	NM_005549	KCNA10	$3.32E-01$	−1.62		
Potassium voltage-gated channel, shaker-related subfamily, beta member 1, transcript variant 2	NM_003471	KCNAB1	$2.70E-01$	1.46		
Potassium voltage-gated channel, shaker-related subfamily, beta member 1, transcript variant 2	NM_003471	KCNAB1	**3.60E − 02**	**2.42**		
Potassium voltage-gated channel, shaker-related subfamily, beta member 1, transcript variant 2	NM_003471	KCNAB1	$7.87E-02$	3.06		
Potassium voltage-gated channel, shaker-related subfamily, beta member 2, transcript variant 1	NM_003636	KCNAB2	$5.35E-01$	−1.35		
Potassium voltage-gated channel, shaker-related subfamily, beta member 2, transcript variant 1	NM_003636	KCNAB2	$2.20E-01$	1.26		
Potassium voltage-gated channel, shaker-related subfamily, beta member 3 [Source: HGNC Symbol; Acc: 6230]	ENST00000303790	KCNAB3	$8.14E-02$	1.62		
Potassium voltage-gated channel, shaker-related subfamily, beta member 3	NM_004732	KCNAB3	$3.66E-01$	1.35		
Potassium voltage-gated channel, Shab-related subfamily, member 1	NM_004975	KCNB1	**7.42E − 08**	**16.32**	**2.59**	
Potassium voltage-gated channel, Shab-related subfamily, member 2	NM_004770	KCNB2	**1.54E − 05**	**4.58**		
Potassium voltage-gated channel, Shaw-related subfamily, member 1, transcript variant A	NM_001112741	KCNC1	$1.47E-01$	1.75		
Potassium voltage-gated channel, Shaw-related subfamily, member 1, transcript variant B	NM_004976	KCNC1	**4.86E − 08**	**13.97**		
Potassium voltage-gated channel, Shaw-related subfamily, member 1, transcript variant A	NM_001112741	KCNC1	$2.17E-01$	1.56		
Potassium voltage-gated channel, Shaw-related subfamily, member 2, transcript variant 1	NM_139136	KCNC2	$8.53E-01$	1.06		
Potassium voltage-gated channel, Shaw-related subfamily, member 2, transcript variant 2	NM_139137	KCNC2	$4.04E-01$	1.34		
Potassium voltage-gated channel, Shaw-related subfamily, member 3	NM_004977	KCNC3	$3.56E-01$	1.20		
Potassium voltage-gated channel, Shaw-related subfamily, member 4, transcript variant 3	NM_001039574	KCNC4	$7.70E-02$	−1.40		
Potassium voltage-gated channel, Shal-related subfamily, member 1	NM_004979	KCND1	**1.48E − 04**	**7.11**		
Potassium voltage-gated channel, Shal-related subfamily, member 2	NM_012281	KCND2	**1.62E − 12**	**91.08**	**2.76**	*−2.57*

(j) Continued.

Gene name	Accession number	Gene symbol	P	Fold change Ker → hiPSC	Fold change hiPSC → Neuron	Fold change hiPSC → CM
Potassium voltage-gated channel, Shal-related subfamily, member 2	NM_012281	KCND2	**2.76E − 09**	**21.83**		
Potassium voltage-gated channel, Shal-related subfamily, member 3 [Source: HGNC Symbol; Acc: 6239]	ENST00000369697	KCND3	5.36E − 01	−1.36		
Potassium voltage-gated channel, Shal-related subfamily, member 3, transcript variant 1	NM_004980	KCND3	1.05E − 01	1.55		
Potassium voltage-gated channel, Shal-related subfamily, member 3, transcript variant 1	NM_004980	KCND3	4.41E − 01	1.37		
Potassium voltage-gated channel, Shal-related subfamily, member 3 [Source: HGNC Symbol; Acc: 6239]	ENST00000369697	KCND3	3.86E − 04	−1.84		
Potassium voltage-gated channel, Isk-related family, member 1, transcript variant 2	NM_000219	KCNE1	3.53E − 01	−1.45		
Potassium voltage-gated channel, Isk-related family, member 1, transcript variant 2	NM_000219	KCNE1	3.59E − 01	1.25		
KCNE1-like	NM_012282	KCNE1L	**1.34E − 08**	**4.44**		*−2.18*
KCNE1-like	NM_012282	KCNE1L	**1.11E − 08**	**3.65**		
KCNE1-like	NM_012282	KCNE1L	6.41E − 03	1.88		
Potassium voltage-gated channel, Isk-related family, member 2	NM_172201	KCNE2	**1.41E − 04**	**3.93**		
Potassium voltage-gated channel, Isk-related family, member 3	NM_005472	KCNE3	**8.65E − 15**	**52.36**		
Potassium voltage-gated channel, Isk-related family, member 4	NM_080671	KCNE4	5.04E − 01	1.20		
Potassium voltage-gated channel, subfamily F, member 1	NM_002236	KCNF1	**2.25E − 05**	**6.48**	**2.84**	
Potassium voltage-gated channel, subfamily G, member 1	NM_002237	KCNG1	8.51E − 03	−1.82		
Potassium voltage-gated channel, subfamily G, member 1	NM_002237	KCNG1	1.55E − 01	−1.65		
Potassium voltage-gated channel, subfamily G, member 2	NM_012283	KCNG2	6.21E − 02	1.32		
Potassium voltage-gated channel, subfamily G, member 3, transcript variant 1	NM_133329	KCNG3	**3.74E − 11**	**58.95**		*−2.93*
Potassium voltage-gated channel, subfamily G, member 4	NM_172347	KCNG4	*3.36 E−03*	*−3.33*		
Potassium voltage-gated channel, subfamily G, member 4, (cDNA clone IMAGE: 3028985)	BC008969	KCNG4	*2.24 E−04*	*−3.29*		
Potassium voltage-gated channel, subfamily H (eag-related), member 1, transcript variant 1	NM_172362	KCNH1	8.05E − 01	−1.15		
Potassium voltage-gated channel, subfamily H (eag-related), member 2, transcript variant 1	NM_000238	KCNH2	**5.94E − 04**	**37.53**		
Potassium voltage-gated channel, subfamily H (eag-related), member 2, transcript variant 2	NM_172056	KCNH2	5.70E − 03	1.73		
Potassium voltage-gated channel, subfamily H (eag-related), member 3	NM_012284	KCNH3	9.65E − 01	1.01		
Potassium voltage-gated channel, subfamily H (eag-related), member 4	NM_012285	KCNH4	3.18E − 01	−1.24		

(j) Continued.

Gene name	Accession number	Gene symbol	P	Fold change Ker → hiPSC	Fold change hiPSC → Neuron	Fold change hiPSC → CM
Potassium voltage-gated channel, subfamily H (eag-related), member 5, transcript variant 2	NM_172376	KCNH5	**3.04E − 03**	**2.96**		
Potassium voltage-gated channel, subfamily H (eag-related), member 5, transcript variant 1	NM_139318	KCNH5	$5.41E-01$	1.47		
Potassium voltage-gated channel, subfamily H (eag-related), member 6, transcript variant 2	NM_173092	KCNH6	**2.93E − 02**	**3.04**		
cDNA FLJ33650 fis, clone BRAMY2024514, highly similar to Rattus norvegicus Potassium channel (erg2)	AK090969	KCNH6	**2.08E − 05**	**12.42**		
Potassium voltage-gated channel, subfamily H (eag-related), member 6, transcript variant 2	NM_173092	KCNH6	**2.55E − 02**	**2.29**		
Potassium voltage-gated channel, subfamily H (eag-related), member 7, transcript variant 2	NM_173162	KCNH7	$4.63E-01$	−1.40		
Potassium voltage-gated channel, subfamily H (eag-related), member 7, transcript variant 1	NM_033272	KCNH7	$7.58E-01$	−1.09		
Potassium voltage-gated channel, subfamily H (eag-related), member 8	NM_144633	KCNH8	**3.00E − 09**	**24.57**	**2.97**	
Kv channel interacting protein 1, transcript variant 1	NM_001034837	KCNIP1	$8.33E-02$	1.96	**4.24**	
Kv channel interacting protein 2, transcript variant 7	NM_173197	KCNIP2	$6.43E-01$	1.21		
Kv channel interacting protein 2, transcript variant 1	NM_014591	KCNIP2	$2.53E-03$	1.96		
Kv channel interacting protein 3, calsenilin, transcript variant 1	NM_013434	KCNIP3	*1.15 E−03*	*−3.47*		
Kv channel interacting protein 4, transcript variant 5	NM_001035003	KCNIP4	$6.73E-01$	1.16		**2.01**
Kv channel interacting protein 4, transcript variant 5	NM_001035003	KCNIP4	$9.26E-01$	1.05		
Potassium voltage-gated channel, KQT-like subfamily, member 1, transcript variant 1	NM_000218	KCNQ1	**3.31E − 09**	**79.52**		
Potassium voltage-gated channel, KQT-like subfamily, member 2, transcript variant 5	NM_172109	KCNQ2	**5.68E − 19**	**3408.43**		
Potassium voltage-gated channel, KQT-like subfamily, member 2, transcript variant 3	NM_004518	KCNQ2	$1.29E-02$	1.82		
Potassium voltage-gated channel, KQT-like subfamily, member 2, (cDNA clone IMAGE: 4154700)	BC020384	KCNQ2	**1.09E − 08**	**37.12**		
Potassium voltage-gated channel, KQT-like subfamily, member 3, transcript variant 1	NM_004519	KCNQ3	$1.10E-04$	−1.69		
Potassium voltage-gated channel, KQT-like subfamily, member 4, transcript variant 1	NM_004700	KCNQ4	$9.77E-01$	1.02		
Potassium voltage-gated channel, KQT-like subfamily, member 5, transcript variant 1	NM_019842	KCNQ5	$9.81E-02$	−1.79		
Potassium voltage-gated channel, delayed-rectifier, subfamily S, member 1	NM_002251	KCNS1	$3.39E-01$	−1.27		*−2.64*
Potassium voltage-gated channel, delayed-rectifier, subfamily S, member 2	NM_020697	KCNS2	$6.19E-02$	−2.45	**2.11**	
Potassium voltage-gated channel, delayed-rectifier, subfamily S, member 3	NM_002252	KCNS3	**1.04E − 04**	**2.22**	*−2.61*	*−2.39*
Potassium channel, subfamily T, member 1 (sodium activated)	NM_020822	KCNT1	$8.51E-02$	−2.17		

(j) Continued.

Gene name	Accession number	Gene symbol	P	Fold change Ker → hiPSC	Fold change hiPSC → Neuron	Fold change hiPSC → CM
Potassium channel, subfamily V, member 1	NM_014379	KCNV1	$7.84E-02$	1.58		
Potassium channel, subfamily V, member 2	NM_133497	KCNV2	$7.63E-01$	−1.16		

(k) Inwardly rectifying potassium channels

Gene name	Accession number	Gene symbol	P	Fold change Ker → hiPSC	Fold change hiPSC → Neuron	Fold change hiPSC → CM
Potassium inwardly-rectifying channel, subfamily J, member 1, transcript variant rom-k5	NM_153767	KCNJ1	**2.54E − 02**	**2.66**		
Potassium inwardly-rectifying channel, subfamily J, member 1, transcript variant rom-k5	NM_153767	KCNJ1	$8.51E-01$	−1.05		
Potassium inwardly-rectifying channel, subfamily J, member 2	NM_000891	KCNJ2	**5.14E − 04**	**4.38**		
Potassium inwardly-rectifying channel, subfamily J, member 3	NM_002239	KCNJ3	$4.56E-01$	1.34		
Potassium inwardly-rectifying channel, subfamily J, member 4, transcript variant 1	NM_152868	KCNJ4	**4.80E − 02**	**2.30**		
Potassium inwardly-rectifying channel, subfamily J, member 5	NM_000890	KCNJ5	*1.88 E−08*	*−45.40*		
Potassium inwardly-rectifying channel, subfamily J, member 5	NM_000890	KCNJ5	*4.42 E−12*	*−109.11*		
Potassium inwardly-rectifying channel, subfamily J, member 6	NM_002240	KCNJ6	**3.29E − 05**	**6.75**	**5.54**	
Potassium inwardly-rectifying channel, subfamily J, member 8	NM_004982	KCNJ8	**1.98E − 04**	**5.97**		**2.74**
Potassium inwardly-rectifying channel, subfamily J, member 9 [Source: HGNC Symbol; Acc: 6270]	ENST00000368088	KCNJ9	$3.17E-01$	1.49		
Potassium inwardly-rectifying channel, subfamily J, member 9	NM_004983	KCNJ9	$3.07E-01$	1.79		
Potassium inwardly-rectifying channel, subfamily J, member 10	NM_002241	KCNJ10	**8.85E − 04**	**4.14**		
Potassium inwardly-rectifying channel, subfamily J, member 10	NM_002241	KCNJ10	$9.56E-01$	1.01		
Potassium inwardly-rectifying channel, subfamily J, member 11, transcript variant 1	NM_000525	KCNJ11	**4.00E − 04**	**2.93**		
Potassium inwardly-rectifying channel, subfamily J, member 12	NM_021012	KCNJ12	$1.00E-01$	1.47		
Potassium inwardly-rectifying channel, subfamily J, member 12	NM_021012	KCNJ12	**3.53E − 06**	**5.81**		
Potassium inwardly-rectifying channel, subfamily J, member 13, transcript variant 1	NM_002242	KCNJ13	$7.75E-01$	1.20		
Potassium inwardly-rectifying channel, subfamily J, member 14, transcript variant 2	NM_170720	KCNJ14	$9.05E-02$	−1.40		
Potassium inwardly-rectifying channel, subfamily J, member 15, transcript variant 1	NM_170736	KCNJ15	*3.41 E−08*	*−150.95*		
Potassium inwardly-rectifying channel, subfamily J, member 16, transcript variant 2	NM_170741	KCNJ16	$2.22E-01$	−1.93		

(l) Two-P potassium channels

Gene name	Accession number	Gene symbol	P	Fold change Ker → hiPSC	Fold change hiPSC → Neuron	Fold change hiPSC → CM
Potassium channel, subfamily K, member 1	NM_002245	KCNK1	$3.02E-04$	−1.68		
Potassium channel, subfamily K, member 2, transcript variant 1	NM_001017424	KCNK2	$3.46E-01$	1.57		
Potassium channel, subfamily K, member 3	NM_002246	KCNK3	$9.98E-01$	1.00	**2.36**	
Potassium channel, subfamily K, member 3	NM_002246	KCNK3	$8.75E-01$	−1.10		
Potassium channel, subfamily K, member 3	NM_002246	KCNK3	$5.34E-01$	−1.30		
Potassium channel, subfamily K, member 3 [Source: HGNC Symbol; Acc: 6278]	ENST00000302909	KCNK3	$2.53E-01$	1.52		
Potassium channel, subfamily K, member 4	NM_033310	KCNK4	$6.21E-01$	−1.14	**2.05**	
Potassium channel, subfamily K, member 5	NM_003740	KCNK5	**1.16E − 14**	**29.46**	*−2.35*	*−2.03*
Potassium channel, subfamily K, member 6	NM_004823	KCNK6	*1.22 E−06*	*−3.48*	*−2.20*	
Potassium channel, subfamily K, member 6	NM_004823	KCNK6	*2.05 E−08*	*−5.11*		
Potassium channel, subfamily K, member 6	NM_004823	KCNK6	*7.04E−06*	*−5.22*		
Potassium channel, subfamily K, member 7, transcript variant A	NM_033347	KCNK7	$1.17E-01$	−1.52		
Potassium channel, subfamily K, member 9	NM_016601	KCNK9	$6.67E-01$	−1.29		
Potassium channel, subfamily K, member 10, transcript variant 1	NM_021161	KCNK10	$2.63E-01$	−1.30		
Potassium channel, subfamily K, member 10, transcript variant 2	NM_138317	KCNK10	$1.41E-02$	1.43		
Potassium channel, subfamily K, member 12	NM_022055	KCNK12	**4.58E − 10**	**23.40**		*−5.58*
Potassium channel, subfamily K, member 13	NM_022054	KCNK13	$7.65E-01$	−1.10		
Potassium channel, subfamily K, member 15	NM_022358	KCNK15	$4.96E-02$	−1.50		
Potassium channel, subfamily K, member 15	NM_022358	KCNK15	$9.10E-01$	−1.09		
Pancreatic potassium channel TALK-1d; alternatively spliced	AY253147	KCNK16	*2.17 E−02*	*−2.43*		
Potassium channel, subfamily K, member 17, transcript variant 1	NM_031460	KCNK17	**1.87E − 11**	**28.60**		
Potassium channel, subfamily K, member 17, transcript variant 1	NM_031460	KCNK17	**1.52E − 05**	**19.62**		
Potassium channel, subfamily K, member 18	NM_181840	KCNK18	$1.77E-01$	1.61		

(m) Calcium-activated potassium channels

Gene name	Accession number	Gene symbol	P	Fold change Ker → hiPSC	Fold change hiPSC → Neuron	Fold change hiPSC → CM
Potassium large conductance calcium-activated channel, subfamily M, alpha member 1, transcript variant 2	NM_002247	KCNMA1	$1.01E-02$	1.84		**2.01**
Potassium large conductance calcium-activated channel, subfamily M, alpha member 1, transcript variant 1	NM_001014797	KCNMA1	$3.19E-01$	1.32		
Potassium large conductance calcium-activated channel, subfamily M, alpha member 1, transcript variant 2	NM_002247	KCNMA1	**3.67E − 03**	**2.27**		
Potassium large conductance calcium-activated channel, subfamily M, alpha member 1, transcript variant 2	NM_002247	KCNMA1	$8.53E-02$	1.44		
Maxi-K channel HSLO	AF349445	KCNMA1	$3.04E-01$	1.44		

(m) Continued.

Gene name	Accession number	Gene symbol	P	Fold change Ker → hiPSC	Fold change hiPSC → Neuron	Fold change hiPSC → CM
Potassium large conductance calcium-activated channel, subfamily M, alpha member 1, transcript variant 2	NM_002247	KCNMA1	$2.15E-01$	−1.23		
Potassium large conductance calcium-activated channel, subfamily M, beta member 1	NM_004137	KCNMB1	$7.12E-02$	−1.41		
Potassium large conductance calcium-activated channel, subfamily M, beta member 1	NM_004137	KCNMB1	**2.23E − 06**	**7.82**		
Potassium large conductance calcium-activated channel, subfamily M, beta member 2, transcript variant 1	NM_181361	KCNMB2	$3.36E-01$	1.56		
Potassium large conductance calcium-activated channel, subfamily M, beta member 2, transcript variant 1	NM_181361	KCNMB2	$1.17E-01$	1.47		
Potassium large conductance calcium-activated channel, subfamily M beta member 3, transcript variant 1	NM_171828	KCNMB3	**1.41E − 05**	**2.63**		
Potassium large conductance calcium-activated channel, subfamily M, beta member 4	NM_014505	KCNMB4	**8.85E − 12**	**103.99**		
Potassium large conductance calcium-activated channel, subfamily M, beta member 4 [Source: HGNC Symbol; Acc: 6289]	ENST00000258111	KCNMB4	**9.22E − 10**	**18.40**		
Potassium intermediate/small conductance calcium-activated channel, subfamily N, member 1	NM_002248	KCNN1	**3.40E − 05**	**4.67**		
Potassium intermediate/small conductance calcium-activated channel, subfamily N, member 2, transcript variant 1	NM_021614	KCNN2	**1.88E − 13**	**22.23**	*−3.63*	
Potassium intermediate/small conductance calcium-activated channel, subfamily N, member 3, transcript variant 1	NM_002249	KCNN3	**2.58E − 06**	**8.25**		
Potassium intermediate/small conductance calcium-activated channel, subfamily N, member 3, transcript variant 3	NM_001204087	KCNN3	**1.11E − 07**	**15.29**		
Potassium intermediate/small conductance calcium-activated channel, subfamily N, member 4	NM_002250	KCNN4	$1.06E-02$	−1.84		

(n) P2X receptors

Gene name	Accession number	Gene symbol	P	Fold change Ker → hiPSC	Fold change hiPSC → Neuron	Fold change hiPSC → CM
Purinergic receptor P2X, ligand-gated ion channel, 1	NM_002558	P2RX1	$7.71E-01$	1.14		
Purinergic receptor P2X, ligand-gated ion channel, 2, transcript variant 4	NM_170683	P2RX2	$5.25E-02$	−1.66		
Purinergic receptor P2X, ligand-gated ion channel, 3	NM_002559	P2RX3	$2.43E-02$	−1.76		
Purinergic receptor P2X, ligand-gated ion channel, 4	NM_002560	P2RX4	$8.68E-01$	−1.03		
Purinergic receptor P2X, ligand-gated ion channel, 5, transcript variant 1	NM_002561	P2RX5	**7.68E − 08**	**6.97**		

(n) Continued.

Gene name	Accession number	Gene symbol	P	Fold change Ker → hiPSC	Fold change hiPSC → Neuron	Fold change hiPSC → CM
Purinergic receptor P2X, ligand-gated ion channel, 5, transcript variant 2	NM_175080	P2RX5	$6.13E-02$	1.54		
Purinergic receptor P2X, ligand-gated ion channel, 6 [Source: HGNC Symbol; Acc: 8538]	ENST00000413302	P2RX6	$4.13E-01$	1.68		
Purinergic receptor P2X, ligand-gated ion channel, 7, transcript variant 1	NM_002562	P2RX7	$6.13E-01$	1.23		
Purinergic receptor P2X, ligand-gated ion channel, 7, transcript variant 1	NM_002562	P2RX7	$9.17E-01$	1.04		

(o) Transient receptor potential channels

Gene name	Accession number	Gene symbol	P	Fold change Ker → hiPSC	Fold change hiPSC → Neuron	Fold change hiPSC → CM
Polycystic kidney disease 2 (autosomal dominant)	NM_000297	PKD2	$7.48E-07$	1.79		
Polycystic kidney disease 2 (autosomal dominant)	NM_000297	PKD2	$2.38E-05$	1.98		
Polycystic kidney disease 2-like 1	NM_016112	PKD2L1	**1.29E − 03**	**4.66**		
Polycystic kidney disease 2-like 2	NM_014386	PKD2L2	$1.94E-01$	1.49		
Polycystic kidney disease 2-like 2	NM_014386	PKD2L2	$7.43E-01$	1.19		
Polycystic kidney disease 2-like 2	NM_014386	PKD2L2	$6.74E-01$	1.09		
Transient receptor potential cation channel, subfamily A, member 1	NM_007332	TRPA1	$2.99E-01$	1.74		
Transient receptor potential cation channel, subfamily A, member 1	NM_007332	TRPA1	$5.64E-02$	2.70		
Transient receptor potential cation channel, subfamily C, member 1	NM_003304	TRPC1	**4.30E − 06**	**2.01**		
Transient receptor potential cation channel, subfamily C, member 3, transcript variant 2	NM_003305	TRPC3	**1.12E − 07**	**5.78**		**2.45**
Transient receptor potential cation channel, subfamily C, member 4, transcript variant alpha	NM_016179	TRPC4	**3.25E − 07**	**25.38**		
Transient receptor potential cation channel, subfamily C, member 5	NM_012471	TRPC5	$1.20E-01$	1.28		
Transient receptor potential cation channel, subfamily C, member 6	NM_004621	TRPC6	$1.21E-01$	2.33		
Transient receptor potential cation channel, subfamily C, member 7, transcript variant 1	NM_020389	TRPC7	$6.18E-01$	–1.36		
Transient receptor potential cation channel, subfamily M, member 1	NM_002420	TRPM1	$2.29E-01$	1.31		
Transient receptor potential cation channel, subfamily M, member 2, transcript variant 1	NM_003307	TRPM2	$1.22E-01$	1.97		
Transient receptor potential cation channel, subfamily M, member 2, transcript variant 1	NM_003307	TRPM2	$5.04E-02$	2.53		
Transient receptor potential cation channel, subfamily M, member 3, transcript variant 7	NM_206948	TRPM3	**3.04E − 09**	**10.69**		
Transient receptor potential cation channel, subfamily M, member 3 [Source: HGNC Symbol; Acc: 17992]	ENST00000354500	TRPM3	**2.34E − 03**	**3.74**		
Transient receptor potential cation channel, subfamily M, member 3, transcript variant 7	NM_206948	TRPM3	**3.41E − 06**	**6.23**		
Transient receptor potential cation channel, subfamily M, member 3, transcript variant 9	NM_001007471	TRPM3	$7.23E-01$	1.13		
Transient receptor potential cation channel, subfamily M, member 3, transcript variant 9	NM_001007471	TRPM3	**1.54E − 05**	**2.60**		

(o) Continued.

Gene name	Accession number	Gene symbol	P	Fold change Ker → hiPSC	Fold change hiPSC → Neuron	Fold change hiPSC → CM
Transient receptor potential cation channel, subfamily M, member 4, transcript variant 1	NM_017636	TRPM4	$3.72E-02$	−1.89		
Transient receptor potential cation channel, subfamily M, member 5	NM_014555	TRPM5	$8.21E-01$	−1.08		
Transient receptor potential cation channel, subfamily M, member 6, transcript variant a	NM_017662	TRPM6	$3.80E-01$	1.64		
Transient receptor potential cation channel, subfamily M, member 6, transcript variant a	NM_017662	TRPM6	$9.10E-01$	1.05		
Transient receptor potential cation channel, subfamily M, member 6, transcript variant a	NM_017662	TRPM6	**5.32E − 07**	**5.59**		
Transient receptor potential cation channel, subfamily M, member 6, transcript variant a	NM_017662	TRPM6	$3.32E-01$	1.36		
Transient receptor potential cation channel, subfamily M, member 7	NM_017672	TRPM7	$2.16E-02$	−1.25		
Transient receptor potential cation channel, subfamily M, member 7	NM_017672	TRPM7	$3.64E-03$	−1.38		
Transient receptor potential cation channel, subfamily M, member 8	NM_024080	TRPM8	$2.04E-01$	1.89		
Transient receptor potential cation channel, subfamily V, member 1, transcript variant 3	NM_080706	TRPV1	$3.59E-05$	1.92		
Transient receptor potential cation channel, subfamily V, member 1, transcript variant 3	NM_080706	TRPV1	**4.14E − 05**	**2.25**		
Transient receptor potential cation channel, subfamily V, member 2	NM_016113	TRPV2	**8.02E − 08**	**4.68**		
Transient receptor potential cation channel, subfamily V, member 3	NM_145068	TRPV3	$4.64E-01$	1.35		
Transient receptor potential cation channel, subfamily V, member 3	NM_145068	TRPV3	$1.35E-01$	−2.39		
Transient receptor potential cation channel, subfamily V, member 4, transcript variant 2	NM_147204	TRPV4	$4.33E-01$	1.39		
Transient receptor potential cation channel, subfamily V, member 5, (cDNA clone MGC: 34269 IMAGE: 5186668)	BC034740	TRPV5	$1.00E-01$	1.38		
Transient receptor potential cation channel, subfamily V, member 5	NM_019841	TRPV5	$3.14E-01$	−1.40		
Transient receptor potential cation channel, subfamily V, member 6	NM_018646	TRPV6	$1.57E-01$	−1.38		

(p) Voltage-gated sodium channels

Gene name	Accession number	Gene symbol	P	Fold change Ker → hiPSC	Fold change hiPSC → Neuron	Fold change hiPSC → CM
Sodium channel, voltage-gated, type I, alpha subunit, transcript variant 2	NM_006920	SCN1A	$1.98E-01$	1.54		
Sodium channel, voltage-gated, type I, beta, transcript variant b	NM_199037	SCN1B	$9.95E-01$	−1.00		
Sodium channel, voltage-gated, type II, alpha subunit, transcript variant 1	NM_021007	SCN2A	$4.16E-01$	1.62	**5.00**	
Sodium channel, voltage-gated, type II, beta	NM_004588	SCN2B	$3.61E-01$	−1.58		
Sodium channel, voltage-gated, type II, beta	NM_004588	SCN2B	*8.16 E−04*	*−2.41*		

(p) Continued.

Gene name	Accession number	Gene symbol	P	Fold change Ker → hiPSC	Fold change hiPSC → Neuron	Fold change hiPSC → CM
Sodium channel, voltage-gated, type III, alpha subunit, transcript variant 1	NM_006922	SCN3A	$2.87E-01$	−2.00	**2.85**	
Sodium channel, voltage-gated, type III, alpha subunit, transcript variant 1	NM_006922	SCN3A	$1.89E-01$	1.49		
Sodium channel, voltage-gated, type III, beta, transcript variant 1	NM_018400	SCN3B	$8.74E-01$	−1.06	**4.70**	
Sodium channel, voltage-gated, type III, beta, transcript variant 1	NM_018400	SCN3B	$1.57E-01$	−1.46		
Sodium channel, voltage-gated, type III, beta, transcript variant 1	NM_018400	SCN3B	$1.56E-01$	1.96		
Sodium channel, voltage-gated, type IV, alpha subunit	NM_000334	SCN4A	**1.62E − 08**	**9.91**		
Sodium channel, voltage-gated, type IV, beta, transcript variant 1	NM_174934	SCN4B	*3.25 E−04*	*−3.66*		
Sodium channel, voltage-gated, type V, alpha subunit, transcript variant 1	NM_198056	SCN5A	**2.43E − 08**	**14.10**		
Sodium channel, voltage-gated, type V, alpha subunit, transcript variant 2	NM_000335	SCN5A	$4.93E-02$	1.95		
Sodium channel, voltage-gated, type VII, alpha	NM_002976	SCN7A	$4.49E-03$	1.63		
Sodium channel, voltage-gated, type VII, alpha	NM_002976	SCN7A	$2.07E-01$	1.72		
Sodium channel, voltage gated, type VIII, alpha subunit, transcript variant 1	NM_014191	SCN8A	**1.89E − 09**	**15.61**		
Sodium channel, voltage gated, type VIII, alpha subunit, transcript variant 1	NM_014191	SCN8A	**4.06E − 07**	**11.23**		
Sodium channel, voltage-gated, type IX, alpha subunit	NM_002977	SCN9A	**4.08E − 08**	**11.51**		
Sodium channel, voltage-gated, type IX, alpha subunit	NM_002977	SCN9A	$1.62E-01$	1.66		
Sodium channel, voltage-gated, type IX, alpha subunit	NM_002977	SCN9A	**3.38E − 03**	**2.57**		
Sodium channel, voltage-gated, type X, alpha subunit	NM_006514	SCN10A	$4.06E-01$	1.35		
Sodium channel, voltage-gated, type XI, alpha subunit	NM_014139	SCN11A	$3.02E-01$	1.57		
Sodium channel, voltage-gated, type XI, alpha subunit [Source: HGNC Symbol; Acc: 10583]	ENST00000444237	SCN11A	$8.83E-03$	1.94		

(q) Nonvoltage-gated sodium channels

Gene name	Accession number	Gene symbol	P	Fold change Ker → hiPSC	Fold change hiPSC → Neuron	Fold change hiPSC → CM
Sodium channel, nonvoltage-gated 1 alpha, transcript variant 1	NM_001038	SCNN1A	**1.33E − 09**	**51.49**	*−21.13*	*−10.71*
Sodium channel, nonvoltage-gated 1, beta	NM_000336	SCNN1B	$2.11E-01$	1.64		
Sodium channel, nonvoltage-gated 1, beta	NM_000336	SCNN1B	$5.52E-01$	1.09		
Sodium channel, nonvoltage-gated 1, delta, transcript variant 1	NM_001130413	SCNN1D	$8.43E-02$	1.49		
Sodium channel, nonvoltage-gated 1, gamma	NM_001039	SCNN1G	$2.33E-01$	1.59		
Gamma subunit of epithelial amiloride-sensitive sodium channel	X87160	SCNN1G	$3.99E-01$	1.27		

(r) Two-pore channels

Gene name	Accession number	Gene symbol	P	Fold change Ker → hiPSC	Fold change hiPSC → Neuron	Fold change hiPSC → CM
Two-pore segment channel 1, transcript variant 1	NM_001143819	TPCN1	$6.20E-04$	−1.76		
Two-pore segment channel 1, transcript variant 2	NM_017901	TPCN1	*1.71 E−03*	*−2.10*		
Two-pore segment channel 1, transcript variant 2	NM_017901	TPCN1	*3.55 E−04*	*−2.44*		
Two-pore segment channel 1, transcript variant 1	NM_001143819	TPCN1	$8.06E-03$	−1.83		
Two-pore segment channel 2	NM_139075	TPCN2	$5.06E-01$	−1.15		

(s) Zinc-activated ligand-gated ion channels

Gene name	Accession number	Gene symbol	P	Fold change Ker → hiPSC	Fold change hiPSC → Neuron	Fold change hiPSC → CM
Zinc-activated ligand-gated ion channel	NM_180990	ZACN	$9.24E-02$	1.45		

During reprogramming 14 (33%) of them are significantly upregulated while only 1 (2%) is significantly downregulated. From iPSCs to neurons, as expected, neuronal alpha-subunits *CACNA1D, CACNA1E* areupregulated together with several neuronal channel subunits ($\alpha_2\delta$, β, and γ). In cardiomyocytes, solely the alpha subunit of the cardiac *CACNA1C* is upregulated. Of note, none of the differentiated progeny downregulated any voltage-gated calcium channels.

3.3. Sperm-Associated Cation Channels. Sperm-associated cation channels or CatSper channels are calcium ion channels. They are flagellar proteins involved in sperm motility and therefore affect fertility [27]. During reprogramming to iPSCs, from seven used probes just one showed a significant downregulation and none had a significant upregulation. We observed nothing noteworthy in the differentiated progeny.

3.4. Nicotinic Acetylcholine Receptors. Nicotinic acetylcholine receptors play a role in interneuronal synapses and neuromuscular junctions. They are composed of five subunits as homomeric or heteromeric receptors. They are located at the postsynaptic site and upon binding of acetylcholine they allow the transmission of cations, especially sodium and potassium ions, in some versions also calcium ions. This leads to a depolarization of the membrane and triggers further signaling pathways [28]. Several acetylcholine receptors and subunits are thought to play roles in a variety of pathomechanisms, for example, psychiatric disorders, cardiovascular diseases, or cancer [29–31]. From 21 probes, 5 (24%) showed a significant upregulation while 3 (14%) showed a significant downregulation from keratinocytes to iPSCs. In neurons, solely the neuronal nicotinic acetylcholine receptor *CHRNA6* alpha subunit was upregulated, none in cardiomyocytes.

3.5. Cyclic Nucleotide-Gated Channels. Cyclic nucleotide-gated channels form tetrameric channels which—upon binding of cGMP—allow a flow of cations. For that, these channels track the intracellular concentration of cNMPs to produce a voltage response [32]. Their major role is the depolarization of rod photoreceptors, but they are also found in other tissues like olfactory sensory neurons [33], testis, kidney, or heart [34] and play a role in cellular development such as neuronal growth cone guidance [35]. Defects in these genes are reported to cause retinitis pigmentosa [36]. From 7 used probes one showed a significant upregulation and one showed a significant downregulation (both 14%) during reprogramming, while none was differentially regulated in differentiated neurons or cardiomyocytes.

3.6. GABA Receptors. GABA (gamma-aminobutyric acid) receptors are ligand-gated chloride channels. Since GABA is the main inhibitory neurotransmitter in the central nervous system GABA receptors play an important role for the brain function. The receptors are composed of five subunits which form heteromers. The GABA receptors are a drug target for anesthetics and other psychoactive drugs. We have analyzed 29 probes within GABA receptor subunits. From keratinocytes to iPSCs, 6 (21%) of them are significantly upregulated while just one (3%) is significantly downregulated. Interestingly, none was up- or downregulated in differentiated neurons, while *GABRB3* was downregulated and *GABRP* was upregulated in cardiomyocytes. Up to now, more or less nothing is known about GABA receptors or their subunits in cardiac cells.

3.7. Glycine Receptors. Glycine receptors are inhibitory receptors of the postsynaptic site. They are activated by glycine and mediate an influx of chloride ions. Accordingly, GlyRs regulate not only the excitability of motor and sensory neurons but are also essential for the processing of photoreceptor signals, neuronal development, and inflammatory pain sensitization [37]. The heteromeric pore is formed by five subunits. Concerning their role in pathomechanisms, it was reported that mutations are causing hyperekplexia (also known as startle disease) [38]. We have analyzed 7 probes and none of them was significantly altered in hiPSCs.

Transcript levels for the alpha2 subunit and the beta subunit were highly upregulated in differentiated neurons, pointing to their functional role in the nervous system.

3.8. Ionotropic Glutamate Receptors. Glutamate is the predominant excitatory neurotransmitter in the central nervous system. Therefore, ionotropic glutamate receptors play a key role for learning and memory processes. They are located in the postsynaptic membrane and are composed of several heteromeric subunits. Ionotropic glutamate receptors are further divided into AMPA (alpha-amino-3-hydroxy-5-methyl-4-isoxazole propionate), NMDA (N-Methyl-D-aspartate) or kainate receptors depending on their sensitivity for the agonists. From 36 probes, 5 (14%) showed a significantly increased expression and 2 (6%) showed a decreased expression in iPSCs compared to keratinocytes. As expected, several subunits were upregulated in neurons (none downregulated). None was upregulated in cardiomyocytes, while the kainate subtype *GRIK5* was downregulated.

3.9. Hyperpolarization-Activated Cyclic Nucleotide-Gated Channels. Hyperpolarization-activated cyclic nucleotide-gated channels are homodimers or heterodimers and form a hyperpolarization-activated potassium channel. CNG channels display a very complex heteromeric structure with various subunits and domains that play a critical role in their function [39]. They contribute to pacemaker currents in the heart [40] but are also found in neurons [41]. We have analyzed 5 probes and 3 (60%) of them showed a significant upregulation while none was downregulated after reprogramming. In neurons the *HCN3* channel transcript was upregulated, which plays a role in several neuronal functions including excitability of basal ganglia output neurons [42]. Although *HCN4* for example plays a critical role in the conduction system of the heart, we did not observe a specific regulation in cardiomyocytes.

3.10. Serotonin Receptors. Serotonin (or 5-hydroxytryptamine) receptors are ligand-gated receptors mainly found presynaptically in neurons. The type 3 receptor is the only ion channel while the other serotonin receptors are G-protein-coupled receptors. It forms a heteropentameric pore which upon activation by serotonin allows the flow of sodium and potassium, leading to a depolarization. Serotonin receptors modulate neuronal function and are therefore involved in various brain functions. The analysis of 6 probes for type 3 serotonin receptors showed a significant upregulation of 2 (33%, both for *HTR3A*) probes while none was downregulated in hiPSCs. Although we expected serotonin receptors to be upregulated during neuronal differentiation, no subunit was upregulated in neurons or cardiomyocytes, while only the receptor transcript for *HTR3A* was downregulated in neurons.

3.11. Voltage-Gated Potassium Channels. Voltage-gated potassium channels are composed of a large group of subunits with different characteristics concerning for example their inactivation speed. Functional channels are formed by heterotetramers. The channels are highly specific for potassium with a low affinity for sodium or other cations. Voltage-gated potassium channels are responsible for the repolarization of excitable cells following the sodium-mediated excitation of an action potential and are therefore found in neurons and other cells displaying action potentials. We have analyzed 81 probes. From keratinocytes to hiPSCs, 25 (31%) were significantly upregulated while only 3 (4%) were significantly downregulated. In neurons, several subunits were upregulated including *KCNB1*, coding for Kv2.1 and *KCND2*, both are better known for their role in cardiac cell excitability as well as *KCNF1, KCNH8,* and *KCNIP1*, all known for their contribution in neuronal excitability [43]. It should be noted that *KCNT1* is actually sodium activated but is included in the alphabetical list for a better overview. Further, several "S" subunits were upregulated (*KCNS2* in neurons) or downregulated (*KCNS3* in neurons; KCNS1 and 3 in cardiomyocytes). These subunits are unable to form functional channels as homotetramers but instead heterotetramerize with other alpha-subunits to form conductive channels. These subunits are involved in modifying the channels response and conductivity [44]. Few is known about distinct roles in other tissues, but they were associated with for example, pain modulation [45] or airway responsiveness [46].

3.12. Inwardly Rectifying Potassium Channels. Inwardly rectifying potassium channels have a higher tendency to allow the flow of potassium ions into the cell rather than to the outside of the cell. Therefore, they play an important role in the maintenance of the resting membrane potential. Their activation is constitutive or controlled by ATP binding and G-proteins [47]. Functional channels are formed as homo- or heterotetramers. These channels can be found predominantly in neurons, cardiac myocytes, the pancreas, or the kidneys. From 20 analyzed probes in hiPSCs compared to keratinocytes, 8 (40%) showed a significant upregulation and 3 (15%) were significantly downregulated. The GIRK2 channel encoded by *KCNJ6* is upregulated in neurons playing multiple roles in various tissues including the pancreas and brain [48, 49] and is associated with epileptic seizures in mice lacking the gene [50]. On the other hand, Kir6.1, encoded by *KCNJ8,* is upregulated in cardiomyocytes and has been reported to be involved in the pathogenesis of cardiac arrest in the early repolarization syndrome [51].

3.13. Two-P Potassium Channels. Two-P potassium channels contain two pore-forming P domains. After dimerization they form an outward rectifying potassium channel. They can be found in several tissues and are activated by various chemical or physical means (TRAAK channels). We have analyzed 23 probes. 4 (17%) of them were significantly upregulated while 4 (17%) were significantly downregulated. In neurons *KCNK3*, vital for setting the resting membrane potential and primary target for volatile anesthetics [52] as well as *KCNK4,* which is mechanically gated and contributes to axonal pathfinding, growth cone motility, and neurite elongation, as well as possibly having a role in touch or

pain detection [53, 54], were upregulated. *KCNK5* and 6 were downregulated. In cardiomyocytes, downregulation of *KCNK5* and 12 was observed.

3.14. Calcium-Activated Potassium Channels. Calcium-activated potassium channels are mostly activated by intracellular calcium; some family members are also voltage gated. The family consists of large, intermediate, and small conductance family members. Channels are formed by two units (*KCNM* family) or most commonly four units (*KCNN* family). They are involved in, for example, afterhyperpolarization following the action potential and are predominantly found in neurons. Additionally, they are known to play different roles in cellular mechanisms, including stem cell biology [4–6, 55]. We have analyzed 18 probes of which 9 (50%) were significantly upregulated and none was significantly downregulated after reprogramming. In neurons, solely *KCNN2* was downregulated, while in cardiomyocytes *KCNMA1*, encoding the large conductance BK-channel, involved in heart rate regulation [56], was upregulated.

3.15. P2X Receptors. P2X receptors are receptors for extracellular ATP and upon activation open a channel for ions, predominantly calcium. The channel is formed by homo- or heterotrimers. They are found in several tissues, mainly in the nervous system and muscle tissue. They are involved in a range of physiological processes such as modulation of synaptic transmission, vascular tone, cardiac rhythm, and contractility and immune response [57–61]. In stem cells an influence of P2X receptors on embryonic stem cell proliferation was reported [62]. From the 9 analyzed probes 1 (11%) was significantly upregulated and none downregulated. None of these receptors/channels was regulated in differentiated progeny.

3.16. Transient Receptor Potential Channels. Transient receptor potential channels (TRP channels) are nonselective cation channels. They show different preferences for cations, as well as different activation mechanisms and functions. TRP channels are broadly expressed throughout the organism and mediate multiple functions. These include amongst others sensor activity for a wide range of hypertrophic stimuli and mutations in *TRPM4* are now recognized as causes of human cardiac conduction disorders (reviewed in [63]). Furthermore, TRP channels are related to the onset or progression of several diseases, and defects in the genes encoding TRP channels (so-called "TRP channelopathies") underlie certain neurodegenerative disorders due to their abnormal Ca^{2+} signaling properties (reviewed in [64]). Additionally, TRP channels influence stem cell differentiation and survival [65, 66] and are involved in neuronal-stem-cell-derived development [67]. We have analyzed 40 probes. After reprogramming, 11 (28%) of them were significantly upregulated and none was significantly downregulated. In neurons, none of these channels was noteworthily regulated while solely *TRPC3* was upregulated in cardiomyocytes, reported to be involved in conduction disturbances induced by adenosine receptor A1AR by enhanced Ca^{2+} entry through the *TRPC3* channel [68].

3.17. Voltage-Gated Sodium Channels. Voltage-gated sodium channels consist of a main alpha unit and some optional modulating or regulatory subunits. They are highly selective for sodium and are involved in a variety of cellular functions including action potential formation [69]. From 24 probes we have analyzed, 6 (25%) were significantly upregulated and two (8%) were significantly downregulated from keratinocytes to iPS cells. These channels seem to be expressed in different kinds of stem cells and during development [70–72]. It was further reported that, for example, *SCN5A*, highly upregulated in iPS cells, is involved in cancer stem cell invasion [73]. *SCN2A*, *SCN3A,* and *SCN3B* were upregulated in neurons, described to be involved in neuronal excitation and epilepsy pathogenesis [74]. Although voltage-gated sodium channels play multiple roles also in the cardiac system [70, 75, 76], we observed no changes of this channel family in cardiomyocytes.

3.18. Nonvoltage-Gated Sodium Channels. Epithelial nonvoltage-gated sodium channels are amiloride sensitive. They form heterotrimers and are involved in ion and fluid transport across epithelia in several organs. We have analyzed 6 probes and one (17%) of them was significantly upregulated while none was significantly downregulated. Interestingly, the upregulated *SCNN1A* in iPS cells was subsequently downregulated both in neurons and cardiomyocytes, pointing to a possible function in stem cells. Of note, it was shown already that repression of pluripotency by retinoic acid represses the *SCNN1A* gene together with several other pluripotency factors [77].

3.19. Two-Pore Channels. Two-pore channels are cation-selective ion channels activated by the second messenger nicotinic acid adenine dinucleotide phosphate (NAADP). Upon activation calcium is released from intracellular stores [78]. We have analyzed 5 probes and while none of them was significantly upregulated two (40%) were significantly downregulated from keratinocytes to iPS cells. None of these channels was regulated in neurons or cardiomyocytes.

3.20. Zinc-Activated Ligand-Gated Ion Channels. The zinc-activated ligand-gated ion channel is activated upon binding of zinc. Until now just one family member is known that is expressed in several tissues [79]. Its exact function is not known. The expression was not significantly altered as shown by one probe in all cells.

4. Discussion

Although ion channels are mainly known for their role in electrically excitable cells they can be found in almost all tissues and are additionally involved in various processes such as cell differentiation and maturation [3, 4, 6, 12, 24, 47, 70]. These large groups of channel proteins are still underestimated concerning their role during embryonic

development and cell fate determination. One of the most interesting *in vitro* models for the elucidation of both developmental processes and disease-specific cellular impairments is represented by pluripotent stem cells. Therefore we were interested in the set of ion channels expressed in hiPSCs after reprogramming and compared this set with iPSC-derived differentiated progeny, namely, neurons and cardiomyocytes. As little is known about ion channels in hiPSCs we aimed to start the analysis with gene expression microarray data. For a comparison, we chose the cells from which they were produced—namely, keratinocytes—as the reference cell type. The comparison of 6 keratinocyte samples with 9 hiPSC samples should minimize the often observed variances between hiPSC lines. We found out that almost a third (32%) of the ion channel probes we investigated showed a significant change in gene expression. Of note, this was mostly an upregulation. Additionally, while many ion channel genes were not expressed in keratinocytes they were present in hiPSCs. This indicates that several of the analyzed channel groups might play unknown roles in stem cell biology, for example, homeostasis, proliferation, or differentiation. Interestingly, after differentiation into neurons or cardiomyocytes, relatively small groups were subsequently regulated. This includes ion channel transcripts playing important roles in the respective tissues. Nevertheless, we compared already published sets of data from different experimental setups and additionally limited the analysis to a strong fold regulation. This might lead to high dropout rates of regulated genes during measurement. Still, various channel transcripts were "logically" up- or downregulated during differentiation into neurons or cardiomyocytes, following embryonic development. iPS cells and especially patient-specific iPS cells from persons suffering from genetic mutations leading to hereditary syndromes are a very valuable tool to investigate pathogenetic mechanisms and disease associated molecular and cellular changes [80–82]. As various channel subtypes are involved in multiple pathogenetic mechanisms it would be further interesting to analyze channel transcript regulation in patient specific iPS cells and their differentiated progeny to elucidate possible disease-specific pathways.

Concerning the presented study it is clear that gene regulations on transcript level do not explicitly mimic either protein levels and posttranslational modifications or protein activity. This set of data is sought to describe a global overview on transcript regulation of ion channels during distinct steps of development. It should be noted that in cases where several probes bind within one gene they do not indicate the same upregulation. Sometimes they show the same trend but miss significance, but for some cases there are considerable differences. This could hint for some yet unknown splicing variants. More detailed studies of these hypothesized splice variants could give insights into their function and broaden the still scarce knowledge.

This work is intended to be a guide and start point for future work focusing on single channels and their composition, localization, and function in hiPSCs and their differentiated progeny. These studies could lead to better *in vitro* differentiation protocols but also explain some of the many disease pathomechanisms related to mutations in ion channel genes.

Conflict of Interests

There is no conflict of interests to declare.

Acknowledgments

The authors thank Sabine Seltenheim for excellent technical assistance enabling research conducted in our laboratories. The research that enabled this paper was funded by a fellowship from the Medical Faculty of Ulm University (Bausteinprogramm, L. SBR.0011) and by the Deutsche Forschungsgemeinschaft (Alexander Kleger KL2544/1-1, Stefan Liebau BO1718/4-1), the German Foundation for Heart Research (F/34/11; to Alexander Kleger and Stefan Liebau), the Else-Kröner-Fresenius-Stiftung (2011_A200; to Alexander Kleger and Stefan Liebau), Boehringer-Ingelheim BIU (N5 to Stefan Liebau; C1 to Alexander Kleger), and the Helmholtz Gesellschaft (VH-VI-510 to Tobias M. Boeckers and Stefan Liebau). Alexander Kleger is indebted to the Baden-Württemberg Stiftung for the financial support of this research project by the Eliteprogramm for Postdocs.

References

[1] B. Malissen, "A voltage-gated sodium channel mediates positive selection of T cells," *Nature Immunology*, vol. 13, pp. 810–812, 2012.

[2] P. Rorsman and M. Braun, "Regulation of insulin secretion in human pancreatic islets," *Annual Review of Physiology*, vol. 75, pp. 155–179, 2012.

[3] A. O. Grant, "Cardiac ion channels," *Circulation*, vol. 2, no. 2, pp. 185–194, 2009.

[4] S. Liebau, J. Steinestel, L. Linta et al., "An SK3 channel/nWASP/Abi-1 complex is involved in early neurogenesis," *PLoS ONE*, vol. 6, no. 3, Article ID e18148, 2011.

[5] S. Liebau, B. Vaida, C. Proepper et al., "Formation of cellular projections in neural progenitor cells depends on SK3 channel activity," *Journal of Neurochemistry*, vol. 101, no. 5, pp. 1338–1350, 2007.

[6] A. Kleger, T. Seufferlein, D. Malan et al., "Modulation of calcium-activated potassium channels induces cardiogenesis of pluripotent stem cells and enrichment of pacemaker-like cells," *Circulation*, vol. 122, no. 18, pp. 1823–1836, 2010.

[7] K. Takahashi, K. Tanabe, M. Ohnuki et al., "Induction of pluripotent stem cells from adult human fibroblasts by defined factors," *Cell*, vol. 131, no. 5, pp. 861–872, 2007.

[8] K. Takahashi and S. Yamanaka, "Induction of pluripotent stem cells from mouse embryonic and adult fibroblast cultures by defined factors," *Cell*, vol. 126, no. 4, pp. 663–676, 2006.

[9] X. Carvajal-Vergara, A. Sevilla, S. L. Dsouza et al., "Patient-specific induced pluripotent stem-cell-derived models of LEOPARD syndrome," *Nature*, vol. 465, no. 7299, pp. 808–812, 2010.

[10] M. Stockmann, L. Linta, K. J. Fohr et al., "Developmental and functional nature of human iPSC derived motoneurons," *Stem Cell Reviews and Reports*, 2011.

[11] M. D. Harrell, S. Harbi, J. F. Hoffman, J. Zavadil, and W. A. Coetzee, "Large-scale analysis of ion channel gene expression in the mouse heart during perinatal development," *Physiological Genomics*, vol. 28, no. 3, pp. 273–283, 2007.

[12] M. P. Davies, R. H. An, P. Doevendans, S. Kubalak, K. R. Chien, and R. S. Kass, "Developmental changes in ionic channel activity in the embryonic murine heart," *Circulation Research*, vol. 78, no. 1, pp. 15–25, 1996.

[13] H. Jäger, T. Dreker, A. Buck, K. Giehl, T. Gress, and S. Grissmer, "Blockage of intermediate-conductance Ca^{2+}-Activated K^+ channels inhibit human pancreatic cancer cell growth in vitro," *Molecular Pharmacology*, vol. 65, no. 3, pp. 630–638, 2004.

[14] M. Müller, M. Stockmann, D. Malan et al., "Ca^{2+} activated K channels-new tools to induce cardiac commitment from pluripotent stem cells in mice and men," *Stem Cell Reviews and Reports*, vol. 8, no. 3, pp. 720–740, 2012.

[15] S. P. Wang, J. A. Wang, R. H. Luo, W. Y. Cui, and H. Wang, "Potassium channel currents in rat mesenchymal stem cells and their possible roles in cell proliferation," *Clinical and Experimental Pharmacology and Physiology*, vol. 35, no. 9, pp. 1077–1084, 2008.

[16] K. J. Brennand, A. Simone, J. Jou et al., "Modelling schizophrenia using human induced pluripotent stem cells," *Nature*, vol. 473, pp. 221–225, 2011.

[17] G. H. Liu, B. Z. Barkho, S. Ruiz et al., "Recapitulation of premature ageing with iPSCs from Hutchinson-Gilford progeria syndrome," *Nature*, vol. 472, no. 7342, pp. 221–225, 2011.

[18] R. Maehr, S. Chen, M. Snitow et al., "Generation of pluripotent stem cells from patients with type 1 diabetes," *Proceedings of the National Academy of Sciences of the United States of America*, vol. 106, no. 37, pp. 15768–15773, 2009.

[19] N. Hofman, A. A. M. Wilde, S. Kääb et al., "Diagnostic criteria for congenital long QT syndrome in the era of molecular genetics: do we need a scoring system?" *European Heart Journal*, vol. 28, no. 5, pp. 575–580, 2007.

[20] M. E. Curran, I. Splawski, K. W. Timothy, G. M. Vincent, E. D. Green, and M. T. Keating, "A molecular basis for cardiac arrhythmia: HERG mutations cause long QT syndrome," *Cell*, vol. 80, no. 5, pp. 795–803, 1995.

[21] T. Aasen, A. Raya, M. J. Barrero et al., "Efficient and rapid generation of induced pluripotent stem cells from human keratinocytes," *Nature Biotechnology*, vol. 26, no. 11, pp. 1276–1284, 2008.

[22] T. Aasen and J. C. I. Belmonte, "Isolation and cultivation of human keratinocytes from skin or plucked hair for the generation of induced pluripotent stem cells," *Nature Protocols*, vol. 5, no. 2, pp. 371–382, 2010.

[23] L. Linta, M. Stockmann, K. N. Kleinhans et al., "Rat embryonic fibroblasts improve reprogramming of human keratinocytes into induced pluripotent stem cells," *Stem Cells and Development*, vol. 21, no. 6, pp. 965–976, 2011.

[24] W. A. Catterall, "Voltage-gated calcium channels," *Cold Spring Harbor Perspectives in Biology*, vol. 3, no. 8, Article ID a003947, 2011.

[25] A. C. Dolphin, "A short history of voltage-gated calcium channels," *British Journal of Pharmacology*, vol. 147, supplement 1, pp. S56–S62, 2006.

[26] D. Magis, E. Boon, G. Coppola, A. Daron, and J. Schoenen, "A novel CACNA1A mutation results in episodic ataxia with migrainous features without headache," *Cephalalgia*, vol. 32, pp. 1147–1149, 2012.

[27] H. Qi, M. M. Moran, B. Navarro et al., "All four CatSper ion channel proteins are required for male fertility and sperm cell hyperactivated motility," *Proceedings of the National Academy of Sciences of the United States of America*, vol. 104, no. 4, pp. 1219–1223, 2007.

[28] J. P. Changeux, "The nicotinic acetylcholine receptor: the founding father of the pentameric ligand-gated ion channel superfamily," *The Journal of Biological Chemistry*, vol. 287, pp. 40207–40215, 2012.

[29] F. M. Benes, "Nicotinic receptors and functional regulation of GABA cell microcircuitry in bipolar disorder and schizophrenia," in *Handbook of Experimental Pharmacology*, pp. 401–417, Springer, Berlin, Germany, 2012.

[30] C. Liu and D. Su, "Nicotinic acetylcholine receptor alpha7 subunit: a novel therapeutic target for cardiovascular diseases," *Frontiers of Medicine*, vol. 6, pp. 35–40, 2012.

[31] H. M. Schuller, "Regulatory role of the alpha7nAChR in cancer," *Current Drug Targets*, vol. 13, pp. 680–687, 2012.

[32] A. Cukkemane, R. Seifert, and U. B. Kaupp, "Cooperative and uncooperative cyclic-nucleotide-gated ion channels," *Trends in Biochemical Sciences*, vol. 36, no. 1, pp. 55–64, 2011.

[33] U. B. Kaupp and R. Seifert, "Cyclic nucleotide-gated ion channels," *Physiological Reviews*, vol. 82, no. 3, pp. 769–824, 2002.

[34] M. Biel, X. Zong, M. Distler et al., "Another member of the cyclic nucleotide-gated channel family, expressed in testis, kidney, and heart," *Proceedings of the National Academy of Sciences of the United States of America*, vol. 91, no. 9, pp. 3505–3509, 1994.

[35] K. Togashi, M. J. von Schimmelmann, M. Nishiyama et al., "Cyclic GMP-gated CNG channels function in Sema3A-induced growth cone repulsion," *Neuron*, vol. 58, no. 5, pp. 694–707, 2008.

[36] Q. Zhang, F. Zulfiqar, S. A. Riazuddin et al., "Autosomal recessive retinitis pigmentosa in a Pakistani family mapped to CNGA1 with identification of a novel mutation," *Molecular Vision*, vol. 10, pp. 884–889, 2004.

[37] H. Betz and B. Laube, "Glycine receptors: recent insights into their structural organization and functional diversity," *Journal of Neurochemistry*, vol. 97, no. 6, pp. 1600–1610, 2006.

[38] J. W. Lynch, "Molecular structure and function of the glycine receptor chloride channel," *Physiological Reviews*, vol. 84, no. 4, pp. 1051–1095, 2004.

[39] M. Biel and S. Michalakis, "Function and dysfunction of CNG channels: insights from channelopathies and mouse models," *Molecular Neurobiology*, vol. 35, no. 3, pp. 266–277, 2007.

[40] S. Herrmann, B. Layh, and A. Ludwig, "Novel insights into the distribution of cardiac HCN channels: an expression study in the mouse heart," *Journal of Molecular and Cellular Cardiology*, vol. 51, pp. 997–1006, 2011.

[41] J. Klueva, A. D. Lima, S. Meis, T. Voigt, and T. Munsch, "Hyperpolarization-activated cation current contributes to spontaneous network activity in developing neocortical cultures," *Neurosignals*, vol. 20, pp. 35–47, 2012.

[42] B. H. Meurers, G. Dziewczapolski, A. Bittner, T. Shi, F. Kamme, and C. W. Shults, "Dopamine depletion induced up-regulation of HCN3 enhances rebound excitability of basal ganglia output neurons," *Neurobiology of Disease*, vol. 34, no. 1, pp. 178–188, 2009.

[43] G. A. Gutman, K. G. Chandy, S. Grissmer et al., "International Union of Pharmacology. LIII. Nomenclature and molecular relationships of voltage-gated potassium channels," *Pharmacological Reviews*, vol. 57, no. 4, pp. 473–508, 2005.

[44] F. C. Richardson and L. K. Kaczmarek, "Modification of delayed rectifier potassium currents by the Kv9.1 potassium channel subunit," *Hearing Research*, vol. 147, no. 1-2, pp. 21–30, 2000.

[45] M. Costigan, I. Belfer, R. S. Griffin et al., "Multiple chronic pain states are associated with a common amino acid-changing allele in KCNS1," *Brain*, vol. 133, no. 9, pp. 2519–2527, 2010.

[46] K. Hao, T. Niu, X. Xu, Z. Fang, and X. Xu, "Single-nucleotide polymorphisms of the KCNS3 gene are significantly associated with airway hyperresponsiveness," *Human Genetics*, vol. 116, no. 5, pp. 378–383, 2005.

[47] H. Hibino, A. Inanobe, K. Furutani, S. Murakami, I. Findlay, and Y. Kurachi, "Inwardly rectifying potassium channels: their structure, function, and physiological roles," *Physiological Reviews*, vol. 90, no. 1, pp. 291–366, 2010.

[48] N. Patil, D. R. Cox, D. Bhat, M. Faham, R. M. Myers, and A. S. Peterson, "A potassium channel mutation in weaver mice implicates membrane excitability in granule cell differentiation," *Nature Genetics*, vol. 11, no. 2, pp. 126–129, 1995.

[49] J. Ferrer, C. G. Nichols, E. N. Makhina et al., "Pancreatic islet cells express a family of inwardly rectifying K^+ channel subunits which interact to form G-protein-activated channels," *The Journal of Biological Chemistry*, vol. 270, no. 44, pp. 26086–26091, 1995.

[50] S. Signorini, Y. J. Liao, S. A. Duncan, L. Y. Jan, and M. Stoffel, "Normal cerebellar development but susceptibility to seizures in mice lacking G protein-coupled, inwardly rectifying K^+ channel GIRK2," *Proceedings of the National Academy of Sciences of the United States of America*, vol. 94, no. 3, pp. 923–927, 1997.

[51] J. B. Gourraud, S. le Scouarnec, F. Sacher et al., "Identification of large families in early repolarization syndrome," *Journal of the American College of Cardiology*, vol. 61, pp. 164–172, 2013.

[52] L. Gabriel, A. Lvov, D. Orthodoxou et al., "The acid-sensitive, anesthetic-activated potassium leak channel, KCNK3, is regulated by 14-3-3beta-dependent, protein kinase C, (PKC)-mediated endocytic trafficking," *The Journal of Biological Chemistry*, vol. 287, pp. 32354–32366, 2012.

[53] D. H. Vandorpe and C. E. Morris, "Stretch activation of the *Aplysia* S-channel," *Journal of Membrane Biology*, vol. 127, no. 3, pp. 205–214, 1992.

[54] F. Maingret, M. Fosset, F. Lesage, M. Lazdunski, and E. Honoré, "TRAAK is a mammalian neuronal mechano-gated K^+ channel," *The Journal of Biological Chemistry*, vol. 274, no. 3, pp. 1381–1387, 1999.

[55] A. Kleger and S. Liebau, "Calcium-activated potassium channels, cardiogenesis of pluripotent stem cells, and enrichment of pacemaker-like cells," *Trends in Cardiovascular Medicine*, vol. 21, pp. 74–83, 2011.

[56] W. L. Imlach, S. C. Finch, J. H. Miller, A. L. Meredith, and J. E. Dalziel, "A role for BK channels in heart rate regulation in rodents," *PLoS ONE*, vol. 5, no. 1, Article ID e8698, 2010.

[57] W. Guo, X. Xu, X. Gao, G. Burnstock, C. He, and Z. Xiang, "Expression of $P2X_5$ receptors in the mouse CNS," *Neuroscience*, vol. 156, no. 3, pp. 673–692, 2008.

[58] M. Ryten, S. Y. Yang, P. M. Dunn, G. Goldspink, and G. Burnstock, "Purinoceptor expression in regenerating skeletal muscle in the mdx mouse model of muscular dystrophy and in satellite cell cultures," *The FASEB Journal*, vol. 18, no. 12, pp. 1404–1406, 2004.

[59] M. Ryten, P. M. Dunn, J. T. Neary, and G. Burnstock, "ATP regulates the differentiation of mammalian skeletal muscle by activation of a $P2X_5$ receptor on satellite cells.," *Journal of Cell Biology*, vol. 158, no. 2, pp. 345–355, 2002.

[60] D. Sonin, S. Y. Zhou, C. Cronin et al., "Role of P2X purinergic receptors in the rescue of ischemic heart failure," *American Journal of Physiology*, vol. 295, no. 3, pp. H1191–H1197, 2008.

[61] S. Feske, E. Y. Skolnik, and M. Prakriya, "Ion channels and transporters in lymphocyte function and immunity," *Nature Reviews Immunology*, vol. 12, pp. 532–547, 2012.

[62] S. H. Jung and J. H. Ho, "ATP stimulates mouse embryonic stem cell proliferation via protein kinase C, phosphatidylinositol 3-kinase/Akt, and mitogen-activated protein kinase signaling pathways," *Stem Cells*, vol. 24, no. 12, pp. 2637–2648, 2006.

[63] H. Watanabe, K. Iino, T. Ohba, and H. Ito, "Possible involvement of TRP channels in cardiac hypertrophy and arrhythmia," *Current Topics in Medicinal Chemistry*. In press.

[64] Y. Takada, T. Numata, and Y. Mori, "Targeting TRPs in neurodegenerative disorders ," *Current Topics in Medicinal Chemistry*. In press.

[65] H. Cheng, J. M. Feng, M. L. Figueiredo et al., "Transient receptor potential melastatin type 7 channel is critical for the survival of bone marrow derived mesenchymal stem cells," *Stem Cells and Development*, vol. 19, no. 9, pp. 1393–1403, 2010.

[66] E. den Dekker, D. G. M. Molin, G. Breikers et al., "Expression of transient receptor potential mRNA isoforms and Ca^{2+} influx in differentiating human stem cells and platelets," *Biochimica et Biophysica Acta*, vol. 1539, no. 3, pp. 243–255, 2001.

[67] J. P. Weick, M. A. Johnson, and S. C. Zhang, "Developmental regulation of human embryonic stem cell-derived neurons by calcium entry via transient receptor potential channels," *Stem Cells*, vol. 27, no. 12, pp. 2906–2916, 2009.

[68] J. Sabourin, F. Antigny, E. Robin, M. Frieden, and E. Raddatz, "Activation of transient receptor potential canonical 3 (TRPC3)-mediated Ca^{2+} entry by A_1 adenosine receptor in cardiomyocytes disturbs atrioventricular conduction," *The Journal of Biological Chemistry*, vol. 287, pp. 26688–26701, 2012.

[69] A. Haythornthwaite, S. Stoelzle, A. Hasler et al., "Characterizing human ion channels in induced pluripotent stem cell-derived neurons," *Journal of Biomolecular Screening*, vol. 17, pp. 1264–1272, 2012.

[70] S. S. Chopra, D. M. Stroud, H. Watanabe et al., "Voltage-gated sodium channels are required for heart development in zebrafish," *Circulation Research*, vol. 106, no. 8, pp. 1342–1350, 2010.

[71] G. R. Li, H. Sun, X. Deng, and C. P. Lau, "Characterization of ionic currents in human mesenchymal stem cells from bone marrow," *Stem Cells*, vol. 23, no. 3, pp. 371–382, 2005.

[72] P. Jiang, S. N. Rushing, C. W. Kong et al., "Electrophysiological properties of human induced pluripotent stem cells," *American Journal of Physiology*, vol. 298, no. 3, pp. C486–C495, 2010.

[73] C. D. House, C. J. Vaske, A. M. Schwartz et al., "Voltage-gated Na^+ channel SCN5A is a key regulator of a gene transcriptional network that controls colon cancer invasion," *Cancer Research*, vol. 70, no. 17, pp. 6957–6967, 2010.

[74] M. H. Meisler, J. E. O'Brien, and L. M. Sharkey, "Sodium channel gene family: epilepsy mutations, gene interactions and modifier effects," *The Journal of Physiology*, vol. 588, no. 11, pp. 1841–1848, 2010.

[75] D. E. Arking and N. Sotoodehnia, "The genetics of sudden cardiac death," *Annual Review of Genomics and Human Genetics*, vol. 13, pp. 223–239, 2012.

[76] R. P. Davis, S. Casini, C. W. van den Berg et al., "Cardiomyocytes derived from pluripotent stem cells recapitulate electrophysiological characteristics of an overlap syndrome of cardiac sodium channel disease," *Circulation*, vol. 125, pp. 3079–3091, 2012.

[77] C. J. Giuliano, J. S. Kerley-Hamilton, T. Bee et al., "Retinoic acid represses a cassette of candidate pluripotency chromosome 12p genes during induced loss of human embryonal carcinoma tumorigenicity," *Biochimica et Biophysica Acta*, vol. 1731, no. 1, pp. 48–56, 2005.

[78] V. Rybalchenko, M. Ahuja, J. Coblentz et al., "Membrane potential regulates nicotinic acid adenine dinucleotide phosphate (NAADP) dependence of the pH- and Ca^{2+}-sensitive organellar two-pore channel TPC1," *The Journal of Biological Chemistry*, vol. 287, pp. 20407–20416, 2012.

[79] P. A. Davies, W. Wang, T. G. Hales, and E. F. Kirkness, "A novel class of ligand-gated ion channel is activated by Zn^{2+}," *The Journal of Biological Chemistry*, vol. 278, no. 2, pp. 712–717, 2003.

[80] J. A. Kaye and S. Finkbeiner, "Modeling Huntington's disease with induced pluripotent stem cells," *Molecular and Cellular Neurosciences*, 2013.

[81] S. Nedelec, B. Onteniente, M. Peschanski, and C. Martinat, "Genetically-modified stem cells for the treatment of neurological diseases," *Current Gene Therapy*, vol. 4, pp. 1170–1181, 2013.

[82] H. Okano, M. Nakamura, K. Yoshida et al., "Steps toward safe cell therapy using induced pluripotent stem cells," *Circulation Research*, vol. 112, pp. 523–533, 2013.

Hindawi Publishing Corporation
Stem Cells International
Volume 2012, Article ID 353491, 16 pages
doi:10.1155/2012/353491

Research Article

Neurally Derived Tissues in *Xenopus laevis* Embryos Exhibit a Consistent Bioelectrical Left-Right Asymmetry

Vaibhav P. Pai, Laura N. Vandenberg, Douglas Blackiston, and Michael Levin

Department of Biology and Tufts Center for Regenerative and Developmental Biology, Tufts University, Medford, MA 02155, USA

Correspondence should be addressed to Michael Levin, michael.levin@tufts.edu

Received 19 September 2012; Accepted 7 November 2012

Academic Editor: Alexander Kleger

Consistent left-right asymmetry in organ morphogenesis is a fascinating aspect of bilaterian development. Although embryonic patterning of asymmetric viscera, heart, and brain is beginning to be understood, less is known about possible subtle asymmetries present in anatomically identical paired structures. We investigated two important developmental events: physiological controls of eye development and specification of neural crest derivatives, in *Xenopus laevis* embryos. We found that the striking hyperpolarization of transmembrane potential (V_{mem}) demarcating eye induction usually occurs in the right eye field first. This asymmetry is randomized by perturbing visceral left-right patterning, suggesting that eye asymmetry is linked to mechanisms establishing primary laterality. Bilateral misexpression of a depolarizing channel mRNA affects primarily the right eye, revealing an additional functional asymmetry in the control of eye patterning by V_{mem}. The ATP-sensitive K^+ channel subunit transcript, SUR1, is asymmetrically expressed in the eye primordia, thus being a good candidate for the observed physiological asymmetries. Such subtle asymmetries are not only seen in the eye: consistent asymmetry was also observed in the migration of differentiated melanocytes on the left and right sides. These data suggest that even anatomically symmetrical structures may possess subtle but consistent laterality and interact with other developmental left-right patterning pathways.

1. Introduction

Consistent (directionally biased) left-right asymmetry of viscera, heart, and brain is overlaid upon the overall bilaterally symmetric body plan of a wide range of organisms [1, 2]. Errors in this process form an important class of human birth defects [3–5]. Thus, understanding left-right patterning and the interaction of individual organ systems with the axial polarity of the body is of great interest for both basic evolutionary developmental biology and for the biomedicine of birth defects. Likewise, the highly lateralized functions of the brain (e.g., language, speech, and handedness) and their partial disconnect from anatomical left-right asymmetry have been a fascinating topic under study for several decades [6, 7].

Recent studies have identified numerous genetic [8–13], biophysical [14–16], and physiological [17–21] mechanisms that underlie large-scale left-right asymmetry and the *situs* of asymmetric organs. However, much less well-understood are subtle asymmetries occurring in paired body structures which are anatomically symmetrical [14].

Such asymmetries manifest in several ways. First, quantitative morphometrics of paired structures can reveal cryptic polarity that may not be apparent from gross morphological examination [22]; insect wings are a good example of this phenomenon [23, 24], as are human foot size [25] and sex organ placement [26]. It is crucial to note that such biased examples of left-right patterning (where the asymmetry is coordinated in a consistent fashion with the other two major axes) are a distinct phenomenon from fluctuating asymmetry, which involves simple differences between the left and right sides derived from developmental noise [27, 28].

Second, differences of gene expression have been described in seemingly symmetric body structures. These include consistent differences in the timing of highly

dynamic bilateral transcriptional waves that drive the segmentation clock of somitogenesis [29–31], as well as long-term asymmetries in expression of markers such as EGF-like growth factors and MLC3F [32, 33].

Perhaps the most interesting types of subtle asymmetries are those that are revealed only under functional perturbation. It has long been known that consistently sided unilateral limb defects are induced in rodents by some compounds such as cadmium [34–36]. Spontaneous genetic defects sometimes uncover biased asymmetries, as seen in several human syndromes that unilaterally affect the limbs [37], face [38], or hips [39]. Holt-Oram syndrome (Tbx5 related) presents upper limb malformations which are much more common on the left side [37, 40–42], while fibular hypoplasia affects the right side more often [43]. Indeed, a variety of human syndromes affecting paired organs have a significant bias for one side [39]. Curiously, unilateral defects in otherwise symmetrically placed structures (e.g., teeth) in monozygotic twins exhibit a mirroring-opposite sidedness in the two twins (reviewed in [44]). Hemihyperplasia [45, 46], a rare phenomenon where one side of the body abnormally overgrows, is right biased [47]. Importantly, targeted molecular-genetic experiments in tractable model systems are beginning to reveal entry points into this process; for example, attenuated FGF8 signaling results in consistently biased left-right asymmetric development of the pharyngeal arches and craniofacial skeleton in zebrafish [48].

Most studies of asymmetry use cardiac and visceral *situs* as readout, focusing on mechanisms that determine the laterality of major body organs. However, the consistent asymmetries revealed in the above examples hint at the possibility that left-right identity (resulting from tissues' interactions with the pathways that establish the left-right axis) could be far more prevalent throughout the body than is currently appreciated. What signaling pathways might underlie laterality information in anatomically symmetrical tissues? While most work on morphogenetic controls focuses on biochemical pathways [49, 50] and physical forces [51, 52], exciting recent as well as classical data demonstrate the importance of endogenous bioelectrical determinants of cell behavior and large-scale patterning [53–59]. We thus focused our search on asymmetries that manifest at the level of functional physiology.

Prior work in the planarian flatworm model system revealed that during head regeneration, the right eye was significantly more sensitive to inhibition of the H, K-ATPase ion pump than the left, in terms of frequency of induced patterning defects [60]. In our efforts to understand the functions of spatial gradients in transmembrane potential (V_{mem}) during vertebrate development and regeneration [18, 61–65], we examined eye development in embryos of *Xenopus laevis*. Using a noninvasive assay with a fluorescent reporter of V_{mem} [66, 67], it was found that the nascent eye fields are demarcated by a localized hyperpolarization of V_{mem} [68, 69]; strikingly, this physiological signature of eye fate is consistently biased, with cells on the right side of the midline hyperpolarizing first. We also report similar consistent subtle asymmetries in the migratory behavior of neural crest-derived melanocytes. Here, we molecularly characterize this novel asymmetry, revealing that physiological analysis can uncover cryptic differences in patterning information not apparent from molecular marker analysis or anatomical examination. Understanding such subtle functional asymmetries may become useful in addressing and targeting diseases with asymmetric manifestations.

2. Results

2.1. Eye Field Cells Exhibit a Consistently Asymmetric V_{mem}. V_{mem} plays a crucial functional role in defining the eye fields during the development of the *Xenopus* embryo [68, 70]. Using the fluorescent voltage-sensitive reporter dye CC2-DMPE [71] *in vivo* to characterize real-time changes in membrane potential [17, 65, 72], we discovered a novel physiological asymmetry between the left and right eye primordia. At stage 18, normal *Xenopus* embryos exhibit bilateral clusters of cells with a more strongly polarized V_{mem} than their neighbors around the putative eye region (Figure 1(a), red arrowheads [68]). Surprisingly, real-time imaging analysis revealed that the right eye field is polarized first, followed by polarization of the left eye field (Figures 1(a) and 1(b)). Though not absolute, this physiological asymmetry is consistently biased, since more than 3-fold as many embryos polarized first on the right compared to those that began polarization on the left (Figure 1(b); $N = 44$, $P < 0.001$, Chi-squared test comparison with an unbiased expectation). In addition to the significant asymmetry at one key timepoint, we followed 6 individual embryos (imaged through eye development stages) to estimate the temporal difference between hyperpolarization events on the two sides. At 20°C, 4 embryos exhibited a 30 min delay in the hyperpolarization of the left eye spot, while 2 embryos exhibited a 20 min delay in the appearance of the left eye spot hyperpolarization. We conclude that eye development in *Xenopus* is inherently asymmetric, with the right eye field most often initiating the endogenous program of polarization.

Previous studies in chick and mouse embryos have shown that somites, though anatomically symmetrical, also exhibit an underlying asymmetry [30, 73]. Somites are shielded from this inherent asymmetry by the action of retinoic acid (RA) signaling, resulting in symmetrical development. In order to determine whether the asymmetry in eye signals is due to an incomplete shielding effect of RA-dependent signaling, we treated embryos with 1.5 μM of the broad-spectrum RA receptor inhibitor Ro-415253. Ro-41-5253 at this concentration has previously been shown to affect RA signaling in *Xenopus* [74]. We used a previously documented midline marker—Sonic Hedgehog (Shh), to further confirm the effect of Ro-41-5253. *Xenopus* embryos were left untreated (Controls) or treated with Ro-41-5253 (1.5 μM), and the Shh expression was evaluated at stage 18 by *in situ* hybridization (Figure 1(c)). Control embryos showed Shh expression as a thin line along the dorsal midline (Figure 1(c), (i) white arrowhead). However, Ro-41-5253-treated embryos (>90%) showed a clear increase in Shh expression along the midline (Figure 1(c), (ii) blue arrowhead) as previously documented [74]. This change

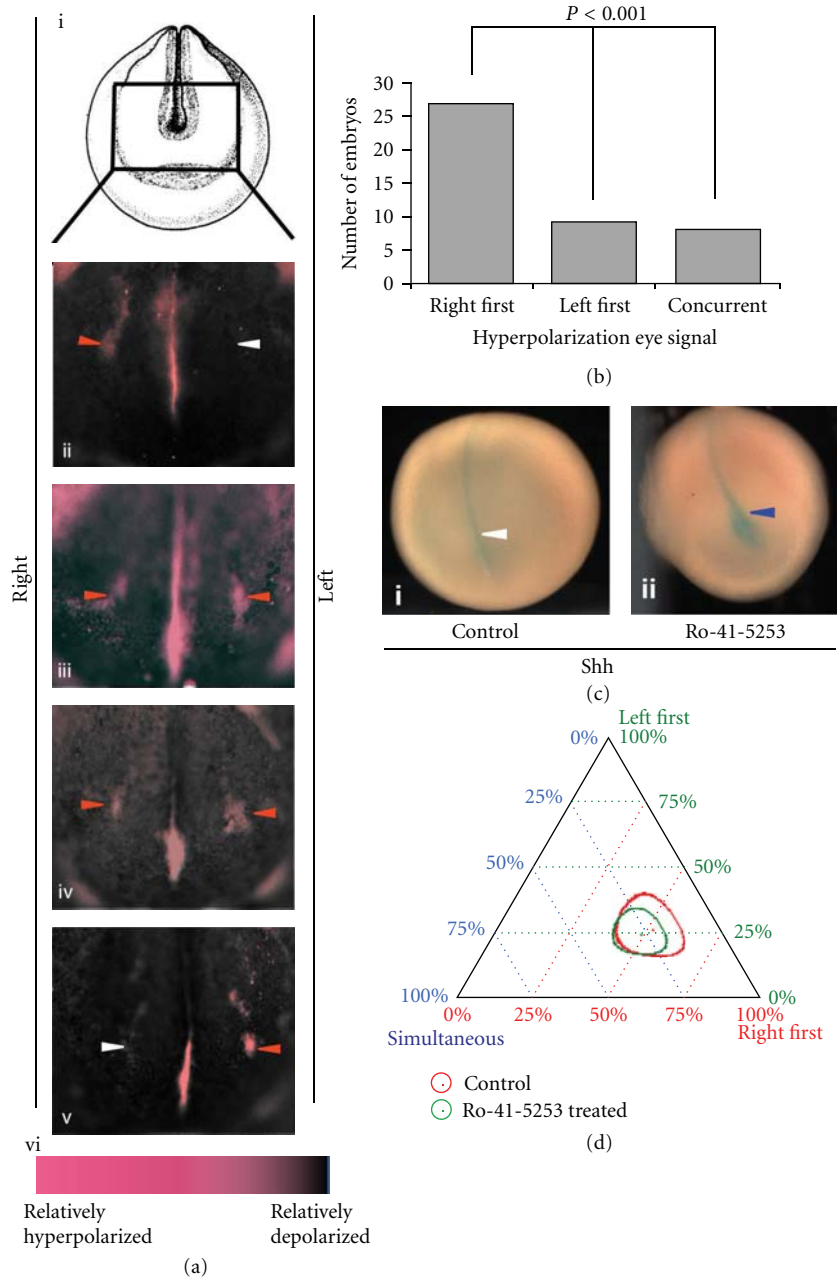

Figure 1: Rightward bias in induction of polarization signal regulating eye development. (a) Incubation in voltage-sensitive CC2-DMPE dye of multiple *Xenopus* embryos tracked from stage 18 to stage 20 shows the representative temporal progression of hyperpolarization signal (red arrowheads) during development (ii)–(v). White arrowheads indicate the lack of a coherent (contiguous) spot of signal. (vi) Color bar representing the scale of relative depolarization and hyperpolarization as seen with the CC2-DMPE dye. (b) Bar graph comparing a group of *Xenopus* embryos ($n = 44$) that were tracked individually and analyzed for the first detectable hyperpolarization signal using CC2-DMPE; a significant bias is observed favoring the right side. A pairwise comparison and Chi-squared test analysis were done between the groups. (c) *In situ* hybridization analysis of Sonic Hedgehog (Shh) signal in stage 18 *Xenopus* embryos either untreated (control) ((i) white arrowhead) or treated with 1.5 μM retinoic acid receptor inhibitor Ro-41-5253 ((ii) blue arrowhead) from midgastrula stage. Ro-41-5253 treatment significantly enhances the Shh expression signal in 92% of treated embryos ($n = 29$). (d) Categorical data analysis using a ternary plot shows that the treatment with Ro-41-5253 (1.5 μM) that inhibits retinoic acid receptor signal resulted in no significant change in the rightward bias of polarization signal (as observed via CC2-DMPE staining) involved in *Xenopus* eye development. In control (untreated) embryos the polarization was 51.5% right first, 26.5% left first, and 22% simultaneous ($n = 72$). In the Ro-41-5253-treated embryos the polarization was 48% right first, 25% left first, and 27% simultaneous ($n = 126$). The circles in the plot represent 95% confidence intervals. Using the calculations provided by a ternary plot algorithm (https://webscript.princeton.edu/~rburdine/stat/three_categories), the results are statistically significant only when there is no overlap of the confidence intervals.

in Shh expression confirms that at 1.5 μM Ro-41-5253 is effective in inhibiting RA receptor signaling.

The effect of Ro-41-5253 on the asymmetric eye polarization signal was analyzed in stage 18 embryos using the CC2-DMPE voltage reporter dye. Each treatment (control and Ro-41-5253) was plotted on a ternary graph using three measures of eye-related polarization signal (right first, left first, and simultaneous) according to the methods described previously [75] (Figure 1(d)). The circles in the plot represent respective error regions of 95% confidence intervals. Using the calculations provided by a ternary plot algorithm (https://webscript.princeton.edu/~rburdine/stat/three_categories), the results are considered statistically significant ($P < 0.05$) when there is no overlap of the 95% confidence intervals. Analysis of the polarization signal in the Ro-41-5253-treated embryos at stage 18 showed a significant right side first bias ($n = 126$) (right first 48%, left first 25%, and simultaneous 27%) (Figure 1(d), green circle), similar to that of control/untreated embryos ($n = 72$) (right first 51.5%, left first 26.5%, and simultaneous 22%) (Figure 1(d), red circle; $P > 0.05$, ternary plot algorithm). Thus, RA signaling does not play a role in the right-side-first bias of V_{mem} signal in the eye primordia.

2.2. Eye Field V_{mem} Asymmetry Is Perturbed by Disruption of pH-Mediated Left-Right Patterning. We next asked whether eye asymmetry is controlled by the same pathway that governs left-right patterning of the heart and viscera. We used low-pH treatment at cleavage stages to specifically induce randomization of asymmetric gene expression and subsequent organ *situs*; this is known to interfere with the earliest steps of left-right patterning by inhibiting the proton efflux of the plasma-membrane H^+ V-ATPase which is required for normal laterality [17]. The very early timing of this treatment ensured that it could not affect eye development directly but rather allowed us to ask whether randomization of the body's main left-right patterning pathway likewise randomized the observed physiological eye asymmetry. The efficacy of our loss-of-function treatment upon normal left-right asymmetry was confirmed by scoring the tadpoles at stage 45 for altered sidedness of the heart, gut, or gallbladder. Normal tadpoles (untreated, Figure 2(a)(i)) have a right-ward looping heart (red arrow), a left-sided gut coil (yellow arrow), and a right-sided gallbladder (green arrow). In contrast, treated tadpoles (Figure 2(a), (ii)-(iii)) showed randomization of the positions of the heart, gut, and gallbladder (independent assortment of organs), as described previously [76, 77], in the absence of generalized toxicity or other malformations (including any dorsoanterior defects). Heterotaxia was induced in 19% of embryos (Figure 2(b)) (the degree of the pH perturbation was kept well below extreme values to be compatible with continued development, to avoid dorsoanterior malformations that might confound analysis of eye development, resulting in a submaximal randomization penetrance). Each treatment (control and pH) was plotted on a ternary graph as described above; the results are considered statistically significant ($P < 0.05$, ternary plot algorithm) when there is no overlap of the 95% confidence intervals. Analysis of the polarization signal in the siblings of treated embryos at stage 18 showed that the rightward bias seen in the normal embryos ($n = 191$) (right first 51%, left first 23%, and simultaneous 26%) (Figure 2(c)) was significantly randomized in treated embryos ($n = 105$, $P < 0.05$, ternary plot algorithm) (right first 31%, left first 39%, and simultaneous 30%) (Figure 2(c)). We conclude that the determination of eye field voltage asymmetry is downstream of early ion flow dynamics, as is the positioning of the heart and viscera [8, 78].

2.3. Eye Fields Are Asymmetrically Sensitive to Perturbation of V_{mem}. To determine whether functional asymmetries (differential sensitivity to perturbation of voltage levels, as previously observed in planaria by [60]) are present in the eye field in addition to the asymmetric endogenous sequence of polarization, we experimentally depolarized the cells' V_{mem} using a carefully titered strategy that allowed us to manipulate V_{mem} and affect subtle bioelectrically controlled processes without inducing generalized toxicity or massive malformation [68]. We capitalized upon the glycine-gated chloride channel [79], which can be opened by exposure to the compound Ivermectin (IVM) [80]—a convenient method of controlling cellular potential that we have previously used to probe the role of V_{mem} in eye induction and metastatic-like transformation [62, 68]. Under normal conditions and standard 0.1X MMR external medium supplemented with Ivermectin, misexpression of these channels depolarizes cells (since the negatively charged chloride ion leaves GlyR-expressing cells down its concentration gradient [62]). We recently showed that injection of GlyR mRNA indeed alters the polarization pattern observed in the putative eye region and affects eye patterning [68].

Because the eyes are derived from the dorsal blastomeres at the 4-cell stage [88], we injected GlyR mRNA into the 2 dorsal cells and developed the embryos to stage 42. On average 45% of the affected embryos showed defects in only one eye; interestingly, there was a significant bias (2.5-fold) towards defects in the patterning of the right eye (Figure 2(d); $P = 0.0007$, Chi-squared test). As a control, we injected in a similar manner a dominant-negative *Pax6* (DNPax6) mRNA which had been previously shown to disrupt *Xenopus* eye development [68, 89]. No statistically significant bias toward right (30%) or left (27%) eye malformation was observed among animals with only 1 eye affected (total 57% with one eye defect) ($P > 0.05$; $n = 294$ Chi-squared test in comparison with an unbiased expectation; Figure 2(e)), suggesting that the Pax6 signal during eye patterning is left-right neutral.

From these results, we conclude that morphogenesis of the right eye is more sensitive to perturbation of V_{mem} than is that of the left.

2.4. K_{ATP} Channel Probes Reveal Asymmetric Expression in the Eye Tissues of Developing Embryos. We next sought to determine the molecular basis for the observed asymmetry in transmembrane potential of the eye fields. Asymmetries

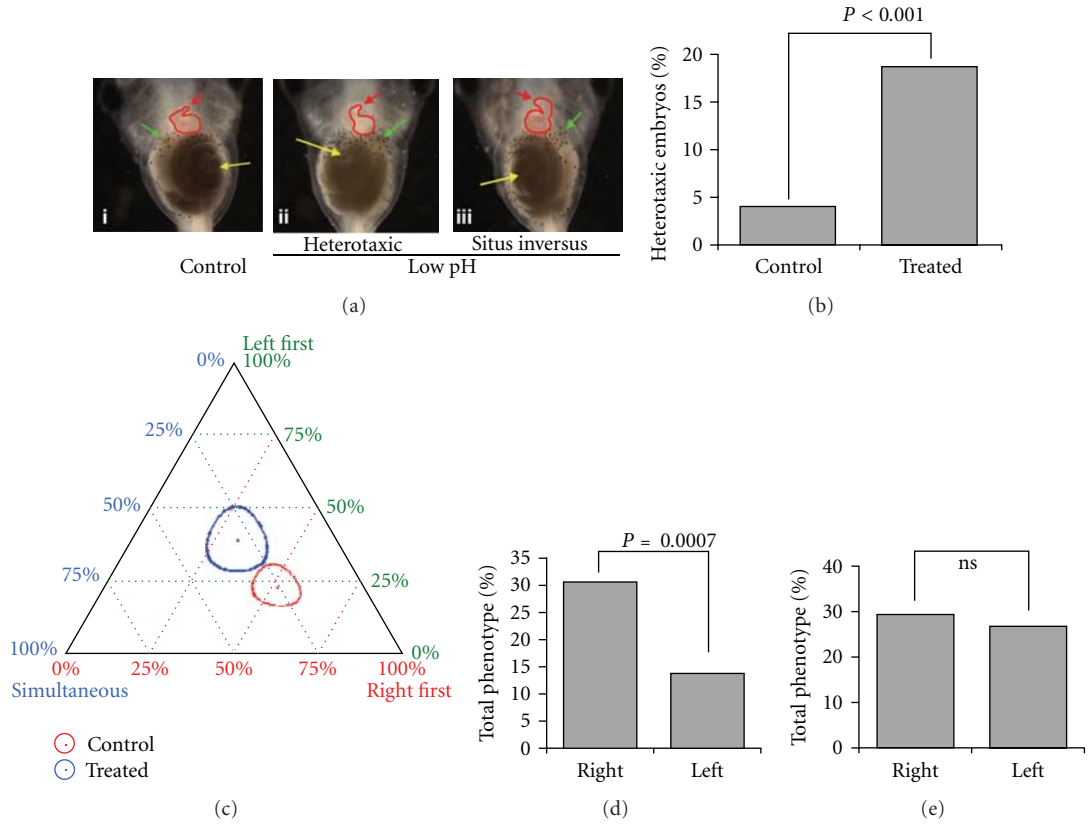

Figure 2: Right-ward bias in eye development is linked to the body left-right axis. (a) (i) Brightfield images of tadpoles at stage 45 showing normal positioning of the organs (*situs solitus*); rightward looping heart (red arrow), leftward coiling of gut (yellow arrow), and right side placement of gallbladder (green arrow) along the left-right axis in untreated controls. (ii)-(iii) Brightfield images of tadpoles at stage 45 after incubation in pH 4.00 0.1XMMR. (ii) Showing heterotaxic positioning of organs; rightward looping heart (red arrow) rightward coiling of gut (yellow arrow), and left side placement of gallbladder (green arrow). (iii) Showing inverse positioning of the organs (*situs inversus*); leftward looping heart (red arrow), rightward coiling of gut (yellow arrow), and left side placement of gallbladder (green arrow) along the left-right axis in tadpoles. (b) Bar graph showing percentage of embryos with heterotaxia upon incubation in 0.1XMMR (pH 4) ($n = 481$) in comparison to untreated controls ($n = 419$). The controls and treated groups were analyzed using Chi-squared test. (c) Categorical data analysis using a ternary plot shows that treatment with pH = 4 0.1XMMR that induced left-right body axis randomization also resulted in randomization and loss of the rightward bias of the polarization signal (observed via CC2-DMPE staining) involved in *Xenopus* eye development. In control embryos the polarization bias was 51% right first, 23% left first, and 26% simultaneous. The pH = 4 0.1XMMR-incubated embryos showed randomization of polarization signal 31% right first, 39% left first, and 30% simultaneous. The circles in the plot represent 95% confidence intervals. Using the calculations provided by a ternary plot algorithm (https://webscript.princeton.edu/~rburdine/stat/three_categories), the results are statistically significant ($P < 0.05$) when there is no overlap of the confidence intervals. (d) Bar graph showing right-ward bias in malformed eye upon perturbation of polarization signal. Embryos were injected with GlyR in the dorsal two cells (eye precursor cells) at the 4-cell stage and treated with IVM to induce depolarization in injected cells. Percentages of phenotypic embryos with a single malformed eye are depicted ($n = 763$). Data was analyzed using a Chi-square test comparing the right and left groups. (e) Bar graph showing no left-right bias in malformed eye upon perturbation of Pax6. Embryos were injected with DNPax6 in the dorsal two cells (eye precursor cells) at 4-cell stage. Percentages of phenotypic embryos with a single malformed eye are depicted. Data was analyzed using a Chi-squared test ($n = 294$).

in V_{mem} with significant consequences for cell behavior are often driven by differential expression of ion channels [90–92]. K_{ATP} channels [93] are octamers formed from 4 proteins from the inward-rectifying potassium family $K_{ir}6.x$ (either $K_{ir}6.1$ or $K_{ir}6.2$) associated with 4 sulphonylurea receptors (SUR1 and SUR2). We had previously found that altering the bioelectric state with dominant negative K_{ir} constructs that target endogenous K_{ATP} channels result in the formation of ectopic eyes [68]. Hence, we analyzed the expression pattern of K_{ATP} channel subunits in *Xenopus* embryos [94] by *in situ* hybridization at stage 18 and stage 30. Previously characterized K_{ATP} channel genes [87, 95] showed no asymmetric expression in the relevant tissues; however, probes made against the murine K_{ATP} genes revealed a striking set of expression patterns.

Probes for all four K_{ATP} channel subunits revealed signal mainly in the head, including the putative eye regions at stage 18 (Figure 3(a), (i)–(iv) blue arrowheads) and intensely stained the developing eye at stage 30 (Figure 3(a), (v)–(viii) blue arrowheads). Stage 30 embryos also showed expression in the neural tube (Figure 3(a), (v), (viii)). Stage 30 embryos were sectioned as illustrated in Figure 3(b).

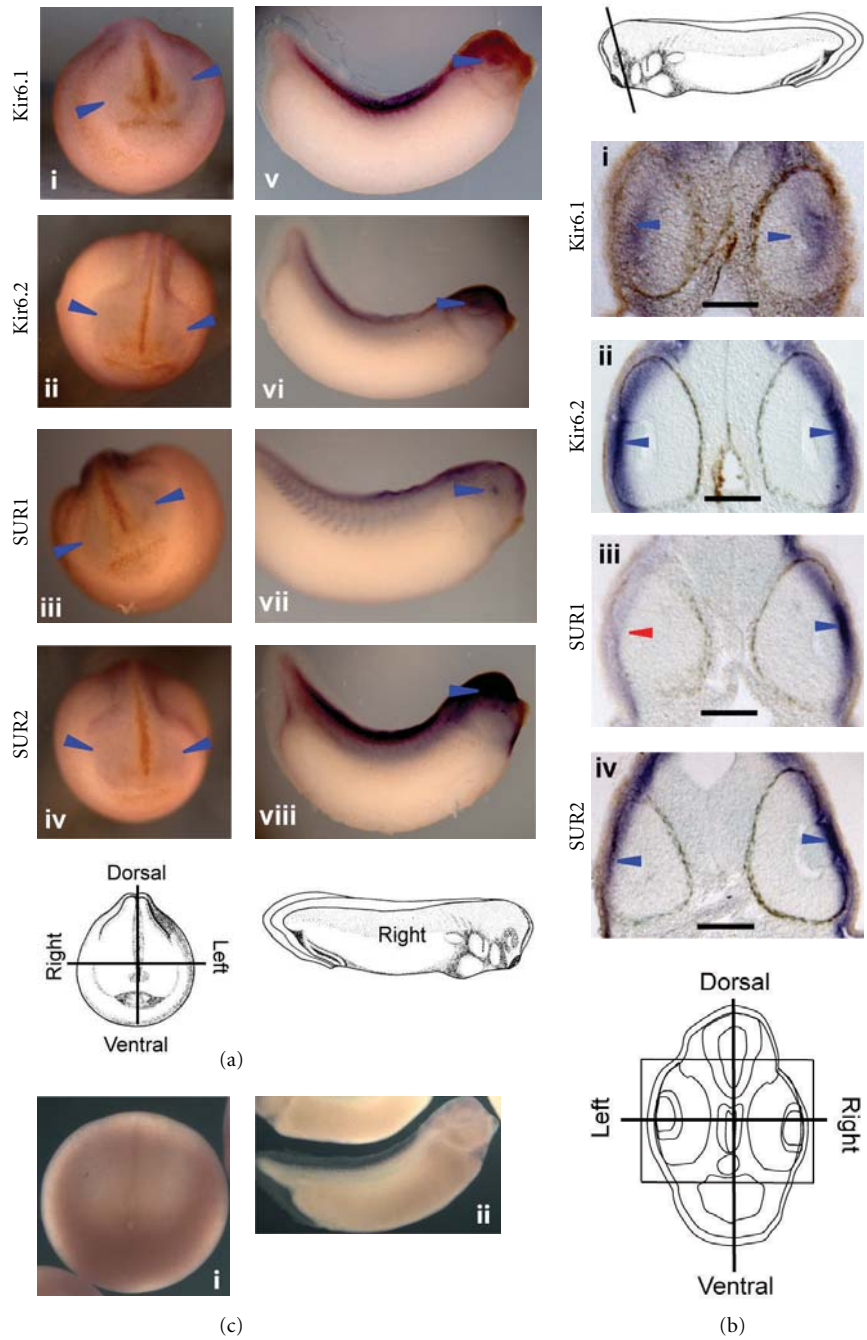

Figure 3: K_{ATP} channels are expressed in the putative eye regions and in the eye tissue in a left-right asymmetric manner. (a) *Xenopus* embryos at stage 18 (i)–(iv) and stage 30 (v)–(viii) were analyzed by *in situ* hybridization for K_{ATP} channel subunits showing their presence in the putative eye region ((i)–(iv) blue arrowheads) as well as in differentiated eye tissue ((v)–(viii) blue arrowheads). All four subunits ($K_{ir}6.1$, $K_{ir}6.2$, SUR1, and SUR2) were found to be present in the putative and developed eye tissue. In addition to the eye tissue, the K_{ATP} channel subunits were also present in the general head region and the dorsal region of the trunk. Illustration shows a stage 18 embryo with the dorsal-ventral and the left-right axes. (b) Transverse JB4 sections of *in situ* hybridized *Xenopus* embryos at stage 30 (i)–(iv) showing left-right distribution of the K_{ATP} channel subunits. Illustration shows the plane of sectioning of the stage 30 embryo. $K_{ir}6.1$ expression is found in the inner retinal part of the eye vesicle ((i) blue arrowheads) and in the brain especially in the cells lining the ventricle and in some cells surrounding the eye tissue. $K_{ir}6.2$, SUR1, and SUR2 expression is found in the inner layer of the 2-layer epidermis with intense staining at the lens placode ((ii)–(iv) blue arrowheads). $K_{ir}6.1$, $K_{ir}6.2$, and SUR2 expression is symmetric ((i), (ii), and (iv) blue arrowheads). SUR1 shows asymmetric distribution ((iii) red and blue arrowheads) where red arrowheads indicate the side with lessened expression. Scale bars = 100 μm. Schematic shows a transverse section of a stage 30 embryo with the dorsal-ventral and the left-right axes indicated. (c) Sense probes showed no signal detected at neurula (i) or tailbud (ii) stages.

Probes to $K_{ir}6.2$, SUR1, and SUR2 showed signal in the inner layer of the epidermis with intense expression in the lens placode (Figure 3(b), (ii)–(iv) blue arrowheads). $K_{ir}6.1$ expression was found in the retinal layer of the developing eye (Figure 3(b), (i) blue arrowheads). $K_{ir}6.1$ was also found in the cells surrounding the eye tissue and along the brain ventricle (Figure 3(b), (i)). Strikingly, expression of the SUR1 transcript was asymmetric, being expressed strongly in the right eye (Figure 3(b), (iii)-(iv), $n = 8$). No-probe controls and SUR1 and 2 sense probes, exposed for the same length of time as embryos probed with antisense RNA, exhibited no signal at any stage tested (Figure 3(c), (i), (ii)). These data reveal a novel left-right asymmetric marker distinguishing the left and right eyes at the transcriptional level. In our previous study we implicated the K_{ATP} channel in regulating the eye-specific polarization signal [68]. Although the native *Xenopus* transcripts matching the expression of these probes remain to be identified within the incompletely sequenced *X. laevis* genome, the current findings of asymmetry revealed by mouse K_{ATP} channel probes are consistent with endogenous K_{ATP} channels as a basis for the physiological differences between the left and right eyes.

2.5. Melanocyte Colonization of Lateral Trunk Is Consistently Left-Right Asymmetric. The discovery of a cryptic functional and physiological asymmetry in a paired organ led us to examine other processes for asymmetries that may have heretofore escaped notice; we were especially interested in other descendants of neural precursors. Pigment cells (melanocytes, derived from neural crest cells) were identified using *in situ* hybridization with a probe against *Trp2* (also known as *Dct*), a definitive marker of melanocytes [96] at stage 30. We observed that 79% of embryos had significantly more *Trp2*-positive cells (melanocytes) on their left side compared to their right side (Figures 4(a) and 4(b) and Table 1 ($n = 28$ and $P = 0.002$, paired t-test)).

This bias in melanocyte numbers could be a result of left-right-biased differentiation of neural crest cells into melanocytes or due to biased migration of differentiated melanocytes. To test whether the observed asymmetry in melanocytes was due to asymmetric melanocyte differentiation before migration (greater number of melanocytes being produced on one side at the very beginning of melanocyte specification), we performed *in situ* hybridization with *Trp2* at an earlier stage 26 (before melanocyte migration begins). At this stage, in sections taken through the trunk, quantitative analysis of the area of *Trp2*-positive regions showed no significant difference between the right and left sides ($n = 10$) (Figure 4(c)). These results show that the left-side bias seen in melanocyte numbers at stage 30 is likely not due to biased differentiation of melanocytes from neural crest cells and favors a mechanism based on biased migration rates of differentiated melanocytes. From these results we also conclude that subtle left-right asymmetry in symmetric structures is not unique to the eye but also extends to the behavior of migratory neural crest derivatives (Figure 5).

3. Discussion

3.1. Development of Xenopus Eyes Is Asymmetric. Previously, we showed that a specific range of relatively hyperpolarized membrane voltage regulates *Xenopus* eye development [68, 69]. While the eyes are paired organs and have been assumed to be symmetric, here we show that the bioelectric signal that endogenously regulates their formation exhibits a distinct and consistent left-right asymmetry. Hyperpolarization of the right eye occurs first (Figure 1), and the right side is consistently more sensitive to functional perturbations (Figures 2(d) and 2(e)). This observation of a right-side-first bioelectrical signal coincides with previous documentation of a morphological right-sided asymmetry of neural structures in *Xenopus*, including retina, olfactory placode, and ganglia of nerve viii [97] and is consistent with developmental asymmetries of the visual system described in flatfish [98], *Ciona intestinalis* [99], and chicken [100–102].

While consistent and statistically significant, the degree of this asymmetry (61%) is not as high as that of crucial visceral organs like heart and gut (99% in wild-type *Xenopus*). Other groups have suggested that developmental asymmetries observed in symmetric structures arise as a side effect from incomplete shielding of symmetrical structures from the left-right signaling pathway coincident in time and space and have demonstrated that retinoic acid signaling has a role in protecting developing symmetric structures from these left-right signals. Since blocking retinoic acid signaling does not exacerbate the level of asymmetry in the eye signal in our studies (Figure 1(d)), our data do not support the role of retinoic acid in the shielding of this asymmetry. However, it is possible that another (yet unknown) pathway exists that serves to reduce or mask an inherent asymmetry of the eye formation process, derived from the influence of body-wide left-right patterning signals. Another intriguing possibility is that this asymmetry is not a side effect but instead has been evolutionarily conserved due to functional relevance.

Consistent asymmetry in handedness is seen in 60% of nonhuman primates but in 90% of humans [6, 103]. Moreover, a number of studies have reported left-right asymmetries in visual function related to food/prey and predatory responses in fish, amphibians, reptiles, birds, and mammals [104–110]. It is possible that subtle differences in the bioelectrical patterning signals of the visual system, along with asymmetries of brain and cognitive processing, are involved in establishing these behavioral and functional asymmetries. In *C. elegans,* for example, a stochastic lateral inhibition system involving ion channels results in lateralized neural differentiation and function [111–115]. It is tempting to speculate that this asymmetric bioelectric signal could trigger differential genetic, chemical, and/or biophysical patterns that overlay upon the universal eye development pattern allowing the left and right sides of the visual system to develop differing visual functionality. This is supported by our observation that depolarization-mediated disruption of endogenous bilateral polarization cues results in a right-biased disruption of eye formation. However, further functional studies will be required to test this hypothesis. In addition, this mechanism appears to

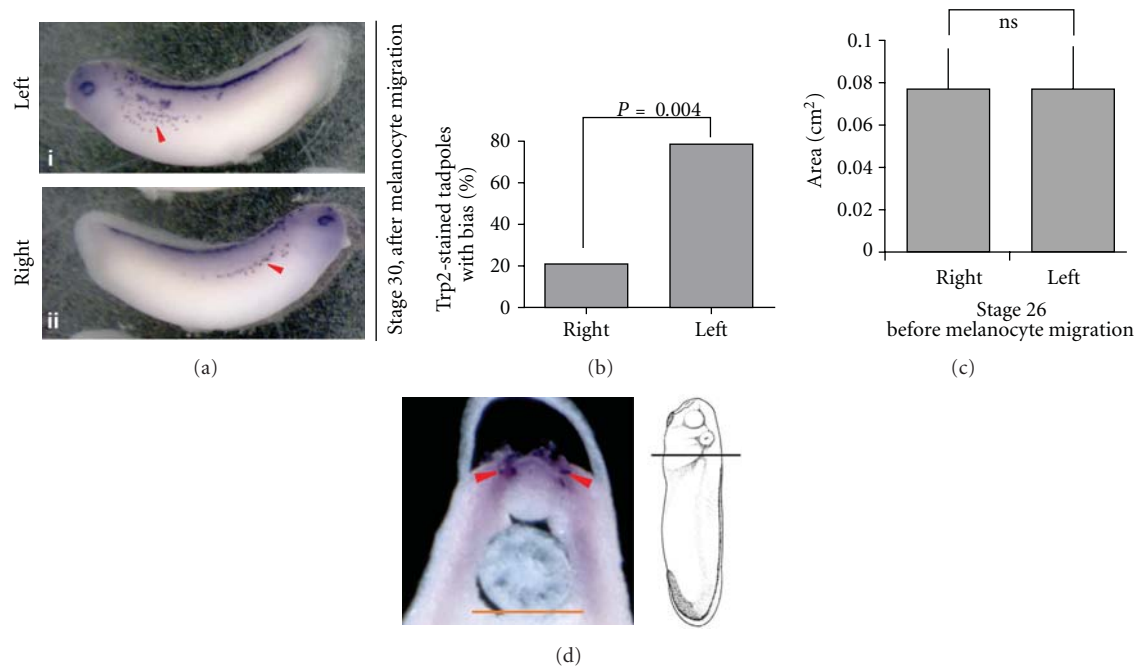

Figure 4: Biased migration of melanocytes along the left-right axis. (a) *Xenopus* embryos at stage 30 analyzed by *in situ* hybridization for melanocyte marker trp2 show a higher number of melanocytes on the left side (i) as compared to the right side (ii) of the embryo. Red arrowheads indicate the melanocytes being counted. (b) Quantification of a number of stage 30 embryos showing biased trp2 spots indicates that 78.6% of embryos show a leftward bias of trp2 staining. 21.4% of embryos showed higher trp2 staining on the right side. The data were analyzed using a two-tailed Binomial calculation; $n = 28$. (See Table 1 for details). (c) Quantification of *Xenopus* embryos at stage 26 analyzed by *in situ* hybridization for trp2 shows no asymmetry in melanocyte number prior to their migration. Due to dense staining at this early stage individual stained cells could not be resolved and counted, hence the stained region was marked, and the area was quantified. Quantification of the *trp2* stain on the left and right sides of embryos ($n = 10$) shows no significant difference in the staining. The areas of the signal on right and left sides were compared using a *t*-test. (d) Transverse agarose sections of *in situ* hybridized *Xenopus* embryo at stage 26 showing left-right distribution of the melanocyte marker *trp2* as measured. Illustration shows the plane of sectioning of the stage 26 embryo. Symmetric *trp2* expression (red arrowheads) is found in the area around the neural tube. Scale bar = 200 μ.

be conserved, as a similar right-biased disruption of eye regeneration is observed in planaria upon depolarization [60]. Thus, comparative studies of possible asymmetries of developmental physiology and subsequent function of eyes (and other structures) among taxa may pay off in the discovery of novel asymmetries in paired organs.

3.2. Eye Asymmetry versus Body Asymmetry. In the past few years, the zebrafish has become a good model for studies of asymmetry in developmental physiology, as they not only show lateralized functions but also show distinct left-right asymmetries in brain structure [116–119]. In *Xenopus*, however, no consistent marker of brain laterality has been described. The endogenous hyperpolarization described above is a convenient novel readout of neural asymmetry because it can be imaged in live animals and is thus compatible with behavioral testing and other experimental paradigms requiring the raising of animals with known neural laterality to older stages.

What is the link between the subtle asymmetries of neural derived organs and the main pathway that determines left-right asymmetry of the body? One of the fascinating aspects of left-right asymmetry determination is the disconnect between the sidedness of the major body organs and the brain. Human *situs inversus* patients (who exhibit complete reversal of the left-right body axis) show normal levels of right handedness and language lateralization [120, 121]. However, certain other behavioral traits (e.g., the hand on which the wristwatch is worn) are found to be reversed [7].

In zebrafish, the asymmetry of the diencephalic region, habenula and parapineal nuclei [116] were found to be reversed in *situs inversus* animals, along with a subset of their visual laterality behavior [110]. Moreover, it is now known that individual neurites have a consistent clockwise chirality of outgrowth [122] and turning [123]. Our data in *Xenopus* demonstrate the linkage of basic body asymmetry to the cryptic asymmetry of the eye: a treatment that randomized the major visceral organs also eliminated the right-side-first bias of the eye patterning signal, suggesting that the asymmetry of the eye derives from the same pathway that patterns the major left-right axis in *Xenopus*.

3.3. The Physiological Origin of the Asymmetry. What is responsible for the consistently different V_{mem} in the left and right sides of the developing head? The K_{ATP} channel consists of K_{ir} and SUR subunits and is responsible for setting resting

Table 1: Biased migration of melanocytes. Embryos were stained with the melanocyte marker Trp2 using *in situ* hybridization to identify pigment cells. The pigment spots on both the left and the right side of each embryo were counted. Student's *t*-test analysis of the raw data shows a significantly higher ($P = 0.002$) melanocyte migration on the left side of the embryos.

Embryo	Left	Right
1	25	16
2	10	9
3	18	27
4	11	13
5	7	4
6	15	17
7	29	24
8	19	13
9	15	10
10	1	2
11	27	18
12	10	6
13	8	3
14	7	3
15	45	25
16	7	4
17	11	10
18	9	14
19	7	5
20	10	4
21	6	4
22	12	7
23	6	7
24	16	8
25	15	5
26	7	5
27	10	7
28	7	4
Average	13.21	9.78
Stddev	9.11	7.08
t-test (paired)	0.002088	
Embryos with more melanocytes	22 (78%)	6 (22%)

potential in a number of cell types [124]. K_{ATP} channel activity depends on the resting V_{mem}, ATP levels in the cell, the external potassium levels, and the limiting levels of each subunit. Our expression data (Figure 3, which extends and complements early immunohistochemistry data on K_{ATP} channels in the hatching gland, [125]) reveal a consistent left-right asymmetry in the levels of a transcript with homology to the mouse SUR K_{ATP} channel subunit. Comparison of the mouse SUR probe sequence to the completed *Xenopus tropicalis* genome using BLAST [126] gives matches with SUR1 ($P = 2E-10$), SUR2 ($P = 2E-75$), but no other target (the next best match is PGER2 at nonsignificant $P = 0.39$), which supports the high probability of the probe picking up a SUR-like mRNA in *Xenopus laevis*. While we have not yet identified the native transcript corresponding to this signal, the high specificity of the staining pattern and the stringency of the *in situ* hybridization conditions make it likely that the mouse probe of SUR is picking up a native SUR-like mRNA that has not yet been characterized within the incompletely sequenced *X. laevis* genome.

The observed asymmetry in the presence of SUR1 subunits is likely to result in a larger number of functional K_{ATP} channels on the side with greater SUR1 expression. On a background of equal initial V_{mem} and external potassium levels on the left and right sides, the asymmetry in subunits available for the formation of functional K_{ATP} channels may explain the difference in the V_{mem} on the left and right sides. It is possible that the asymmetry in functional K_{ATP} channels is also responsible for the observed asymmetry in sensitivity to eye malformation upon perturbing the V_{mem}. Other channels may be involved in generating the observed asymmetric polarization. Comparative expression profiling and functional testing on both sides in the eye region may reveal other candidate/s that cooperate with K_{ATP} to generate the asymmetric polarization eye patterning signal.

The K_{ATP} subunits are expressed mainly in the surface ectoderm, which forms the eye placode. Interaction between the ectodermal placode and the underlying neuroectodermal and mesodermal layers results in invagination of the optic cup and eye formation [127–130]. The K_{ATP} ion channels in the surface ectoderm, and the bioelectric cell properties they regulate, may participate in modulating these signaling interactions.

One important feature of the observed bioelectric asymmetry is its temporal properties: although the right eye signal is seen first, the eye-specific V_{mem} signature is ultimately seen on both sides (the left side delayed by 20–30 minutes), resulting in anatomically symmetrical and equal sized eyes. As the function of ion channels is gated by posttranslational events, physiological feedback loops implemented by voltage-sensitive channels could amplify stable differences in V_{mem}, leading to distinct voltage gradients in cell groups expressing similar complements of ion channel proteins. Future work will profile the other major conductances present in eye cells and quantitatively characterize and model the molecular-genetic and temporal details of the circuit that functions in eye precursor cells to control resting potential. Such circuits are likely to exhibit distinct stable V_{mem} states, as has been shown in mouse (muscle) cells to be due to potassium inward rectifying channels [131].

3.4. Neural Crest Derivatives Are Also Consistently Left-Right Asymmetric. A similar asymmetry was observed in neural crest-derived pigment cells, melanocytes. Melanocytes follow specific migration paths along the side of the *Xenopus* embryo after differentiation from neural crest. Interestingly, a consistent left-right asymmetry in the number of melanocytes was found upon careful analysis. Our analysis of Trp2-positive cells prior to onset of migration (stage

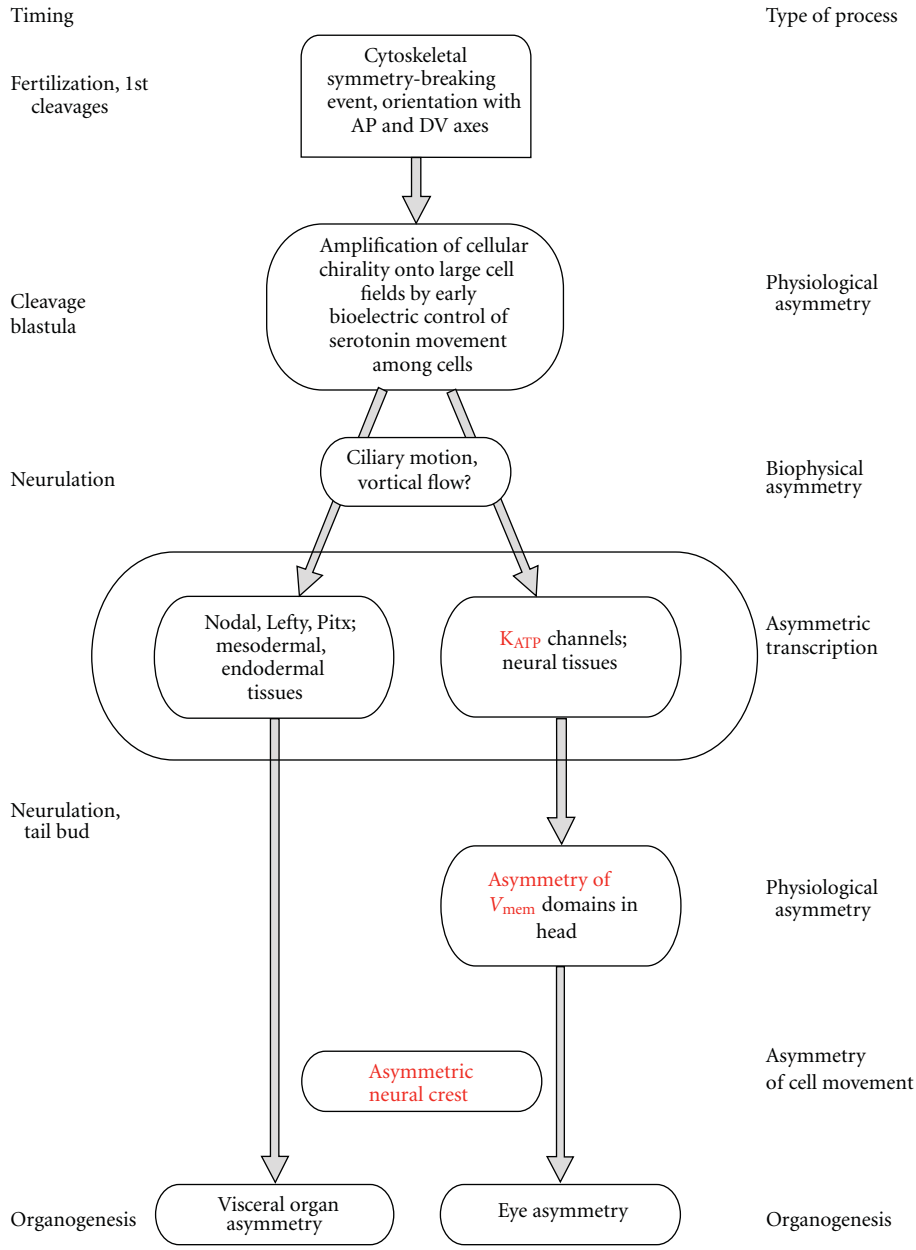

Figure 5: A model of physiological asymmetries within the overall scheme of the left-right patterning pathway. In *Xenopus*, bilateral symmetry is first broken, and the left-right axis is consistently oriented with respect to the dorsoventral and anterior-posterior axes, during early cleavage stages [8, 81]. The intracellular chirality is amplified onto multicellular cell fields during cleavage and blastula stages by the voltage-dependent movement of small molecule determinants through gap junctions [82–84]. The transduction of voltage gradient differences by epigenetic mechanisms [85] and other biophysical events such as ciliary movement [86] initiates at least two asymmetric transcriptional cascades. The first is the well-known Nodal, Lefty, and Pitx2 cassette that drives asymmetric organogenesis of the visceral organs. The other is the asymmetry of K_{ATP} channel subunits expressed in neural tissues, which results in asymmetric gradients of resting potential that directs development of the eye [87]. Future work will determine the functional linkage of the reported asymmetry in neural crest cell movement.

26) revealed that there is no apparent asymmetry in the extent of melanocyte differentiation from the neural crest cells, suggesting that the observed asymmetry is due to asymmetric migration patterns. The source of asymmetric migratory cues or mechanisms ensuring left-right asymmetrically biased response of cells to migration cues (as has been observed in mammalian cells [132, 133]) remains to be analyzed in future work. The evolutionary or developmental role of such asymmetric melanocyte distributions is not yet known; indeed, it is possible that careful quantification of cell number or other properties in other developmental events may reveal other heretofore-unrecognized consistent

asymmetries in systems that are currently considered to be symmetrical.

3.5. Conclusion. The identification of subtle physiological and cell positioning asymmetries in *Xenopus* development raises a number of open questions. It is possible that consistent asymmetries in bioelectric state, cell number, and sensitivity to specific perturbations remain to be discovered in many different paired (symmetric) organs. The anatomical and genetic profiling studies carried out to date may have only scratched the surface of the developmental information embedded in various somatic tissues at the level of mRNA and protein profiles and would likely not reveal physiology differences. The identification of such asymmetries, as well as their molecular origins, and the characterization of their interactions with the major left-right axial patterning cascade are likely to reveal fascinating aspects of developmental biology with significant evolutionary implications. Moreover, a mechanistic understanding of these subtle asymmetries will provide insight into the form, function, and robustness of the nervous system and may help address the lateralized diseases of both nervous and nonnervous organs.

4. Materials and Methods

4.1. Animal Husbandry. Xenopus laevis embryos were collected and fertilized *in vitro* according to standard protocols [134], in 0.1X Modified Marc's Ringers (MMR; pH 7.8). *Xenopus* embryos were housed at 14–18°C and staged according to Nieuwkoop and Faber [135]. All experiments were approved by the Tufts University Animal Research Committee in accordance with the *Guide for Care and Use of Laboratory Animals*, protocol number: M2011-70.

4.2. Imaging of Membrane Voltage Patterns Using CC2-DMPE. CC2-DMPE (molecular probes) stocks (stock: 1 mg/mL in DMSO) were diluted 1 : 1000 in 0.1X MMR for a final concentration of 0.2 μM. Stage 15-16 embryos were soaked in dye for 1.5 h. Embryos in solution were imaged using the CC2 cube set on an Olympus BX61 microscope with an ORCA digital CCD camera (Hamamatsu) with Metamorph software. See [66, 67] for additional details. For determining the bias in eye CC2-DMPE signal, embryos were imaged at regular intervals. The side of the embryo that first showed the eye CC2-DMPE signal was noted, and the embryos were kept under observation until signal was seen on both sides. Time difference between the right and left eye CC2-DMPE signals was measured by taking images at regular intervals of 10 minutes. While CC2-DMPE used alone cannot precisely quantify V_{mem} levels, the strong fluorescence from this positively charged dye has been shown previously to reliably identify hyperpolarized regions as confirmed by electrophysiological impalement [65–67, 136] and to identify the same locations of hyperpolarized cells in the early face as did prior studies using ratiometric imaging [69].

4.3. Microinjection. Capped, synthetic mRNAs were generated using the Ambion mMessage mMachine kit, resuspended in water, and injected (2.7 nL per blastomere) into embryos in 3% Ficoll. Results of injections are reported as percentage of injected embryos showing eye phenotypes, sample size (n) and P values comparing treated groups to controls. For lineage tracing, 4-cell embryos were injected with mRNA encoding β-galactosidase. At stage 45, fixed embryos were stained by incubation with X-gal substrate.

4.4. In Situ Hybridization. In situ hybridization was performed according to standard protocols [137]. Accession numbers for the sequences used as probes were $K_{ir}6.1$ NM_008428.4, $K_{ir}6.2$ NM_001204411.1, SUR1 NM_011510.3, and SUR2 NM_001044720.1. *Xenopus* embryos were collected and fixed in MEMFA. Prior to *in situ* hybridization, embryos were washed in PBS + 0.1% Tween-20 and then transferred to ethanol through a 25%/50%/75% series. *In situ* probes were generated *in vitro* from linearized templates using DIG labeling mix (Invitrogen, Carlsbad, CA, USA). Chromogenic reaction times were optimized to maximize signal and minimize background. Histological sections were obtained by embedding embryos after *in situ* hybridization in JB4 according to manufacturer's instructions (Polysciences). Prior to sectioning, one corner of the block was physically marked to allow unambiguous orientation of section images with respect to the left-right axis (for sections in Figure 3(b)).

4.4.1. Quantification of In Situ Signal. Trp2 *in situ* hybridized embryos were embedded in 4% low melting point agarose as previously described and sectioned at 100 μm [138]. The sections were imaged using a Nikon SMZ1500 microscope with a Q-imaging Retiga 2000R camera. Using NIH's ImageJ software the regions exhibiting purple signal on the left and right side of the sections were marked using the freehand selection tool, and the area of the Trp2 stain was automatically quantified. The 3rd section from the last section containing eye was selected from each of the 10 different embryos and used for quantification.

4.5. Heterotaxia-Inducing Treatment. Embryos were kept in 0.1X MMR (pH 4.0–4.05) from fertilization until stage 12-13 and then moved to 0.1x MMR (pH 7.8) for the remainder of the experiment. At stage 45, the *situs* of the internal organs was scored by visual inspection of the heart, gut, and gallbladder as previously reported [17]. Categorical data analysis of the CC2-DMPE staining following drug treatment was done using ternary plots [75].

4.6. Retinoic Acid Receptor Inhibitor (Ro-41-5253) Treatment. Embryos were kept in 0.1X MMR from fertilization. At ~ stage 11 Ro-41-5253 was added into 0.1X MMR with a final concentration of 1.5 μM. At stage 18, a portion of the embryos were fixed and used for *in situ* hybridization. Categorical data analysis of the CC2-DMPE staining following drug treatment was done on the remaining live embryos using ternary plots [75].

4.7. Statistics. All Statistical analyses were performed using Graphpad Prism (GraphPad Software, La Jolla, CA, USA), except in case of the categorical data analyses where ternary plots algorithms were used (https://webscript.princeton.edu/~rburdine/stat/three_categories). For data pooled from various iterations, Chi-square test or two-tailed Binomial calculation was used. Nonpooled data was analyzed by *t*-test (for 2 groups) or ANOVA (for more than two groups).

Authors' Contribution

V. P. Pai and M. Levin designed research, V. P. Pai, M. Levin, L. N. Vandenberg, and D. Blackiston performed research, and M. Levin and V. P. Pai wrote the paper.

Acknowledgments

The authors thank Punita Koustubhan, Amber Currier, Joan Lemire, and Claire Stevenson for *Xenopus* husbandry and general lab assistance and Daryl Davies and Miriam Fine for the GlyCl expression construct. They also especially thank Dany S. Adams and Brook Chernet for microscopy assistance and Sherry Aw for many helpful ideas and discussions on this project. This work was supported by NIH Grants EY018168, MH081842, and GM077425 to M. Levin. The authors are also grateful for the support of the G. Harold and Leila Y. Mathers Charitable Foundation.

References

[1] A. C. Neville, *Animal Asymmetry*, Edward Arnold, London, UK, 1976.

[2] A. R. Palmer, "From symmetry to asymmetry: phylogenetic patterns of asymmetry variation in animals and their evolutionary significance," *Proceedings of the National Academy of Sciences of the United States of America*, vol. 93, no. 25, pp. 14279–14286, 1996.

[3] H. Peeters and K. Devriendt, "Human laterality disorders," *European Journal of Medical Genetics*, vol. 49, no. 5, pp. 349–362, 2006.

[4] A. F. Ramsdell, "Left-right asymmetry and congenital cardiac defects: getting to the heart of the matter in vertebrate left-right axis determination," *Developmental Biology*, vol. 288, no. 1, pp. 1–20, 2005.

[5] B. W. Bisgrove, S. H. Morelli, and H. J. Yost, "Genetics of human laterality disorders: insights from vertebrate model systems," *Annual Review of Genomics and Human Genetics*, vol. 4, pp. 1–32, 2003.

[6] I. McManus, *Right Hand, Left Hand: The Origins of Asym metry in Brains, Bodies, Atoms and Cultures*, Harvard University Press, 2002.

[7] I. C. McManus, N. Martin, G. F. Stubbings, E. M. K. Chung, and H. M. Mitchison, "Handedness and situs inversus in primary ciliary dyskinesia," *Proceedings of the Royal Society B*, vol. 271, no. 1557, pp. 2579–2582, 2004.

[8] L. N. Vandenberg and M. Levin, "Far from solved: a perspective on what we know about early mechanisms of left-right asymmetry," *Developmental Dynamics*, vol. 239, no. 12, pp. 3131–3146, 2010.

[9] M. Levin, "Left-right asymmetry in embryonic development: a comprehensive review," *Mechanisms of Development*, vol. 122, no. 1, pp. 3–25, 2005.

[10] P. Spéder, A. Petzoldt, M. Suzanne, and S. Noselli, "Strategies to establish left/right asymmetry in vertebrates and invertebrates," *Current Opinion in Genetics and Development*, vol. 17, no. 4, pp. 351–358, 2007.

[11] T. Sun and C. A. Walsh, "Molecular approaches to brain asymmetry and handedness," *Nature Reviews Neuroscience*, vol. 7, no. 8, pp. 655–662, 2006.

[12] B. Basu and M. Brueckner, "Chapter Six Cilia. Multifunctional organelles at the center of vertebrate left-right asymmetry," *Current Topics in Developmental Biology*, vol. 85, pp. 151–174, 2008.

[13] R. P. Harvey, "Links in the left/right axial pathway," *Cell*, vol. 94, no. 3, pp. 273–276, 1998.

[14] S. Aw, D. S. Adams, D. Qiu, and M. Levin, "H,K-ATPase protein localization and Kir4.1 function reveal concordance of three axes during early determination of left-right asymmetry," *Mechanisms of Development*, vol. 125, no. 3-4, pp. 353–372, 2008.

[15] M. V. Danilchik, E. E. Brown, and K. Riegert, "Intrinsic chiral properties of the Xenopus egg cortex: an early indicator of left-right asymmetry," *Development*, vol. 133, no. 22, pp. 4517–4526, 2006.

[16] C. Pohl, "Left-right patterning in the *C. elegans* embryo: unique mechanisms and common principles," *Communicative and Integrative Biology*, vol. 4, no. 1, pp. 34–40, 2011.

[17] D. S. Adams, K. R. Robinson, T. Fukumoto et al., "Early, H^+-V-ATPase-dependent proton flux is necessary for consistent left-right patterning of non-mammalian vertebrates," *Development*, vol. 133, no. 9, pp. 1657–1671, 2006.

[18] M. Levin, T. Thorlin, K. R. Robinson, T. Nogi, and M. Mercola, "Asymmetries in H^+/K^+-ATPase and cell membrane potentials comprise a very early step in left-right patterning," *Cell*, vol. 111, no. 1, pp. 77–89, 2002.

[19] Á. Raya, Y. Kawakami, C. Rodríguez-Esteban et al., "Notch activity acts as a sensor for extracellular calcium during vertebrate left-right determination," *Nature*, vol. 427, no. 6970, pp. 121–128, 2004.

[20] A. Garic-Stankovic, M. Hernandez, G. R. Flentke, M. H. Zile, and S. M. Smith, "A ryanodine receptor-dependent $Cai2^+$ asymmetry at Hensen's node mediates avian lateral identity," *Development*, vol. 135, no. 19, pp. 3271–3280, 2008.

[21] J. A. Kreiling, Z. L. Balantac, A. R. Crawford et al., "Suppression of the endoplasmic reticulum calcium pump during zebrafish gastrulation affects left-right asymmetry of the heart and brain," *Mechanisms of Development*, vol. 125, no. 5-6, pp. 396–410, 2008.

[22] U. Sienknecht, "Genetic stabilization of vertebrate bilateral limb symmetry as an example of cryptic polarity," *Developmental Biology*, vol. 295, pp. 414–415, 2006.

[23] C. P. Klingenberg, G. S. McIntyre, and S. D. Zaklan, "Left-right asymmetry of flywings and the evolution of body axes," *Proceedings of the Royal Society B*, vol. 265, no. 1413, p. 2455, 1998.

[24] C. P. Klingenberg, G. S. McIntyre, and S. D. Zaklan, "Left-right asymmetry of fly wings and the evolution of body axes," *Proceedings of the Royal Society of London B*, vol. 265, pp. 1255–1259, 1998.

[25] J. Levy and J. M. Levy, "Human lateralization from head to foot: sex-related factors," *Science*, vol. 200, no. 4347, pp. 1291–1292, 1978.

[26] U. Mittwoch, "Genetics of mammalian sex determination: some unloved exceptions," *Journal of Experimental Zoology*, vol. 290, no. 5, pp. 484–489, 2001.

[27] C. P. Klingenberg and G. S. Mcintyre, "Geometric morphometrics of developmental instability: analyzing patterns of fluctuating asymmetry with procrustes methods," *Evolution*, vol. 52, no. 5, pp. 1363–1375, 1998.

[28] M. V. Angelopoulou, V. Vlachou, and D. J. Halazonetis, "Fluctuating molar asymmetry in relation to environmental radioactivity," *Archives of Oral Biology*, vol. 54, no. 7, pp. 666–670, 2009.

[29] G. C. Vilhais-Neto, M. Maruhashi, K. T. Smith et al., "Rere controls retinoic acid signalling and somite bilateral symmetry," *Nature*, vol. 463, no. 7283, pp. 953–957, 2010.

[30] J. Vermot and O. Pourquié, "Retinoic acid coordinates somitogenesis and left-right patterning in vertebrate embryos," *Nature*, vol. 435, no. 7039, pp. 215–220, 2005.

[31] L. Saúde, R. Lourenço, A. Gonçalves, and I. Palmeirim, "terra is a left-right asymmetry gene required for left-right synchronization of the segmentation clock," *Nature Cell Biology*, vol. 7, no. 9, pp. 918–920, 2005.

[32] J. P. Golding, T. A. Partridge, J. R. Beauchamp et al., "Mouse myotomes pairs exhibit left-right asymmetric expression of MLC3F and α-skeletal actin," *Developmental Dynamics*, vol. 231, no. 4, pp. 795–800, 2004.

[33] J. P. Golding, S. Tsoni, M. Dixon et al., "Heparin-binding EGF-like growth factor shows transient left-right asymmetrical expression in mouse myotome pairs," *Gene Expression Patterns*, vol. 5, no. 1, pp. 3–9, 2004.

[34] J. Milaire, "Histological changes induced in developing limb buds of C57BL mouse embryos submitted in utero to the combined influence of acetazolamide and cadmium sulphate," *Teratology*, vol. 32, no. 3, pp. 433–451, 1985.

[35] M. Barr Jr., "The teratogenicity of cadmium chloride in two stocks of Wistar rats," *Teratology*, vol. 7, no. 3, pp. 237–242, 1973.

[36] W. M. Layton Jr. and M. W. Layton, "Cadmium induced limb defects in mice: strain associated differences in sensitivity," *Teratology*, vol. 19, no. 2, pp. 229–235, 1979.

[37] A. T. Smith, G. H. Sack, and G. J. Taylor, "Holt-oram syndrome," *Journal of Pediatrics*, vol. 95, no. 4, pp. 538–543, 1979.

[38] M. Delaney and T. K. Boyd, "Case report of unilateral clefting: is sonic hedgehog to blame?" *Pediatric and Developmental Pathology*, vol. 10, no. 2, pp. 117–120, 2007.

[39] L. J. Paulozzi and J. M. Lary, "Laterality patterns in infants with external birth defects," *Teratology*, vol. 60, no. 5, pp. 265–271, 1999.

[40] R. A. Newbury-Ecob, R. Leanage, J. A. Raeburn, and I. D. Young, "Holt-Oram syndrome: a clinical genetic study," *Journal of Medical Genetics*, vol. 33, no. 4, pp. 300–307, 1996.

[41] C. J. Hatcher, M. M. Goldstein, C. S. Mah, C. S. Delia, and C. T. Basson, "Identification and localization of TBX5 transcription factor during human cardiac morphogenesis," *Developmental Dynamics*, vol. 219, no. 1, pp. 90–95, 2000.

[42] B. G. Bruneau, M. Logan, N. Davis et al., "Chamber-specific cardiac expression of Tbx5 and heart defects in Holt- Oram syndrome," *Developmental Biology*, vol. 211, no. 1, pp. 100–108, 1999.

[43] S. O. Lewin and J. M. Opitz, "Fibular a/hypoplasia: review and documentation of the fibular developmental field," *American Journal of Medical Genetics. Supplement*, vol. 2, pp. 215–238, 1986.

[44] M. Levin and M. Mercola, "Gap junction-mediated transfer of left-right patterning signals in the early chick blastoderm is upstream of Shh asymmetry in the node," *Development*, vol. 126, no. 21, pp. 4703–4714, 1999.

[45] C. L. Clericuzio, "Clinical phenotypes and Wilms tumor," *Medical and Pediatric Oncology*, vol. 21, no. 3, pp. 182–187, 1993.

[46] J. F. Fraumeni Jr., C. F. Geiser, and M. D. Manning, "Wilms' tumor and congenital hemihypertrophy: report of five new cases and review of literature," *Pediatrics*, vol. 40, no. 5, pp. 886–899, 1967.

[47] H. E. Hoyme, L. H. Seaver, K. L. Jones et al., "Isolated hemihyperplasia (hemihypertrophy): report of a prospective multicenter study of the incidence of neoplasia and review," *American Journal of Medical Genetics Part A*, vol. 79, pp. 274–278, 1998.

[48] R. C. Albertson and P. C. Yelick, "Roles for fgf8 signaling in left-right patterning of the visceral organs and craniofacial skeleton," *Developmental Biology*, vol. 283, no. 2, pp. 310–321, 2005.

[49] C. Niehrs, "On growth and form: a Cartesian coordinate system of Wnt and BMP signaling specifies bilaterian body axes," *Development*, vol. 137, no. 6, pp. 845–857, 2010.

[50] J. S. Kanodia, R. Rikhy, Y. Kim et al., "Dynamics of the Dorsal morphogen gradient," *Proceedings of the National Academy of Sciences of the United States of America*, vol. 106, no. 51, pp. 21707–21712, 2009.

[51] L. V. Beloussov, "Mechanically based generative laws of morphogenesis," *Physical Biology*, vol. 5, no. 1, Article ID 015009, 2008.

[52] L. V. Beloussov and V. I. Grabovsky, "Morphomechanics: goals, basic experiments and models," *International Journal of Developmental Biology*, vol. 50, no. 2-3, pp. 81–92, 2006.

[53] S. Sundelacruz, M. Levin, and D. L. Kaplan, "Role of membrane potential in the regulation of cell proliferation and differentiation," *Stem Cell Reviews and Reports*, vol. 5, no. 3, pp. 231–246, 2009.

[54] D. J. Blackiston, K. A. McLaughlin, and M. Levin, "Bioelectric controls of cell proliferation: ion channels, membrane voltage and the cell cycle," *Cell Cycle*, vol. 8, no. 21, pp. 3519–3528, 2009.

[55] M. Levin, "Errors of Geometry: regeneration in a broader perspective," *Seminars in Cell and Developmental Biology*, vol. 20, no. 6, pp. 643–645, 2009.

[56] C. D. McCaig, B. Song, and A. M. Rajnicek, "Electrical dimensions in cell science," *Journal of Cell Science*, vol. 122, no. 23, pp. 4267–4276, 2009.

[57] C. D. McCaig, A. M. Rajnicek, B. Song, and M. Zhao, "Controlling cell behavior electrically: current views and future potential," *Physiological Reviews*, vol. 85, no. 3, pp. 943–978, 2005.

[58] M. Levin, "Molecular bioelectricity In developmental biology: new tools and recent discoveries," *BioEssays*, vol. 34, no. 3, pp. 205–217, 2011.

[59] D. S. Adams, "A new tool for tissue engineers: ions as regulators of morphogenesis during development and regeneration," *Tissue Engineering A*, vol. 14, no. 9, pp. 1461–1468, 2008.

[60] T. Nogi, Y. E. Yuan, D. Sorocco, R. Perez-Tomas, and M. Levin, "Eye regeneration assay reveals an invariant functional left-right asymmetry in the early bilaterian, Dugesia japonica," *Laterality*, vol. 10, no. 3, pp. 193–205, 2005.

[61] C. Lange, S. Prenninger, P. Knuckles, V. Taylor, M. Levin, and F. Calegari, "The H+ vacuolar ATPase maintains neural stem cells in the developing mouse cortex," *Stem Cells and Development*, vol. 20, no. 5, pp. 843–850, 2011.

[62] D. Blackiston, D. S. Adams, J. M. Lemire, M. Lobikin, and M. Levin, "Transmembrane potential of GlyCl-expressing instructor cells induces a neoplastic-like conversion of melanocytes via a serotonergic pathway," *DMM Disease Models and Mechanisms*, vol. 4, no. 1, pp. 67–85, 2011.

[63] W. S. Beane, J. Morokuma, D. S. Adams, and M. Levin, "A chemical genetics approach reveals H,K-ATPase-mediated membrane voltage is required for planarian head regeneration," *Chemistry and Biology*, vol. 18, no. 1, pp. 77–89, 2011.

[64] A. S. Tseng, W. S. Beane, J. M. Lemire, A. Masi, and M. Levin, "Induction of vertebrate regeneration by a transient sodium current," *Journal of Neuroscience*, vol. 30, no. 39, pp. 13192–13200, 2010.

[65] D. S. Adams, A. Masi, and M. Levin, "H+ pump-dependent changes in membrane voltage are an early mechanism necessary and sufficient to induce Xenopus tail regeneration," *Development*, vol. 134, no. 7, pp. 1323–1335, 2007.

[66] D. S. Adams and M. Levin, "Measuring resting membrane potential using the fluorescent voltage reporters DiBAC4(3) and CC2-DMPE," *Cold Spring Harbor Protocols*, vol. 2012, no. 4, pp. 459–464, 2012.

[67] D. S. Adams and M. Levin, "General principles for measuring resting membrane potential and ion concentration using fluorescent bioelectricity reporters," *Cold Spring Harbor Protocols*, vol. 2012, no. 4, pp. 385–397, 2012.

[68] V. P. Pai, S. Aw, T. Shomrat, J. M. Lemire, and M. Levin, "Transmembrane voltage potential conrols embryonic eye patterning in Xenopus laevis," *Development*, vol. 139, no. 2, pp. 313–323, 2012.

[69] L. N. Vandenberg, R. D. Morrie, and D. S. Adams, "V-ATPase-dependent ectodermal voltage and Ph regionalization are required for craniofacial morphogenesis," *Developmental Dynamics*, vol. 240, no. 8, pp. 1889–1904, 2011.

[70] D. S. Adams and M. Levin, "Endogenous voltage gradientsas mediators of cell-cell communication: strategies for investigating bioelectrical signals during pattern formation," *Cell and Tissue Research*. In press.

[71] C. Wolff, B. Fuks, and P. Chatelain, "Comparative study of membrane potential-sensitive fluorescent probes and their use in ion channel screening assays," *Journal of Biomolecular Screening*, vol. 8, no. 5, pp. 533–543, 2003.

[72] N. J. Oviedo, C. L. Nicolas, D. S. Adams, and M. Levin, "Live imaging of planarian membrane potential using DiBAC4(3)," *Cold Spring Harbor Protocols*, vol. 3, no. 10, 2008.

[73] T. Brend and S. A. Holley, "Balancing segmentation and laterality during vertebrate development," *Seminars in Cell and Developmental Biology*, vol. 20, no. 4, pp. 472–478, 2009.

[74] P. G. Franco, A. R. Paganelli, S. L. Löpez, and A. E. Carrasco, "Functional association of retinoic acid and hedgehog signaling in Xenopus primary neurogenesis," *Development*, vol. 126, no. 19, pp. 4257–4265, 1999.

[75] B. Xu, X. Feng, and R. D. Burdine, "Categorical data analysis in experimental biology," *Developmental Biology*, vol. 348, no. 1, pp. 3–11, 2010.

[76] H. J. Yost, "Development of the left-right axis in amphibians," *Ciba Foundation Symposium*, vol. 162, pp. 165–176, 1991.

[77] M. C. Danos and H. J. Yost, "Linkage of cardiac left-right asymmetry and dorsal-anterior development in Xenopus," *Development*, vol. 121, no. 5, pp. 1467–1474, 1995.

[78] M. Levin, "Is the early left-right axis like a plant, a kidney, or a neuron? The integration of physiological signals in embryonic asymmetry," *Birth Defects Research C*, vol. 78, no. 3, pp. 191–223, 2006.

[79] D. L. Davies, J. R. Trudell, S. J. Mihic, D. K. Crawford, and R. L. Alkana, "Ethanol potentiation of glycine receptors expressed in xenopus oocytes antagonized by increased atmospheric pressure," *Alcoholism: Clinical and Experimental Research*, vol. 27, no. 5, pp. 743–755, 2003.

[80] Q. Shan, J. L. Haddrill, and J. W. Lynch, "Ivermectin, an unconventional agonist of the glycine receptor chloride channel," *Journal of Biological Chemistry*, vol. 276, no. 16, pp. 12556–12564, 2001.

[81] M. Lobikin, G. Wang, J. Xu et al., "Early, nonciliary role for microtubule proteins in left-right patterning is conserved across kingdoms," *Proceedings of the National Academy of Sciences of the United States of America*, vol. 109, pp. 12586–12591, 2012.

[82] N. J. Oviedo and M. Levin, "Gap junctions provide new links in left-right patterning," *Cell*, vol. 129, no. 4, pp. 645–647, 2007.

[83] M. Levin and M. Mercola, "Gap junctions are involved in the early generation of left-right asymmetry," *Developmental Biology*, vol. 203, no. 1, pp. 90–105, 1998.

[84] M. Levin and M. Mercola, "Gap junction-mediated transfer of left-right patterning signals in the early chick blastoderm is upstream of Shh asymmetry in the node," *Development*, vol. 126, no. 21, pp. 4703–4714, 1999.

[85] K. Carneiro, C. Donnet, T. Rejtar et al., "Histone deacetylase activity is necessary for left-right patterning during vertebrate development," *BMC Developmental Biology*, vol. 11, article 29, 2011.

[86] A. Schweickert, T. Weber, T. Beyer et al., "Cilia-driven leftward flow determines laterality in xenopus," *Current Biology*, vol. 17, no. 1, pp. 60–66, 2007.

[87] V. P. Pai, S. Aw, T. Shomrat, J. M. Lemire, and M. Levin, "Transmembrane voltage potential controls embryonic eye patterning in Xenopus laevis," *Development*, vol. 139, pp. 313–323, 2012.

[88] S. A. Moody, "Fates of the blastomeres of the 32-cell-stage Xenopus embryo," *Developmental Biology*, vol. 122, no. 2, pp. 300–319, 1987.

[89] R. L. Chow, C. R. Altmann, R. A. Lang, and A. Hemmati-Brivanlou, "Pax6 induces ectopic eyes in a vertebrate," *Development*, vol. 126, no. 19, pp. 4213–4222, 1999.

[90] E. Aydar, S. Yeo, M. Djamgoz, and C. Palmer, "Abnormal expression, localization and interaction of canonical transient receptor potential ion channels in human breast cancer cell lines and tissues: a potential target for breast cancer diagnosis and therapy," *Cancer Cell International*, vol. 9, article 23, 2009.

[91] A. E. Novak, A. D. Taylor, R. H. Pineda, E. L. Lasda, M. A. Wright, and A. B. Ribera, "Embryonic and larval expression of zebrafish voltage-gated sodium channel α-subunit genes," *Developmental Dynamics*, vol. 235, no. 7, pp. 1962–1973, 2006.

[92] S. M. Jones and A. B. Ribera, "Overexpression of a potassium channel gene perturbs neural differentiation," *Journal of Neuroscience*, vol. 14, no. 5, pp. 2789–2799, 1994.

[93] C. G. Nichols, "KATP channels as molecular sensors of cellular metabolism," *Nature*, vol. 440, no. 7083, pp. 470–476, 2006.

[94] S. Aw, J. C. Koster, W. Pearson et al., "The ATP-sensitive K+-channel (KATP) controls early left-right patterning in

Xenopus and chick embryos," *Developmental Biology*, vol. 346, no. 1, pp. 39–53, 2010.

[95] S. Aw, J. C. Koster, W. Pearson et al., "The ATP-sensitive K+-channel (KATP) controls early left-right patterning in Xenopus and chick embryos," *Developmental Biology*, vol. 346, no. 1, pp. 39–53, 2010.

[96] M. Kumasaka, S. Sato, I. Yajima, and H. Yamamoto, "Isolation and developmental expression of tyrosinase family genes in Xenopus laevis," *Pigment Cell Research*, vol. 16, no. 5, pp. 455–462, 2003.

[97] A. E. Proshchina and S. V. Savel'ev, "Study of amphibian brain asymmetry during normal embryonic and larval development," *Izvestiia Akademii Nauk*, no. 3, pp. 408–411, 1998.

[98] B. Bao, Z. Ke, J. Xing et al., "Proliferating cells in suborbital tissue drive eye migration in flatfish," *Developmental Biology*, vol. 351, no. 1, pp. 200–207, 2011.

[99] K. Yoshida and H. Saiga, "Repression of Rx gene on the left side of the sensory vesicle by Nodal signaling is crucial for right-sided formation of the ocellus photoreceptor in the development of Ciona intestinalis," *Developmental Biology*, vol. 354, no. 1, pp. 144–150, 2011.

[100] R. L. Trelstad and A. J. Coulombre, "Morphogenesis of the collagenous stroma in the chick cornea," *The Journal of Cell Biology*, vol. 50, no. 3, pp. 840–858, 1971.

[101] A. J. Coulombre, "Experimental embryology of the vertebrate eye," *Investigative ophthalmology*, vol. 4, pp. 411–419, 1965.

[102] R. L. Trelstad, "The bilaterally asymmetrical architecture of the submammalian corneal stroma resembles a cholesteric liquid crystal," *Developmental Biology*, vol. 92, no. 1, pp. 133–134, 1982.

[103] P. F. MacNeilagea, M. G. Studdert-Kennedya, and B. Lindbloma, "Primate Handedness reconsidered," *Behavioral and Brain Science*, vol. 10, no. 2, pp. 247–303, 1987.

[104] G. Vallortigara and L. J. Rogers, "Survival with an asymmetrical brain: advantages and disadvantages of cerebral lateralization," *Behavioral and Brain Sciences*, vol. 28, no. 4, pp. 575–589, 2005.

[105] N. Rashid and R. J. Andrew, "Right hemisphere advantage for topographical orientation in the domestic chick," *Neuropsychologia*, vol. 27, no. 7, pp. 937–948, 1989.

[106] L. J. Rogers, R. J. Andrew, and T. H. J. Burne, "Light exposure of the embryo and development of behavioural lateralisation in chicks, I: olfactory responses," *Behavioural Brain Research*, vol. 97, no. 1-2, pp. 195–200, 1998.

[107] G. Lippolis, A. Bisazza, L. J. Rogers, and G. Vallortigara, "Lateralisation of predator avoidance responses in three species of toads," *Laterality*, vol. 7, no. 2, pp. 163–183, 2002.

[108] G. Vallortigara, L. J. Rogers, A. Bisazza, G. Lippolis, and A. Robins, "Complementary right and left hemifield use for predatory and agonistic behaviour in toads," *NeuroReport*, vol. 9, no. 14, pp. 3341–3344, 1998.

[109] A. Bisazza, A. De Santi, S. Bonso, and V. A. Sovrano, "Frogs and toads in front of a mirror: lateralisation of response to social stimuli in tadpoles of five anuran species," *Behavioural Brain Research*, vol. 134, no. 1-2, pp. 417–424, 2002.

[110] G. Vallortigara, L. J. Rogers, and A. Bisazza, "Possible evolutionary origins of cognitive brain lateralization," *Brain Research Reviews*, vol. 30, no. 2, pp. 164–175, 1999.

[111] C. Chang, Y. W. Hsieh, B. J. Lesch, C. I. Bargmann, and C. F. Chuang, "Microtubule-based localization of a synaptic calciumsignaling complex is required for left-right neuronal asymmetry in C. elegans," *Development*, vol. 138, no. 16, pp. 3509–3518, 2011.

[112] C. F. Chuang, M. K. VanHoven, R. D. Fetter, V. K. Verselis, and C. I. Bargmann, "An Innexin-Dependent Cell Network Establishes Left-Right Neuronal Asymmetry in C. elegans," *Cell*, vol. 129, no. 4, pp. 787–799, 2007.

[113] S. L. Bauer Huang, Y. Saheki, M. K. VanHoven et al., "Left-right olfactory asymmetry results from antagonistic functions of voltage-activated calcium channels and the Raw repeat protein OLRN-I in *C. elegans*," *Neural Development*, vol. 2, no. 1, article 24, 2007.

[114] M. K. VanHoven, S. L. Bauer Huang, S. D. Albin, and C. I. Bargmann, "The claudin superfamily protein NSY-4 biases lateral signaling to generate left-right asymmetry in *C. elegans* Olfactory Neurons," *Neuron*, vol. 51, no. 3, pp. 291–302, 2006.

[115] R. J. Poole and O. Hobert, "Early Embryonic Programming of Neuronal Left/Right Asymmetry in C. elegans," *Current Biology*, vol. 16, no. 23, pp. 2279–2292, 2006.

[116] M. L. Concha and S. W. Wilson, "Asymmetry in the epithalamus of vertebrates," *Journal of Anatomy*, vol. 199, no. 1-2, pp. 63–84, 2001.

[117] K. A. Barth, A. Miklosi, J. Watkins, I. H. Bianco, S. W. Wilson, and R. J. Andrew, "fsi zebrafish show concordant reversal of laterality of viscera, neuroanatomy, and a subset of behavioral responses," *Current Biology*, vol. 15, no. 9, pp. 844–850, 2005.

[118] L. Facchin, H. A. Burgess, M. Siddiqi, M. Granato, and M. E. Halpern, "Determining the function of zebrafish epithalamic asymmetry," *Philosophical Transactions of the Royal Society B*, vol. 364, no. 1519, pp. 1021–1032, 2009.

[119] L. Facchin, F. Argenton, and A. Bisazza, "Lines of Danio rerio selected for opposite behavioural lateralization show differences in anatomical left-right asymmetries," *Behavioural Brain Research*, vol. 197, no. 1, pp. 157–165, 2009.

[120] D. N. Kennedy, K. M. O'Craven, B. S. Ticho, A. M. Goldstein, N. Makris, and J. W. Henson, "Structural and functional brain asymmetries in human situs inversus totalis," *Neurology*, vol. 53, no. 6, pp. 1260–1265, 1999.

[121] S. Tanaka, R. Kanzaki, M. Yoshibayashi, T. Kamiya, and M. Sugishita, "Dichotic listening in patients with situs inversus:Brain asymmetry and situs asymmetry," *Neuropsychologia*, vol. 37, no. 7, pp. 869–874, 1999.

[122] A. M. Heacock and B. W. Agranoff, "Clockwise growth of neurites from retinal explants," *Science*, vol. 198, no. 4312, pp. 64–66, 1977.

[123] A. Tamada, S. Kawase, F. Murakami, and H. Kamiguchi, "Autonomous right-screw rotation of growth cone filopodia drives neurite turning," *Journal of Cell Biology*, vol. 188, no. 3, pp. 429–441, 2010.

[124] A. P. Babenko, L. Aguilar-Bryan, and J. Bryan, "A view of SUR/K(IR)6.X, k(atp) channels," *Annual Review of Physiology*, vol. 60, pp. 667–687, 1998.

[125] S. M. Cheng, I. Chen, and M. Levin, "KATP channel activity is required for hatching in Xenopus embryos," *Developmental Dynamics*, vol. 225, no. 4, pp. 588–591, 2002.

[126] S. F. Altschul, T. L. Madden, A. A. Schäffer et al., "Gapped BLAST and PSI-BLAST: a new generation of protein database search programs," *Nucleic Acids Research*, vol. 25, no. 17, pp. 3389–3402, 1997.

[127] M. E. Zuber, "Eye field specification in Xenopus laevis," *Current Topics in Developmental Biology*, vol. 93, pp. 29–60, 2010.

[128] C. Holt, "Cell movements in Xenopus eye development," *Nature*, vol. 287, no. 5785, pp. 850–852, 1980.

[129] M. S. Saha, C. L. Spann, and R. M. Grainger, "Embryonic lens induction: more than meets the optic vesicle," *Cell Differentiation and Development*, vol. 28, no. 3, pp. 153–172, 1989.

[130] T. Harada, C. Harada, and L. F. Parada, "Molecular regulation of visual system development: more than meets the eye," *Genes and Development*, vol. 21, no. 4, pp. 367–378, 2007.

[131] J. Gallaher, M. Bier, and J. S. van Heukelom, "First order phase transition and hysteresis in a cell's maintenance of the membrane potential-An essential role for the inward potassium rectifiers," *BioSystems*, vol. 101, no. 3, pp. 149–155, 2010.

[132] L. Q. Wan, K. Ronaldson, M. Park et al., "Micropatterned mammalian cells exhibit phenotype-specific left-right asymmetry," *Proceedings of the National Academy of Sciences of the United States of America*, vol. 108, no. 30, pp. 12295–12300, 2011.

[133] T. H. Chen, J. J. Hsu, X. Zhao et al., "Left-right symmetry breaking in tissue morphogenesis via cytoskeletal mechanics," *Circulation Research*, vol. 110, pp. 551–559, 2012.

[134] H. Sive, R. M. Grainger, and R. Harland, *Early Development of Xenopus laevis*, Cold Spring Harbor Laboratory Press, New York, NY, USA, 2000.

[135] P. D. Nieuwkoop and J. Faber, *Normal table of Xenopus laevis (Daudin). Normal table of Xenopus laevis (Daudin)*, 1967.

[136] R. Burgstahler, H. Koegel, F. Rucker, D. Tracey, P. Grafe, and C. Alzheimer, "Confocal ratiometric voltage imaging of cultured human keratinocytes reveals layer-specific responses to ATP," *American Journal of Physiology*, vol. 284, no. 4, pp. C944–C952, 2003.

[137] R. M. Harland, "In situ hybridization: an improved whole-mount method for Xenopus embryos," *Methods in Cell Biology*, vol. 36, pp. 685–695, 1991.

[138] D. Blackiston, L. N. Vandenberg, and M. Levin, "High-throughput Xenopus laevis immunohistochemistry using agarose sections," *Cold Spring Harbor Protocols*, vol. 2010, no. 12, 2010.

Hindawi Publishing Corporation
Stem Cells International
Volume 2012, Article ID 462161, 9 pages
doi:10.1155/2012/462161

Review Article

Ion Flux Dependent and Independent Functions of Ion Channels in the Vertebrate Heart: Lessons Learned from Zebrafish

Mirjam Keßler, Steffen Just, and Wolfgang Rottbauer

Department of Internal Medicine II, University of Ulm, 89081 Ulm, Germany

Correspondence should be addressed to Wolfgang Rottbauer, wolfgang.rottbauer@uniklinik-ulm.de

Received 19 August 2012; Accepted 14 October 2012

Academic Editor: Alexander Kleger

Ion channels orchestrate directed flux of ions through membranes and are essential for a wide range of physiological processes including depolarization and repolarization of biomechanical activity of cells. Besides their electrophysiological functions in the heart, recent findings have demonstrated that ion channels also feature ion flux independent functions during heart development and morphogenesis. The zebrafish is a well-established animal model to decipher the genetics of cardiovascular development and disease of vertebrates. In large scale forward genetics screens, hundreds of mutant lines have been isolated with defects in cardiovascular structure and function. Detailed phenotyping of these lines and identification of the causative genetic defects revealed new insights into ion flux dependent and independent functions of various cardiac ion channels.

1. Introduction

Ion channels are pore-forming proteins that warrant controlled and directed flux of ions through membranes. Temporal and spatial coordination of ion movements is essential for a wide range of physiological processes including the generation and propagation of the membrane action potential that is critical for the biomechanical activity of muscle cells. Despite their well-established canonical electrophysiological functions in the heart, recent findings have demonstrated that ion channels also might feature ion flux independent functions during heart development and morphogenesis long before acting as ion-conducting pores. For example, targeted knockout of the cardiac sodium channel SCN5A in mice leads to embryonic lethality due to defective cardiogenesis. Besides the expected electrophysiological alterations, hearts of SCN5a-deficient mice develop a common hypoplastic ventricular chamber with reduced trabeculae whereas the endocardial cushions of the atrio-ventricular (AV) canal or the truncus arteriosus form normally [1]. These findings implicate that regular ion channel function is crucial not only for the regulation of heart rhythm but also for cardiogenesis.

Whereas the study of heart development in mice is hindered by the *in utero* development of the embryo and the high mortality of embryos with cardiac defects, animal models such as the zebrafish (*Danio rerio*) emerged as a powerful model organism to study cardiac development and function in the last few years.

The advantages of this animal model are external fertilization and fast development. The embryos can easily be reared in aqueous medium and are accessible for manipulation at all developmental stages. Meanwhile their organogenesis can be observed continuously due to their optical transparency [2]. During its embryonic development the zebrafish does not entirely depend upon a functional cardiovascular system and circulation, since oxygen is distributed by passive diffusion [3]. This facilitates extended studies on severe congenital cardiovascular defects. Besides, the almost completely sequenced genome of the zebrafish and the highly conserved gene functions compared to humans further strengthen the zebrafish's role for cardiovascular research [2, 4]. Large scale forward genetic screens in zebrafish expanded our knowledge on genetic networks that mediate development and maintenance of cardiac form and function. Genes identified in these screens encode for a wide variety of different proteins: transcription factors, signaling molecules, as well as several structural proteins of cardiomyocytes including the contractile apparatus.

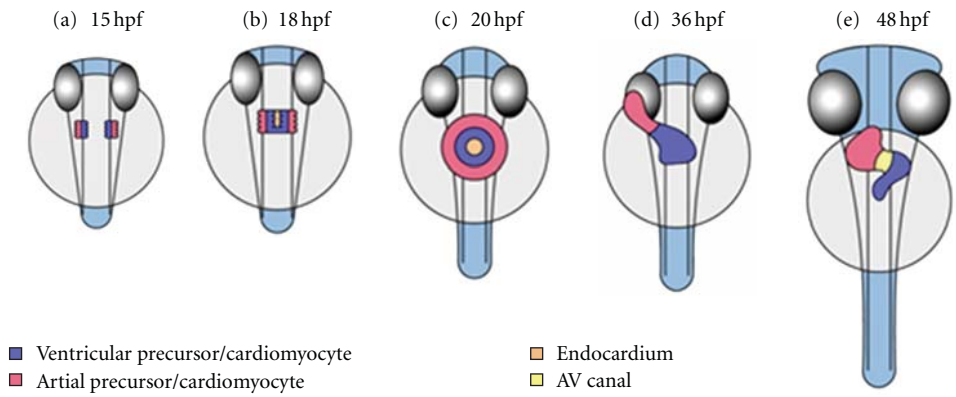

Figure 1: Stages of heart development in zebrafish embryos in a ventral view. (a) At 15 hpf cardiac precursors move towards the anterior lateral plate mesoderm; the atrial precursors are located laterally, the ventricular precursors medially. (b) Cardiac fusion starts at about 18 hpf at the posterior end of the bilateral heart fields; first, endocardial cells arrive at midline, followed by ventricular cells. The atrial precursors do so slightly later. (c) After cardiac fusion the cells form the cardiac cone. Viewed ventrally, this structure resembles a ring: endocardial cells lining the central lumen, and ventricular cells are surrounded by atrial precursors. The cardiac cone starts to transform into the heart tube by 21 hpf. (d) Cardiac looping of the heart tube occurs between 26 hpf and 48 hpf. The linear heart tube bends and creates an S-shaped loop. By 36 hpf the atrium and ventricle become distinguishable. (e) The heart tube rotates. The different parts of the heart tube do not rotate equally and therefore torsion occurs. The AV canal develops by constriction of the boundary between atrium and ventricle. Ventricular maturation by appositional growth takes place.

The key steps of heart development in zebrafish resemble those in humans and other mammals. Differentiation of cardiac precursors is required to form a heart tube that finally loops and builds an atrial and ventricular chamber separated by an atrio-ventricular (AV) valve. At 5 hours after fertilization (hpf) cardiac progenitor cells are located bilaterally in the lateral marginal zone. During gastrulation cardiac progenitor cells migrate towards the embryonic midline to end up at the anterior lateral plate mesoderm (Figure 1(a)). The cells continue to converge at midline at about 18 hpf (*cardiac fusion*; Figure 1(b)) and form the cardiac cone (Figure 1(c)). The shallow cone shifts from midline towards the left side (*cardiac jogging*). By 21 hpf a linear heart tube forms and exhibits regular peristaltic contractions. Endocardial cells lie within the inner lining of the lumen, myocardial cells peripherally. The heart tube elongates (*cardiac extension*) and bends to the right to create an S-shaped form (*cardiac looping*, Figure 1(d)). The future ventricle and atrium become distinguishable and, by 36 hpf, show sequential contractions with a characteristic AV delay. The AV canal becomes detectable and by 48 hpf the endocardial cells lining this canal form the endocardial cushions (Figure 1(e)). Gradually, between 48 hpf and 72 hpf, ventricular maturation proceeds, the ventricular wall thickens by appositional growth (*cardiac ballooning*), and trabeculae are formed. Endocardial cushions enlarge and, by 105 hpf, have differentiated into valve leaflets of the AV valve.

Heart morphogenesis is accompanied by cardiomyocyte specification and differentiation. Myocardial cell precursors start to express cardiac myosin genes including myosin light chain polypeptide 7 (myl7, cmlc2). At 16 hpf the medial cells differentiate into ventricular cells expressing ventricle myosin heavy chain (vmhc) and at 22 hpf the lateral, atrial myosin heavy chain (amhc) positive cells differentiate into atrial cells. The transcription factor nkx2.5 is needed to generate myocardial and endocardial progenitor cells, which is regulated by bone morphogenetic protein (Bmp), gata5, and hand2 (for reviews see [5–8]).

The role of ion channels in adulthood for the generation and the propagation of action potentials in excitable cells and the contraction of myocytes and cardiomyocytes is well understood [9]. Additionally, recent findings mainly from the zebrafish model demonstrate that ion channels also play a crucial and unexpected role in heart development. The presence of ion channels is required for normal cardiogenesis. A knockout or Morpholino antisense oligonucleotide mediated knockdown of ion channel genes in zebrafish causes disruptions of heart development. Besides their role as ion-conducting pores, ion channels seem to impinge on cardiogenesis in an ion flux independent manner. However, further studies are required to learn more about the mechanisms how ion channels exert influence on heart development. This paper focuses on the recent findings on the role of ion channels in cardiac development in zebrafish.

2. Role of Ion Channels in Heart Development

2.1. Sodium Channels. In excitable cells, voltage-gated sodium channels permit the rapid sodium influx and thus are accountable for the initial upstroke of the action potential (phase 0 depolarization). The structure of voltage-gated sodium channels resembles the assembly of calcium channels and other ion channels. Each channel consists of a pore-forming α subunit (Na_v 1) and auxiliary β subunits [9]. In chick and mouse it is already known that coordinated electric activity of cardiomyocytes is not required for early heart development [10–12]. Furthermore, results of studies on the zebrafish troponin T mutant *silent heart* showed that

these mutants lack both contraction and circulation but cardiogenesis proceeds normally [13].

In zebrafish, eight genes encode for α subunits of sodium channels: four sets of duplicated genes are termed as scn1Laa & scn1Lab, scn4aa & scn4ab, scn5Laa & scn5Lab, and scn8aa & scn8ab [14–16]. scn5Laa and scn5Lab are phylogenetically related to SCN5A in mammals (Na_v 1.5) [9, 17]. At 24 hpf scn5Laa mRNA is detected by whole mount in situ hybridisation in regions of the future heart tube [18]. At later stages of embryonic and larval development (at 52 hpf and 104 hpf) scn5Laa and scn5Lab expression is observed in the heart and the nervous system [17]. Transcripts of both genes can be identified by reverse transcriptase polymerase chain reaction assays already in early embryonic stages (0 to 12 hpf) [17]. Morpholino antisense oligonucleotide-mediated knockdown of the cardiac sodium channels scn5Laa or scn5Lab in zebrafish lead to dysmorphic and hypoplastic hearts. scn5Laa morphant hearts show significant defects of both atrial and ventricular chamber morphogenesis and cardiac looping by 58 hpf. During later stages of heart development both chambers remain small. The ventricle displays a single cardiomyocyte layer; trabeculae are missing. Quantification of cardiomyocyte numbers by 62 hpf reveals a significant reduction in comparison to controls. The reason for this reduction of heart cells seems to be a decreased number of differentiating cardiomyocytes at early embryonic stages. Quantification of future heart cells in the cardiac cone at the 22-somite stage, approximately at 20 hpf, reveals significantly reduced numbers compared to wild-type and control-injected embryos. Double knockdown of both cardiac sodium channel genes scn5Laa and scn5Lab leads to an even more severe disruption of cardiac development compared to a single knockdown of either gene. These scn5Laa scn5Lab morphants show even fewer numbers of heart cells. The defects in the heart are not caused by an increase of apoptosis. Thus, these abnormalities seem to be due to early disruption of cardiomyocyte differentiation and proliferation [17].

Injection of either scn5Laa or scn5Lab translation inhibitor Morpholino resulted in a reduction of cardiogenic transcription factors nkx2.5, gata4, and hand2 at the 6-somite stage in the anterior lateral mesoderm. This effect on nkx2.5 expression is dose dependent. Expression of gata5 as a potent positive regulator of nkx2.5 is unaffected. Additionally the expression of the sarcomeric genes cmlc2 and vmhc is decreased at 16-somite stage [17].

When the voltage-gated sodium channel Na_v 1.5 in zebrafish is blocked either by injection of different sodium channel blockers into the pericardial space of the embryonic heart or by penetration via bathing solution, normal formation of the heart tube is observed. In addition rearing in sodium-free media causes no disruption of cardiogenesis. As expected, at later stages conduction abnormalities are caused by blockage of the voltage-gated sodium channel. Activation of this channel by Anemone toxin II or Veratridine delivered by either bathing solution or injection leads to convulsions, but the cardiac development remains unaffected [17]. These findings indicate that the voltage-gated sodium channel exerts influence on cardiac development independent of ion flux.

In summary, the studies on the voltage-gated sodium channel Na_v 1.5 in zebrafish suggest that the expression of the channel is essential for heart development. Morpholino knockdown of scna5Laa and scna5Lab causes a decreased number of differentiating cells as well as hypoplastic and dysmorphic hearts. Sodium currents seem to be redundant for this effect. Reduced expression levels of nkx2.5, gata4, and hand2 in scna5Laa and scna5Lab morphants imply an essential role of sodium channels in fate determination and differentiation of cardiac cells.

2.2. Calcium Channels. Calcium channels are important for the function of the adult heart. The voltage-gated entry of calcium into cardiomyocytes is permitted by the L-type (for long lasting) and the T-type (for threshold or tiny) calcium channel. The L-type channel is the major route for calcium inward current. Calcium entry via L-type channels (LTCC) is crucial to sustain the characteristically long action potential of cardiomyocytes, conduction, and excitation-contraction coupling [9]. In mammals the T-type channel is predominantly expressed in the sinus node, atrio-ventricular node, and atrial cells where it facilitates automaticity and pace-making activities [9]. Adult zebrafish displays a significant T-type-Ca^{2+} current in both atrial and ventricular cardiomyocytes [19]. Intracellularly, calcium facilitates the contraction mechanism by triggering the release of calcium from the sarcoplasmatic reticulum via ryanodine receptor [9]. Furthermore calcium regulates as a second messenger growth and hypertrophy of cells by less understood mechanisms [20]. In addition the C terminus of the LTCC encodes a transcription factor and autoregulates transcription of the channel [21, 22].

LTCC are heteromeric protein complexes usually consisting of a pore-forming $\alpha 1$ subunit, a modulatory cytoplasmatic β subunit, and an ancillary extracellular $\alpha 2$ subunit with a transmembrane δ subunit and a function-modifying γ subunit in noncardiac cells [23–25].

The ion-conducting pore and the voltage sensor lie within the $\alpha 1$ subunit of cardiac-specific isoform $\alpha 1C$. The subunit consists of four transmembrane domains each containing of six transmembrane segments. It has been reported that LTCC blockers such as 1,4-dihydropyridine applied to chick embryos cause a reduction of the heart size and thickness of the myocardium [26] whereas targeted mutagenesis of the LTCC $\alpha 1C$-subunit did not interfere with embryonic cardiac function and growth in mice [27].

In zebrafish the embryonic lethal *island beat* mutant is an excellent model to determine the role of LTCC in cardiac development since its pore-forming $\alpha 1C$ subunit is defective. In *island beat (isl)* mutant embryos a morphologically normal heart tube is formed in its correct position. Endocardium and myocardium are present. Already at that early stage of heart development, defects become noticeable. The embryos lack the characteristic peristaltic contraction of the heart tube. During cardiac development two chambers are generated in *isl* mutants. In contrast to wild-type embryos

the mutants display a smaller ventricular chamber with single-layer cardiac cells. At 60 hpf appositional addition of cardiomyocytes is absent. Consequently the thickening and thereby growth along the long axis of the heart does not occur. At 72 hpf it becomes clear that the number of cardiomyocytes is reduced in mutants compared to wild type. Apoptosis is not evident in *isl* hearts. The atrium remains morphologically normal throughout the early stages of cardiac development. The atrial cells continue to contract in sporadic, uncoordinated manner resembling atrial fibrillation whereas in ventricular cells contraction and blood flow remain absent. At an ultrastructural level myocardial cells of *isl* mutants appear to be normal [28].

The cytoplasmatic β subunit of the calcium channel modulates the electrophysiological properties of the channel and is capable of increasing calcium channel activity when coexpressed with α1 subunits [25]. Additionally, the β subunit of the LTCC belongs to the group of membrane associated guanylate kinases (MAGUK) which have scaffolding function [29]. β2 is the predominantly expressed β subunit in the heart. β2 null mutant mice die during embryogenesis due to absence of cardiac contraction. Knockout of other calcium channel β subunits in mice did not lead to embryonic lethal heart failure [30–32]. The calcium channel β4 subunit is expressed in fetal hearts of rats and precedes the expression of the β2 subunit [33].

In zebrafish the following β subunit genes were identified: cacnb1 for the β1 subunit, and for β2 cacnb2a and -b, β3 cacnb3a and -b and for β4 cacnb4a and -b. Similar to the results in mice, in zebrafish cacnb4a is expressed in the embryonic heart at 48–72 hpf. cacnb4b is not expressed in the developing heart tube in zebrafish. At this stage neither cacnb2a nor cacnb2b were detected in cardiac tissue by in situ hybridisation [34]. Interestingly, an antisense oligonucleotide mediated Morpholino knockdown either by translation initiation block or by missplicing of the β2.1 subunit causes disruptions of heart development in zebrafish. At 48 hpf the knockdown morphants exhibit defects in chamber shaping, cardiac looping, and contractility. By 72 hpf the heart remains linear and a pericardial edema is present. The atria appear to be dilated whereas the ventricle is collapsed. In β2.1 depleted zebrafish specification and differentiation of the cardiomyocyte precursors proceeds without any makeable differences compared to wild type. Nevertheless, in the ventricle of morphants at 48 hpf, reduced numbers of cardiomyocytes were detected, whereas in the atrium equal numbers of cells were counted. A decreased rate of proliferating cardiomyocytes seems to be causative since an increased apoptosis rate was not observed. In addition, the β2.1 depleted cardiomyocytes differ from wild-type cells morphologically. While normally the cardiomyocytes undergo a transition from a round to a larger, elongated shape during chamber ballooning, the β2.1 knockdown cardiomyocytes remain round. The surface of individual cardiomyocytes at the outer curvature of the heart is markedly reduced. Besides these morphological distinctions, the heart function is compromised in β2.1 knockdown morphants. Heart rate, ventricle volume, stroke volume, and cardiac output are decreased at 48 hpf. Moreover upon externally applied mechanical shear stress the β2.1 morphant heart tube ruptures since cardiomyocytes express less N-cadherin and lack the characteristic banding of sarcomeric actin. These findings implicate besides its role for proliferation and contractility an important scaffolding function of the β2.1 subunit [29].

In conclusion, the α1C subunit as well as the β2.1 subunit influence heart development in zebrafish. Loss of function of the channel subunits, either by mutation or by Morpholino oligonucleotide antisense mediated knockdown, leads to reduced numbers of cardiomyocytes and disruption of chamber morphogenesis. In *island beat* mutants the appositional growth of the ventricle is disturbed and remains mechanically silent. The β2.1 subunit Morpholino knockdown morphants exhibit defects in cardiac looping, contractility, and cell integrity.

2.3. Sodium-Calcium-Exchanger. Calcium inward currents drive excitation of excitable cells and contraction of myocytes and cardiomyocytes. In order to prepare for the next contraction, calcium must be extruded from the intracellular cytosol to return to a resting state. Two major routes contribute to this extrusion in myocytes and cardiomyocytes: the sarcoplasmatic reticulum Ca^{2+}-ATPase (SERCA2), which sequesters intracellular calcium into sarcoplasmatic reticulum and the Sodium-Calcium-Exchanger (NCX1). This exchanger regulates Ca^{2+} concentration according to the electrochemical gradient and catalyzes the exchange of three extracellular sodium ions for one intracellular calcium ion. The relative contributions of both NCX and SERCA2 to the intracellular calcium concentration change during development and vary by species [35–38]. Homozygous NCX1-deficient mice showed the absence of a normally beating heart and enhanced apoptosis of cardiomyocytes. A dilated pericardium has been described. The homozygous mice died at approximately day 10 of embryonic development *in utero* [39, 40]. In chick embryos disruption of cardiac development and contraction was observed when treated with a NCX inhibitor [41].

Expression of the cardiac isoform NCX1h in zebrafish manifests first at the 12-somite stage in bilateral cardiac primordia. The expression of NCX1h is restricted to the heart throughout the first 5 days of zebrafish embryonic development [35]. It is prominent in the myocardium of ventricle and atrium and barely noticeable in the outflow tract [42]. Embryonic lethal mutation of the cardiac isoform NCX1h in zebrafish causes atrial arrhythmias and a nearly silent ventricle in the zebrafish mutant *tremblor (tre)*. Length and morphology of the heart tube appear to be normal. At later stages of cardiac development an abnormal heart function is observed in homozygous *tre* embryos. These defects appear when the cells of the heart tube differentiate into ventricular and atrial cells. The cardiomyocytes of the heart tube fibrillate, contract arrhythmically and rhythmically. Compared to the wild type the ventricle is markedly smaller. Electron microscopy at 48 hpf reveals sparse sarcomeres with uncoordinated assembly in ventricular cells whereas the atrium of *tre* mutants displays no obvious abnormalities

in sarcomere formation. The posterior end of the atrium collapses. At 6 days after fertilization embryonic lethality occurs [35, 42].

Injection of a calcium sensitive dye reveals nearly constant and in relation to the atrium elevated calcium levels of ventricular cells in *tre* mutants suggestive of calcium overload [35].

Early cardiac specification and differentiation seems to be unaffected by disruptions in NCX1h since *tre* mutants display normal expression levels of *vmhc*, *cmlc2*, *tbx5*, *irx1*, *amhc*, and *hand2*. These data imply defects in later cardiac differentiation in *tre* mutants leading to dysmorphogenesis and arrhythmias of both cardiac chambers [35, 42].

2.4. Ca^{2+}-ATPase. The second major route for the extrusion of calcium from the intracellular space is by sequestering calcium into the sarcoplasmatic reticulum via the sarcoplasmatic reticulum Ca^{2+}-ATPase2 (SERCA2). The cardiac-specific isoform SERCA2a plays an essential role in excitation-contraction-coupling in the heart. Calcium cations are transported into the sarcoplasmatic reticulum in order to reduce the intracellular cytosolic calcium concentration and to refill the calcium stores of cardiomyocytes [36].

Zebrafish SERCA2 is expressed bilaterally in the cardiac precursors throughout heart development and in skeletal muscle. Knockdown of SERCA2 either by Morpholino injection or by treatment with cyclopiazonic acid, a specific inhibitor of SERCA-activity, resulted in defects of cardiogenesis [43, 44]. The hearts of these embryos fail to expand. Heart looping is absent. In contrast to *tre* mutants, both heart chambers contract continuously without fibrillation. The heart rate is reduced and the chamber contractions are weak. At 6 days after fertilization embryonic lethality occurs [35].

When a calcium sensitive dye is injected into SERCA2 morphants waves of calcium entry are observed correlating with their bradycardic heart rate. Unlike in NCX1h mutants a calcium overload is not detectable in SERCA2 morphants [35].

Thus, both Ca^{2+} extrusion routes, NCX1h and SERCA2, are each important for zebrafish heart formation and function, but their loss of function phenotypes are distinct.

2.5. Na^+K^+-ATPase. Na^+K^+-ATPase obtains a crucial role for the establishment of a proper electrochemical gradient across the plasma membrane. Sodium and potassium are pumped across the cell boundaries, ATP is utilized. Both, the cation and ATP-binding sites are located in the α subunit and are essential for the catalytic and transport function of the integral membrane protein. Dimerization of α and β subunit is required for enzyme activity (for review see [52]).

In mammals it has been demonstrated that four isoformes of the α subunit of Na^+K^+-ATPases and three isoformes of the β subunit exist, each showing distinct expression patterns and different affinities to glycosides [52]. Cardiac function is modified by Na^+K^+-ATPases through interaction with the Sodium-Calcium-Exchanger NCX. Blockade of Na^+K^+-ATPases leads to an increase of Na^+ concentration in cardiomyocytes. Consequently NCX is inhibited, the intracellular calcium concentration rises and thereby the contractility of cardiomyocytes is enhanced [53, 54].

Studies on mice demonstrated that Na^+K^+-ATPase activity is crucial for embryogenesis. α1 homozygous knockout mice are embryonic lethal and heterozygous mice have hypocontractile heart beats; α2 homozygous knockout mice die during the first day after birth and heterozygous mice show hypercontractility of the myocardium that correlates with the elevated calcium level in cardiomyocytes [55]. Pharmacological inhibition of Na^+K^+-ATPase by Ouabain in chick embryos leads to disruptions of early heart development [56].

In zebrafish eight isoformes of the α subunit and five β subunits exist. Three Na^+K^+-ATPase isoformes are expressed in the developing heart: α1B1 (also known as α1a1), α2, and β1a [57].

Heart and mind (had) mutants carry defects in Na^+K^+-ATPase α1B1 isoform. *had* embryos develop a curved body and severe abnormalities in brain and heart. Circulation is not established and the embryos die five days after fertilization [45]. By 21 hpf bilateral cardiac primordia fuse at midline and a shallow heart cone becomes evident. At 24 hpf the *had* mutant's heart remains as a shallow heart cone, whereas in wild type at the same stage development of the primitive heart tube is nearly finished. The heart usually starts beating in the stage of the primitive heart tube. *had* mutants reveal a small heart without contraction after 28 hpf. By 48 hpf both cardiac chambers and both cardiac cell types, endocardium and myocardium, exist. However the heart remains small, the ventricle thin, and the myocardial-endocardial distance is enlarged in Na^+K^+-ATPase α1B1 defective zebrafish [45]. The expression patterns of the early cardiac development genes *vmhc*, *nkx2.5*, and *cmlc2* are normal in these mutants at approximately 24 hpf, suggesting that *had* is not required for the determination of early cardiac cell fate. After 48 hpf *vmhc* and *irx1* become specific for the ventricle in wild-type zebrafish, whereas *versican* expression usually is localized between atrium and ventricle. In *had* mutants a significant reduction of *irx1* can be observed, whereas *vmhc* is evident in the atrium as well as in the ventricle. *Versican* spreads throughout the whole heart, suggesting a disruption of cardiac chamber specific differentiation [45].

Quantification of cardiomyocytes by counting transgenic green-fluorescent-protein- (GFP-) positive cells reveals similar numbers in both wild-type and *had* mutant. The primitive heart is markedly shorter and thereby the GFP signal more intense. Hence, extension of the heart tube seems to be disrupted in *had* mutants [45].

As mentioned above, the heart of *had* mutants does not beat at 24 hpf. After 48 hours of development a bradycardic heart rhythm is established, and cardiac contractility is diminished. Treatment with Ouabain, a Na^+K^+-ATPase inhibitor, and injection of a Morpholino antisense oligonucleotide to wild-type zebrafish phenocopies *had* mutants [45, 56].

The α2 subunit of Na^+K^+-ATPase is also expressed in the developing heart of zebrafish. By injection of a Morpholino

Table 1: Affected ion channel and effect on heart development.

Affected ion channel	Zebrafish phenotype and effect on heart development	Reference
Na_v 1.5 (scn5Laa, scn5Lab)	(i) Morpholino knockdown: hypoplastic, dysmorphic heart, reduced numbers of cardiomyocytes (ii) pharmacological modification: normal heart tube formation	[17]
LTCC α1C subunit	(i) *Island beat (isl):* loss of function; hypoplastic and silent ventricle, reduced numbers of ventricular cardiomyocytes; atrial fibrillation	[28]
LTCC β2.1 subunit	(i) Morpholino knockdown: defects in cardiac looping and ballooning, reduced numbers and proliferation of cardiomyocytes, disrupted cell integrity; bradycardiac and weakly contractile heart rhythm (ii) pharmacological modification with nifedipin resembles the morphants' phenotype	[29]
NCX1h	(i) *Tremblor (tre):* loss of function; hypoplastic and nearly silent ventricle, disruptions of sarcomere assembly in the ventricle; atrial fibrillation	[35]
SERCA2a	(i) Morpholino knockdown, pharmacological modification: absent cardiac looping, no expanding of cardiac chambers, bradycardia	[35]
Na^+K^+-ATPase α1B1 subunit	(i) *heart and mind (had):* loss of function, disturbed heart tube elongation and cardiogenic differentiation	[45]
Na^+K^+-ATPase α2 subunit	(i) Morpholino knockdown: perturbed cardiac looping and laterality	[45]
zERG	(i) *reggae (reg):* gain of function; Short-QT-Syndrome, no effect on heart development (ii) *breakdance (bre):* loss of function; Long-QT-Syndrome, no effect on heart development (iii) $S290^{-/-}$, $S213^{-/-}$: loss of function; Long-QT-Syndrome (iv) Morpholino knockdown, pharmacological modification: no effects on heart development	[46–51]

antisense oligonucleotide targeting the translation initiation site of this isoform a distinct phenotype occurs. The proper cardiac laterality is perturbed; whereas in wild-type embryos the hearts shifts to the left side by 24 hpf (*cardiac jogging*), the heart of α2 knockdowns remains in midline or is displaced to the right side in 51% of all injected embryos. Cardiac looping is abnormal in half of the knockdown morphants [45].

In summary in zebrafish both Na^+K^+-ATPase isoformes α1B1 and α2 contribute to cardiac development in zebrafish in different ways: α1B1 defective mutants exhibit abnormalities in heart tube extension and ventricular cardiomyocyte differentiation as well as bradycardia and hypocontractility. α2 isoform contributes to cardiac laterality [45].

2.6. Potassium Channels. Cardiac repolarization depends mainly upon outward currents of potassium cations. Different potassium channels are involved in the repolarization process. The outward current is provided by three delayed rectifier K^+-currents in humans (rapidly activating I_{kr}, slow I_{ks}, and ultrarapid I_{kur}). Inward currents are provided by cardiac inward rectifier potassium channels encoded by the Kir superfamily [9, 46].

KCNH2 or hERG (human ether-á-go-go related gene) encodes the α subunit underlying rapidly activating delayed rectifier K^+-current I_{kr} [9]. In zebrafish hearts a highly expressed orthologue has been found: zERG. Both hERG and zERG contain six transmembrane segments, one Per-Arnt-Sim (PAS) domain and a cyclic-nucleotide-binding region. An overall amino acid identity between the two species of 59% is shared, whereas in certain domains such as the transmembrane and the catalytic domains, a markedly higher homology is observed [47, 58]. Both ERG channels, hERG and zERG, feature similar biophysical properties [48]. Several arrhythmias are linked to mutations in zERG channels including Short-QT-Syndrome and Long-QT-Syndrome [47, 49].

A gain of function mutation in the homozygous zebrafish mutant *reggae (reg)* prevents ERG channel inactivation. This recessive mutation resides within the voltage sensor of zERG. As a consequence accelerated repolarization, shortened action potential duration, and premature channel reactivation occur. *Reg* mutants display intermittent cardiac arrest, sinuatrial block, and atrial fibrillation already at embryonic stages. In adulthood the zebrafish demonstrates shortened QT-intervals on surface electrocardiograms. Besides the arrhythmias, no disruptions in cardiac development are observed. Essential steps of zebrafish heart development proceed properly in homozygous *reg* mutant embryos without any abnormalities [47, 50].

The zebrafish mutant *breakdance (bre)* is the first animal model for Long-QT-Syndrome. Ventricular bradycardia and 2 : 1 block between atrium and ventricle occur. Causative is a loss of function mutation in the PAS-domain of zERG which leads to an impairment of ERG protein trafficking and hence reduced expression of zERG at the cell membrane. Cardiac repolarization and thereby the QT-interval is prolonged. Besides arrhythmias the *bre* mutants exhibit no specific phenotype. Cardiac development appears to be normal [49, 58]. Another zebrafish model for Long-QT-Syndrome is provided by mutants with defects residing in KCNH2, respectively, zERG. Two different loss of function mutations ($S290^{-/-}$, $S213^{-/-}$) cause a mechanically silent ventricle and pericardial edema. By 33 hpf the ventricle does not contract and appears to be collapsed. Atrial function and morphology

seem to be unaffected in these mutants at this developmental stage. At the 48 hpf stage pericardial edema is noticeable and increases gradually. After 10 days after fertilization the homozygous zebrafish mutants die [51].

Neither Morpholino antisense oligonucleotide translation block of zERG nor incubation with zERG inhibitor E-4031 in bathing solution cause disruptions in cardiac development whereas arrhythmias, particularly bradycardia and irregular atrial rhythms, can be provoked [17].

In summary, the different mutations of zERG cause no specific cardiac phenotype. The regular heart rhythm is disturbed and arrhythmias occur, whereas no major structural alterations appear in the developing heart.

3. Conclusion

Several studies on chick, mouse, zebrafish, and other species highlight the impact of ion channels on heart development. Owing to the advantage of survival without circulation, the zebrafish facilitates research on these cardiovascular defects without distortion by hypoxia and opens up new possibilities. Various methods enforced the results of studies on mammals and extended the previous knowledge: ion channel mutants, knockdown by Morpholino antisense oligonucleotides, and pharmacological modulation exhibit perturbed heart development at different time points (Table 1).

Voltage-gated sodium channels impinge on early cardiogenic differentiation, whereas the Sodium-Calcium-Exchanger NCX1h influences later stages of the differentiation. Heart looping hinges on proper function of Ca^{2+}-ATPase SERCA2, while the voltage-gated L-type calcium channel affects ventricular morphogenesis. The $Na^{+}K^{+}$-ATPase isoformes have distinct functions: α1B1 facilitates cardiac differentiation and extension of the heart tube. α2 isoform modifies laterality of cardiac precursors. The impact of the variety of potassium channels is least understood. Mutations in zERG cause no major structural alterations during heart development.

The zebrafish's heart proved to be a valuable model for congenital and acquired cardiovascular disease in humans. The findings on the role of ion channels in zebrafish embryos provide new insights into cardiac development. In addition to human pedigree studies and candidate gene screens the zebrafish model might help to understand the underlying mechanisms leading to congenital heart disease in humans. As a consequence the invention of causative treatment targeting the ion channels might become possible.

However the heart begins to function during its formation. Cardiogenic differentiation and morphogenesis occur simultaneously and interact mutually. Some of the developmental steps of the heart seem to be independent of proper cardiomyocyte function while others depend on normal function. The recent findings on ion channels and heart development highlight the crucial role of ion channels for specification, differentiation, and morphogenesis. Yet, the mechanisms how the ion conducting pores exert influence on heart development remain unclear. Ion flux dependent and independent functions of ion channels in the developing heart seem to exist. Hence there is still a lot to be learned from zebrafish.

References

[1] G. A. Papadatos, P. M. R. Wallerstein, C. E. G. Head et al., "Slowed conduction and ventricular tachycardia after targeted disruption of the cardiac sodium channel gene Scn5a," *Proceedings of the National Academy of Sciences of the United States of America*, vol. 99, no. 9, pp. 6210–6215, 2002.

[2] D. Y. R. Stainier and M. C. Fishman, "The zebrafish as a model system to study cardiovascular development," *Trends in Cardiovascular Medicine*, vol. 4, no. 5, pp. 207–212, 1994.

[3] B. Pelster and W. W. Burggren, "Disruption of hemoglobin oxygen transport does not impact oxygen- dependent physiological processes in developing embryos of zebra fish (Danio rerio)," *Circulation Research*, vol. 79, no. 2, pp. 358–362, 1996.

[4] T. Dahme, H. A. Katus, and W. Rottbauer, "Fishing for the genetic basis of cardiovascular disease," *DMM Disease Models and Mechanisms*, vol. 2, no. 1-2, pp. 18–22, 2009.

[5] J. Bakkers, "Zebrafish as a model to study cardiac development and human cardiac disease," *Cardiovascular Research*, vol. 91, no. 2, pp. 279–288, 2011.

[6] N. S. Glickman and D. Yelon, "Cardiac development in zebrafish: coordination of form and function," *Seminars in Cell and Developmental Biology*, vol. 13, no. 6, pp. 507–513, 2002.

[7] D. Yelon, "Cardiac patterning and morphogenesis in zebrafish," *Developmental Dynamics*, vol. 222, no. 4, pp. 552–563, 2001.

[8] D. Y. R. Stainier, "Zebrafish genetics and vertebrate heart formation," *Nature Reviews Genetics*, vol. 2, no. 1, pp. 39–48, 2001.

[9] D. M. Roden, J. R. Balser, A. L. George, and M. E. Anderson, "Cardiac ion channels," *Annual Review of Physiology*, vol. 64, pp. 431–475, 2002.

[10] M. P. Davies, R. H. An, P. Doevendans, S. Kubalak, K. R. Chien, and R. S. Kass, "Developmental changes in ionic channel activity in the embryonic murine heart," *Circulation Research*, vol. 78, no. 1, pp. 15–25, 1996.

[11] N. Sperelakis and A. J. Pappano, "Physiology and pharmacology of developing heart cells," *Pharmacology and Therapeutics*, vol. 22, no. 1, pp. 1–39, 1983.

[12] J. F. Renaud, G. Romey, A. Lombet, and M. Lazdunski, "Differentiation of the fast Na^{+} channel in embryonic heart cells: interaction of the channel with neurotoxins," *Proceedings of the National Academy of Sciences of the United States of America*, vol. 78, no. 9, pp. 5348–5352, 1981.

[13] A. J. Sehnert, A. Huq, B. M. Weinstein, C. Walker, M. Fishman, and D. Y. R. Stainier, "Cardiac troponin T is essential in sarcomere assembly and cardiac contractility," *Nature Genetics*, vol. 31, no. 1, pp. 106–110, 2002.

[14] A. E. Novak, M. C. Jost, Y. Lu, A. D. Taylor, H. H. Zakon, and A. B. Ribera, "Gene duplications and evolution of vertebrate voltage-gated sodium channels," *Journal of Molecular Evolution*, vol. 63, no. 2, pp. 208–221, 2006.

[15] R. B. Rogart, L. L. Cribbs, L. K. Muglia, D. D. Kephart, and M. W. Kaiser, "Molecular cloning of a putative tetrodotoxin-resistant rat heart Na^{+} channel isoform," *Proceedings of*

the National Academy of Sciences of the United States of America, vol. 86, no. 20, pp. 8170–8174, 1989.

[16] M. E. Gellens, A. L. George, L. Chen et al., "Primary structure and functional expression of the human cardiac tetrodotoxin-insensitive voltage-dependent sodium channel," *Proceedings of the National Academy of Sciences of the United States of America*, vol. 89, no. 2, pp. 554–558, 1992.

[17] S. S. Chopra, D. M. Stroud, H. Watanabe et al., "Voltage-gated sodium channels are required for heart development in zebrafish," *Circulation Research*, vol. 106, no. 8, pp. 1342–1350, 2010.

[18] A. E. Novak, A. D. Taylor, R. H. Pineda, E. L. Lasda, M. A. Wright, and A. B. Ribera, "Embryonic and larval expression of zebrafish voltage-gated sodium channel α-subunit genes," *Developmental Dynamics*, vol. 235, no. 7, pp. 1962–1973, 2006.

[19] P. Nemtsas, E. Wettwer, T. Christ, G. Weidinger, and U. Ravens, "Adult zebrafish heart as a model for human heart? An electrophysiological study," *Journal of Molecular and Cellular Cardiology*, vol. 48, no. 1, pp. 161–171, 2010.

[20] N. Frey, T. A. McKinsey, and E. N. Olson, "Decoding calcium signals involved in cardiac growth and function," *Nature Medicine*, vol. 6, no. 11, pp. 1221–1227, 2000.

[21] E. Schroder, M. Byse, and J. Satin, "L-type calcium channel C terminus autoregulates transcription," *Circulation Research*, vol. 104, no. 12, pp. 1373–1381, 2009.

[22] N. Gomez-Ospina, F. Tsuruta, O. Barreto-Chang, L. Hu, and R. Dolmetsch, "The C terminus of the L-type voltage-gated calcium channel CaV1.2 encodes a transcription factor," *Cell*, vol. 127, no. 3, pp. 591–606, 2006.

[23] A. C. Dolphin, "β subunits of voltage-gated calcium channels," *Journal of Bioenergetics and Biomembranes*, vol. 35, no. 6, pp. 599–620, 2003.

[24] S. Herlitze, M. Xie, J. Han et al., "Targeting mechanisms of high voltage-ativated Ca^{2+} channels," *Journal of Bioenergetics and Biomembranes*, vol. 35, no. 6, pp. 621–637, 2003.

[25] A. Castellano, X. Wei, L. Birnbaumer, and E. Perez-Reyes, "Cloning and expression of a neuronal calcium channel β subunit," *Journal of Biological Chemistry*, vol. 268, no. 17, pp. 12359–12366, 1993.

[26] D. Sedmera, T. Pexieder, N. Hu, and E. B. Clark, "A quantitative study of the ventricular myoarchitecture in the stage 21–29 chick embryo following decreased loading," *European Journal of Morphology*, vol. 36, no. 2, pp. 105–119, 1998.

[27] C. Seisenberger, V. Specht, A. Welling et al., "Functional embryonic cardiomyocytes after disruption of the L-type α1C (Cav1.2) calcium channel gene in the mouse," *Journal of Biological Chemistry*, vol. 275, no. 50, pp. 39193–39199, 2000.

[28] W. Rottbauer, K. Baker, Z. G. Wo, M. A. P. K. Mohideen, H. F. Cantiello, and M. C. Fishman, "Growth and function of the embryonic heart depend upon the cardiac-specific L-type calcium channel α1 subunit," *Developmental Cell*, vol. 1, no. 2, pp. 265–275, 2001.

[29] Y. Chernyavskaya, A. M. Ebert, E. Milligan, and D. M. Garrity, "Voltage-gated calcium channel CACNB2 (β2.1) protein is required in the heart for control of cell proliferation and heart tube integrity," *Developmental Dynamics*, vol. 241, pp. 648–662, 2012.

[30] A. M. Ebert, C. A. McAnelly, A. Srinivasan, R. L. Mueller, D. B. Garrity, and D. M. Garrity, "The calcium channel β2 (CACNB2) subunit repertoire in teleosts," *BMC Molecular Biology*, vol. 9, article 38, 2008.

[31] P. Weissgerber, B. Held, W. Bloch et al., "Reduced cardiac L-type Ca^{2+} current in Cav$\beta 2^{-/-}$ embryos impairs cardiac development and contraction with secondary defects in vascular maturation," *Circulation Research*, vol. 99, no. 7, pp. 749–757, 2006.

[32] S. L. Ball, P. A. Powers, H. S. Shin, C. W. Morgans, N. S. Peachey, and R. G. Gregg, "Role of the β2 subunit of voltage-dependent calcium channels in the retinal outer plexiform layer," *Investigative Ophthalmology and Visual Science*, vol. 43, no. 5, pp. 1595–1603, 2002.

[33] H. Haase, B. Pfitzmaier, M. W. McEnery, and I. Morano, "Expression of Ca(2+) channel subunits during cardiac ontogeny in mice and rats: identification of fetal alpha(1C) and beta subunit isoforms," *Journal of Cellular Biochemistry*, vol. 76, pp. 695–703, 2000.

[34] W. Zhou, E. J. Horstick, H. Hirata, and J. Y. Kuwada, "Identification and expression of voltage-gated calcium channel β subunits in zebrafish," *Developmental Dynamics*, vol. 237, no. 12, pp. 3842–3852, 2008.

[35] A. M. Ebert, G. L. Hume, K. S. Warren et al., "Calcium extrusion is critical for cardiac morphogenesis and rhythm in embryonic zebrafish hearts," *Proceedings of the National Academy of Sciences of the United States of America*, vol. 102, no. 49, pp. 17705–17710, 2005.

[36] T. D. Reed, G. J. Babu, Y. Ji et al., "The expression of SR calcium transport atpase and the Na^+/Ca^{2+} exchanger are antithetically regulated during mouse cardiac development and in hypo/hyperthyroidism," *Journal of Molecular and Cellular Cardiology*, vol. 32, no. 3, pp. 453–464, 2000.

[37] I. Lüss, P. Boknik, L. R. Jones et al., "Expression of cardiac calcium regulatory proteins in atrium v ventricle in different species," *Journal of Molecular and Cellular Cardiology*, vol. 31, no. 6, pp. 1299–1314, 1999.

[38] N. Tohse, S. Seki, T. Kobayashi, M. Tsutsuura, M. Nagashima, and Y. Yamada, "Development of excitation-contraction coupling in cardiomyocytes," *Japanese Journal of Physiology*, vol. 54, no. 1, pp. 1–6, 2004.

[39] C. H. Cho, S. S. Kim, M. J. Jeong, C. O. Lee, and H. S. Shin, "The Na^+ -Ca^{2+} exchanger is essential for embryonic heart development in mice," *Molecules and cells*, vol. 10, no. 6, pp. 712–722, 2000.

[40] K. Wakimoto, K. Kobayashi, M. Kuro-o et al., "Targeted disruption of Na^+/Ca^{2+} exchanger gene leads to cardiomyocyte apoptosis and defects in heartbeat," *Journal of Biological Chemistry*, vol. 275, no. 47, pp. 36991–36998, 2000.

[41] K. K. Linask, M. D. Han, M. Artman, and C. A. Ludwig, "Sodium-calcium exchanger (NCX-1) and calcium modulation: NCX protein expression patterns and regulation of early heart development," *Developmental Dynamics*, vol. 221, no. 3, pp. 249–264, 2001.

[42] A. D. Langenbacher, Y. Dong, X. Shu et al., "Mutation in sodium-calcium exchanger 1 (NCX1) causes cardiac fibrillation in zebrafish," *Proceedings of the National Academy of Sciences of the United States of America*, vol. 102, no. 49, pp. 17699–17704, 2005.

[43] N. J. Yard, M. Chiesi, and H. A. Ball, "Effect of cyclopiazonic acid, an inhibitor of sarcoplasmic reticulum Ca^{2+}-ATPase, on the frequency-dependence of the contraction-relaxation cycle of the guinea-pig isolated atrium," *British Journal of Pharmacology*, vol. 113, no. 3, pp. 1001–1007, 1994.

[44] S. Takahashi, Y. Kato, M. Adachi, N. Agata, H. Tanaka, and K. Shigenobu, "Effects of cyclopiazonic acid on rat myocardium: inhibition of calcium uptake into sarcoplasmic reticulum,"

Journal of Pharmacology and Experimental Therapeutics, vol. 272, no. 3, pp. 1095–1100, 1995.

[45] X. Shu, K. Cheng, N. Patel et al., "Na,K-ATPase is essential for embryonic heart development in the zebrafish," *Development*, vol. 130, no. 25, pp. 6165–6173, 2003.

[46] C. Zhang, T. Miki, T. Shibasaki, M. Yokokura, A. Saraya, and S. Seino, "Identification and characterization of a novel member of the ATP-sensitive K^+ channel subunit family, Kir6.3, in zebrafish," *Physiological Genomics*, vol. 24, no. 3, pp. 290–297, 2006.

[47] D. Hassel, E. P. Scholz, N. Trano et al., "Deficient zebrafish ether-à-go-go-related gene channel gating causes short-QT syndrome in zebrafish reggae mutants," *Circulation*, vol. 117, no. 7, pp. 866–875, 2008.

[48] E. P. Scholz, N. Niemer, D. Hassel et al., "Biophysical properties of zebrafish ether-à-go-go related gene potassium channels," *Biochemical and Biophysical Research Communications*, vol. 381, no. 2, pp. 159–164, 2009.

[49] B. Meder, E. P. Scholz, D. Hassel et al., "Reconstitution of defective protein trafficking rescues Long-QT syndrome in zebrafish," *Biochemical and Biophysical Research Communications*, vol. 408, no. 2, pp. 218–224, 2011.

[50] Y. H. Zhang, C. K. Colenso, R. B. Sessions, C. E. Dempsey, and J. C. Hancox, "The hERG K^+ channel S4 domain L532P mutation: characterization at 37°C," *Biochimica et Biophysica Acta*, vol. 1808, no. 10, pp. 2477–2487, 2011.

[51] R. Arnaout, T. Ferrer, J. Huisken et al., "Zebrafish model for human long QT syndrome," *Proceedings of the National Academy of Sciences of the United States of America*, vol. 104, no. 27, pp. 11316–11321, 2007.

[52] G. Blanco and R. W. Mercer, "Isozymes of the Na-K-ATPase: heterogeneity in structure, diversity in function," *American Journal of Physiology*, vol. 275, no. 5, pp. F633–F650, 1998.

[53] R. H. G. Schwinger, H. Bundgaard, J. Müller-Ehmsen, and K. Kjeldsen, "The Na, K-ATPase in the failing human heart," *Cardiovascular Research*, vol. 57, no. 4, pp. 913–920, 2003.

[54] R. H. G. Schwinger, J. Wang, K. Frank et al., "Reduced sodium pump $\alpha 1$, $\alpha 3$, and $\beta 1$-isoform protein levels and Na^+, K^+-ATPase activity but unchanged Na^+-Ca^{2+} exchanger protein levels in human heart failure," *Circulation*, vol. 99, no. 16, pp. 2105–2112, 1999.

[55] P. F. James, I. L. Grupp, G. Grupp et al., "Identification of a specific role for the Na,K-ATPase $\alpha 2$ isoform as a regulator of calcium in the heart," *Molecular Cell*, vol. 3, no. 5, pp. 555–563, 1999.

[56] K. K. Linask and Y. H. Gui, "Inhibitory effects of ouabain on early heart development and cardiomyogenesis in the chick embryo," *Developmental Dynamics*, vol. 203, no. 1, pp. 93–105, 1995.

[57] S. J. R. Rajarao, V. A. Canfield, M. A. P. K. Mohideen et al., "The repertoire of Na,K-ATPase α and β subunit genes expressed in the Zebrafish, Danio rerio," *Genome Research*, vol. 11, no. 7, pp. 1211–1220, 2001.

[58] U. Langheinrich, G. Vacun, and T. Wagner, "Zebrafish embryos express an orthologue of HERG and are sensitive toward a range of QT-prolonging drugs inducing severe arrhythmia," *Toxicology and Applied Pharmacology*, vol. 193, no. 3, pp. 370–382, 2003.

Hindawi Publishing Corporation
Stem Cells International
Volume 2012, Article ID 816049, 10 pages
doi:10.1155/2012/816049

Review Article

Bioelectric State and Cell Cycle Control of Mammalian Neural Stem Cells

Julieta Aprea and Federico Calegari

DFG-Research Center and Cluster of Excellence for Regenerative Therapies, Medical Faculty, Dresden University of Technology, Fetscherstrasse 105, 01307 Dresden, Germany

Correspondence should be addressed to Federico Calegari, federico.calegari@crt-dresden.de

Received 2 May 2012; Accepted 22 July 2012

Academic Editor: Stefan Liebau

The concerted action of ion channels and pumps establishing a resting membrane potential has been most thoroughly studied in the context of excitable cells, most notably neurons, but emerging evidences indicate that they are also involved in controlling proliferation and differentiation of nonexcitable somatic stem cells. The importance of understanding stem cell contribution to tissue formation during embryonic development, adult homeostasis, and regeneration in disease has prompted many groups to study and manipulate the membrane potential of stem cells in a variety of systems. In this paper we aimed at summarizing the current knowledge on the role of ion channels and pumps in the context of mammalian corticogenesis with particular emphasis on their contribution to the switch of neural stem cells from proliferation to differentiation and generation of more committed progenitors and neurons, whose lineage during brain development has been recently elucidated.

1. Introduction

An extensive literature has described the features and properties of bioelectric gradients and signaling in a variety of tissues of many species during development, adulthood, and regeneration [1–5]. In particular for the developing nervous system, it has become clear that the concerted action of membrane channels and ion pumps establishing a resting membrane potential (V_{mem}) and other bioelectric parameters plays important roles in migration, survival, maturation, and functionality of newborn neurons [6–8]. Certainly less investigated is whether similar parameters may also play a role in controlling the switch of neural stem and progenitor cells (altogether referred to as NSC) from proliferative to neurogenic divisions but various evidences have accumulated in recent years making this possibility likely; in particular, when considering the multiple factors coupling bioelectric gradients and cell cycle progression [1, 7, 9, 10] as well as the effects of cell cycle length on proliferation versus differentiation of neural, and other somatic, stem cells [11, 12].

However, the limits of our knowledge in this area are particularly evident during mammalian brain development in which the establishment of new, sophisticated tools has only recently allowed the characterization of the physiological lineage of NSC. Specifically, during embryonic development of the mammalian cortex, polarized radial-glial cells, also referred to as apical progenitors (AP) forming the ventricular zone (VZ), progressively switch from divisions that generate additional AP to divisions that generate more committed, neurogenic progenitors leaving the VZ to form the subventricular zone (SVZ) at its pial, or basal, boundary; hence the name basal progenitors (BP) [13, 14]. BP lose polarity, have limited self-renewal potential, and are soon consumed through symmetric neurogenic divisions to generate a pair of postmitotic neurons that migrate towards the pial surface to form the various neuronal layers of the mammalian cortex [13, 14] (Figure 1). Currently, most mammalian cortical neurons are thought to be derived from BP, rather than AP, and, interestingly, the appearance of this subpopulation of cells specifically in mammals has been proposed to be a critical step through which the massive enlargement in

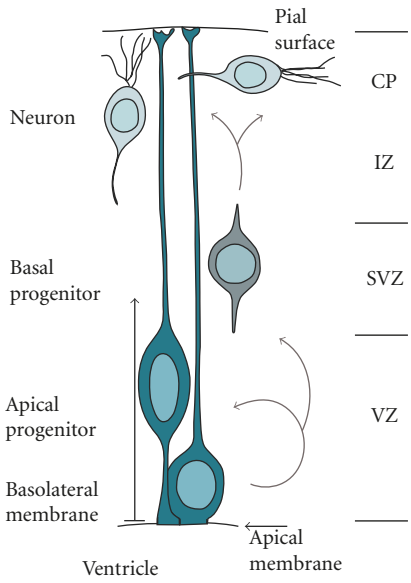

Figure 1: Scheme representing cell types in the developing mammalian cortex with (from top to bottom) neurons, basal (BP), and apical (AP) progenitors forming the cortical plate (CP), intermediate (IZ), subventricular (SVZ), and ventricular (VZ) zones, respectively. Lineages are depicted (arrows). Note the distinction between apical and basolateral plasma membrane of AP establishing the apicobasal polarity of the developing cortex.

cortical surface area has been achieved during evolution of our species [15–17].

Unfortunately, major technical limitations in investigating the role of bioelectric signals in neurogenic commitment during development have prompted most groups to use nonmammalian organisms, lacking BP, as model systems. Moreover, of the few reports in which mammalian NSC have been used, the vast majority were carried out in cultures of dissociated cells in which the loss of positional information and polarity makes it difficult to identify and compare characteristics of AP and BP. For these reasons, our knowledge about bioelectric signaling during mammalian brain development is very limited and its role in controlling the switch from proliferating AP to neurogenic BP can only be retrospectively inferred from previous studies in which these questions were, if any, only indirectly addressed.

Other authors have already summarized our current knowledge about a potential role of bioelectric signaling in stem cell function in various tissues or, within the nervous system, without considering progenitor lineages of the mammalian cortex [1–4, 7–9]. Thus, in this paper we attempted to make the retrospective links that may help address its role in the switch of mammalian NSC from proliferation to neurogenesis, which is fundamental towards understanding brain development and, perhaps, designing novel approaches of therapy of the mammalian central nervous system. Considering the extensive breadth of this area of research, we decided to focus our attention exclusively on the role of ion channels and pumps and their role in establishing a resting membrane potential in mammalian NSC of the developing embryo without discussing other bioelectric features, such as capacitance and input resistance, or additional roles of ion channels and metabotropic transporters involved in intracellular Ca^{2+} signaling, that were discussed elsewhere [1–8].

2. Establishing a Resting Membrane Potential in NSC

The fundamental mechanisms controlling the resting membrane potential of NSC are essentially identical to those of any other cell type being regulated by the permeability of ion channels and the activity of ion pumps and exchangers establishing ion gradients across membranes [8, 18–20]. Members of the first group include "leak" as well as voltage- and ligand-gated channels that allow the passive diffusion of ions through membranes after opening as a result of a change in voltage or binding to a specific ligand, respectively [18, 20]. Examples of the second group include various types of ATPases and other enzymatic complexes exchanging ions through membranes against their gradients by consumption of energy, including the ubiquitous Na^+/K^+, H^+, Ca^{2+} ATPases, and $Na^+/K^+/Cl^-$ cotransporters covering almost the whole spectrum of biologically relevant ions [18, 19]. The roles of the three major classes of ion channels and pumps in embryonic mammalian neurogenesis will be discussed separately.

2.1. Voltage-Gated Ion Channels. The study of voltage-gated ion channels has been particularly important for understanding the origin of action potentials, but recent evidences suggest that they may play important roles also in nonexcitable cells such as NSC. Several channels responsible for establishing a V_{mem} in NSC during development [21] and adulthood [22] have been characterized, but many discrepancies and uncertainties remain with regard to the specific features of the bioelectric state and signaling in different subpopulations of NSC. In particular, of the main types of voltage-gated K^+ currents both outward, delayed rectifier [21, 23–25] and inward rectifier currents in response to hyperpolarizing pulses [21] were detected. On the other hand, fast, A-type, transient outward K^+ currents were detected in NSC cultures [21, 23–25] but not in the VZ of organotypic slices [26].

Since the resting membrane potential of most animal cells is slightly higher than the reversal potential of K^+, the overall effect of blocking K^+ channels is to promote depolarization; this most typically correlates with increased cell proliferation. In fact, voltage-gated K^+ currents are involved in the regulation of the ce ll cycle, in particular G1, in many cell types [1, 7, 9, 10, 27], including NSC [8, 22], and treating NSC with certain K^+ channels antagonists promoted their proliferation in a number of assays [23, 28–30]. For example, blockage of voltage-gated delayed rectifier K^+ channels in cells isolated from rat midbrain increased the proportion of dividing precursors from ca. 10 to 30% [23]. In 12-week human fetal NSC, inhibition of delayed-rectifier K^+ channels either did not affect proliferation or increased it,

depending on the blocker used, while inhibition of A-type K^+ channels impaired cell viability [29]. This proliferation effect of certain blockers of K^+ channels has also been confirmed in adult neurogenic or embryonic gliogenic progenitors in which increased or decreased proliferation has been observed depending on which particular subtype of K^+ channels has been blocked [28, 30]. Along these lines, a block in K^+ channels in oligodendrocyte progenitors correlated with inhibited proliferation and an increase in the levels of the G1-specific cyclin-dependent kinase inhibitors p21 and p27 [31].

Reconciling these partly contrasting results is difficult not only because the pharmacological approaches and origin of NSC varied among studies but also because effects on membrane potential as a result of a block of one given type of K^+ channel were rarely measured to corroborate effects on de- versus hyperpolarization.

The K^+ currents found in NSC are also present in immature neurons in which inward Na^+ currents soon appear that increase their amplitude during neuronal maturation until reaching values characteristic of mature neurons [26, 32]. In contrast to K^+, the presence of voltage-gated Na^+ channels in NSC is controversial. Several studies have detected low Na^+ currents in NSC preparations, but these were present only in a relatively small subpopulation of cells of which most have been classified as early born neurons [21, 33], a conclusion that was also corroborated by direct measurement of NSC in the VZ of mouse cortical slices [34]. Nevertheless, it cannot be excluded that Na^+ currents may appear in more committed neurogenic progenitors, such as BP, since these cells were reported to initiate the expression of genes characteristically identifying postmitotic neurons [35, 36]. This possibility is consistent with the detection of Na^+ current in only a subpopulation of cortical progenitors [33] and is not invalidated by the absence of Na^+ currents in the VZ [34] since this latter study was limited to cells with radial morphology, that is, AP.

Direct evidence for the appearance of depolarizing Na^+ currents in the transition from AP to BP can be retrospectively inferred from a study by Bahrey and Moody in which organotypic slice cultures from the embryonic day (E) 14 mouse brain were used to measure bioelectrical parameters of different progenitor subtypes [26]. Upon labeling with vital dyes, the authors could identify radial versus nonradial cells within the VZ observing a bias for the presence of Na^+ currents in the latter population [26]. Interestingly, the proportion of cells in the VZ displaying Na^+ currents increased during development from 0, 30, and then 50% at E9, E14 and E16, respectively [26]. Not only these values fit remarkably well with the proportion of BP detected in the VZ [37], but one year after the study by Bahrey and Moody three independent reports could also demonstrate that the vast majority of nonradial cell in the VZ are, indeed, BP [38–40]. Thus, it can now be retrospectively concluded that the work by Bahrey and Moody provided the first strong evidence for a difference in AP versus BP currents at a time when, remarkably, cellular and molecular features of BP were not even characterized.

Similar to K^+, the presence of voltage-gated Ca^{2+} currents in NSC is consistently reported by various studies. Inward currents were detected in cells within the VZ in brain slices and dissociated cultures [26, 41, 42], and since similar currents were elicited also in preparations from E10 rat spinal cord [21], that are known to lack BP, it is likely that voltage-gated Ca^{2+} channels are a feature of all NSC. In cells isolated from human embryonic central nervous sytem [43] and P0 mouse cortex [44] small Ca^{2+} currents were only detected upon differentiation conditions in cells with neuronal morphology. Treating NSC with blockers of L-type voltage-gated Ca^{2+} channels has been found to reduce the number of neurons in differentiation conditions while, conversely, activating the channels triggered the opposite effect [44]. Yet, since the same experiments failed to detect Ca^{2+} currents in undifferentiated NSC [44], it may be concluded that the different number of neurons detected in this study may be attributed to effects on neuronal survival or an altered timing in the expression of neuronal markers in postmitotic cells rather than to a change in the fate of NSC proper.

The expression pattern during development of the fourth type of ion channels, Cl^-, has also been described [45], but functional experiments on their role in NSC differentiation are missing.

Altogether, several reports point to a role of voltage-gated ion channels in NSC proliferation with K^+ channels being more consistently implicated in this process. Most studies in this area were performed using dissociated cells, or in slice cultures but without considering different progenitor subtypes, thus making it difficult to infer differences between AP and BP; the latter probably being characterized by the presence of Na^+ currents [26]. It has been suggested that depolarization has a positive effect on proliferation [1, 7, 9], and many of the studies discussed above extend this view to NSC via manipulations that alter the activity of voltage-gated ion channels (Figure 2). Yet, the molecular mechanisms underlying this correlation are unknown.

2.2. Ligand-Gated Ion Channels. The study of ligand-gated ion channels is most typically associated with the understanding of neurotransmitter-dependent excitability of neurons and neuroendocrine cells, but evidences collected over the years have shown that at least two ligands, γ-aminobutyric acid (GABA) and glutamate, play important roles in NSC activity not only in the adult [46] but also in the developing brain even before functional synapses are formed [41, 47, 48].

Among the most extensively studied, the $GABA_A$ receptor is a ligand-gated Cl^- channel and because of the particular pattern of Cl^- transporters expressed in NSC of the embryonic brain [49, 50], these cells present a low Cl^- reversal potential implying that during development GABA depolarizes NSC and immature neurons instead of hyperpolarizing them as it does in the mature brain [48]. Functional $GABA_A$ receptors and GABA are expressed in mammalian NSC during brain development [41, 51] acting through paracrine/autocrine signaling [47, 52, 53], and NSC in the VZ start to respond to GABA by depolarizing V_{mem} at E15 but not before [41]. The cellular origin of nonsynaptic

Parameter manipulated	Type of manipulation	Proliferation	Developmental stage/region	Reference
I_k	Kv1.3 block, Psora-4		rE14.5 mid, dissociated cells	[23]
	Kv3.1 block, TEA		rE14.5 mid, dissociated cells	[23]
	Inhibition, QND (low dose)	=	hW12, dissociated cells	[29]
	Inhibition, DTX		hW12, dissociated cells	[29]
	Inhibition, FSK		rE20 Cx,O-2A prog.	[31]
I_A	Inhibition, 4-AP/PTX/NH_4Cl		hW12, dissociated cells	[29]
$[K^+]_e$	20 mM KCl (depolarization)		rE17 Cx, slices VZ + SVZ	[41]
	5 mM KCl (depolarization)		rE15 LGE, dissociated cells	[64]
$GABA_A$ receptor	Agonist, GABA	=	rE14Cx, slices VZ+SVZ	[41]
	Agonist, GABA		rE16 and 19 Cx, slices VZ + SVZ	[41]
	Agonist, GABA/muscitol		mE13 and 14 Cx, slices, VZ	[56]
	Agonist, GABA/muscitol		mE13 and 14 Cx, slices, SVZ	[56]
	Agonist, GABA/muscitol		rE16 Cx, dissociated cells	[54]
	Antagonist, BMI	=	rE16 Cx, slices VZ + SVZ	[41]
	Antagonist, BMI		rE19 Cx, slices VZ + SVZ	[41]
	Antagonist, BMI	=	mE13 and 14 Cx, slices, VZ	[56]
	Antagonist, BMI		mE13 and 14 Cx, slices, SVZ	[56]
GlutamateR	Agonist, glutamate		rE16 and 19 Cx, slices VZ + SVZ	[41]
	Agonist, glutamate		hW10-16 Cx, dissociated cells	[65]
NMDA receptor	Agonist, glutamate + MK-801	=	hW10-16 Cx, dissociated cells	[65]
	Agonist, NMDA	=	rE16 and 19 Cx, slices VZ + SVZ	[41]
	Agonist, NMDA		rE15 LGE, dissociated cells	[64]
	Agonist, NMDA		rE16 Hp, dissociated cells	[42]
	Antagonist, D-APV		rE17 Cx, slices, VZ and SVZ/cells	[62]
	Antagonist, MK-801/CGS-19755	(1)	rE15–18, in utero	[64]
	Antagonist, MK-801	= (2)	rE15–18, in utero	[64]
	Antagonist, MK-801		rE15-16 LGE, in utero, VZ	[64]
	Antagonist, MK-801	=	rE15-16 LGE, in utero, SVZ	[64]
	Antagonist, MK-801/CGS-19755		rE15 LGE, dissociated cells	[64]
	Antagonist, MK-801	=	rE16 Hp, dissociated cells	[42]
Non-NMDA receptor	Agonist, kainate	=	rE14 Cx, slices VZ + SVZ	[41]
	Agonist, kainate		rE16 and 19 Cx, slices VZ + SVZ	[41]
	Agonist, glutamate/kainate		mE13 and 14 Cx, slices, VZ	[56]
	Agonist, glutamate/kainate		mE13 and 14 Cx, slices, SVZ	[56]
	Antagonist, CNQX	=	rE16 Cx, slices VZ + SVZ	[41]
	Antagonist, CNQX		rE19 Cx, slices VZ + SVZ	[41]
	Antagonist, CNQX		mE13 and 14 Cx, slices, VZ	[56]
	Antagonist, CNQX		mE13 and 14 Cx, slices, SVZ	[56]
	Antagonist, NQBX	= (1)	rE15–18, in utero	[64]
	Antagonist, NQBX	=	rE15 LGE, dissociated cells	[64]

Figure 2: Effects upon manipulation of ion channels or extracellular ionic composition on the proliferation of NSC. Green and red arrows indicate increased or decreased proliferation, respectively, as deduced from incorporation of thymidine analogues or number of neurons in the adult striatum (1) or motor cortex (2). Agonists and antagonists used (Psora-4 = 5-(4-phenylbutoxy)psoralen; TEA = tetraethylammonium chloride; QND = quinidine; DTX = α-dendrotoxin; FSK = forskolin; 4-AP = 4-aminopyridine; PTX = phrixotoxin; BMI = biculline methionine; D-APV = D(-)-2-amino-5-phosphonopentanoicacid; CNQX = 6-cyano-7-dinitroquinoxaline-2,3-dione; NQBX = 1,2,3,4-tetrahydro-6-nitro-2,3-dioxo-benzol(f)-quinoxaline-7-sulfonamide) as well as source of NSC form different species (r = rat; h = human; m = mouse), developmental stage (E = embryonic day; W = embryonic week), or region (mid = midbrain; Cx = cortex; LGE = lateral ganglionic eminence; Hp = hippocampus; VZ = ventricular zone; SVZ = subventricular zone) are indicated. *reduced viability; **only in the presence of bFGF; O-2A = oligodendrocyte progenitors.

GABA release is still controversial, but there is evidence for the presence of a synthetic machinery in NSC [51].

Several studies have pointed to an effect of GABA on NSC proliferation. LoTurco et al. found that GABA inhibits DNA synthesis in embryonic rat cortical explants and since GABA caused a reversible increase in $[Ca^{2+}]_i$, and depolarization by K^+ had similar effects to GABA, the authors hypothesized that the effect on proliferation is mediated through activation of voltage-gated Ca^{2+} channels [41]. Consistently, GABA administration on dissociated cells was found to inhibit proliferation while promoting differentiation [54, 55]. On the other hand, Haydar et al. subsequently observed that GABA increased proliferation with a shortening of the cell cycle and decreased differentiation in the VZ while, interestingly, the opposite effect was found in the SVZ, where BP reside [56]. Clearly, differences between AP and BP were lost when NSC were pulled together [41] or studied using dissociated cultures [54, 55]. Other reports have also pointed to a positive effect of GABA on proliferation [57], and a vast literature has described its many effects on survival, migration, maturation, and synaptogenesis of newborn neurons [48, 52, 53].

Glutamate is the principal excitatory neurotransmitter in the adult cerebral cortex whose signals, as for GABA, are mediated by ionotropic and metabotropic receptors. The former group is further subdivided into three types based on their pharmacological and electrophysiological properties and named after their specific agonists: NMDA, AMPA, and KA receptors [58]. Considering the similar effect of GABA and glutamate on depolarization, it is not surprising that both neurotransmitters elicited similar effects on NSC.

The presence of NMDA receptors in NSC has been reported in several systems including NSC lines, primary cultures, and organotypic slice preparations displaying low expression levels of this receptor and small NMDA-mediated currents [59–62]. The fact that the NMDA-elicited currents observed in the VZ are all but a small fraction of those in the cortical plate, where neurons reside, [62] may explain why these currents were not detected by previous studies [41].

One early work reported increased proliferation upon block of NMDA receptors in NSC of the VZ and SVZ in slice cultures [62], but later studies consistently reached the opposite conclusion by showing that agonists of NMDA receptors increase proliferation while, conversely, antagonists trigger the opposite effect in vitro and in vivo [42, 63–65].

AMPA and KA receptors are expressed during development as early as E10 [60, 66]. In rat cortical slices, an increasing proportion of cells in the VZ depolarized upon AMPA or KA exposure as a function of developmental time from 0 to 100% between E14 and E16 [41]. Exposure to KA in rat cortical slices decreased NSC proliferation [41], while exposure to AMPA or KA agonists in mouse cortical slices shortened the cell cycle in the VZ but had the opposite effect on the SVZ while inhibiting neurogenesis [56].

Other ionotropic receptors for glycine, acetylcholine, and serotonin have also been implicated in neuronal development but primarily in the maturation, migration, synaptogenesis, and circuit formation of postmitotic neurons rather than in the regulation of NSC proliferation versus differentiation proper [52, 53].

Most of the limitations discussed in the context of voltage-dependent ion channels with regard to their involvement in AP to BP transition during mammalian cortical development hold true for ligand-dependent ion channels, and equally valid is the overall positive correlation between manipulations that depolarize NSC and increased proliferation (Figure 2).

2.3. Ion Pumps. The third big family of proteins essential for establishing an electric potential across membranes comprises enzymatic macrocomplexes converting energy, most typically chemical in the form of ATP or electrochemical gradients, to pump ions against their concentration gradient [18, 19]. An additional, and equally important, role of certain pumps is to regulate the concentration of ions in intracellular compartments as, for example, in the case of the ubiquitous H^+ ATPase responsible for the acidification of endosomes and other organelles [67, 68].

Despite their importance in a number of fundamental biological processes, few studies have addressed the effects of manipulating the activity of ion pumps in neural development; even fewer were focused on mammalian corticogenesis. For example, the Na^+/K^+ and Ca^{2+} ATPases have been shown to mediate dendritic outgrowth of mammalian cortical neurons [69] and midline signaling in zebrafish embryos [70]. Loss of function of the H^+ ATPase in *Xenopus* has been shown to inhibit development and regeneration [71, 72], while gain of function had the opposite effect [71].

Due to their multiple roles [67, 68], it is currently difficult to determine to which extent the effects induced by manipulations of ATPases are primarily due to a change in membrane potential as compared to other functions including endocytosis, trafficking, and signaling. Nevertheless, several observations suggest that the latter functions may be the most relevant ones during development. In particular, manipulations of the Na^+/K^+ ATPase during dendritogenesis of rat cortical neurons were not accompanied by a change in membrane potential but rather by a change in Ca^{2+}/calmodulin-dependent protein kinase signaling and cAMP-responsive element gene expression [69]. Moreover, the inhibition of Ca^{2+} ATPases that was shown to induce developmental defects in zebrafish was achieved by manipulating pumps specifically of the endoplasmic reticulum leading to increased intracellular Ca^{2+} and, thus altering the complex Ca^{2+}-dependent signaling events occurring during development more than changing V_{mem} proper [70]. Finally, with regard to the role of the H^+ ATPase various laboratories have independently shown that its inhibition affects the transduction of important signaling molecules, such as Notch [73, 74] and Wnt [75], that are known to control proliferation, tissue patterning, and development throughout the animal kingdom [76–79].

While essentially all experiments on the role of the H^+ ATPase in stem cell differentiation were performed in non-mammalian species, recent evidences from our laboratory could extend the role of this proton pump in Notch signaling

during mammalian cortical development [80]. In these experiments, a dominant-negative subunit of the H^+ ATPase was overexpressed during mouse embryonic development in NSC triggering their premature differentiation through a reduction of endogenous Notch signaling [80]. These and other experiments [73, 74, 80] support the notion that intracellular cleavage of activated Notch requires trafficking through acidic endosomes [81–83], but the intrinsic difficulties in distinguishing between cell autonomous versus extrinsic effects, and reports showing that Notch signaling may not require endocytosis [84–86], have led to a long debate in the field. Nevertheless, the fact that ATPases can have multiple effects at the level of (i) the cell biophysical state, (ii) signaling of differentiation molecules, and (iii) cell cycle length, places these enzymatic complexes in an ideal position to control the differentiation of NSC during mammalian corticogenesis.

Cation-chloride cotransporters are a family of membrane proteins that use the Na^+/K^+ transmembrane electrochemical gradient to transport Cl^- against its gradient. This family is composed by seven members, most of which are expressed in neurons, with only one K^+ (KCC4) and one Na^+ (NKCC1) coupled cotransporters being detected in the proliferative zones of the developing cortex and being responsible for pumping Cl^- outside or inside the cell, respectively [49, 50, 87]. KCC4 expression is specific for the VZ and SVZ and its levels seem to increase during development from E12 to E14 and disappear perinatally [50]. NKCC1 expression in NSC similarly increases during development, but it then switches from NSC to neurons before birth [50].

The high expression of NKCC1 in the embryonic VZ [50] provides an explanation for the high $[Cl^-]_i$ underlying $GABA_A$ depolarization response in AP [50, 88]. In addition to NSC, NKCC1 is also highly expressed in immature cortical neurons from E18 to the first postnatal week [49, 50] while KCC2 shows a marked increase only after the first postnatal week [45, 49, 50]. These changes in the composition of Cl^- transporters during the first weeks of life are probably the cause for the reduced $[Cl^-]_i$ responsible for the excitatory versus inhibitory effects of GABA [88–91].

3. Membrane Potential and Proliferation versus Differentiation of NSC

The primary role of the concerted action of ion channels and pumps is to regulate the V_{mem} of cells and, thus, it is reasonable to assume that their effect on proliferation of NSC should be interpreted in the context of this function.

Various groups have measured the membrane potential of mammalian NSC during embryonic development by different approaches resulting in V_{mem} values that ranged from a maximum of −40 mV to a minimum of −70 mV [21, 25, 26, 50, 88, 92–94]. Because a higher proliferative activity is known to correlate with a less negative, or depolarized, V_{mem} [1, 7, 9] and NSC, in particular BP, lengthen their cell cycle as development proceed [12, 95], it would be expected that the different V_{mem} measured by the different authors should reflect the use of NSC at different developmental stages. Reinforcing this expectation, more negative, or hyperpolarized, V_{mem} during development may also be deduced from the fact that (i) adult NSC tend to be more hyperpolarized than embryonic NSCs [22], (ii) the activity of the $K^+/Na^+/2\ Cl^-$ transporter decreases during development [88], and (iii) developmentally regulated growth factors and signaling molecules influencing the cell cycle also influence the activity of ion channels [32, 96]. Yet, while comparing the measurements performed at different developmental stages, or from different regions of the central nervous system that contain, or lack, BP, [21, 25, 26, 50, 88, 92–94] we were unable to detect any specific trend.

Certainly, the lack of evidence for a change in V_{mem} during development, and in particular between AP and BP, should not be considered as an evidence for its lack since this comparison has never been directly pursued. Many of the reports discussed above are consistent with the view that an artificial depolarization of NSC may increase their proliferative potential and delay neurogenesis, but some are not and reconciling them is particularly difficult if one considers the diverse approaches and experimental condition used among studies including NSC of different origins and culture conditions, diverse pharmacological approaches to manipulate the activity of various ion channels or pumps without necessarily measuring an effect on V_{mem} or, even less so, cell cycle length. Moreover, in nearly all studies discussed, it is difficult to assess whether hyperpolarization is a cell-intrinsic feature of a given subpopulation of differentiating NSC, such as BP that increase in number during development, or, alternatively, an overall characteristic of tissues at different embryonic stages, as would be expected from the fact that ion concentrations in the cerebrospinal fluid fluctuate during mammalian development [97]. In fact, discriminating between these possibilities would require the measurement and manipulation of V_{mem} concomitantly in two coexisting subpopulations of cells, such as multipotent AP and more committed BP, at one given developmental time. Clearly, the ideal conditions to performing such experiments are those in which other bioelectric features of NSC, including capacitance, conductivity, and electric coupling mediated by junctions are preserved within an intact tissue.

The technical limitations intrinsic in these experiments are daunting, but recent developments provide the key towards addressing the role of V_{mem} in mammalian neurogenesis.

4. Conclusions

For many years the lineage of NSC during mammalian corticogenesis has been indirectly inferred from fixed tissues or retrospectively deduced upon S-phase labeling in vivo. Only recently has the establishment of time-lapse videomicroscopy and transgenesis evolved to the point that direct visualization of AP and BP divisions in organotypic slice cultures became possible [38–40]. Moreover, the identification of molecular markers for BP [37], the generation of

transgenic reporter mice allowing their visualization in alive tissues [98, 99], and new methods to genetically manipulate individual cells in brain cortical slices [100] while also monitoring G1/S/G2 progression [101] currently allow us to directly investigate the role of ion channels, pumps, and their effects on membrane potential during mammalian corticogenesis at the single-cell level. Overcoming the use of dissociated cells cultures and uncertainties with regard to the identity of different progenitors subtypes, these powerful new tools may allow us to reveal a new role of bioelectric signaling in NSC differentiation and likely reconcile the different reports that were discussed in this paper.

Similarly, great emphasis on the role of apicobasal polarity in AP/BP transition and neurogenesis has recently come to light in particular in the context of asymmetric cleavage plane orientation [102], subcellular localization of cell cycle regulators [103], and evolution of the mammalian brain [104]. This in turn triggers the question as to whether or not the subcellular localization of certain channels or pumps, rather than their absolute expression levels, might be important for cell fate change. Unfortunately, however, identification of ion pumps and channels in tissues has been historically established by electrophysiology or, alternatively, by in situ hybridization, neither of which provides any information about protein localization. When immunohistochemical characterization was undertaken [23, 25, 44, 54, 55, 64, 65], this was performed either on dissociated cells where apicobasal polarity is lost or in intact tissue but exclusively for the Na-K-Cl cotransporter that showed no preferential localization in the apicobasal axis [50].

Apparently, the two big fields comprising (i) cell biologists studying the cell cycle, lineage, and polarity of NSC and (ii) physiologists studying their channels, pumps, and membrane potential have seldom met. We hope that our paper may underline the importance of this interdisciplinary field.

Acknowledgments

J. Aprea and F. Calegari are supported by the DFG-funded Center for Regenerative Therapies, the Medical Faculty of the Dresden University of Technology, the Max Planck Institute of Molecular Cell Biology and Genetics, and the DFG-Collaborative Research Center SFB655 (subproject A20).

References

[1] M. Levin, "Large-scale biophysics: ion flows and regeneration," *Trends in Cell Biology*, vol. 17, no. 6, pp. 261–270, 2007.

[2] K. R. Robinson and M. A. Messerli, "Left/right, up/down: the role of endogenous electrical fields as directional signals in development, repair and invasion," *BioEssays*, vol. 25, no. 8, pp. 759–766, 2003.

[3] M. Zhao, "Electrical fields in wound healing—an overriding signal that directs cell migration," *Seminars in Cell and Developmental Biology*, vol. 20, no. 6, pp. 674–682, 2009.

[4] C. D. McCaig, A. M. Rajnicek, B. Song, and M. Zhao, "Controlling cell behavior electrically: current views and future potential," *Physiological Reviews*, vol. 85, no. 3, pp. 943–978, 2005.

[5] R. H. W. Funk and T. K. Monsees, "Effects of electromagnetic fields on cells: physiological and therapeutical approaches and molecular mechanisms of interaction. A review," *Cells Tissues Organs*, vol. 182, no. 2, pp. 59–78, 2006.

[6] R. B. Borgens, "Voltage gradients and ionic currents in injured and regenerating axons," *Advances in neurology*, vol. 47, pp. 51–66, 1988.

[7] C. D. McCaig, B. Song, and A. M. Rajnicek, "Electrical dimensions in cell science," *Journal of Cell Science*, vol. 122, no. 23, pp. 4267–4276, 2009.

[8] N. C. Spitzer, "Electrical activity in early neuronal development," *Nature*, vol. 444, no. 7120, pp. 707–712, 2006.

[9] D. J. Blackiston, K. A. McLaughlin, and M. Levin, "Bioelectric controls of cell proliferation: ion channels, membrane voltage and the cell cycle," *Cell Cycle*, vol. 8, no. 21, pp. 3519–3528, 2009.

[10] L. A. Pardo, "Voltage-gated potassium channels in cell proliferation," *Physiology*, vol. 19, no. 5, pp. 285–292, 2004.

[11] C. Lange and F. Calegari, "Cdks and cyclins link G(1) length and differentiation of embryonic, neural and hematopoietic stem cells," *Cell Cycle*, vol. 9, no. 10, pp. 1893–1900, 2010.

[12] P. Salomoni and F. Calegari, "Cell cycle control of mammalian neural stem cells: putting a speed limit on G1," *Trends in Cell Biology*, vol. 20, no. 5, pp. 233–243, 2010.

[13] M. Götz and W. B. Huttner, "The cell biology of neurogenesis," *Nature Reviews Molecular Cell Biology*, vol. 6, no. 10, pp. 777–788, 2005.

[14] A. Kriegstein and A. Alvarez-Buylla, "The glial nature of embryonic and adult neural stem cells," *Annual Review of Neuroscience*, vol. 32, pp. 149–184, 2009.

[15] A. Pontious, T. Kowalczyk, C. Englund, and R. F. Hevner, "Role of intermediate progenitor cells in cerebral cortex development," *Developmental Neuroscience*, vol. 30, no. 1–3, pp. 24–32, 2007.

[16] A. Kriegstein, S. Noctor, and V. Martínez-Cerdeño, "Patterns of neural stem and progenitor cell division may underlie evolutionary cortical expansion," *Nature Reviews Neuroscience*, vol. 7, no. 11, pp. 883–890, 2006.

[17] J. H. Lui, D. V. Hansen, and A. R. Kriegstein, "Development and evolution of the human neocortex," *Cell*, vol. 146, no. 1, pp. 18–36, 2011.

[18] E. Gouaux and R. MacKinnon, "Principles of selective ion transport in channels and pumps," *Science*, vol. 310, no. 5753, pp. 1461–1465, 2005.

[19] R. Blostein, "Ion pumps," *Current Opinion in Cell Biology*, vol. 1, no. 4, pp. 746–752, 1989.

[20] N. Unwin, "Neurotransmitter action: opening of ligand-gated ion channels," *Cell*, vol. 72, no. 1001, supplement, pp. 31–41, 1993.

[21] J. Cai, A. Cheng, Y. Luo et al., "Membrane properties of rat embryonic multipotent neural stem cells," *Journal of Neurochemistry*, vol. 88, no. 1, pp. 212–226, 2004.

[22] T. Yasuda and D. J. Adams, "Physiological roles of ion channels in adult neural stem cells and their progeny," *Journal of Neurochemistry*, vol. 114, no. 4, pp. 946–959, 2010.

[23] S. Liebau, C. Pröpper, T. Böckers et al., "Selective blockage of Kv1.3 and Kv3.1 channels increases neural progenitor cell proliferation," *Journal of Neurochemistry*, vol. 99, no. 2, pp. 426–437, 2006.

[24] T. Li, L. Jiang, H. Chen, and X. Zhang, "Characterization of excitability and voltage-gated ion channels of neural

progenitor cells in rat hippocampus," *Journal of Molecular Neuroscience*, vol. 35, no. 3, pp. 289–295, 2008.

[25] D. O. Smith, J. L. Rosenheimer, and R. E. Kalil, "Delayed rectifier and A-type potassium channels associated with Kv 2.1 and Kv 4.3 expression in embryonic rat neural progenitor cells," *PLoS One*, vol. 3, no. 2, Article ID e1604, 2008.

[26] H. L. P. Bahrey and W. J. Moody, "Voltage-gated currents, dye and electrical coupling in the embryonic mouse neocortex," *Cerebral Cortex*, vol. 13, no. 3, pp. 239–251, 2003.

[27] W. F. Wonderlin and J. S. Strobl, "Potassium channels, proliferation and G1 progression," *Journal of Membrane Biology*, vol. 154, no. 2, pp. 91–107, 1996.

[28] S. N. MacFarlane and H. Sontheimer, "Changes in ion channel expression accompany cell cycle progression of spinal cord astrocytes," *Glia*, vol. 30, pp. 39–48, 2000.

[29] G. Schaarschmidt, F. Wegner, S. C. Schwarz, H. Schmidt, and J. Schwarz, "Characterization of voltage-gated potassium channels in human neural progenitor cells," *PLoS One*, vol. 4, no. 7, Article ID e6168, 2009.

[30] T. Yasuda, P. F. Bartlett, and D. J. Adams, "Kir and Kv channels regulate electrical properties and proliferation of adult neural precursor cells," *Molecular and Cellular Neuroscience*, vol. 37, no. 2, pp. 284–297, 2008.

[31] C. A. Ghiani, X. Yuan, A. M. Eisen et al., "Voltage-activated K^+ channels and membrane depolarization regulate accumulation of the cyclin-dependent kinase inhibitors $p27^{Kip1}$ and $p21^{CIP1}$ in glial progenitor cells," *Journal of Neuroscience*, vol. 19, no. 13, pp. 5380–5392, 1999.

[32] J. Leng, L. Jiang, H. Chen, and X. Zhang, "Brain-derived neurotrophic factor and electrophysiological properties of voltage-gated ion channels during neuronal stem cell development," *Brain Research*, vol. 1272, no. C, pp. 14–24, 2009.

[33] D. H. Feldman, J. S. Thinschmidt, A. L. Peel, R. L. Papke, and P. J. Reier, "Differentiation of ionic currents in CNS progenitor cells: dependence upon substrate attachment and epidermal growth factor," *Experimental Neurology*, vol. 140, no. 2, pp. 206–217, 1996.

[34] S. C. Noctor, A. C. Flint, T. A. Weissman, R. S. Dammerman, and A. R. Kriegstein, "Neurons derived from radial glial cells establish radial units in neocortex," *Nature*, vol. 409, no. 6821, pp. 714–720, 2001.

[35] A. Attardo, F. Calegari, W. Haubensak, M. Wilsch-Bräuninger, and W. B. Huttner, "Live imaging at the onset of cortical neurogenesis reveals differential appearance of the neuronal phenotype in apical versus basal progenitor progeny," *PLoS One*, vol. 3, no. 6, Article ID e2388, 2008.

[36] Y. Ishii, S. Nakamura, and N. Osumi, "Demarcation of early mammalian cortical development by differential expression of fringe genes," *Developmental Brain Research*, vol. 119, no. 2, pp. 307–320, 2000.

[37] C. Englund, A. Fink, C. Lau et al., "Pax6, Tbr2, and Tbr1 are expressed sequentially by radial glia, intermediate progenitor cells, and postmitotic neurons in developing neocortex," *Journal of Neuroscience*, vol. 25, no. 1, pp. 247–251, 2005.

[38] S. C. Noctor, V. Martinez-Cerdeño, L. Ivic, and A. R. Kriegstein, "Cortical neurons arise in symmetric and asymmetric division zones and migrate through specific phases," *Nature Neuroscience*, vol. 7, no. 2, pp. 136–144, 2004.

[39] W. Haubensak, A. Attardo, W. Denk, and W. B. Huttner, "Neurons arise in the basal neuroepithelium of the early mammalian telencephalon: a major site of neurogenesis," *Proceedings of the National Academy of Sciences of the United States of America*, vol. 101, no. 9, pp. 3196–3201, 2004.

[40] T. Miyata, A. Kawaguchi, K. Saito, M. Kawano, T. Muto, and M. Ogawa, "Asymmetric production of surface-dividing and non-surface-dividing cortical progenitor cells," *Development*, vol. 131, no. 13, pp. 3133–3145, 2004.

[41] J. J. LoTurco, D. F. Owens, M. J. S. Heath, M. B. E. Davis, and A. R. Kriegstein, "GABA and glutamate depolarize cortical progenitor cells and inhibit DNA synthesis," *Neuron*, vol. 15, no. 6, pp. 1287–1298, 1995.

[42] J. Y. Joo, B. W. Kim, J. S. Lee et al., "Activation of NMDA receptors increases proliferation and differentiation of hippocampal neural progenitor cells," *Journal of Cell Science*, vol. 120, no. 8, pp. 1358–1370, 2007.

[43] D. R. Piper, T. Mujtaba, M. S. Rao, and M. T. Lucero, "Immunocytochemical and physiological characterization of a population of cultured human neural precursors," *Journal of Neurophysiology*, vol. 84, no. 1, pp. 534–548, 2000.

[44] M. D'Ascenzo, R. Piacentini, P. Casalbore et al., "Role of L-type Ca^{2+} channels in neural stem/progenitor cell differentiation," *European Journal of Neuroscience*, vol. 23, no. 4, pp. 935–944, 2006.

[45] G. H. Clayton, K. J. Staley, C. L. Wilcox, G. C. Owens, and R. L. Smith, "Developmental expression of ClC-2 in the rat nervous system," *Developmental Brain Research*, vol. 108, no. 1-2, pp. 307–318, 1998.

[46] S. Z. Young, M. M. Taylor, and A. Bordey, "Neurotransmitters couple brain activity to subventricular zone neurogenesis," *European Journal of Neuroscience*, vol. 33, no. 6, pp. 1123–1132, 2011.

[47] M. Demarque, A. Represa, H. E. Becq, I. Khalilov, Y. Ben-Ari, and L. Aniksztejn, "Paracrine intercellular communication by a Ca^{2+}- and SNARE-independent release of GABA and glutamate prior to synapse formation," *Neuron*, vol. 36, no. 6, pp. 1051–1061, 2002.

[48] D. D. Wang and A. R. Kriegstein, "Defining the role of GABA in cortical development," *Journal of Physiology*, vol. 587, no. 9, pp. 1873–1879, 2009.

[49] C. Wang, C. Shimizu-Okabe, K. Watanabe et al., "Developmental changes in KCC1, KCC2, and NKCC1 mRNA expressions in the rat brain," *Developmental Brain Research*, vol. 139, no. 1, pp. 59–66, 2002.

[50] H. Li, J. Tornberg, K. Kaila, M. S. Airaksinen, and C. Rivera, "Patterns of cation-chloride cotransporter expression during embryonic rodent CNS development," *European Journal of Neuroscience*, vol. 16, no. 12, pp. 2358–2370, 2002.

[51] W. Ma and J. L. Barker, "Complementary expressions of transcripts encoding GAD67 and GABA(A) receptor $\alpha 4$, $\beta 1$, and $\gamma 1$ subunits in the proliferative zone of the embryonic rat central nervous system," *Journal of Neuroscience*, vol. 15, no. 3, pp. 2547–2560, 1995.

[52] H. Le-Corronc, J. M. Rigo, P. Branchereau, and P. Legendre, "GABAA receptor and glycine receptor activation by paracrine/autocrine release of endogenous agonists: more than a simple communication pathway," *Molecular Neurobiology*, vol. 44, no. 1, pp. 28–52, 2011.

[53] L. Nguyen, J. M. Rigo, V. Rocher et al., "Neurotransmitters as early signals for central nervous system development," *Cell and Tissue Research*, vol. 305, no. 2, pp. 187–202, 2001.

[54] J. Antonopoulos, "Activation of the GABAA receptor inhibits the proliferative effects of bFGF in cortical progenitor cells," *European Journal of Neuroscience*, vol. 9, no. 2, pp. 291–298, 1997.

[55] L. Nguyen, B. Malgrange, I. Breuskin et al., "Autocrine/paracrine activation of the $GABA_A$ receptor inhibits the proliferation of neurogenic polysialylated neural cell adhesion

molecule-positive (PSA-NCAM$^+$) precursor cells from postnatal striatum," *Journal of Neuroscience*, vol. 23, no. 8, pp. 3278–3294, 2003.

[56] T. F. Haydar, F. Wang, M. L. Schwartz, and P. Rakic, "Differential modulation of proliferation in the neocortical ventricular and subventricular zones," *Journal of Neuroscience*, vol. 20, no. 15, pp. 5764–5774, 2000.

[57] T. Cesetti, T. Fila, K. Obernier et al., "GABAA receptor signaling induces osmotic swelling and cell cycle activation of neonatal prominin+ precursors," *Stem Cells*, vol. 29, no. 2, pp. 307–319, 2011.

[58] S. Nakanishi, "Molecular diversity of glutamate receptors and implications for brain function," *Science*, vol. 258, no. 5082, pp. 597–603, 1992.

[59] E. Muth-Köhne, S. Pachernegg, M. Karus, A. Faissner, and M. Hollmann, "Expression of NMDA receptors and Ca^{2+}-impermeable AMPA receptors requires neuronal differentiation and allows discrimination between two different types of neural stem cells," *Cellular Physiology and Biochemistry*, vol. 26, no. 6, pp. 935–946, 2010.

[60] N. Nakamichi, T. Takarada, and Y. Yoneda, "Neurogenesis mediated by γ-aminobutyric acid and glutamate signaling," *Journal of Pharmacological Sciences*, vol. 110, no. 2, pp. 133–149, 2009.

[61] D. W. Y. Sah, J. Ray, and F. H. Gage, "Regulation of voltage- and ligand-gated currents in rat hippocampal progenitor cells in vitro," *Journal of Neurobiology*, vol. 32, no. 1, pp. 95–110, 1997.

[62] T. Hirasawa, H. Wada, S. Kohsaka, and S. Uchino, "Inhibition of NMDA receptors induces delayed neuronal maturation and sustained proliferation of progenitor cells during neocortical development," *Journal of Neuroscience Research*, vol. 74, no. 5, pp. 676–687, 2003.

[63] K. Toriumi, A. Mouri, S. Narusawa et al., "Prenatal NMDA receptor antagonism impaired proliferation of neuronal progenitor, leading to fewer glutamatergic neurons in the prefrontal cortex," *Neuropsychopharmacology*, vol. 37, no. 6, pp. 1387–1396, 2012.

[64] K. C. Luk, T. E. Kennedy, and A. F. Sadikot, "Glutamate promotes proliferation of striatal neuronal progenitors by an NMDA receptor-mediated mechanism," *Journal of Neuroscience*, vol. 23, no. 6, pp. 2239–2250, 2003.

[65] M. Suzuki, A. D. Nelson, J. B. Eickstaedt, K. Wallace, L. S. Wright, and C. N. Svendsen, "Glutamate enhances proliferation and neurogenesis in human neural progenitor cell cultures derived from the fetal cortex," *European Journal of Neuroscience*, vol. 24, no. 3, pp. 645–653, 2006.

[66] V. Gallo, M. Pende, S. Scherer, M. Molne, and P. Wright, "Expression and regulation of kainate and AMPA receptors in uncommitted and committed neural progenitors," *Neurochemical Research*, vol. 20, no. 5, pp. 549–560, 1995.

[67] M. Forgac, "Vacuolar ATPases: rotary proton pumps in physiology and pathophysiology," *Nature Reviews Molecular Cell Biology*, vol. 8, no. 11, pp. 917–929, 2007.

[68] V. Marshansky and M. Futai, "The V-type H^+-ATPase in vesicular trafficking: targeting, regulation and function," *Current Opinion in Cell Biology*, vol. 20, no. 4, pp. 415–426, 2008.

[69] L. Desfrere, M. Karlsson, H. Hiyoshi et al., "Na,K-ATPase signal transduction triggers CREB activation and dendritic growth," *Proceedings of the National Academy of Sciences of the United States of America*, vol. 106, no. 7, pp. 2212–2217, 2009.

[70] R. Creton, "The calcium pump of the endoplasmic reticulum plays a role in midline signaling during early zebrafish development," *Developmental Brain Research*, vol. 151, no. 1-2, pp. 33–41, 2004.

[71] D. S. Adams, A. Masi, and M. Levin, "H^+ pump-dependent changes in membrane voltage are an early mechanism necessary and sufficient to induce *Xenopus* tail regeneration," *Development*, vol. 134, no. 7, pp. 1323–1335, 2007.

[72] L. N. Vandenberg, R. D. Morrie, and D. S. Adams, "V-ATPase-dependent ectodermal voltage and Ph regionalization are required for craniofacial morphogenesis," *Developmental Dynamics*, vol. 240, no. 8, pp. 1889–1904, 2011.

[73] Y. Yan, N. Denef, and T. Schüpbach, "The vacuolar proton pump, V-ATPase, is required for notch signaling and endosomal trafficking in *Drosophila*," *Developmental Cell*, vol. 17, no. 3, pp. 387–402, 2009.

[74] T. Vaccari, S. Duchi, K. Cortese, C. Tacchetti, and D. Bilder, "The vacuolar ATPase is required for physiological as well as pathological activation of the Notch receptor," *Development*, vol. 137, no. 11, pp. 1825–1832, 2010.

[75] C. M. Cruciat, B. Ohkawara, S. P. Acebron et al., "Requirement of prorenin receptor and vacuolar H^+-ATPase-mediated acidification for Wnt signaling," *Science*, vol. 327, no. 5964, pp. 459–463, 2010.

[76] R. Kopan and M. X. G. Ilagan, "The canonical notch signaling pathway: unfolding the activation mechanism," *Cell*, vol. 137, no. 2, pp. 216–233, 2009.

[77] M. E. Fortini, "Notch signaling: the core pathway and its posttranslational regulation," *Developmental Cell*, vol. 16, no. 5, pp. 633–647, 2009.

[78] A. C. Tien, A. Rajan, and H. J. Bellen, "A notch updated," *Journal of Cell Biology*, vol. 184, no. 5, pp. 621–629, 2009.

[79] R. van Amerongen and R. Nusse, "Towards an integrated view of Wnt signaling in development," *Development*, vol. 136, no. 19, pp. 3205–3214, 2009.

[80] C. Lange, S. Prenninger, P. Knuckles, V. Taylor, M. Levin, and F. Calegari, "The H^+ vacuolar ATPase maintains neural stem cells in the developing mouse cortex," *Stem Cells and Development*, vol. 20, no. 5, pp. 843–850, 2011.

[81] S. H. Pasternak, R. D. Bagshaw, M. Guiral et al., "Presenilin-1, nicastrin, amyloid precursor protein, and γ-secretase activity are co-localized in the lysosomal membrane," *Journal of Biological Chemistry*, vol. 278, no. 29, pp. 26687–26694, 2003.

[82] L. Seugnet, P. Simpson, and M. Haenlin, "Requirement for dynamin during notch signaling in *Drosophila* neurogenesis," *Developmental Biology*, vol. 192, no. 2, pp. 585–598, 1997.

[83] N. Gupta-Rossi, E. Six, O. LeBail et al., "Monoubiquitination and endocytosis direct γ-secretase cleavage of activated Notch receptor," *Journal of Cell Biology*, vol. 166, no. 1, pp. 73–83, 2004.

[84] G. Struhl and A. Adachi, "Requirements for presenilin-dependent cleavage of notch and other transmembrane proteins," *Molecular Cell*, vol. 6, no. 3, pp. 625–636, 2000.

[85] D. D. Shaye and I. Greenwald, "Endocytosis-mediated downregulation of LIN-12/Notch upon Ras activation in *Caenorhabditis elegans*," *Nature*, vol. 420, no. 6916, pp. 686–690, 2002.

[86] E. B. Sorensen and S. D. Conner, "γ-secretase-dependent cleavage initiates notch signaling from the plasma membrane," *Traffic*, vol. 11, no. 9, pp. 1234–1245, 2010.

[87] G. H. Clayton, G. C. Owens, J. S. Wolff, and R. L. Smith, "Ontogeny of cation-Cl- cotransporter expression in rat neocortex," *Developmental Brain Research*, vol. 109, no. 2, pp. 281–292, 1998.

[88] D. F. Owens, L. H. Boyce, M. B. E. Davis, and A. R. Kriegstein, "Excitatory GABA responses in embryonic and neonatal cortical slices demonstrated by gramicidin perforated-patch recordings and calcium imaging," *Journal of Neuroscience*, vol. 16, no. 20, pp. 6414–6423, 1996.

[89] C. Rivera, J. Voipio, J. A. Payne et al., "The K^+/Cl^- co-transporter KCC2 renders GABA hyperpolarizing during neuronal maturation," *Nature*, vol. 397, no. 6716, pp. 251–255, 1999.

[90] C. A. Hübner, V. Stein, I. Hermans-Borgmeyer, T. Meyer, K. Ballanyi, and T. J. Jentsch, "Disruption of KCC2 reveals an essential role of K-Cl cotransport already in early synaptic inhibition," *Neuron*, vol. 30, no. 2, pp. 515–524, 2001.

[91] D. F. Owens and A. R. Kriegstein, "Is there more to GABA than synaptic inhibition?" *Nature Reviews Neuroscience*, vol. 3, no. 9, pp. 715–727, 2002.

[92] T. Cesetti, K. Obernier, C. P. Bengtson et al., "Analysis of stem cell lineage progression in the neonatal subventricular zone identifies EGFR+/NG2- cells as transit-amplifying precursors," *Stem Cells*, vol. 27, no. 6, pp. 1443–1454, 2009.

[93] S. C. Noctor, A. C. Flint, T. A. Weissman, W. S. Wong, B. K. Clinton, and A. R. Kriegstein, "Dividing precursor cells of the embryonic cortical ventricular zone have morphological and molecular characteristics of radial glia," *Journal of Neuroscience*, vol. 22, no. 8, pp. 3161–3173, 2002.

[94] L. Nguyen, B. Malgrange, S. Belachew et al., "Functional glycine receptors are expressed by postnatal nestin-positive neural stem/progenitor cells," *European Journal of Neuroscience*, vol. 15, no. 8, pp. 1299–1305, 2002.

[95] Y. Arai, J. N. Pulvers, C. Haffner et al., "Neural stem and progenitor cells shorten S-phase on commitment to neuron production," *Nature Communications*, vol. 2, no. 1, article 154, 2011.

[96] A. F. Pla, D. Maric, S. C. Brazer et al., "Canonical transient receptor potential 1 plays a role in basic fibroblast growth factor (bFGF)/FGF receptor-1-induced Ca^{2+} entry and embryonic rat neural stem cell proliferation," *Journal of Neuroscience*, vol. 25, no. 10, pp. 2687–2701, 2005.

[97] M. W. Bradbury, J. Crowder, S. Desai, J. M. Reynolds, M. Reynolds, and N. R. Saunders, "Electrolytes and water in the brain and cerebrospinal fluid of the foetal sheep and guinea-pig," *Journal of Physiology*, vol. 227, no. 2, pp. 591–610, 1972.

[98] S. J. Arnold, J. Sugnaseelan, M. Groszer, S. Srinivas, and E. J. Robertson, "Generation and analysis of a mouse line harboring GFP in the Eomes/Tbr2 locus," *Genesis*, vol. 47, no. 11, pp. 775–781, 2009.

[99] R. D. Hodge, T. D. Kowalczyk, S. A. Wolf et al., "Intermediate progenitors in adult hippocampal neurogenesis: Tbr2 expression and coordinate regulation of neuronal output," *Journal of Neuroscience*, vol. 28, no. 14, pp. 3707–3717, 2008.

[100] E. Taverna, C. Haffner, R. Pepperkok, and W. B. Huttner, "A new approach to manipulate the fate of single neural stem cells in tissue," *Nature Neuroscience*, vol. 15, no. 2, pp. 329–337, 2012.

[101] A. Sakaue-Sawano, H. Kurokawa, T. Morimura et al., "Visualizing spatiotemporal dynamics of multicellular cell-cycle progression," *Cell*, vol. 132, no. 3, pp. 487–498, 2008.

[102] Y. Kosodo and W. B. Huttner, "Basal process and cell divisions of neural progenitors in the developing brain," *Development Growth and Differentiation*, vol. 51, no. 3, pp. 251–261, 2009.

[103] Y. Tsunekawa, J. M. Britto, M. Takahashi, F. Polleux, S.-S. Tan, and N. Osumi, "Cyclin D2 in the basal process of neural progenitors is linked to non-equivalent cell fates," *EMBO Journal*, vol. 31, no. 8, pp. 1879–1892, 2012.

[104] S. A. Fietz and W. B. Huttner, "Cortical progenitor expansion, self-renewal and neurogenesis-a polarized perspective," *Current Opinion in Neurobiology*, vol. 21, no. 1, pp. 23–35, 2011.

Hindawi Publishing Corporation
Stem Cells International
Volume 2012, Article ID 167265, 10 pages
doi:10.1155/2012/167265

Research Article

The Flatworm *Macrostomum lignano* Is a Powerful Model Organism for Ion Channel and Stem Cell Research

Daniil Simanov,[1] Imre Mellaart-Straver,[1] Irina Sormacheva,[2] and Eugene Berezikov[1,3]

[1] *Hubrecht Institute, KNAW, University Medical Center Utrecht, 3584 CT Utrecht, The Netherlands*
[2] *Institute of Cytology and Genetics SB RAS, 630090 Novosibirsk, Russia*
[3] *European Research Institute for the Biology of Ageing and University Medical Center Groningen, University of Groningen, 9713 AV Groningen, The Netherlands*

Correspondence should be addressed to Eugene Berezikov, e.berezikov@umcg.nl

Received 27 April 2012; Accepted 2 August 2012

Academic Editor: Michael Levin

Bioelectrical signals generated by ion channels play crucial roles in many cellular processes in both excitable and nonexcitable cells. Some ion channels are directly implemented in chemical signaling pathways, the others are involved in regulation of cytoplasmic or vesicular ion concentrations, pH, cell volume, and membrane potentials. Together with ion transporters and gap junction complexes, ion channels form steady-state voltage gradients across the cell membranes in nonexcitable cells. These membrane potentials are involved in regulation of such processes as migration guidance, cell proliferation, and body axis patterning during development and regeneration. While the importance of membrane potential in stem cell maintenance, proliferation, and differentiation is evident, the mechanisms of this bioelectric control of stem cell activity are still not well understood, and the role of specific ion channels in these processes remains unclear. Here we introduce the flatworm *Macrostomum lignano* as a versatile model organism for addressing these topics. We discuss biological and experimental properties of *M. lignano*, provide an overview of the recently developed experimental tools for this animal model, and demonstrate how manipulation of membrane potential influences regeneration in *M. lignano*.

1. Introduction

Ion channels represent a diverse family of pore-forming proteins. They are crucial for establishing voltage gradients across plasma membranes by allowing the flow of inorganic ions (such as Na^+, K^+, Ca^{2+}, or Cl^-) down their electrochemical gradients. Ionic flux through the channels provides the foundation for membrane excitability, which is essential for the proper functioning of neurons, cardiac, and muscle cells [1]. At the same time, ion channels serve many functions apart from electrical signal transduction. For example, Ca^{2+} is an important messenger, and changes in its intracellular concentrations influence numerous cellular processes in virtually all types of nonexcitable cells [2–4], including stem cells [5–7]. Besides, a number of ion channels are known to be directly involved in chemical signaling pathways in different cell types [8, 9]. As a result, mutations in genes encoding ion channel proteins have been associated with many disorders (so-called "channelopathies"), caused by dysfunction of both excitable (epilepsy, hypertension, cardiac arrhythmia) and nonexcitable (diabetes, osteopetrosis, and cystic fibrosis) cells [10]. Here we briefly describe the crucial role ion channels play in maintenance, proliferation, and differentiation of stem cells on the level of single cell and the whole organism. We discuss the importance of animal model systems, such as flatworms, for studying bioelectric signaling in complex morphogenesis during development and regeneration. Finally, we introduce the new flatworm model, *Macrostomum lignano*, and discuss its experimental potential for dissecting the roles of ion channels in stem cell regulation.

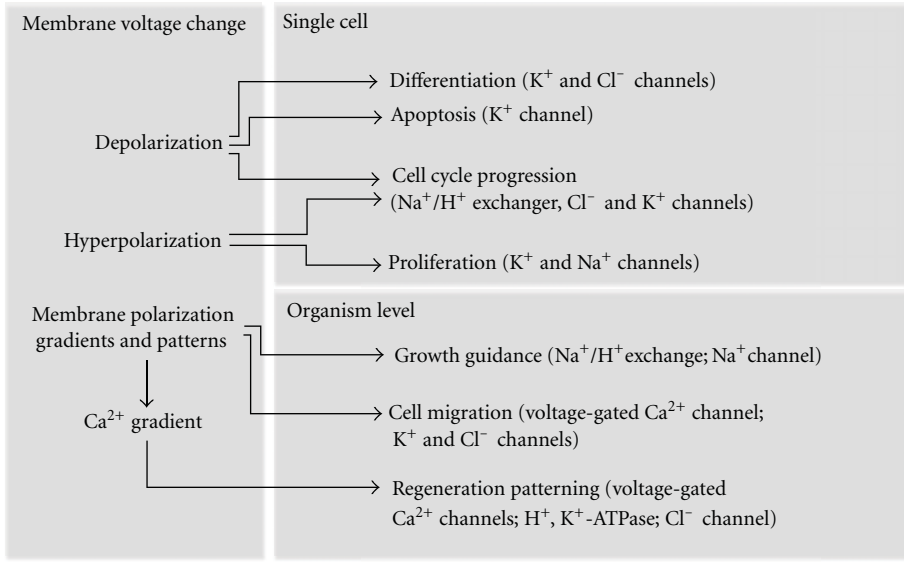

Figure 1: Ion channels and membrane voltage during regeneration. Changes of membrane potentials can directly affect different aspects of cell behavior and large-scale morphogenetic processes during regeneration. Ion channels and transporters implicated in these processes are mentioned in brackets.

2. Ion Channels and Membrane Potential in Stem Cells

Numerous ion channels and pumps together with gap junction complexes form transmembrane voltage gradients. While quick changes of these membrane potentials (V_{mem}) are best described in neurons, muscle, and cardiac cells, long-term steady-state V_{mem} levels are present in all other cells [11, 12]. Membrane potentials strongly correlate with the mitotic ability of different cell types, with the high resting potential associated with differentiated nondividing cells [13]. V_{mem} fluctuations during progression through the cell cycle have been reported in a number of cell types, and changes of membrane potential appear to be required for both G1/S and G2/S phase transitions [14–16]. Modulation of V_{mem} through applied electric fields or by inhibition of ion channels leads to cell cycle arrest in dividing cells [17–20], and artificial membrane hyperpolarization induces differentiation of mesenchymal stem cells [21]. On the other hand, electroporation (supposedly followed by membrane depolarization) activates cell hyperproliferation and de-differentiation [22].

On the level of multicellular organism, progression through the cell cycle should be strictly regulated and synchronized during such processes as development and regeneration in order to achieve a proper body patterning. Accordingly, stable and reproducible membrane polarization patterns have been recently described in various model organisms. Artificial modulation of these patterns during development or regeneration has a large impact on left-right asymmetry and anterior-posterior identity [23–27]. The role of bioelectric signaling in regeneration is comprehensively reviewed in [28] and schematically shown in Figure 1. Finally, modulations of membrane voltage have been observed in a large number of oncological disorders, and ion channels were proposed as cancer treatment targets [29, 30].

Thus, bioelectric signaling is an important mechanism of cell regulation, including stem cell maintenance, proliferation and differentiation. Recent findings suggest this control system to be well conserved in a wide range of animal phyla. However, the mechanisms linking membrane potential to the cell cycle, proliferation and differentiation, and the role of specific ion channels in this process remain largely unclear. The picture becomes even more complicated on the level of multicellular organism. Our understanding of the ways cells produce and receive bioelectric signals and translate them into positional information during development and regeneration is still fairly poor. While considerable knowledge about the role of membrane potential in stem cells was gathered recently from different species, the number of models used in this field is still limited. Expanding the range of model organisms used for functional studies of bioelectric signaling is crucial for better understanding of this control system and its role in complex morphogenesis.

3. Planarian Models in Ion Channel Research

Planarian flatworms are long-established models for stem cell and regeneration research. The adult stem cell system and regeneration capacity of the species *Planaria maculata* and *Planaria lugubris* were described by Morgan as early as in the end of 19th century [31, 32]. In our days the favorite planarian species for research in the regeneration field are *Schmidtea mediterranea* and *Dugesia japonica* [33, 34]. Planaria were also one of the first species in which stable membrane potential patterns were described, and their role in regeneration postulated. In 1940s and 1950s Marsh

and Beams were able to specifically control establishing of anterior-posterior axis by providing bioelectrical signals to regenerating planaria fragments [35–37].

In the last 5 years considerable work was done in planaria on understanding the molecular and genetic mechanisms that allow cells to establish and maintain long-term membrane potential patterns and transduce bioelectric signals into proliferation and differentiation decisions. The importance of gap junction signaling in establishing anterior-posterior polarity during regeneration was shown [38], and the specific innexin gene, *Smedinx-11*, responsible for blastema (regenerating tissue) formation and stem cell maintenance identified [39].

The role of ion channels and pumps in the establishment of anterior-posterior axis during regeneration of planaria *D. japonica* was recently highlighted by groups of Michael Levin and Jonathan Marchant. *D. japonica*, which can regenerate an entire animal from a small part of a cut worm, has highly depolarized cell membranes in the head region, and highly polarized in the posterior part. In the cut worm this pattern is reestablished rapidly, regardless of the cutting plane [26]. After the wound is closed, blastema at all anterior-facing wounds gives origin to heads, while tails are regenerated from the posterior-facing wounds. The polarization pattern is altered by highly specific drugs against different ion channels and transporters, such as SCH-28080 (inhibitor of H^+, K^+-ATPase), ivermectin (IVM, activator of the invertebrate GluCl channels), or praziquantel (PZQ, activator of voltage-operated Ca^{2+}-channels). Remarkably, induced depolarization itself is sufficient to drive ectopic anterior (head) regeneration even in posterior-facing blastemas, whereas membrane polarization of anterior-facing wounds blocks the head regeneration [25, 26]. The role of specific voltage-operated Ca^{2+} channels in regenerative patterning was addressed in the followup experiments [27].

Thus, planarian flatworms can be successfully used for ion channel and stem cell studies. Fascinating regeneration capacity of these animals, together with a wide range of research techniques established and optimized over the last 100 years, make planaria a very attractive model for studying bioelectric signaling during regenerative morphogenesis. However, due to inefficient sexual reproduction under laboratory conditions, classical genetic methods are not available in planarians, and reverse genetics methods are limited to RNA interference. Since genetic manipulation of these animals is difficult, no reproducible transgenesis methods are available for planaria [40].

4. Experimental Properties of the Flatworm *Macrostomum lignano*

During the last decade another flatworm, *Macrostomum lignano*, has emerged as a complementary model organism for regeneration research [41–44]. This marine free-living basal flatworm is about 1.5 mm long and consists of roughly 25000 cells. *M. lignano* is easy to culture in laboratory conditions, and populations of this animal are continuously maintained in the number of laboratories for over a decade. The generation time of the flatworm is short, with about two weeks of postembryonic development to sexually mature adult. Both juvenile and adult worms have clear morphology and are highly transparent (Figure 2(a)), greatly facilitating phenotyping and both fluorescent and non-fluorescent staining. The regeneration capacity of *M. lignano* is provided by roughly 1600 neoblasts (adult stem cells) located mesodermally. Proliferation activity of these cells can be easily studied using BrdU labeling, performed by simple soaking [43, 45] (Figure 2(b)). Importantly, *M. lignano* is nonself fertilizing hermaphrodite and has exclusively sexual reproduction. Well-fed adult animals generate a lot of embryos all year through (one animal lies on average one egg a day), making it accessible for genetic manipulation. *In situ* hybridization [43] and RNA interference (by soaking) [45] protocols are established and optimized for *M. lignano*, and a number of tissue-specific monoclonal antibodies are available [41]. Basic culturing and experimental properties of *M. lignano* are summarized in Table 1.

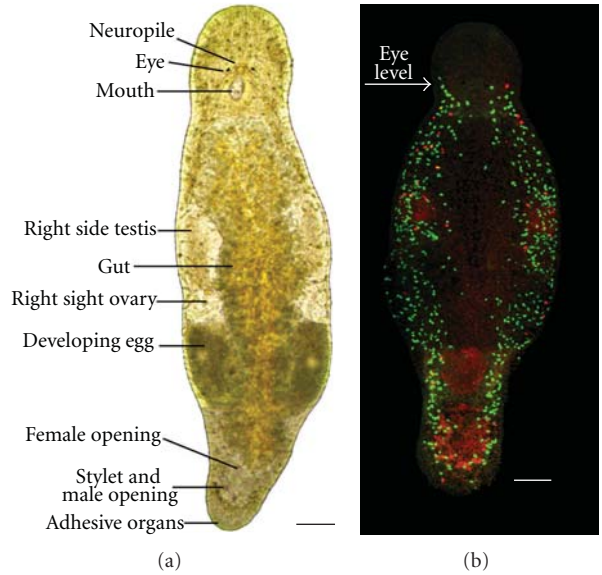

Figure 2: *Macrostomum lignano* as a model organism. (a) Bright field image of a living specimen. (b) Confocal projection of BrdU and phospho-histone H3 immunostaining after 30 minutes BrdU pulse in an adult worm (green: S-phase cells, red: mitotic cells). Scalebar 100 μm.

Considerable progress has been made in the past three years towards establishing *M. lignano* as versatile stem cell research model for the genomics era. The work on *M. lignano* genome assembly and annotation is in progress (Berezikov and colleagues), and draft genome and transcriptome assemblies are publicly available at http://www.macgenome.org/. Comparing transcriptome data obtained from irradiated (neoblast-depleted) and control worms provided the insight into the role of a number of genes in regeneration, while stage-specific transcriptome data showed the temporal expression of *Macrostomum* genes through development

Table 1: Biological and experimental properties of *M. lignano*.

Size	1 mm
Total cell number	±25.000
Neoblasts	±1600
Transparency	Highly transparent
Culturing media	f/2 (sea water based)
Feeding	Diatom algae (*Nitzschia curvilineata*)
Embryogenesis	5 days
Generation time	18 days
Nervous, muscle system, and gonads	Simple
Stem cell system	Pluripotent
BrdU/H3 staining	Yes (easy by soaking)
RNA interference	Yes (easy by soaking)
Accessibility to eggs	Single eggs (one egg/day per animal)
Transgenics	Possible, by injection into eggs

(Simanov et al., in preparation). Most importantly, proof-of-principle for transgenesis in *M. lignano* has been demonstrated and first stable transgenic GFP-expressing lines of *M. lignano* have been established (Demircan, De Mulder, Berezikov et al., in preparation). Thus, biological and experimental properties of *M. lignano*, combined with its rapidly expanding experimental toolbox, make this animal an attractive and powerful model organism for stem cell and regeneration research. Its astonishing ability to resist γ-irradiation and recover after being exposed to it makes the neoblast system of this animal exceptional even for flatworms [46]. Moreover, fascinating but yet poorly understood link between regeneration and rejuvenation provides an exciting opportunity of using *M. lignano* as a model for ageing research [47].

5. Ion Channels and Regeneration in *M. lignano*

Unlike planarian flatworm species, *M. lignano* is unable to regenerate the head under normal circumstances. Posterior-facing blastemas give origin to fully functioning tails with all its organs and structures, whereas anterior-facing wounds develop blastema layer but the actual regeneration can only happen if the worm was amputated in front of the brain (at the very tip of the head). Thus, anterior fragments of the worm, having a functional head, can regenerate the whole body in 2-3 weeks, while posterior fragments normally die 5–10 days after losing the head [42]. These differences in the head regeneration capacity between *M. lignano* and planarians, and the ability to induce ectopic head regeneration in *D. japonica* by the manipulation of membrane voltage gradients, prompted us to investigate how these findings in planarians translate into *M. lignano.*

$DiBAC_4(3)$ voltage-reporting dye stainings (as described in [48]) showed that membrane voltage pattern in *M. lignano* is similar to the one observed in *D. japonica* [26]—the anterior part is highly depolarized, while the tail is relatively polarized. In the cut worms this pattern is quickly reestablished in the anterior head-containing fragments, while the posterior headless fragments do not show any clear anterior-posterior polarization gradient and do not regenerate (Figure 3(a)). Just like in planarians, membrane polarization patterns in *M. lignano* can be altered using drugs against ion channels. IVM induces depolarization of the membranes of intact and cut worms, both in anterior and posterior regions (Figure 3(b)). Posterior-facing blastemas still regenerate the tails after treatment, though the full regeneration takes longer than normally. Anterior-facing wounds treated with IVM develop blastema, and some tissue growth is often observed within a week after wound closure. IVM-treated headless fragments always move more actively and survive longer comparing to control fragments. Strikingly, 1.5% of posterior fragments after IVM treatment are able to regenerate head-specific structures and, in a few cases, a fully functional head (Figures 3(c) and 3(c′)). PZQ causes the same depolarization effect but does not have any effect on regeneration patterning at tested concentrations (data not shown). Intact animals exposed to high doses of IVM or PZQ display phenotypes that in planarian flatworms are stereotypically associated with stem cell loss or disorder [49–52]. *M. lignano* animals treated with 2 μM IVM gradually lose anterior identity, with no head-specific structures left 7–9 days after treatment (Figure 3(d)). After exposure to higher doses of IVM (3-4 μM), worms develop characteristic square head due to partial tissue loss in the most anterior part of the body, get paralyzed and die 3-4 days after treatment (Figure 3(d′)). High concentration of PZQ in culturing media causes formation of bulges, mainly in the posterior part of the body (Figure 3(d′′)). This phenotype is completely different from the one observed after IVM treatment, suggesting specific action of the drugs.

These pilot experimental results show that *M. lignano* can be successfully used as a model for ion channel and stem cell studies. The complete transcriptome and established *in situ* hybridization and RNA interference methods, in combination with chemical treatment make it possible to address the function of specific ion channels in development, tissue turnover, and regeneration. For example, comparison of transcriptome data from irradiated (stem cell-deficient) and nonirradiated animals (Simanov et al., in preparation)

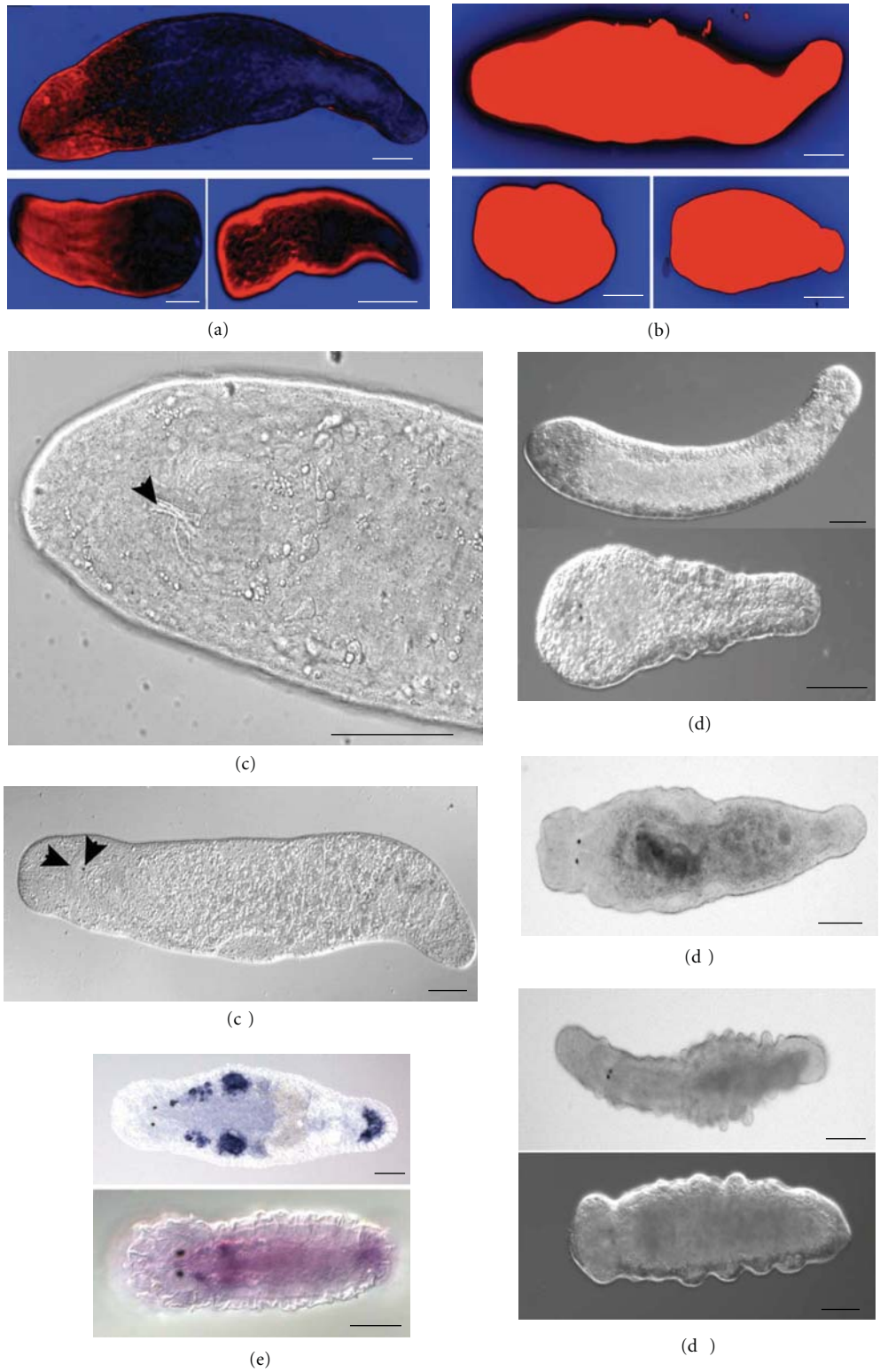

Figure 3: Bioelectric signaling and stem cells in *M. lignano*. (a-b) $DiBAC_4(3)$ staining of intact worm (top), anterior (left bottom) and posterior (right bottom) fragments. (a) control worm, (b) worm treated with 1 μM IVM. Blue is more polarized than black, black is more polarized than red. (c-c′) Regeneration of head-specific structures after 1 μM IVM treatment. Arrowheads in (c) indicate regenerated pharynx, in (c′) regenerated eye and half of the brain. (d-d′′) intact worms exposed to high doses of IVM (2 μM in d and 4 μM in d′) and PZQ (150 μM in d′′). (d) head regression; (d′) square head; (d′′) bulges and outgrowth. (e) *In situ* hybridization results in adult (top) and juvenile (bottom) animals with the probe against RNA815_5834 transcript from ML110815 transcriptome assembly (voltage-gated sodium channel). In juvenile worm this gene is expressed almost ubiquitously, and in adults expression is only detected in gonads and (likely) in somatic stem cells. Strong signal in the adhesive glands in the tail is likely a common artifact.

Table 2: Major categories of ion channel genes conserved between *H. sapiens* and *M. lignano*.

GO term	Description	*H*	*M*	Human genes
GO:0004889	Acetylcholine-activated cation-selective channel activity	13	132	CHRNA4, CHRNE, CHRNA10, CHRNB1, CHRNB3, CHRNA6, CHRNA3, CHRND, CHRNB2, CHRNB4, CHRNA9, CHRNA2, CHRNA7
GO:0004931	Extracellular ATP-gated cation channel activity	5	15	P2RX6, P2RX7, P2RX5, P2RX4, P2RX2
GO:0004970	Ionotropic glutamate receptor activity	12	67	GRIN1, GRIA4, GRIN2A, GRIK2, GRIK1, GRIA1, GRIK4, GRIA2, GRIK3, GRID1, GRIN3A, GRIK5
GO:0005216	Ion channel activity	6	23	PKD1L2, MCOLN3, MCOLN2, PKD2L2, PKD2L1, PKDREJ
GO:0005221	Intracellular cyclic nucleotide activated cation channel activity	2	5	KCNA10, CNGA3
GO:0005222	Intracellular cAMP activated cation channel activity	1	2	HCN4
GO:0005223	Intracellular cGMP activated cation channel activity	1	1	CNGB3
GO:0005229	Intracellular calcium activated chloride channel activity	2	3	ANO1, ANO2
GO:0005232	Serotonin-activated cation-selective channel activity	2	3	HTR3B, HTR3A
GO:0005237	Inhibitory extracellular ligand-gated ion channel activity	2	3	GABRA6, GABRB2
GO:0005242	Inward rectifier potassium channel activity	6	26	KCNH6, KCNJ12, KCNK6, KCNJ8, KCNQ5, KCNH7
GO:0005245	Voltage-gated calcium channel activity	8	27	CACNA1C, CATSPER1, CACNG7, CACNG5, CACNB1, CACNA1B, CACNB2, CACNA1E
GO:0005247	Voltage-gated chloride channel activity	6	14	CLCN7, CLCN4, CLIC1, CLIC4, CLIC6, CLCN3
GO:0005248	Voltage-gated sodium channel activity	8	19	SCN3A, SCN2A, SCN4A, PKD2, SCN8A, SCN5A, SCN9A, SCN11A
GO:0005249	Voltage-gated potassium channel activity	23	75	KCTD12, KCTD21, KCNH3, KCTD10, KCTD3, KCTD6, KCNAB3, KCTD2, KCTD15, KCTD7, KCNH4, KCNB1, KCTD9, KCNH8, KCNC3, KCNC2, KCTD16, KCND1, KCNC1, KCNV2, KCNH5, KCTD1, KCTD20
GO:0005250	A-type (transient outward) potassium channel activity	3	11	KCNIP2, KCND3, KCND2
GO:0005251	Delayed rectifier potassium channel activity	8	26	KCNA3, KCNB2, KCNH2, KCNA1, KCNA5, KCNQ1, KCNA2, KCNH1
GO:0005254	Chloride channel activity	17	55	CLCA1, ANO3, GABRB3, GABRA2, GABRB1, ANO7, ANO9, ANO4, GABRG2, CLCA4, CLCC1, ANO6, GABRQ, GABRG1, ANO10, GABRA4, GABRG3
GO:0005261	Cation channel activity	7	33	TRPM3, TRPV4, TRPM6, TRPC7, TMEM38A, TRPV1, HCN2
GO:0005262	Calcium channel activity	7	51	TRPM1, TRPM7, TRPM8, TRPV5, TRPM5, TRPM4, TRPV6

Table 2: Continued.

GO term	Description	*H*	*M*	Human genes
GO:0005267	Potassium channel activity	13	27	KCNC4, KCNK16, KCNK10, KCNG1, KCNK2, KCNK5, KCNK3, KCNK12, KCNQ4, KCNK17, KCNIP1, KCNIP4, KCNK9
GO:0005272	Sodium channel activity	4	40	HCN1, NALCN, ACCN4, TRPM2
GO:0008308	Voltage-gated anion channel activity	2	3	VDAC1, VDAC2
GO:0008331	High voltage-gated calcium channel activity	7	38	CACNA1A, CACNA2D4, CACNA1D, CACNA2D1, CACNA1S, CACNA2D3, CACNA2D2
GO:0008332	Low voltage-gated calcium channel activity	3	18	CACNA1H, CACNA1I, CACNA1G
GO:0015269	Calcium-activated potassium channel activity	9	49	KCNMA1, KCNN1, KCNT2, KCNN2, KCNT1, KCNU1, KCNMB2, KCNK18, KCNN3
GO:0015276	Ligand-gated ion channel activity	2	4	CLCA2, CNGB1
GO:0015279	Store-operated calcium channel activity	5	40	TRPC4, TRPC6, ORAI1, TRPA1, TRPC3
GO:0015280	Ligand-gated sodium channel activity	8	97	SCNN1B, SCNN1G, ACCN1, ACCN3, SCNN1A, ACCN5, ACCN2, SCNN1D
GO:0022824	Transmitter-gated ion channel activity	4	34	GLRA2, GLRA4, GLRA1, GLRA3
GO:0030171	Voltage-gated proton channel activity	1	3	HVCN1
GO:0072345	NAADP-sensitive calcium-release channel activity	2	3	TPCN1, TPCN2
	Total	199	947	
	Total number of genes in these GO categories	390		

H: number of different ion channel genes in human with homologs in *M. lignano*. *M*: number of transcripts in *M. lignano de novo* transcriptome assembly ML110815 with homology to ion channel genes in human. Note that alternatively spliced transcripts are counted separately in the *M. lignano* transcriptome assembly, hence the total reported number of transcripts is higher than the number of corresponding human genes. For this classification, genes were assigned to the least frequent available GO term within predefined list of ion channel-related GO terms (molecular function domain).

highlights a number of ion channel genes expressed specifically in dividing cells (Figure 3(e)), and future elaborated studies of such genes may provide novel insights into the role of bioelectric signaling in stem cell maintenance and differentiation. Importantly, a significant number of ion channels are well-conserved between *M. lignano* and human (Table 2), increasing the relevance of findings in flatworms to understanding ion channels and stem cells in human situation.

6. Future Directions

We advocate that *Macrostomum lignano* has great potential as a model for ion channel and stem cell research. The genetic toolbox available for this organism is already useful enough to address a wide range of scientific problems, and more methods and approaches will be optimized and used in this flatworm in the near future. *M. lignano* is a small animal and it is cultured in water, which makes it easy to apply different chemicals to the worms. Another major advantage of the animal is its high transparency. Phenotypic changes, fluorescent signals or certain transgene expression can be observed in any part of the body, as well is on the whole organism scale. For example, various fluorescent reporter dyes can be just added to culturing media in order to enable real-time *in vivo* monitoring of membrane potentials, pH, and ion flows [53]. Short generation time and efficient reproduction of *M. lignano* make logistics of large-scale experiments, such as drug screens, feasible in this animal.

As a model, *M. lignano* offers an exciting opportunity to bridge the gap between bioelectric signaling and genetic pathways involved in stem cell functions. The expression pattern and function of any gene can be determined by *in situ* hybridization and RNAi protocols, but it is transgenics that can bring such studies to the whole new level. Transgenic reporter lines expressing pH-sensitive or Ca^{2+}-sensitive fluorescent proteins [54, 55] would make a perfect tool to visualize bioelectric phenotypes during drug- or RNAi-screens. Overexpression of ion channels or even certain subunits would help to better understand their functions and interactions. Targeted genome editing by Zinc Finger Nucleases have not been tested yet in this animal but should

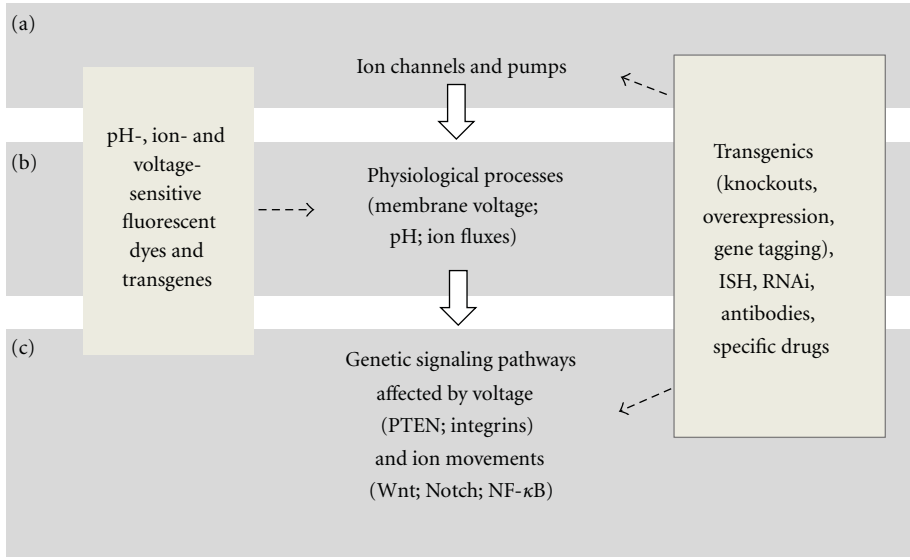

Figure 4: Approaches to study the roles of ion channels in regulation of stem cells in *M. lignano.* (a) Expression, localization, and function of ion channels and pumps that give rise to bioelectric signals can be addressed in *M. lignano* by established methods such as RNAi or *in situ* hybridization (ISH) in combination with specific drugs, antibodies, and transgenics. (b) Changes in ion flows, pH and membrane voltage caused by these channels and pumps can be detected with sensitive fluorescent dyes or followed *in vivo* in mutants expressing pH- or ion-sensitive forms of fluorescent proteins. (c) These processes affect known (and possibly unknown) genetic signaling pathways via different mechanisms including changes of Ca^{2+} concentrations, voltage-sensing domains of proteins, and voltage-gated transport of signaling molecules. These pathways and functional links between genetic and epigenetic mechanisms of stem cell function regulation can be studied in transgenic mutant lines with the help of RNAi and ISH techniques.

be also feasible and potentially can be used to generate ion channel knockout and knock-in lines [56, 57]. The same method allows fluorescent tagging of genes of interest and analysis of their expression, localization, and functions at the endogenous level [58]. Sexual reproduction and lack of self-fertilization make possible crossing different lines of *M. lignano* and hence to use the power of classical genetics approaches in this animal. Taken all together, we are convinced that *M. lignano* is poised to become a productive model to study relations between ion channels and stem cell regulation (Figure 4).

Acknowledgments

The authors thank S. Mouton and T. Demircan for critical comments on the paper, and S. Mouton for providing the image of the BrdU-labeled *M. lignano* animal.

References

[1] B. Hille, *Ion Channels of Excitable Membranes*, Sinauer, Sunderland, Mass, USA, 2001.

[2] C. Fewtrell, "Ca^{2+} oscillations in non-excitable cells," *Annual Review of Physiology*, vol. 55, pp. 427–454, 1993.

[3] A. P. Thomas, G. S. T. J. Bird, G. Hajnóczky, L. D. Robb-Gaspers, and J. W. Putney, "Spatial and temporal aspects of cellular calcium signaling," *The FASEB Journal*, vol. 10, no. 13, pp. 1505–1517, 1996.

[4] S. Schuster, M. Marhl, and T. Höfer, "Modelling of simple and complex calcium oscillations from single-cell responses to intercellular signalling," *European Journal of Biochemistry*, vol. 269, no. 5, pp. 1333–1355, 2002.

[5] F. M. Tonelli, A. K. Santos, D. A. Gomes et al., "Stem cells and calcium signaling," *Advances in Experimental Medicine and Biology*, vol. 740, pp. 891–916, 2012.

[6] A. Apáti, K. Pászty, Z. Erdei, K. Szebényi, L. Homolya, and B. Sarkadi, "Calcium signaling in pluripotent stem cells," *Molecular and Cellular Endocrinology*, vol. 353, pp. 57–67, 2012.

[7] E. J. Paredes-Gamero, C. M. Barbosa, and A. T. Ferreira, "Calcium signaling as a regulator of hematopoiesis," *Frontiers in Bioscience*, vol. 4, pp. 1375–1384, 2012.

[8] M. Sheng and D. T. S. Pak, "Ligand-gated ion channel interactions with cytoskeletal and signaling proteins," *Annual Review of Physiology*, vol. 62, pp. 755–778, 2000.

[9] A. Arcangeli and A. Becchetti, "Complex functional interaction between integrin receptors and ion channels," *Trends in Cell Biology*, vol. 16, no. 12, pp. 631–639, 2006.

[10] C. A. Hübner and T. J. Jentsch, "Ion channel diseases," *Human Molecular Genetics*, vol. 11, no. 20, pp. 2435–2445, 2002.

[11] A. Pandiella, M. Magni, D. Lovisolo, and J. Meldolesi, "The effects of epidermal growth factor on membrane potential. Rapid hyperpolarization followed by persistent fluctuations," *Journal of Biological Chemistry*, vol. 264, no. 22, pp. 12914–12921, 1989.

[12] F. Lang, F. Friedrich, E. Kahn et al., "Bradykinin-induced oscillations of cell membrane potential in cells expressing the Ha-ras oncogene," *Journal of Biological Chemistry*, vol. 266, no. 8, pp. 4938–4942, 1991.

[13] R. Binggeli and R. C. Weinstein, "Membrane potentials and sodium channels: hypotheses for growth regulation and

cancer formation based on changes in sodium channels and gap junctions," *Journal of Theoretical Biology*, vol. 123, no. 4, pp. 377–401, 1986.

[14] C. D. Cone, "Electroosmotic interactions accompanying mitosis initation in sarcoma cells in vitro," *Transactions of the New York Academy of Sciences*, vol. 31, no. 4, pp. 404–427, 1969.

[15] B. D. Freedman, M. A. Price, and C. J. Deutsch, "Evidence for voltage modulation of IL-2 production in mitogen-stimulated human peripheral blood lymphocytes," *Journal of Immunology*, vol. 149, no. 12, pp. 3784–3794, 1992.

[16] D. J. Blackiston, K. A. McLaughlin, and M. Levin, "Bioelectric controls of cell proliferation: ion channels, membrane voltage and the cell cycle," *Cell Cycle*, vol. 8, no. 21, pp. 3519–3528, 2009.

[17] T. E. DeCoursey, K. G. Chandy, S. Gupta, and M. D. Cahalan, "Voltage-gated K^+ channels in human T lymphocytes: a role in mitogenesis?" *Nature*, vol. 307, no. 5950, pp. 465–468, 1984.

[18] S. Y. Chiu and G. F. Wilson, "The role of potassium channels in Schwann cell proliferation in Wallerian degeneration of explant rabbit sciatic nerves," *Journal of Physiology*, vol. 408, pp. 199–222, 1989.

[19] S. Amigorena, D. Choquet, J. L. Teillaud, H. Korn, and W. H. Fridman, "Ion channel blockers inhibit B cell activation at a precise stage of the G1 phase of the cell cycle. Possible involvement of K^+ channels," *Journal of Immunology*, vol. 144, no. 6, pp. 2038–2045, 1990.

[20] E. Wang, Y. Yin, M. Zhao, J. V. Forrester, and C. D. McCaig, "Physiological electric fields control the G1/S phase cell cycle checkpoint to inhibit endothelial cell proliferation," *The FASEB Journal*, vol. 17, no. 3, pp. 458–460, 2003.

[21] S. Sundelacruz, M. Levin, and D. L. Kaplan, "Membrane potential controls adipogenic and osteogenic differentiation of mesenchymal stem cells," *PLoS ONE*, vol. 3, no. 11, Article ID e3737, 2008.

[22] D. L. Atkinson, T. J. Stevenson, E. J. Park, M. D. Riedy, B. Milash, and S. J. Odelberg, "Cellular electroporation induces dedifferentiation in intact newt limbs," *Developmental Biology*, vol. 299, no. 1, pp. 257–271, 2006.

[23] D. S. Adams, K. R. Robinson, T. Fukumoto et al., "Early, H^+-V-ATPase-dependent proton flux is necessary for consistent left-right patterning of non-mammalian vertebrates," *Development*, vol. 133, no. 9, pp. 1657–1671, 2006.

[24] D. S. Adams, A. Masi, and M. Levin, "H^+ pump-dependent changes in membrane voltage are an early mechanism necessary and sufficient to induce *Xenopus* tail regeneration," *Development*, vol. 134, no. 7, pp. 1323–1335, 2007.

[25] T. Nogi, D. Zhang, J. D. Chan, and J. S. Marchant, "A novel biological activity of praziquantel requiring voltage-operated Ca^{2+} channel β subunits: subversion of flatworm regenerative polarity," *PLoS Neglected Tropical Diseases*, vol. 3, no. 6, article e464, 2009.

[26] W. S. Beane, J. Morokuma, D. S. Adams, and M. Levin, "A chemical genetics approach reveals H,K-ATPase-mediated membrane voltage is required for planarian head regeneration," *Chemistry and Biology*, vol. 18, no. 1, pp. 77–89, 2011.

[27] D. Zhang, J. D. Chan, T. Nogi, and J. S. Marchant, "Opposing roles of voltage-gated Ca^{2+} channels in neuronal control of regenerative patterning," *The Journal of Neuroscience*, vol. 31, pp. 15983–15995, 2011.

[28] M. Levin, "Bioelectric mechanisms in regeneration: unique aspects and future perspectives," *Seminars in Cell and Developmental Biology*, vol. 20, no. 5, pp. 543–556, 2009.

[29] K. Kunzelmann, "Ion channels and cancer," *Journal of Membrane Biology*, vol. 205, no. 3, pp. 159–173, 2005.

[30] A. Arcangeli, O. Crociani, E. Lastraioli, A. Masi, S. Pillozzi, and A. Becchetti, "Targeting ion channels in cancer: a novel frontier in antineoplastic therapy," *Current Medicinal Chemistry*, vol. 16, no. 1, pp. 66–93, 2009.

[31] T. H. Morgan, "Experimental studies of the regeneration of *Planaria maculata*," *Archiv für Entwickelungsmechanik der Organismen*, vol. 7, no. 2-3, pp. 364–397, 1898.

[32] T. H. Morgan, "Growth and regeneration in *Planaria lugubris*," *Archiv Für Entwicklungsmechanik der Organismen*, vol. 13, pp. 1179–2212, 1901.

[33] A. Sánchez Alvarado, "Regeneration and the need for simpler model organisms," *Philosophical Transactions of the Royal Society B*, vol. 359, no. 1445, pp. 759–763, 2004.

[34] K. Agata, E. Nakajima, N. Funayama, N. Shibata, Y. Saito, and Y. Umesono, "Two different evolutionary origins of stem cell systems and their molecular basis," *Seminars in Cell and Developmental Biology*, vol. 17, no. 4, pp. 503–509, 2006.

[35] G. Marsh and H. W. Beams, "Electrical control of growth polarity in regenerating *Dugesia tigrina*," *Federation Proceedings*, vol. 6, article 163, 1947.

[36] G. Marsh and H. W. Beams, "Electrical control of morphogenesis in regenerating *Dugesia tigrina*. I. Relation of axial polarity to field strength," *Journal of Cellular Physiology*, vol. 39, pp. 191–213, 1952.

[37] J. Dimmitt and G. Marsh, "Electrical control of morphogenesis in regenerating *Dugesia tigrina*. II. Potential gradient vs. current density as control factors," *Journal of Cellular Physiology*, vol. 40, no. 1, pp. 11–23, 1952.

[38] T. Nogi and M. Levin, "Characterization of innexin gene expression and functional roles of gap-junctional communication in planarian regeneration," *Developmental Biology*, vol. 287, no. 2, pp. 314–335, 2005.

[39] N. J. Oviedo and M. Levin, "Smedinx-11 is a planarian stem cell gap junction gene required for regeneration and homeostasis," *Development*, vol. 134, no. 17, pp. 3121–3131, 2007.

[40] K. D. Poss, "Advances in understanding tissue regenerative capacity and mechanisms in animals," *Nature Reviews Genetics*, vol. 11, no. 10, pp. 710–722, 2010.

[41] P. Ladurner, D. Pfister, C. Seifarth et al., "Production and characterisation of cell- and tissue-specific monoclonal antibodies for the flatworm *Macrostomum* sp," *Histochemistry and Cell Biology*, vol. 123, no. 1, pp. 89–104, 2005.

[42] B. Egger, P. Ladurner, K. Nimeth, R. Gschwentner, and R. Rieger, "The regeneration capacity of the flatworm *Macrostomum lignano*—on repeated regeneration, rejuvenation, and the minimal size needed for regeneration," *Development Genes and Evolution*, vol. 216, no. 10, pp. 565–577, 2006.

[43] D. Pfister, K. De Mulder, I. Philipp et al., "The exceptional stem cell system of *Macrostomum lignano*: screening for gene expression and studying cell proliferation by hydroxyurea treatment and irradiation," *Frontiers in Zoology*, vol. 4, article 9, 2007.

[44] K. De Mulder, D. Pfister, G. Kuales et al., "Stem cells are differentially regulated during development, regeneration and homeostasis in flatworms," *Developmental Biology*, vol. 334, no. 1, pp. 198–212, 2009.

[45] D. Pfister, K. De Mulder, V. Hartenstein et al., "Flatworm stem cells and the germ line: developmental and evolutionary implications of macvasa expression in *Macrostomum lignano*," *Developmental Biology*, vol. 319, no. 1, pp. 146–159, 2008.

[46] K. De Mulder, G. Kuales, D. Pfister et al., "Potential of *Macrostomum lignano* to recover from γ-ray irradiation," *Cell and Tissue Research*, vol. 339, no. 3, pp. 527–542, 2010.

[47] S. Mouton, M. Willems, B. P. Braeckman et al., "The free-living flatworm *Macrostomum lignano*: a new model organism for ageing research," *Experimental Gerontology*, vol. 44, no. 4, pp. 243–249, 2009.

[48] N. J. Oviedo, C. L. Nicolas, D. S. Adams, and M. Levin, "Live imaging of planarian membrane potential using $DiBAC_4(3)$," *Cold Spring Harbor Protocols*, vol. 2008, Article ID pdb.prot5055, 2008.

[49] P. W. Reddien, N. J. Oviedo, J. R. Jennings, J. C. Jenkin, and A. Sánchez Alvarado, "Developmental biology: SMEDWI-2 is a PIWI-like protein that regulates planarian stem cells," *Science*, vol. 310, no. 5752, pp. 1327–1330, 2005.

[50] T. Guo, A. H. F. M. Peters, and P. A. Newmark, "A bruno-like gene is required for stem cell maintenance in planarians," *Developmental Cell*, vol. 11, no. 2, pp. 159–169, 2006.

[51] B. J. Pearson and A. S. Alvarado, "A planarian p53 homolog regulates proliferation and self-renewal in adult stem cell lineages," *Development*, vol. 137, no. 2, pp. 213–221, 2010.

[52] M. W. Cowles, A. Hubert, and R. M. Zayas, "A Lissencephaly-1 homologue is essential for mitotic progression in the planarian *Schmidtea mediterranea*," *Developmental Dynamics*, vol. 241, pp. 901–910, 2012.

[53] C. Wolff, B. Fuks, and P. Chatelain, "Comparative study of membrane potential-sensitive fluorescent probes and their use in ion channel screening assays," *Journal of Biomolecular Screening*, vol. 8, no. 5, pp. 533–543, 2003.

[54] M. J. Mahon, "pHluorin2: an enhanced, ratiometric, pH-sensitive green florescent protein," *Advances in Bioscience and Biotechnology*, vol. 2, pp. 132–137, 2011.

[55] Y. Zhao, S. Araki, J. Wu et al., "An expanded palette of genetically encoded Ca^{2+} indicators," *Science*, vol. 333, pp. 1888–1891, 2011.

[56] P. Q. Liu, E. M. Chan, G. J. Cost et al., "Generation of a triple-gene knockout mammalian cell line using engineered zinc-finger nucleases," *Biotechnology and Bioengineering*, vol. 106, no. 1, pp. 97–105, 2010.

[57] J. Wang, G. Friedman, Y. Doyon et al., "Targeted gene addition to a predetermined site in the human genome using a ZFN-based nicking enzyme," *Genome Research*, vol. 22, no. 7, pp. 1316–1326, 2012.

[58] J. B. Doyon, B. Zeitler, J. Cheng et al., "Rapid and efficient clathrin-mediated endocytosis revealed in genome-edited mammalian cells," *Nature Cell Biology*, vol. 13, no. 3, pp. 331–337, 2011.

Hindawi Publishing Corporation
Stem Cells International
Volume 2012, Article ID 217910, 9 pages
doi:10.1155/2012/217910

Review Article

Ion Channels in Hematopoietic and Mesenchymal Stem Cells

Serena Pillozzi[1] and Andrea Becchetti[2]

[1] *Department of Experimental Pathology and Oncology, University of Florence, Viale Morgagni 50, 50134 Florence, Italy*
[2] *Department of Biotechnology and Biosciences, University of Milano-Bicocca, Piazza della Scienza 2, 20126 Milano, Italy*

Correspondence should be addressed to Andrea Becchetti, andrea.becchetti@unimib.it

Received 28 May 2012; Accepted 5 July 2012

Academic Editor: Stefan Liebau

Hematopoietic stem cells (HSCs) reside in bone marrow niches and give rise to hematopoietic precursor cells (HPCs). These have more restricted lineage potential and eventually differentiate into specific blood cell types. Bone marrow also contains mesenchymal stromal cells (MSCs), which present multilineage differentiation potential toward mesodermal cell types. In bone marrow niches, stem cell interaction with the extracellular matrix is mediated by integrin receptors. Ion channels regulate cell proliferation and differentiation by controlling intracellular Ca^{2+}, cell volume, release of growth factors, and so forth. Although little evidence is available about the ion channel roles in true HSCs, increasing information is available about HPCs and MSCs, which present a complex pattern of K^+ channel expression. K^+ channels cooperate with Ca^{2+} and Cl^- channels in regulating calcium entry and cell volume during mitosis. Other K^+ channels modulate the integrin-dependent interaction between leukemic progenitor cells and the niche stroma. These channels can also regulate leukemia cell interaction with MSCs, which also involves integrin receptors and affects the MSC-mediated protection from chemotherapy. Ligand-gated channels are also implicated in these processes. Nicotinic acetylcholine receptors regulate cell proliferation and migration in HSCs and MSCs and may be implicated in the harmful effects of smoking.

1. Introduction

In early embryos, totipotent blastomeres are defined as cells able to produce every cell type of the adult organism. During development, a progressive restriction in differentiation potency occurs, with primordial pluripotent cells being able to yield other stem cells (*self-renewal*) and originate all cell lineages except the extraembryonic ones [1]. Further restriction is observed in adult tissues, in which cell lineages comprise slowly dividing stem cells. These, besides self-renewing, divide to generate *transit amplifying cells* which undergo many mitotic cycles before differentiating into the tissue cell types. For example, neural stem cells, located in restricted regions of the brain, can differentiate into neurons, astrocytes, and oligodendrocytes. Whether the spectrum of possible differentiation outcomes depends on extrinsic regulation or is founded on the existence of heterogeneous stem cell populations is uncertain [2]. A similar pattern is thought to exist in cancer tissue, in which a few stem cells maintain the neoplastic cell population, whereas the majority of cells composing the tumor rapidly divide and display only limited self-renewal properties [3].

The contribution of ion channels and transporters to the regulation of cell proliferation and differentiation is increasingly recognized. The field has greatly expanded in the last ten years and cannot be fully discussed here. The reader is referred to several recent reviews that cover the main aspects and provide introduction to specialized literature [4–11]. Although the precise mechanisms are still debated, evidence exists about the involvement of both voltage-gated and ligand-gated channels. As a first approximation, the well-known correlation between depolarization and proliferation seems to hold in embryonic stem cells. For example, inhibition of KCNQ1 potassium channels by altered expression of the accessory β subunit XKCNE1 depolarizes neural crest cells in *Xenopus.* This effect is accompanied by hyperproliferation [12]. Conversely, paracrine stimulation of $GABA_A$ receptors, which tends to hyperpolarize embryonic stem cells and peripheral neural crest stem cells in mice, is accompanied by inhibition of cell proliferation [13].

A cell's decision to divide or differentiate is regulated by both intracellular molecular cascades and local environmental cues. Ion channels appear often to behave as signaling pivots that coordinate these upstream and downstream signals. By governing membrane potential (V_m) and transmembrane calcium flux, ion channels regulate the calcium signals that punctuate the mitotic cycle as well as processes such as neurite extension and exocytosis of autocrine or angiogenetic factors [8]. Moreover, transmembrane ion fluxes drive the cell volume oscillations typical of cycling and migrating cells [14, 15]. However, these examples certainly do not exhaust the range of ion channel functions in cell proliferation and differentiation and other regulatory roles may or may not depend on ion transport. For instance, the channel proteins can form macromolecular complexes with growth factor receptors, cell adhesion receptors and related proteins [16–19]. These mechanisms have been especially studied in mature and immature blood cells [16, 19, 20], and their alteration can promote neoplastic invasiveness. Because of such complexity, a simple comprehensive picture of the physiology of ion channels in cell cycle and differentiation is not available and probably cannot be reached. In the following, we discuss some of these issues as related to the hematopoietic system. Since relatively few studies have addressed ion channel physiology in adult and embryonic stem cells, we believe an ample and potentially fruitful field is offered to future research.

2. Hematopoietic and Mesenchymal Stem Cells: The Fundamentals

Hematopoiesis allows the lifelong turnover of blood cells. In adult mammals, small populations of hematopoietic stem cells (HSCs) reside in the bone marrow (BM). HSCs originate hematopoietic precursor cells (HPCs) with more restricted lineage potential, which eventually differentiate into specific blood cells. Permanence of a functional HSC population throughout life is guaranteed by stem cell self-renewal as well as HSC dwelling in protected *BM niches*, in which 90–95% of HSCs are maintained in a quiescent state [21, 22]. The exact proportions of different cell populations and the rate of cell cycle entry vary in rodents and humans [23]. Adult quiescent HSCs arise from actively proliferating fetal HSC [24]. These are first located in placenta and aorta-gonad-mesonephros, which are subsequently substituted by the fetal liver. Fetal HSCs initially rapidly produce red blood cells and in a second phase generate all blood cell lineages plus engrafting HSCs [21, 25]. These latter actively proliferate during development by mainly generating erythroid and myeloid lineages, to produce the blood system. In rodents, HSCs colonize BM between embryonic day 17 and postnatal day 14. Subsequently, they remain anchored to the BM niche by integrin-dependent mechanisms [26, 27].

The BM stroma is constituted by stromal cells (fibroblasts, endothelial cells, macrophages, and osteoblasts) and extracellular matrix proteins. Stroma contributes to regulate hematopoiesis through signals triggered by adhesion-dependent and soluble factors. In the adult, HSCs and HPCs mostly reside in BM, whereas they actively migrate between the hematopoietic tissues during fetal development. Integrins exert a central regulatory role, as they mediate most of the functional interactions between hematopoietic cells and the bone marrow microenvironment [26–28]. The regulated expression of specific integrin subunits and their localization in selected areas of the BM confirm that these molecules exert a variety of functions in hematopoiesis [26]. The expression of cell-matrix and cell-cell adhesion receptors in HSCs and HPCs has been extensively reviewed elsewhere [20].

Mesenchymal stromal cells (MSCs), formerly known as mesenchymal stem cells, are adult stem cells originally isolated from BM. Subsequent studies have shown that MSCs are stromal progenitors also found in other adult tissues. They are endowed with multilineage differentiation potential toward mesodermal cell lineages and extensive immunomodulatory properties. MSCs actively proliferate in some tissues, but remain quiescent in others [29]. Three main criteria have been identified by the International Society of Cellular Therapy to define MSCs: (i) adhesion to plastic, (ii) expression of specific immunophenotypic marker combinations (CD73, CD90, and CD105), accompanied by lack of expression of hematopoietic markers (CD14, CD34, and CD45) and class II major histocompatibility complex (MHC) molecules; (iii) capability of differentiating into mesodermal lineages (adipocytes, cardiomyocytes, osteoblasts, and chondrocytes) [30, 31]. All cultured MSCs tend to present these features, although some differences are observed among the MSCs from a given tissue such as expression of surface CD34 and CD54 in MSCs derived from adipose tissue. In addition, MSCs may show *in vitro*, under specific experimental conditions, some features of differentiation into tissues of endodermal and neuroectodermal lineages, such as hepatocytes, epithelia, and neurons, although their genuine differentiation into nonmesodermal cells is still matter of debate [31]. Because of their properties, MSCs have drawn considerable interest as potentially useful material for tissue engineering and cell-based therapy. Human BM is now the major MSC source for both experimental and clinical studies [32–36].

3. Ion Channels in HSCs and HPCs

3.1. K^+ Channels and Other Channels Related to the Voltage-Gated Superfamily. To the best of our knowledge, no studies have been published about the K^+ channel expression in *bona fide* HSCs. However, inward rectifying K^+ currents (K_{IR}) have been measured in primitive HPCs (CD34+ CD38−), after stimulation with interleukin-3 (IL-3) plus stem cell factor (SCF [37]). The term inward rectifier applies to those ion channels that tend to be more permeable to ions flowing toward the cytoplasm. However, it should be remembered that not all channels known to belong to the K_{IR} structural family (Kir subunits) display prominent inward rectification. Interestingly, measurements in HPCs showed expression of both strongly rectifying (Kir4.3) and weakly rectifying (Kir1.1) K^+ channels. Evidence that this

is necessary to generate committed progenitors *in vitro* was obtained in umbilical cord blood CD34+ CD38− cells, in which inhibiting either channel type suppresses the generation of progenitor cells stimulated by IL-3- and SCF [38]. These observation are consistent with the notion that different K^+ channel types give distinct contributions to proliferation and differentiation. In general, the strong inward rectifiers and the background channels K_{2P} (two-pore domain K^+ channels) seem to be mainly responsible to regulate the resting V_m. In immature B cells, Nam et al. [39] recently identified two kinds of K_{2P} channels, namely, TREK-2 (TWIK-related K^+ channel type 2) and TASK-2 (TWIK-related acid-sensitive K^+ channel type 2). TASK-2 is activated by stimulation of B cells receptors (BCRs ligation) and participates in the BCR-ligation-dependent apoptosis [39]. Other types of K^+ channel are thought to cooperate with the other membrane transport systems to regulate cell volume, secretion of paracrine factors, calcium influx, and so forth. These processes may be accompanied by oscillations in V_m, cell volume, and intracellular calcium [8]. The whole picture can thus be very complex, as is now made clear by extensive expression studies. In $CD34^+/CD45^+/CD133^{high}$ cells from peripheral blood [40], RT-PCR showed expression of $K_V1.3$, $K_V7.1$, $Na_V1.7$, TASK 2, TALK 2 (TWIK-related alkaline pH-activated K^+ channel type 2), TWIK 2 (tandem of pore domains in a weak inward rectifying K^+ channel, type 2), TRPC4, 6, TRPM2,7, and TRPV2 and patch-clamp recordings identified voltage gated K^+ currents, TASK 2-like K^+ currents, TRPM2 currents, and TRPC6-like currents [40].

Some voltage-dependent K^+ channels, particularly $K_V11.1$ (also known as hERG1), are directly implicated in regulating the integrin-dependent cell adhesion, which is potentially important for cell physiology inside the BM marrow niches [20, 41]. In leukemic osteoclastic progenitors, hERG1 activates during cell adhesion to fibronectin. Channel activation mediates a complex regulatory network that control cell adhesion, as it increases expression of $\alpha V\beta 3$ integrin (CD51 [42]). Moreover, hERG1 is upregulated in leukemic hematopoietic cells [43, 44]. In particular, the *Kv11.1* transcript was detected in circulating CD34+ cells stimulated to proliferate by IL-3 (interleukin 3), SCF (stem cell factor), GM-CSF (granulocyte-macrophage colony-stimulating factor), and G-CSF (granulocyte colony-stimulating factor [43]. In stimulated CD34+ cells, $K_V11.1$ associates with β_1 integrin, which is essential for proper bone marrow engraftment of these HPCs [19]. The *Kv11.1* transcript was also detected in $CD34+/CD38-/CD123^{high}$ cells, which constitute the stem cell population critical for perpetuating leukemia [45]. The involvement of $K_V11.1$ in the physiology of leukemic and stem cells is further discussed in Section 4.4.

Overall, relatively ample evidence indicates that K_V channels are important modulators of normal and leukemic HSCs. It is, however, clear that the physiological comprehension of these processes is still in its infancy.

3.2. Neuronal Nicotinic Receptors (nAChRs) and Hematopoiesis. The neuronal nicotinic acetylcholine receptors (nAChRs) are ligand-gated pentameric ion channels that mediate fast excitatory postsynaptic potentials as well as slower paracrine actions of ACh. Growing evidence shows that nAChRs are also widely expressed in nonnervous tissue, including lymphocytes, and in cancer cells [46]. Since nicotine is a well-known risk factor for cancer, these observations have stimulated work aimed to determine whether and how nAChRs contribute to regulate the main cellular events associated with neoplastic progression, that is, cell proliferation and survival, invasiveness, the epithelial-mesenchymal transition and angiogenesis [47]. The nAChRs are homo- or hetero-pentamers of α ($\alpha 2$–$\alpha 9$) and β ($\beta 2$–$\beta 4$) subunits, arranged with different possible stoichiometries, characterized by different physiological and pharmacological properties [46, 47]. Interestingly, recent genomewide association studies attribute to the gene cluster coding for the $\alpha 3/\alpha 5/\beta 4$ nAChR subunits a role in both development of lung cancer and nicotine addiction [48–50]. Many cellular effects of nicotine-and tobacco-derived metabolites are probably caused by nAChR activation, which leads to increased cytosolic calcium. This can stimulate intracellular pathways both directly as well as by increasing the release of autocrine/paracrine factors [51–53]. Nonconductive signals exerted by nAChRs have also been observed [54]. In general, the precise function of nAChRs in normal and neoplastic cells is difficult to determine because many cells express a variety of nicotinic subunits, whose interplay is unclear [47].

In humans, smoking is associated with increased leukocyte count [55–57]. Recent work in mice indicates that treatment with nicotine increases leukocytes in peripheral blood, BM, and spleen [58], in keeping with previous results showing that nicotine stimulates hematopoiesis [59]. The effect is correlated with higher frequency of HSCs in bone marrow [58]. Long-term HSCs isolated from treated mice appear to remain fully competent and express nAChRs, as demonstrated by binding of α-bungarotoxin (specific for $\alpha 7$-containing nAChRs and the muscle isoform). The expression pattern of other nAChR subunits was not reported. Regardless, these results are consistent with the previous observation that mice deficient of $\alpha 7$ display a reduction of myeloid and erythroid lineages [60]. Although the mechanisms of nAChR implication in these processes are unclear, these studies suggest that the cholinergic system is implicated in regulating hematopoiesis. From a pathologic standpoint, some of the effects of prolonged tobacco use may thus be caused by nAChR targeting. However, it should be kept in mind that $\alpha 7$ receptors desensitize rapidly in the presence of agonists. Therefore, to understand their physiological role in hematopoiesis, it will be important to precisely determine how these effects depend on the concentration of nicotine and other tobacco-related compounds. Low doses may sustain steady state nAChR currents, although with low amplitude, whereas higher doses may produce strong channel desensitization. In fact, the available evidence, albeit fragmentary, indicates that high concentrations of nicotine produce inhibition of hematopoiesis, instead of stimulation [60]. Hence, it is possible that different smoking habits produce opposite effects on hematopoiesis.

4. Ion Channels in Mesenchymal Stem Cells

4.1. MSCs from Bone Marrow (BM-MSCs). Although human MSCs have been used for several years in the investigation of cell therapy and differentiation [36, 61, 62], a coherent picture of the physiological functions of the different ion channels expressed in these cells is not available. Not surprisingly, most results concern human BM-MSCs. In these cells, Kawano et al. first observed spontaneous inositol 1,4,5-trisphosphate-dependent Ca^{2+} oscillations, which are regulated by the Na^+-Ca^{2+} exchanger and the plasma membrane Ca^{2+} pump [63, 64]. For review of the calcium handling system in MSCs, see [65]. In addition, approximately 10–15% of BM-MSCs express the L-type calcium current (I_{CaL}) and related mRNAs such as *α1C* [34, 35, 66], although I_{CaL} does not seem to be significantly implicated in controlling the spontaneous cell activity [66]. Nonetheless, the calcium oscillations are completely blocked by removing extracellular calcium and by applying La^{3+}, while the intracellular stores are not depleted. This suggests that an unknown pathway, probably mediated by nonselective cation channels, controls calcium entry in hMSC and contributes to sustain the $[Ca^{2+}]_i$ oscillations [64]. These latter drive the activity of high-conductance Ca^{2+}-dependent K^+ channels (BK_{Ca}), which in turn determines V_m cycling [64, 67]. In human BM-MSCs, K_{Ca} currents and the corresponding *MaxiK* mRNA were also observed by others, along with a slowly activating K^+ current distinct from the rapidly activating K_{Ca} [34]. Significant mRNA expression was also detected for *K_V1.4*, *K_V4.2*, *K_V4.3*, and *HCN2*, but no corresponding functional currents were reported [34]. These were instead reported by Li et al. [35] who, besides BK_{Ca} and I_{CaL}, measured transient outward voltage-dependent K^+ channels sensitive to 4-aminopyridine whose molecular correlates were identified as *K_V1.4* and *K_V4.2* and denoted in the literature as I_A or I_{TO} (for a brief summary of I_K nomenclature, see [68]). These authors also observed expression of K_V10.1-delayed rectifying K^+ channels (also known as ether-à-go-go type 1, EAG1), accompanied by the corresponding mRNA [35]. Finally, in hBM-MSCs, expression of K_{ATP} channels (Kir6.1 and Kir6.2) and the regulatory subunit SUR2A was detected by RT-PCR and immunolabeling. Osteogenic differentiation strongly increased Kir6.2, whereas adipogenic differentiation reduced Kir6.1 and SUR2A [69].

Broadly speaking, the above pattern seems also to apply to BM-MSCs prepared from rats [70–72] and mice [73, 74], where the effects on proliferation of modulating ion channels have been studied in some more detail. Rat BM-MSCs express both high- and intermediate-conductance K_{Ca} (resp., *slo* or *K_{Ca}1.1* and *KCNN4 or K_{Ca}3.1*), I_{KDR} (*K_V1.2 and K_V2.1*), I_A (*K_V1.4* and *K_V4.3*), I_{CaL} and TTX-sensitive Na^+ currents [70–72]. In these cells, K_{DR}-decreased whereas intermediate-conductance K_{Ca}3.1 increased during progression from G1 to S phase. Downregulating these channels with specific interfering RNAs blocked cell proliferation [71]. The partial substitution of K_{DR} with K_{Ca} during cell cycle progression agrees with the model originally proposed in T lymphocytes, in which sequential activation of K_V and K_{Ca} during mitosis triggers and sustains cell hyperpolarization, with ensuing facilitation of Ca^{2+} entry and stimulation of the cell cycle machinery [75]. In murine MSCs, the usual K_{Ca}3.1 channel is accompanied by K_{IR} currents (Kir2.1) and volume-regulated Cl^- channels (CLCN3 [73]). K_{Ca} and Cl^- channels cooperate in regulating cell proliferation by modulating cyclin D1 and cyclin E expression [74]. K_{Ca}, I_{CaL}, and I_A (*K_V1.4*) were also observed in undifferentiated MSCs isolated from chicken embryos [76].

As is often the case, some types of K^+ channels are involved in processes related to cell adhesion and migration. For instance, Hu et al. [77] found that K_V2.1 regulates directed migration and homing of BM-MSCs. Hypoxic preconditioning increases K_V2.1 expression and enhances the channel activity that subsequently augments phosphorylation/activation of the focal adhesion kinase and cell migration, resulting in increased homing of transplanted BM-MSCs to the injured region [77].

Finally, about 30% of human BM-MSC cells were found to express TTX-sensitive voltage-gated Na^+ currents [34]. This observation was also carried out in rodents [70, 73] and chicken embryo MSCs [76], but its physiological meaning is uncertain.

4.2. MSCs from Human Umbilical Cord Vein (hUC-MSCs). The expression of ion channels has been recently studied in undifferentiated hUC-MSCs [78]. Patch-clamp experiments revealed iberiotoxin-sensitive I_{KCa}, I_A, and I_{DR} currents. Once again, about 30% of these cells express functional TTX-sensitive Na^+ currents, whereas no more than 5% of the cells express K_{IR}. The molecular correlates of these currents were investigated by RT-PCR, which revealed the expression of *K_V1.1*, *K_V4.2*, *K_V1.4*, *Kir2.1*, *heag1*, *MaxiK*, *hNE-Na*, and *TWIK-1* [78]. Therefore, the overall pattern is similar to the one shown by BM-derived cells.

4.3. MSCs Derived from Human-Induced Pluripotent Stem Cells (iPSCs). iPSCs produce a high yield of MSCs. Moreover iPSC-derived MSCs present higher proliferation capacity than BM-derived stem cells, thus providing a better option for applications in regenerative medicine. Zhang et al. [79] recently studied whether the different proliferative potential of iPSC-MSCs may be founded on significant differences in ion channel expression compared to BM-MSCs. Patch-clamp measurements revealed five functional ion currents in human iPSC-MSCs: BK_{Ca}, intermediate-conductance K_{Ca}, K_{DR}, K_{IR}, and voltage-gated Cl^- channels, whereas the latter Cl^- currents were not detected in BM-MSCs. RT-PCR revealed significant expression in both cell types of *K_{Ca}1.1, K_{Ca}3.1, K_V10.1, Kir2.1, SCN9A, CACNA1C,* and *Clcn3*. In contrast, *Kir2.2* and *Kir2.3* were only found in iPSC-MSCs. Interestingly, the expression level of *K_V10.1* was much higher in iPSC-MSCs than in BM-MSCs. In agreement with the proliferative potential conferred by K_V10.1 (hEAG1) to different cell types [80], block of hEAG1 tended to inhibit cell proliferation in both cell types. Consistently with the expression pattern, the effect was more pronounced in iPSC-MSCs.

These observations may contribute to explain the greater proliferative capacity of iPSC-MSCs, which may be correlated with specific patterns of channel expression. In general, the diversity of ion channel expression in MSCs might reflect the existence of different cell populations. Differently from immortalized cell lines, pure populations of MSCs have been so far impossible to isolate. As discussed earlier, identification of human MSCs is mainly based on their plastic-adherence features in standard culture conditions and expression or lack of expression of an ensemble of surface markers. As has been observed in other cell types, some channel types seem specifically implicated in controlling cell cycle. Interestingly, evidence summarized in the above sections also suggests that K_{IR} currents tend to be expressed in stem cells at earlier stages, that is, in cells with broader differentiation potential. This may be different from what has been observed in the nervous system, where for example, K_{IR} currents mark late stages of quail neural crest cell differentiation [81].

4.4. K_V11.1 (hERG1) Channels in Leukemic Cells Mediate Cell Interaction with MSCs. BM-MSCs can protect leukemic cells from chemotherapy by secreting the chemokine SDF-1 (also known as CXCL11), which binds to the G-protein-coupled receptor CXCR4 (chemokine receptor CXC 4 [82]) expressed onto leukemia cells [83]. Adhesion between these cell types is consolidated by engagement of the integrin receptors expressed onto leukemic cells, typically $\alpha5\beta1$ (VLA-5) and $\alpha4\beta1$ (VLA-4). These interact with extracellular matrix proteins on the MSCs [84]. MSCs thus regulate intracellular signaling cascades in leukemic cells that lead to antiapoptotic effects, as shown in acute myeloid leukemia [85], chronic lymphocytic leukemia [86–88], and chronic myeloid leukemia [89]. These intracellular signals are thought to require integrin-dependent activation of ILK (integrin-linked kinase), with subsequent recruitment of the MAPK and the phosphoinositide 3-kinase (PI3K)/Akt pathways, at least in myeloid leukemia.

We recently studied the molecular mechanisms underlying the analogous effect observed in acute lymphoblastic leukemia (ALL) cells [90]. Coculture of ALL cells with MSCs induced on the lymphoblast plasma membrane the expression of a signaling complex formed by hERG1, the $\beta1$ integrin subunit, and CXCR4. Such complex is absent in normal B lymphocytes. Moreover MSCs also do not express hERG1. Assembly of the protein complex activated the prosurvival pathways centered on ILK, extracellular signal-related kinase 1/2 (ERK1/2) and PI3K/Akt. In parallel, ALL cells became resistant to chemotherapy-induced apoptosis [90]. Formation of an hERG1/integrin/VEGF receptor complex was previously observed in acute myeloid leukemia [19]. The possibility that interaction with CXCR4 also occurs in these cells is matter for future studies.

Blocking hERG1 channels with specific drugs decreased the protective effect conferred by MSCs to leukemic cells function. Moreover, integrin activation depends on channel activity. The channel role appears to be important for both initiation of pro-survival signals and development of drug resistance. Immunodeficient mice engrafted with ALL cells and treated with channel blockers had increased rate of leukemic cell apoptosis, reduced leukemic infiltration and overall survival rates. What is more, hERG1 blockade enhanced the therapeutic effect produced by corticosteroids.

4.5. MSCs and Nicotinic Receptors. Observations such as the relatively recent one that smoking cessation in chronic smokers produces a rapid increase of circulating endothelial progenitor cells in peripheral blood led to suspect that the tobacco products regulate MSC physiology [91]. In fact, it was subsequently found that human MSCs express the entire machinery for cholinergic signaling, namely, the synthesizing enzyme choline acetyltransferase, the degrading enzyme acetylcholinesterase, ACh itself, the nAChR subunits $\alpha3$, $\alpha5$, and $\alpha7$ and the muscarinic ACh receptor M2 [92]. Human MSCs were also found to express $\beta2$ and $\beta4$ nAChR subunits [93]. Nicotinic and muscarinic receptors are expressed in different MSC populations [92], but stimulation with receptors' agonists leads to a rapid increase of intracellular (Ca^{2+}) in both [92, 93]. As in other cell types [47], this signal converges onto ERK1/2 [92]. These results are consistent with the general notion that nonneuronal tissues can express the entire cholinergic machinery necessary to release ACh for paracrine signaling. Tonic exposure to nicotinic ligands in smokers alters proper regulation of such system. Interestingly, $\alpha7$ nAChRs were found to be implicated in the control of MSC migration [93], in analogy with what was previously observed in human keratinocytes [94]. The balance of the nAChR effects on proliferation/apoptosis and migration is a matter for future studies.

5. Conclusion

Knowledge about the cell physiology of ion channels and transporters in stem cells is at an initial stage. Current evidence indicates that, in analogy with what has been observed in other cell types, stem cells, particularly the better known human MSCs, express a wide variety of ion channels which are implicated in different physiological functions. Broadly speaking, certain classes of K^+ channels cooperate with Ca^{2+} and Cl^- channels in regulating the calcium transients and the volume oscillations that accompany the cell cycle. Other K^+ channel types control cell anchorage with the stromal matrix and cell migration as well as release of paracrine growth factors. The differential expression of ion channel types in individual MSC cells indicates that stem cell populations may be heterogeneous. One possibility is that, as observed in other cell types, MSCs sampled at different cell cycle phases present different channel activity or expression (reviewed in [8]). Another possible explanation is that MSC populations contain progenitor cells at different stages of commitment, which would also affect the pattern of ion channel expression and activity. Recent evidence in both HSCs and MSCs indicates that ligand-gated channels, such as nAChRs, also contribute to regulate stem cell biology.

From a therapeutic standpoint, MSCs have been lately the object of intense interest. The perspectives these cells

offer for clinical applications turn on their easy accessibility, prompt expansibility, and capacity to differentiate. A more thorough understanding of their physiological features, including the details of how different ion channels and transporters interplay, will be necessary for safer and reliable medical applications. Currently, four main therapeutic approaches are being investigated: (i) local implantation of MSC for focalized diseases, (ii) systemic transplantation, (iii) combination of stem cell therapy with gene therapy, and (iv) use of MSC in tissue repair and remodeling. Considering the advantages offered by membrane channels as targets of pharmacological therapy [95], we believe further efforts along this line should suggest potentially fertile novel methods to attempt therapy in both normal and cancer stem cells.

Acknowledgments

The authors' work has been lately supported by the Associazione Genitori Contro le Leucemie e Tumori Infantili Noi per Voi, Associazione Italiana per la Ricerca sul Cancro, the Istituto Toscano Tumori, the Italian Ministry for University and Scientific Research, the Ente Cassa di Risparmio di Firenze, and the University of Milano Bicocca (FAR).

References

[1] M. Dejosez and T. P. Zwaka, "Pluripotency and nuclear reprogramming," *Annual Reviews of Biochemistry*, vol. 81, pp. 737–765, 2012.

[2] H. Suh, W. Deng, and F. H. Gage, "Signaling in adult neurogenesis," *Annual Review of Cell and Developmental Biology*, vol. 25, pp. 253–275, 2009.

[3] M. R. Alison, W. R. Lin, S. M. Lim, and L. J. Nicholson, "Cancer stem cells: in the line of fire," *Cancer Treatment Reviews*, vol. 38, no. 6, pp. 589–598, 2012.

[4] A. Arcangeli, O. Crociani, E. Lastraioli, A. Masi, S. Pillozzi, and A. Becchetti, "Targeting ion channels in cancer: a novel frontier in antineoplastic therapy," *Current Medicinal Chemistry*, vol. 16, no. 1, pp. 66–93, 2009.

[5] D. J. Blackiston, K. A. McLaughlin, and M. Levin, "Bioelectric controls of cell proliferation: ion channels, membrane voltage and the cell cycle," *Cell Cycle*, vol. 8, no. 21, pp. 3519–3528, 2009.

[6] M. D. Cahalan and K. G. Chandy, "The functional network of ion channels in T lymphocytes," *Immunological Reviews*, vol. 231, no. 1, pp. 59–87, 2009.

[7] A. Arcangeli, S. Pillozzi, and A. Becchetti, "Ion channels: novel functional hubs in leukemia," in *Current Cancer Treatment—Novel Beyond Conventional Approaches*, O. Ozdemir, Ed., pp. 227–254, InTech, 2011.

[8] A. Becchetti, "Ion channels and transporters in cancer. 1. Ion channels and cell proliferationin cancer," *American Journal of Physiology*, vol. 301, no. 2, pp. C255–C265, 2011.

[9] S. S. Rosenberg and N. Spitzer, "Calcium signaling in neuronal development," *Cold Spring Harbor Perspectives in Biology*, vol. 3, no. 10, Article ID a004259.

[10] A. Darszon, T. Nishigaki, C. Beltran, and C. L. Treviño, "Calcium channels in the development, maturation, and function of spermatozoa," *Physiological Reviews*, vol. 91, no. 4, pp. 1305–1355, 2011.

[11] E. Shumilina, S. M. Huber, and F. Lang, "Ca^{2+} signaling in the regulation of dendritic cell functions," *American Journal of Physiology*, vol. 300, no. 6, pp. C1205–C1214, 2011.

[12] J. Morokuma, D. Blackiston, D. S. Adams, G. Seebohm, B. Trimmer, and M. Levin, "Modulation of potassium channel function confers a hyperproliferative invasive phenotype on embryonic stem cells," *Proceedings of the National Academy of Sciences of the United States of America*, vol. 105, no. 43, pp. 16608–16613, 2008.

[13] M. Andäng, J. Hjerling-Leffler, A. Moliner et al., "Histone H2AX-dependent $GABA_A$ receptor regulation of stem cell proliferation," *Nature*, vol. 451, no. 7177, pp. 460–464, 2008.

[14] E. K. Hoffmann, I. H. Lambert, and S. F. Pedersen, "Physiology of cell volume regulation in vertebrates," *Physiological Reviews*, vol. 89, no. 1, pp. 193–277, 2009.

[15] V. A. Cuddapah and H. Sontheimer, "Ion channels and transporters in cancer. 2. Ion channels and the control of cancer cell migration," *American Journal of Physiology*, vol. 301, no. 3, pp. C541–C549, 2011.

[16] M. Levite, L. Cahalon, A. Peretz et al., "Extracellular K^+ and opening of voltage-gated potassium channels activate T cell integrin function: physical and functional association between $K_v1.3$ channels and $\beta1$ integrins," *Journal of Experimental Medicine*, vol. 191, no. 7, pp. 1167–1176, 2000.

[17] A. Cherubini, G. Hofmann, S. Pillozzi et al., "Human *ether-a-go-go*-related gene 1 channels are physically linked to $\beta1$ integrins and modulate adhesion-dependent signaling," *Molecular Biology of the Cell*, vol. 16, no. 6, pp. 2972–2983, 2005.

[18] J. F. Wei, L. Wei, X. Zhou et al., "Formation of Kv2.1-FAK complex as a mechanism of FAK activation, cell polarization and enhanced motility," *Journal of Cellular Physiology*, vol. 217, no. 2, pp. 544–557, 2008.

[19] S. Pillozzi, M. F. Brizzi, P. A. Bernabei et al., "VEGFR-1 (FLT-1), $\beta1$ integrin, and hERG K^+ channel for a macromolecular signaling complex in acute myeloid leukemia: role in cell migration and clinical outcome," *Blood*, vol. 110, no. 4, pp. 1238–1250, 2007.

[20] A. Becchetti, S. Pillozzi, R. Morini, E. Nesti, and A. Arcangeli, "New insights into the regulation of ion channels by integrins," *International Review of Cell and Molecular Biology*, vol. 279, pp. 135–190, 2010.

[21] E. M. Pietras, M. R. Warr, and E. Passegué, "Cell cycle regulation in hematopoietic stem cells," *Journal of Cell Biology*, vol. 195, no. 5, pp. 709–720, 2011.

[22] G. Costa, V. Kouskoff, and G. Lacaud, "Origin of blood cells and HSC production in the embryo," *Trends in Immunology*, vol. 33, no. 5, pp. 215–223, 2012.

[23] S. N. Catlin, L. Busque, R. E. Gale, P. Guttorp, and J. L. Abkowitz, "The replication rate of human hematopoietic stem cells in vivo," *Blood*, vol. 117, no. 17, pp. 4460–4466, 2011.

[24] M. B. Bowie, K. D. McKnight, D. G. Kent, L. McCaffrey, P. A. Hoodless, and C. J. Eaves, "Hematopoietic stem cells proliferate until after birth and show a reversible phase-specific engraftment defect," *The Journal of Clinical Investigation*, vol. 116, no. 10, pp. 2808–2816, 2006.

[25] A. Medvinsky, S. Rybtsov, and S. Taoudi, "Embryonic origin of the adult hematopoietic system: advances and questions," *Development*, vol. 138, no. 6, pp. 1017–1031, 2011.

[26] D. Soligo, R. Schiró, R. Luksch et al., "Expression of integrins in human bone marrow," *British Journal of Haematology*, vol. 76, no. 3, pp. 323–332, 1990.

[27] E. B. Voura, F. Billia, N. N. Iscove, and R. G. Hawley, "Expression mapping of adhesion receptor genes during

differentiation of individual hematopoietic precursors," *Experimental Hematology*, vol. 25, no. 11, pp. 1172–1179, 1997.

[28] L. M. Scott, G. V. Priestley, and T. Papayannopoulou, "Deletion of $\alpha 4$ integrins from adult hematopoietic cells reveals roles in homeostasis, regeneration, and homing," *Molecular and Cellular Biology*, vol. 23, no. 24, pp. 9349–9360, 2003.

[29] E. C. Forsberg and S. Smith-Berdan, "Parsing the niche code: the molecular mechanisms governing hematopoietic stem cell adhesion and differentiation," *Haematologica*, vol. 94, no. 11, pp. 1477–1481, 2009.

[30] H. Orbay, M. Tobita, and H. Mizuno, "Mesenchymal stem cells isolated from adipose and other tissues: basic biological properties and clinical applications," *Stem Cells International*, vol. 2012, Article ID 461718, 9 pages, 2012.

[31] Z. J. Liu, Y. Zhuge, and O. C. Velazquez, "Trafficking and differentiation of mesenchymal stem cells," *Journal of Cellular Biochemistry*, vol. 106, no. 6, pp. 984–991, 2009.

[32] M. F. Pittenger, A. M. Mackay, S. C. Beck et al., "Multilineage potential of adult human mesenchymal stem cells," *Science*, vol. 284, no. 5411, pp. 143–147, 1999.

[33] D. Orlic, J. Kajstura, S. Chimenti et al., "Bone marrow cells regenerate infarcted myocardium," *Nature*, vol. 410, no. 6829, pp. 701–705, 2001.

[34] J. F. Heubach, E. M. Graf, J. Leutheuser et al., "Electrophysiological properties of human mesenchymal stem cells," *Journal of Physiology*, vol. 554, no. 3, pp. 659–672, 2004.

[35] G. R. Li, H. Sun, X. Deng, and C. P. Lau, "Characterization of ionic currents in human mesenchymal stem cells from bone marrow," *Stem Cells*, vol. 23, no. 3, pp. 371–382, 2005.

[36] S. Wang, X. Qu, and R. C. Zhao, "Clinical applications of mesenchymal stem cells," *Journal of Hematology & Oncology*, vol. 5, article 19, 2012.

[37] O. Shirihai, S. Merchav, B. Attali, and D. Dagan, "K^+ channel antisense oligodeoxynucleotides inhibit cytokine-induced expansion of human hemopoietic progenitors," *Pflügers Archiv European Journal of Physiology*, vol. 431, no. 4, pp. 632–638, 1996.

[38] O. Shirihai, B. Attali, D. Dagan, and S. Merchav, "Expression of two inward rectifier potassium channels is essential for differentiation of primitive human hematopoietic progenitor cells," *Journal of Cellular Physiology*, vol. 177, no. 2, pp. 197–205, 1998.

[39] J. H. Nam, D. H. Shin, H. Zheng et al., "Expression of TASK-2 and its upregulation by B cell receptor stimulation in WEHI-231 mouse immature B cells," *American Journal of Physiology*, vol. 300, no. 5, pp. C1013–C1022, 2011.

[40] K. S. Park, B. Pang, S. J. Park et al., "Identification and functional characterization of ion channels in $CD34^+$ hematopoietic stem cells from human peripheral blood," *Molecules and Cells*, vol. 32, no. 2, pp. 181–188, 2011.

[41] A. Arcangeli, "Ion channels and transporters in cancer. 3. Ion channels in the tumor cell-microenvironment cross talk," *American Journal of Physiology*, vol. 301, no. 4, pp. C762–C771, 2011.

[42] G. Hofmann, P. A. Bernabei, O. Crociani et al., "HERG K^+ channels activation during $\beta 1$ integrin-mediated adhesion to fibronectin induces an up-regulation of $\alpha_v\beta_3$ integrin in the preosteoclastic leukemia cell line FLG 29.1," *The Journal of Biological Chemistry*, vol. 276, no. 7, pp. 4923–4931, 2001.

[43] S. Pillozzi, M. F. Brizzi, M. Balzi et al., "HERG potassium channels are constitutively expressed in primary human acute myeloid leukemias and regulate cell proliferation of normal and leukemic hemopoietic progenitors," *Leukemia*, vol. 16, no. 9, pp. 1791–1798, 2002.

[44] G. A. M. Smith, H. W. Tsui, E. W. Newell et al., "Functional up-regulation of HERG K^+ channels in neoplastic hematopoietic cells," *The Journal of Biological Chemistry*, vol. 277, no. 21, pp. 18528–18534, 2002.

[45] H. Li, L. Liu, L. Guo et al., "HERG K^+ channel expression in $CD34^+/CD38^-/CD123^{high}$ cells and primary leukemia cells and analysis of its regulation in leukemia cells," *International Journal of Hematology*, vol. 87, no. 4, pp. 387–392, 2008.

[46] I. Wessler and C. J. Kirkpatrick, "Acetylcholine beyond neurons: the non-neuronal cholinergic system in humans," *British Journal of Pharmacology*, vol. 154, no. 8, pp. 1558–1571, 2008.

[47] P. Ambrosi and A. Becchetti, "Targeting neuronal nicotinic receptors in cancer: new ligands and potential side-effects," *Recent Patents on Anticancer Drug Discovery*. In press.

[48] C. I. Amos, X. Wu, P. Broderick et al., "Genome-wide association scan of tag SNPs identifies a susceptibility locus for lung cancer at 15q25.1," *Nature Genetics*, vol. 40, no. 5, pp. 616–622, 2008.

[49] R. J. Hung, J. D. McKay, V. Gaborieau et al., "A susceptibility locus for lung cancer maps to nicotinic acetylcholine receptor subunit genes on 15q25," *Nature*, vol. 452, no. 7187, pp. 633–637, 2008.

[50] T. E. Thorgeirsson, F. Geller, P. Sulem et al., "A variant associated with nicotine dependence, lung cancer and peripheral arterial disease," *Nature*, vol. 452, no. 7187, pp. 638–642, 2008.

[51] M. G. Cattaneo, A. Codignola, L. M. Vicentini, F. Clementi, and E. Sher, "Nicotine stimulates a serotonergic autocrine loop in human small-cell lung carcinoma," *Cancer Research*, vol. 53, no. 22, pp. 5566–5568, 1993.

[52] E. Martínez-García, M. Irigoyen, E. Ansó, J. J. Martínez-Irujo, and A. Rouzaut, "Recurrent exposure to nicotine differentiates human bronchial epithelial cells via epidermal growth factor receptor activation," *Toxicology and Applied Pharmacology*, vol. 228, no. 3, pp. 334–342, 2008.

[53] E. A. Putnam, N. Yen, G. E. Gallick et al., "Autocrine growth stimulation by transforming growth factor-α in human non-small cell lung cancer," *Surgical Oncology*, vol. 1, no. 1, pp. 49–60, 1992.

[54] A. I. Chernyavsky, J. Arredondo, V. Galitovskiy, J. Qian, and S. A. Grando, "Upregulation of nuclear factor-κB expression by SLURP-1 is mediated by $\alpha 7$-nicotinic acetylcholine receptor and involves both ionic events and activation of protein kinases," *American Journal of Physiology*, vol. 299, no. 5, pp. C903–C911, 2010.

[55] F. Corre, J. Lellouch, and D. Schwartz, "Smoking and leucocyte-counts. Results of an epidemiological survey," *The Lancet*, vol. 2, no. 7725, pp. 632–634, 1971.

[56] D. Sparrow, R. J. Glynn, M. Cohen, and S. T. Weiss, "The relationship of the peripheral leukocyte count and cigarette smoking to pulmonary function among adult men," *Chest*, vol. 86, no. 3, pp. 383–386, 1984.

[57] E. J. Jensen, B. Pedersen, R. Frederiksen, and R. Dahl, "Prospective study on the effect of smoking and nicotine substitution on leucocyte blood counts and relation between blood leucocytes and lung function," *Thorax*, vol. 53, no. 9, pp. 784–789, 1998.

[58] E. Chang, E. C. Forsberg, J. Wu et al., "Cholinergic activation of hematopoietic stem cells: role in tobacco-related disease?" *Vascular Medicine*, vol. 15, no. 5, pp. 375–385, 2010.

[59] T. S. Pandit, L. Sikora, G. Muralidhar, S. P. Rao, and P. Sriramarao, "Sustained exposure to nicotine leads to extramedullary hematopoiesis in the spleen," *Stem Cells*, vol. 24, no. 11, pp. 2373–2381, 2006.

[60] L. M. Koval, A. S. Zverkova, R. Grailhe et al., "Nicotinic acetylcholine receptors alpha4beta2 and alpha7 regulate myelo- and erythropoiesis within the bone marrow," *International Journal of Biochemistry & Cell Biology*, vol. 40, no. 5, pp. 980–990, 2008.

[61] A. I. Caplan and S. P. Bruder, "Mesenchymal stem cells: building blocks for molecular medicine in the 21st century," *Trends in Molecular Medicine*, vol. 7, no. 6, pp. 259–264, 2001.

[62] Y. Jiang, B. N. Jahagirdar, R. L. Reinhardt et al., "Pluripotency of mesenchymal stem cells derived from adult marrow," *Nature*, vol. 418, no. 6893, pp. 41–49, 2002.

[63] S. Kawano, S. Shoji, S. Ichinose, K. Yamagata, M. Tagami, and M. Hiraoka, "Characterization of Ca^{2+} signaling pathways in human mesenchymal stem cells," *Cell Calcium*, vol. 32, no. 4, pp. 165–174, 2002.

[64] S. Kawano, K. Otsu, S. Shoji, K. Yamagata, and M. Hiraoka, "Ca^{2+} oscillations regulated by Na^{+}-Ca^{2+} exchanger and plasma membrane Ca^{2+} pump induce fluctuations of membrane currents and potentials in human mesenchymal stem cells," *Cell Calcium*, vol. 34, no. 2, pp. 145–156, 2003.

[65] B. Ye, "Ca^{2+} oscillations and its transporters in mesenchymal stem cells," *Physiological Research*, vol. 59, no. 3, pp. 323–329, 2010.

[66] I. Zahanich, E. M. Graf, J. F. Heubach, U. Hempel, S. Boxberger, and U. Ravens, "Molecular and functional expression of voltage-operated calcium channels during osteogenic differentiation of human mesenchymal stem cells," *Journal of Bone and Mineral Research*, vol. 20, no. 9, pp. 1637–1646, 2005.

[67] S. Kawano, K. Otsu, A. Kuruma et al., "ATP autocrine/paracrine signaling induces calcium oscillations and NFAT activation in human mesenchymal stem cells," *Cell Calcium*, vol. 39, no. 4, pp. 313–324, 2006.

[68] C. Di Resta and A. Becchetti, "Introduction to ion channels," *Advances in Experimental Medicine and Biology*, vol. 674, pp. 9–21, 2010.

[69] A. Diehlmann, S. Bork, R. Saffrich, R. W. Veh, W. Wagner, and C. Derst, "K_{ATP} channels in mesenchymal stromal stem cells: strong up-regulation of Kir6.2 subunits upon osteogenic differentiation," *Tissue and Cell*, vol. 43, no. 5, pp. 331–336, 2011.

[70] G. R. Li, X. L. Deng, H. Sun, S. S. M. Chung, H. F. Tse, and C. P. Lau, "Ion channels in mesenchymal stem cells from rat bone marrow," *Stem Cells*, vol. 24, no. 6, pp. 1519–1528, 2006.

[71] X. L. Deng, C. P. Lau, K. Lai, K. F. Cheung, G. K. Lau, and G. R. Li, "Cell cycle-dependent expression of potassium channels and cell proliferation in rat mesenchymal stem cells from bone marrow," *Cell Proliferation*, vol. 40, no. 5, pp. 656–670, 2007.

[72] S. P. Wang, J. A. Wang, R. H. Luo, W. Y. Cui, and H. Wang, "Potassium channel currents in rat mesenchymal stem cells and their possible roles in cell proliferation," *Clinical and Experimental Pharmacology and Physiology*, vol. 35, no. 9, pp. 1077–1084, 2008.

[73] R. Tao, C. P. Lau, H. F. Tse, and G. R. Li, "Functional ion channels in mouse bone marrow mesenchymal stem cells," *American Journal of Physiology*, vol. 293, no. 5, pp. C1561–C1567, 2007.

[74] R. Tao, C. P. Lau, H. F. Tse, and G. R. Li, "Regulation of cell proliferation by intermediate-conductance Ca^{2+}-activated potassium and volume-sensitive chloride channels in mouse mesenchymal stem cells," *American Journal of Physiology*, vol. 295, no. 5, pp. C1409–C1416, 2008.

[75] K. G. Chandy, H. Wulff, C. Beeton, M. Pennington, G. A. Gutman, and M. D. Cahalan, "K^{+} channels as targets for specific immunomodulation," *Trends in Pharmacological Sciences*, vol. 25, no. 5, pp. 280–289, 2004.

[76] Z. Varga, T. Juhász, C. Matta et al., "Switch of voltage-gated K^{+} channel expression in the plasma membrane of chondrogenic cells affects cytosolic Ca^{2+}-oscillations and cartilage formation," *PLoS ONE*, vol. 6, no. 11, Article ID e27957, 2011.

[77] X. Hu, L. Wei, T. M. Taylor et al., "Hypoxic preconditioning enhances bone marrow mesenchymal stem cell migration via Kv2.1 channel and FAK activation," *American Journal of Physiology*, vol. 301, no. 2, pp. C362–C372, 2011.

[78] K. S. Park, K. H. Jung, S. H. Kim et al., "Functional expression of ion channels in mesenchymal stem cells derived from umbilical cord vein," *Stem Cells*, vol. 25, no. 8, pp. 2044–2052, 2007.

[79] J. Zhang, Y. C. Chan, J. C. Ho, C. W. Siu, Q. Lian, and H. F. Tse, "Regulation of cell proliferation of human induced pluripotent stem cell-derived mesenchymal stem cells via ether-à-go-go 1 (hEAG1) potassium channel," *American Journal of Physiology*, vol. 303, no. 2, pp. C115–C125, 2012.

[80] L. A. Pardo, D. del Camino, A. Sánchez et al., "Oncogenic potential of EAG K^{+} channels," *The EMBO Journal*, vol. 18, no. 20, pp. 5540–5547, 1999.

[81] A. Arcangeli, B. Rosati, A. Cherubini et al., "HERG- and IRK-like inward rectifier currents are sequentially expressed during neuronal development of neural crest cells and their derivatives," *European Journal of Neuroscience*, vol. 9, no. 12, pp. 2596–2604, 1997.

[82] E. A. Berger, P. M. Murphy, and J. M. Farber, "Chemokine receptors as HIV-1 coreceptors: roles in viral entry, tropism, and disease," *Annual Review of Immunology*, vol. 17, pp. 657–700, 1999.

[83] Z. Zeng, I. J. Samudio, M. Munsell et al., "Inhibition of CXCR4 with the novel RCP168 peptide overcomes stroma-mediated chemoresistance in chronic and acute leukemias," *Molecular Cancer Therapeutics*, vol. 5, no. 12, pp. 3113–3121, 2006.

[84] A. Manabe, K. G. Murti, E. Coustan-Smith et al., "Adhesion-dependent survival of normal and leukemic human B lymphoblasts on bone marrow stromal cells," *Blood*, vol. 83, no. 3, pp. 758–766, 1994.

[85] M. Konopleva, S. Konoplev, W. Hu, A. Y. Zaritskey, B. V. Afanasiev, and M. Andreeff, "Stromal cells prevent apoptosis of AML cells by up-regulation of anti-apoptotic proteins," *Leukemia*, vol. 16, no. 9, pp. 1713–1724, 2002.

[86] P. Panayiotidis, D. Jones, K. Ganeshaguru, L. Foroni, and A. V. Hoffbrand, "Human bone marrow stromal cells prevent apoptosis and support the survival of chronic lymphocytic leukaemia cells *in vitro*," *British Journal of Haematology*, vol. 92, no. 1, pp. 97–103, 1996.

[87] L. Lagneaux, A. Delforge, D. Bron, C. De Bruyn, and P. Stryckmans, "Chronic lymphocytic leukemic B cells but not normal B cells are rescued from apoptosis by contact with normal bone marrow stromal cells," *Blood*, vol. 91, no. 7, pp. 2387–2396, 1998.

[88] J. A. Burger, N. Tsukada, M. Burger, N. J. Zvaifler, M. Dell'Aquila, and T. J. Kipps, "Blood-derived nurse-like cells protect chronic lymphocytic leukemia B cells from spontaneous apoptosis through stromal cell-derived factor-1," *Blood*, vol. 96, no. 8, pp. 2655–2663, 2000.

[89] E. Weisberg, R. D. Wright, D. W. McMillin et al., "Stromal-mediated protection of tyrosine kinase inhibitor-treated BCR-ABL-expressing leukemia cells," *Molecular Cancer Therapeutics*, vol. 7, no. 5, pp. 1121–1129, 2008.

[90] S. Pillozzi, M. Masselli, E. De Lorenzo et al., "Chemotherapy resistance in acute lymphoblastic leukemia requires hERG1 channels and is overcome by hERG1 blockers," *Blood*, vol. 117, no. 3, pp. 902–914, 2011.

[91] T. Kondo, M. Hayashi, K. Takeshita et al., "Smoking cessation rapidly increases circulating progenitor cells in peripheral blood in chronic smokers," *Arteriosclerosis, Thrombosis, and Vascular Biology*, vol. 24, no. 8, pp. 1442–1447, 2004.

[92] M. J. Hoogduijn, A. Cheng, and P. G. Genever, "Functional nicotinic and muscarinic receptors on mesenchymal stem cells," *Stem Cells and Development*, vol. 18, no. 1, pp. 103–112, 2009.

[93] I. U. Schraufstatter, R. G. DiScipio, and S. K. Khaldoyanidi, "Alpha 7 subunit of nAChR regulates migration of human mesenchymal stem cells," *Journal of Stem Cells*, vol. 4, no. 4, pp. 203–216, 2010.

[94] A. I. Chernyavsky, J. Arrendondo, L. M. Marubio, and S. A. Grando, "Differential regulation of keratinocyte chemokinesis and chemotaxis through distinct nicotinic receptor subtypes," *Journal of Cell Science*, vol. 117, no. 23, pp. 5665–5679, 2004.

[95] A. Arcangeli and A. Becchetti, "New trends in cancer therapy: targeting ion channels and transporters," *Pharmaceuticals*, vol. 3, no. 4, pp. 1202–1224, 2010.

Hindawi Publishing Corporation
Stem Cells International
Volume 2012, Article ID 247670, 6 pages
doi:10.1155/2012/247670

Review Article

Ion Channel Activities in Neural Stem Cells of the Neuroepithelium

Masayuki Yamashita

Department of Physiology 1, Nara Medical University, Shijo-cho 840, Kashihara 634-8521, Japan

Correspondence should be addressed to Masayuki Yamashita, yama@naramed-u.ac.jp

Received 5 March 2012; Revised 2 May 2012; Accepted 9 May 2012

Academic Editor: Michael Levin

During the embryonic development of the central nervous system, neuroepithelial cells act as neural stem cells. They undergo interkinetic nuclear movements along their apico-basal axis during the cell cycle. The neuroepithelial cell shows robust increases in the nucleoplasmic [Ca^{2+}] in response to G protein-coupled receptor activation in S-phase, during which the nucleus is located in the basal region of the neuroepithelial cell. This response is caused by Ca^{2+} release from intracellular Ca^{2+} stores, which are comprised of the endoplasmic reticulum and the nuclear envelope. The Ca^{2+} release leads to the activation of Ca^{2+} entry from the extracellular space, which is called capacitative, or store-operated Ca^{2+} entry. These movements of Ca^{2+} are essential for DNA synthesis during S-phase. Spontaneous Ca^{2+} oscillations also occur synchronously across the cells. This synchronization is mediated by voltage fluctuations in the membrane potential of the nuclear envelope due to Ca^{2+} release and the counter movement of K^+ ions; the voltage fluctuation induces alternating current (AC), which is transmitted via capacitative electrical coupling to the neighboring cells. The membrane potential across the plasma membrane is stabilized through gap junction coupling by lowering the input resistance. Thus, stored Ca^{2+} ions are a key player in the maintenance of the cellular activity of neuroepithelial cells.

1. Introduction

During the embryonic development of the central nervous system, cells in the neuroepithelium act as neural stem cells. The neuroepithelium forms the neural tube, from which the central nervous system including the spinal cord, retina, and brain is derived. The neuroepithelial cell has a polarized structure: the apical process faces the ventricle, and the furthest portion of the basal process makes contact with the basement membrane. This contact is necessary for the cell to undergo interkinetic nuclear movement along the apico-basal axis during the cell cycle [1–4]. Neuroepithelial cells in S-phase synthesize DNA in their basal region, followed by the movement of the soma towards the apical region prior to cell division during M-phase [3, 4].

To study ion channel activities in the neuroepithelial cell, the retinal neuroepithelium is a suitable model because the retina can be isolated from an optic cup at early stages of embryonic development. The neural tube evaginates laterally to form two optic vesicles, each of which invaginates to form an optic cup. The neuroepithelium on the inner wall of the optic cup becomes the retina. Figure 1 shows the retinal neuroepithelial cells that are undergoing interkinetic nuclear movements and the first differentiated neuron, a retinal ganglion cell. Developmental changes in the cellular activity are summarized as a time diagram in Figure 2. Studies of the retinal neuroepithelial cells have revealed that various ion channels are assembled in these cells and are important for the maintenance of the cellular activity of neuroepithelial cells. The current paper is intended to survey and discuss the functional roles of ion channels found in the retinal neuroepithelial cell, as well as in other neural tube stem cells, and the cell line.

2. Channel-Mediated Release of Ca^{2+} from Intracellular Ca^{2+} Stores

Neuroepithelial cells show a robust response to the activation of G protein-coupled receptors (GPCRs) including

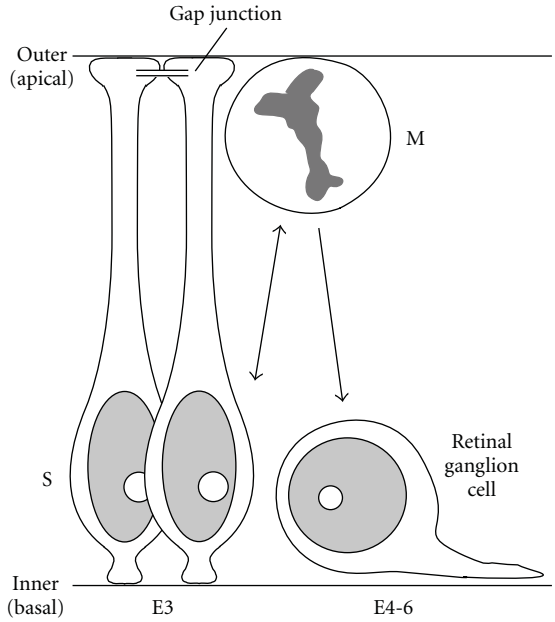

Figure 1: Schematic drawings of retinal neuroepithelial cells in cell cycle and the first differentiated neuron, a retinal ganglion cell. In chick embryo, the retina is composed almost homogeneously of neuroepithelial cells on embryonic day 3 (E3). The retinal ganglion cells are born mainly at E4–6. S: S-phase; M: M-phase. The outer (apical) surface faces the space that is continuous with the ventricle. This figure is cited from [5].

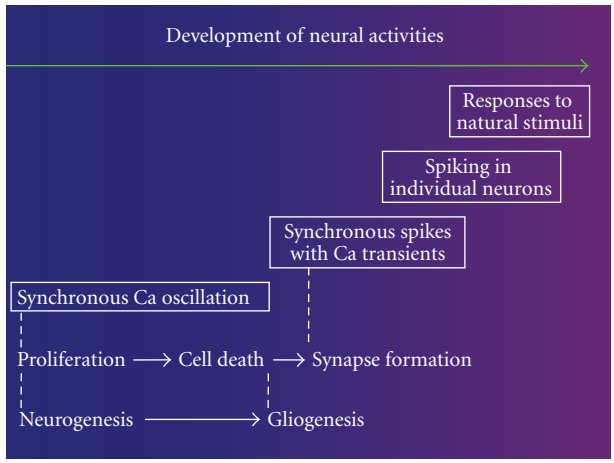

Figure 2: Developmental changes in neural activities. Self-renewing neuroepithelial cells show spontaneous, synchronous calcium oscillations. Newborn neurons show synchronous burst spike discharges before synapse formation. This figure is cited from [6].

muscarinic acetylcholine receptors [7], P2Y purinoceptors [8], and lysophosphatidic acid receptors [9], which leads to increases in intracellular Ca^{2+} concentrations ($[Ca^{2+}]$). Activation of these GPCRs leads to the production of inositol 1,4,5-trisphosphate ($InsP_3$) from phosphatidylinositol 4,5-bisphosphate (PIP_2) via the phospholipase C enzyme. $InsP_3$ activates the $InsP_3$ receptor Ca^{2+} channel to cause the release of Ca^{2+} from intracellular Ca^{2+} stores (Ca^{2+} mobilization) [10]. Another type of Ca^{2+} releasing channel, namely ryanodine receptor channel, is unlikely to be functioning in the retinal neuroepithelial cell because no response was evoked by caffeine (an activator of ryanodine receptor) [8].

Using confocal fluorescence microscopy and a Ca^{2+}-sensitive fluorescent indicator, it was shown that Ca^{2+} mobilization is dependent upon the cell cycle [11]. Increases in intracellular $[Ca^{2+}]$ occur in the nucleoplasm of S-phase cells, of which somata are localized to the basal region of the developing neuroepithelium. In contrast, Ca^{2+} mobilization decreases in M-phase cells, which are located in the apical region. In newborn retinal ganglion cells, which migrate to the basal region (Figure 1), Ca^{2+} mobilization is also reduced. These results suggest that the rise in nucleoplasmic $[Ca^{2+}]$ is necessary for DNA synthesis during S-phase and that the Ca^{2+} mobilization system is less active following neuronal

differentiation [11]. It is not clear whether other phases in cell cycle (i.e., G_1 or G_2) show Ca^{2+} increases.

The GPCR-mediated Ca^{2+} response of the neuroepithelial cell also depends upon the developmental stage of the retina. On embryonic day 3 (E3), nearly all the cells in the neural retina arise from the self-renewal of the neuroepithelial cells (Figure 1), and the Ca^{2+} mobilization is most robust at this stage. Retinal ganglion cells and other types of neurons are born between E4 and E8, and then neurogenesis ceases [12]. Between E3 and E8, the Ca^{2+} response declines in parallel with the decreasing proliferative activity of the retinal cells [7–9, 13]. This developmental profile suggests that Ca^{2+} mobilization may be critical for the proliferation of neuroepithelial cells. In support of this concept, studies using retinal cell cultures have shown that the release of Ca^{2+} from intracellular Ca^{2+} store is essential for DNA synthesis in these cells [14].

Increases in Ca^{2+} mobilization also occur spontaneously as synchronized Ca^{2+} oscillations in the retinal neuroepithelial cells [15] (Figure 2). GPCRs, such as P2Y purinoceptors, may be constitutively activated by ambient ATP, which is released in both an autocrine and paracrine manner [16]. The activation of P2Y purinoceptors has also been shown to promote the proliferation of retinal neuroepithelial cells [16–18]. The inhibitory effects of P2 antagonists on the proliferation of retinal neuroepithelial cells suggest that endogenous ATP activates P2Y purinoceptors constitutively [16]. The mechanism underlying the synchronization of Ca^{2+} oscillations is discussed later in this text.

Increases in the intracellular $[Ca^{2+}]$ of S-phase cells may be involved in the activation of Ca^{2+}-dependent nuclear signaling for proliferation. It has been suggested in various cell types that calcineurin, a Ca^{2+}/calmodulin-dependent phosphatase, dephosphorylates the transcription factor NFAT (nuclear factor of activated T-lymphocytes), which regulates cell cycle progression [19, 20].

3. Store-Operated Ca^{2+} Entry

The release of Ca^{2+} from intracellular Ca^{2+} stores has been shown to instantaneously induce an influx of extracellular Ca^{2+}. This Ca^{2+} influx is called capacitative or store-operated Ca^{2+} entry, and is necessary for the replenishment of the intracellular Ca^{2+} stores [21, 22]. This type of Ca^{2+} influx also occurs in the retinal neuroepithelial cell [23].

The store-operated Ca^{2+} entry in the retinal neuroepithelial cell has also been shown to decline as the cell becomes increasingly differentiated [13, 23]. Store-operated Ca^{2+} entry has also been shown to be essential for DNA synthesis in cultured retinal cells [14]. In a culture model of neural stem cells, neuroblastoma × glioma NG108-15 cell line, store-operated Ca^{2+} entry is most frequent in proliferation, as opposed to neuronal differentiation, medium [24]. It has been suggested that the store-operated Ca^{2+} entry is also involved in the Ca^{2+}-regulated transcription pathways for cell cycle progression via the activation of calcineurin and NFAT [19, 20].

The channels responsible for capacitative Ca^{2+} entry have been supposed to be transient receptor potential (TRP) channels [21, 22]. It is now evident that the STIM molecules function as Ca^{2+} sensors within the endoplasmic reticulum and the orai proteins function as the channel for Ca^{2+} influx [21, 22]. The specific channels involved in the store-operated Ca^{2+} entry in the neuroepithelial cell have not yet been identified.

4. Ligand-Gated Channels

Retinal neuroepithelial cells also express ligand-gated channels. Application of the neurotransmitter gamma-aminobutyric acid (GABA) causes a strong depolarization that leads to the activation of L-type Ca^{2+} channels, allowing Ca^{2+} influx [25]. The GABA-induced depolarization is due to the efflux of Cl^- ions through $GABA_A$ receptor channels, since the intracellular $[Cl^-]$ in the retinal neuroepithelial cell is higher than that in a mature neuron and the equilibrium potential of Cl^- is more positive than the resting membrane potential [25].

The GABA-induced depolarization and Ca^{2+} influx through voltage-dependent Ca^{2+} channels have been shown to inhibit the DNA synthesis in cortical progenitor cells [26] and the cell cycle progression in neuronal precursors from striatum [27]. On the contrary, by causing influx of Cl^- ions and hyperpolarization, GABA has been shown to negatively control the proliferation in embryonic stem (ES) cells and neural crest stem (NCS) cells [28].

In addition to GABA, ATP depolarizes retinal neuroepithelial cells by activating P2X purinoceptor channels as revealed by intracellular recording from these cells (unpublished observation).

5. Gap Junctions as Stabilizers of Membrane Potential

Neuroepithelial cells adhere to each other through gap junctions, which are located at the apical process of the cell [29]. This gap junction coupling between retinal neuroepithelial cells was demonstrated by the intracellular injection of a fluorescent dye and the subsequent dye diffusion (dye coupling) [5]. Following application of the gap junction channel blocker carbenoxolone during intracellular recording from retinal neuroepithelial cells, it was demonstrated that the input resistance was dramatically increased. In addition, the membrane potential was depolarized and rendered unstable showing fluctuations during the recording in the presence of the blocker [5]. These results suggest that the gap junction coupling stabilizes the resting membrane potential of the neuroepithelial cell by lowering the input resistance. This characteristic of gap junction coupling in the neuroepithelial cell may underlie the maintenance of the driving force for Ca^{2+} influx during store-operated Ca^{2+} entry and the prevention of the excess, continuous influx of Ca^{2+} through L-type Ca^{2+} channels.

6. Na^+, Ca^{2+}, and K^+ Channels in the Plasma Membrane

The neuroepithelial cell shows epithelial features including not only the polarized structure but also physiological properties. Studies of the chick retinal neuroepithelium and the amphibian neural tube have shown that neuroepithelial cells are nonexcitable [5, 30]. Instead of voltage-dependent Na^+ channels, amiloride-sensitive epithelial-type Na^+ channels are present in cells of the neural tube [31]. These channels allow a continuous influx of Na^+ from the ventricular space, and Na^+-K^+ pumps extrude Na^+ ions from the cell to generate the transneural tube potential (a lumen-negative DC potential) in the amphibian embryo [31]. An extracellular DC potential was also observed within the retinal neuroepithelium (unpublished observation). The polarized transport of Na^+ from the ventricular space may contribute to the establishment of the DC potential. The retinal neuroepithelium is an electrically tight epithelium since the extracellular resistance is extremely high ($\geq$300 MΩ) in the middle region of the retinal neuroepithelium (unpublished observation).

Voltage-gated Ca^{2+} channels are also present in the retinal neuroepithelial cell. Ca^{2+}-sensitive fluorescence measurements revealed the presence of L-type channels [25]. The L-type Ca^{2+} channel allows a continuous Ca^{2+} influx when the cell is depolarized with a high concentration of extracellular K^+ [25]. Since retinal neuroepithelial cells are interconnected through gap junctions, lowering the input resistance [5], it seems likely that these channels are activated only when a mass of cells are depolarized. A single neuroepithelial cell does not generate any spike-like potential, even following the injections of a strong depolarizing current [5]. Thus, the role of the L-type Ca^{2+} channel in these cells remains to be clarified. It can be supposed that if L-type Ca^{2+} channels are activated by GABA-induced depolarization after losing gap junction, the Ca^{2+} influx through these channels may inhibit cell cycle progression, as revealed in neural progenitor cells [26, 27]. It has also been shown that the influx of Ca^{2+} through L-type Ca^{2+} channels prevents apoptosis in culture models of neuronal death [32].

BK (big potassium, Ca^{2+}- and voltage-dependent potassium) channels in the plasma membrane are activated by increases in intracellular [Ca^{2+}], which may be caused by Ca^{2+} influx through voltage-dependent Ca^{2+} channels during depolarization. Cells expressing BK channels in the plasma membrane show a voltage sag in response to a depolarizing current injection. This is the case in newborn retinal ganglion cells, which do not yet generate a tetrodotoxin-sensitive Na^+-dependent action potential [5]. The newborn ganglion cell loses its gap junction coupling, thus the input resistance is increased and the voltage response in the cell is rendered visible [5]. The voltage sag in response to a depolarizing current injection is also observed in retinal neuroepithelial cells in which the gap junction channels are blocked by carbenoxolone [5]. These data suggest that BK channels are also present in the plasma membrane of retinal neuroepithelial cells. It seems likely that the BK channels in the plasma membrane repolarize the membrane potential when intracellular [Ca^{2+}] is increased.

7. BK Channels in the Nuclear Envelope and Endoplasmic Reticulum

Intracellular Ca^{2+} stores are comprised of the endoplasmic reticulum and the nuclear envelope [33, 34]. The lumen of the endoplasmic reticulum is continuous with the space between the outer and inner nuclear membranes [35]. Ca^{2+} ions are actively transported into this lumen by Ca^{2+} pumps.

The release of Ca^{2+} from intracellular stores via $InsP_3$ receptor channels leads to a charge movement across the store membrane from the lumen to the cytoplasm or to the nucleoplasm, which are electrically interconnected through low-resistance nuclear pores [36]. This charge movement should lead to a negative shift in the luminal potential [37]. Simultaneous measurements of the nuclear membrane potential and intracellular [Ca^{2+}] revealed that the potential of the nuclear membrane changes in a biphasic manner together with the activation of GPCRs, leading to a transient hyperpolarization and a sustained depolarization associated with the release of Ca^{2+} and the electrogenic pumping of Ca^{2+} ions, respectively [38].

To maintain the driving force for Ca^{2+} release from intracellular stores, the counter movement of ions, such as K^+, across the store membrane is absolutely necessary; without counter ion movement, the luminal potential hyperpolarizes to the equilibrium potential of Ca^{2+} and the driving force for Ca^{2+} release is lost [37]. In the sarcoplasmic reticulum, TRIC (trimeric intracellular cation) channels mediate the counter ion movement [39].

Patch clamp recordings from the nuclear envelope membrane have shown that this membrane contains BK channels and that these BK channels are activated by positive changes in the luminal potential (depolarization) and by an increase in the luminal [Ca^{2+}] [15, 40]. Such voltage and Ca^{2+} dependence may suggest that hyperpolarization caused by the release of Ca^{2+} and a decrease in the luminal [Ca^{2+}], together lead to the closure of the BK channel and cessation of Ca^{2+} release from the lumen. This has been proposed to be a hypothetical underlying mechanism to explain the "quantal" manner of Ca^{2+} release, in which Ca^{2+} release terminates after a rapid release of a fraction of stored Ca^{2+} [41].

8. Nuclear Envelope Potential and the Synchronization of Cellular Activity

Spontaneous Ca^{2+} oscillations occur synchronously across the cells in the retinal neuroepithelium, while agonist-induced [Ca^{2+}] rises occur asynchronously [15]. The mechanism underlying the synchronization of Ca^{2+} oscillations has been a matter of debate [42]. The diffusion of $InsP_3$ or Ca^{2+} itself through gap junction channels is unlikely to synchronize a [Ca^{2+}] rise, because an agonist-induced Ca^{2+} release is not synchronized even with the application of a supramaximal concentration of the agonist [15, 42]. Instead, a capacitative, or AC (alternating current), electrical coupling model has been proposed [6]. In this model, the efflux of Ca^{2+} from intracellular stores and the counter

Table 1: Neuroepithelial-cell-ion channels and their functions.

Type of ion channel	Function of ion channel
Ion channels in the plasma membrane	
Gap junction channel	Stabilizing membrane potential by lowering input resistance
Store-operated Ca^{2+} entry channel (TRP or Orai)	Replenishing Ca^{2+} stores after Ca^{2+} release
Epithelial Na^{+} channel	Continuous Na^{+} influx from ventricular space to generate DC potential
L-type voltage-dependent Ca^{2+} channel	Ca^{2+} influx by depolarization
BK channel	Repolarizating after depolarization and intracellular $[Ca^{2+}]$ rise
$GABA_A$ receptor channel	Depolarizing in response to GABA
P2X purinoceptor channel	Depolarizing in response to ATP
Ion channels in the nuclear envelope and the endoplasmic reticulum	
$InsP_3$ receptor channel	Ca^{2+} release by activation of muscarinic acetylcholine receptor, P2Y purinoceptor, and lysophosphatidic acid receptor
BK channel	Counter ion movement for Ca^{2+} release to maintain driving force for Ca^{2+} release

influx of K^{+} into the store lumen cause alternating voltage changes across the store membrane, and this voltage fluctuation induces AC currents. In the neuroepithelial cell, the outer nuclear membrane is closely apposed to the plasma membrane, and the cells are tightly packed [6, 15, 38]. Thus, it is plausible that the voltage fluctuation in the nuclear envelope potential is synchronized across the cells by the AC current being transferred in series via the capacitance of the outer nuclear membrane and the plasma membrane [6, 41]. Real-time confocal fluorescence measurements using an organelle-specific voltage-sensitive dye revealed that the nuclear membrane potential generates spontaneous repeats of high frequency (100–300 Hz) bursts of fluctuations in potential [38]. Furthermore, oscillatory changes in nuclear membrane potential underlie spike burst generation in developing neurons prior to synapse formation [38]. These results support the capacitative coupling model, in which voltage fluctuations in the nuclear membrane potential synchronize Ca^{2+} release across the population of cells and also function as a current noise generator to cause synchronous burst spike discharges in the neurons at an early stage of neural development [6, 38].

9. Concluding Remarks

Table 1 summarizes the different types and functions of ion channels expressed by neuroepithelial cells. While neurons use voltage changes across the plasma membrane, such as action potentials and synaptic potentials, for intercellular communication, the neuroepithelial cell uses stored Ca^{2+} ions to enable proliferation as well as the synchronization of Ca^{2+} oscillations. This synchronization is mediated by voltage fluctuations in the membrane potential of the nuclear envelope that allow capacitative (AC) electrical coupling between the cells. The membrane potential across the plasma membrane is stabilized via gap junction coupling, which lowers the input resistance of the neuroepithelial cell. BK-type potassium channels may also contribute to the stabilization of the plasma membrane potential when intracellular $[Ca^{2+}]$ is increased. Thus, stored Ca^{2+} ions are a key player in the maintenance of the cellular activity of neuroepithelial cells.

References

[1] F. C. Sauer, "Mitosis in the neural tube," *The Journal of Comparative Neurology*, vol. 62, no. 2, pp. 377–405, 1935.

[2] S. Fujita, "Mitotic pattern and histogenesis of the central nervous system," *Nature*, vol. 185, no. 4714, pp. 702–703, 1960.

[3] S. Fujita, "The matrix cell and cytogenesis in the developing central nervous system," *Journal of Comparative Neurology*, vol. 120, no. 1, pp. 37–42, 1963.

[4] Y. Kosodo, T. Suetsugu, M. Suda et al., "Regulation of interkinetic nuclear migration by cell cycle-coupled active and passive mechanisms in the developing brain," *The EMBO Journal*, vol. 30, no. 9, pp. 1690–1704, 2011.

[5] M. Yamashita, "Synchronous Ca^{2+}oscillation emerges from voltage fluctuations of Ca^{2+} stores," *The FEBS Journal*, vol. 275, no. 16, pp. 4022–4032, 2008.

[6] M. Yamashita, "Synchronization of Ca^{2+} oscillations: a capacitative (AC) electrical coupling model in neuroepithelium," *The FEBS Journal*, vol. 277, no. 2, pp. 293–299, 2010.

[7] M. Yamashita, Y. Yoshimoto, and Y. Fukuda, "Muscarinic acetylcholine responses in the early embryonic chick retina," *Journal of Neurobiology*, vol. 25, no. 9, pp. 1144–1153, 1994.

[8] M. Sugioka, Y. Fukuda, and M. Yamashita, "Ca^{2+} responses to ATP via purinoceptors in the early embryonic chick retina," *Journal of Physiology*, vol. 493, no. 3, pp. 855–863, 1996.

[9] W. L. Zhou, M. Sugioka, and M. Yamashita, "Lysophosphatidic acid-induced Ca^{2+} mobilization in the neural retina of chick embryo," *Journal of Neurobiology*, vol. 41, no. 4, pp. 495–504, 1999.

[10] Y. Sakaki, Y. Fukuda, and M. Yamashita, "Muscarinic and purinergic Ca^{2+} mobilizations in the neural retina of early embryonic chick," *International Journal of Developmental Neuroscience*, vol. 14, no. 6, pp. 691–699, 1996.

[11] M. Sugioka and M. Yamashita, "Calcium signaling to nucleus via store-operated system during cell cycle in retinal neuroepithelium," *Neuroscience Research*, vol. 45, no. 4, pp. 447–458, 2003.

[12] C. Prada, J. Puga, L. Pérez-Méndez, R. López, and G. Ramírez, "Spatial andtemporal patterns of neurogenesis in the chick

retina," *European Journal of Neuroscience*, vol. 3, no. 6, pp. 559–569, 1991.

[13] M. Yamashita and M. Sugioka, "Calcium mobilization systems during neurogenesis," *News in Physiological Sciences*, vol. 13, no. 2, pp. 75–79, 1998.

[14] M. Sugioka, W. L. Zhou, H. D. Hofmann, and M. Yamashita, "Ca^{2+} mobilization and capacitative Ca^{2+} entry regulate DNA synthesis in cultured chick retinal neuroepithelial cells," *International Journal of Developmental Neuroscience*, vol. 17, no. 3, pp. 163–172, 1999.

[15] M. Yamashita, M. Sugioka, and Y. Ogawa, "Voltage- and Ca^{2+}-activated potassium channels in Ca^{2+} store control Ca^{2+} release," *The FEBS Journal*, vol. 273, no. 15, pp. 3585–3597, 2006.

[16] M. Sugioka, W. L. Zhou, H. D. Hofmann, and M. Yamashita, "Involvement of P2 purinoceptors in the regulation of DNA synthesis in the neural retina of chick embryo," *International Journal of Developmental Neuroscience*, vol. 17, no. 2, pp. 135–144, 1999.

[17] G. Sanches, L. S. Alencar, and A. L. M. Ventura, "ATP induces proliferation of retinal cells in culture via activation of PKC and extracellular signal-regulated kinase cascade," *International Journal of Developmental Neuroscience*, vol. 20, pp. 21–27, 2002.

[18] I. M. Ornelas and A. L. M. Ventura, "Involvement of the PI3K/AKT pathway in ATP-induced proliferation of developing retinal cells in culture," *International Journal of Developmental Neuroscience*, vol. 28, no. 6, pp. 503–511, 2010.

[19] L. Lipskaia and A. M. Lompré, "Alteration in temporal kinetics of Ca^{2+} signaling and control of growth and proliferation," *Biology of the Cell*, vol. 96, no. 1, pp. 55–68, 2004.

[20] L. Lipskaia, J. S. Hulot, and A. M. Lompré, "Role of sarco/endoplasmic reticulum calcium content and calcium ATPase activity in the control of cell growth and proliferation," *Pflügers Archiv—European Journal of Physiology*, vol. 457, no. 3, pp. 673–685, 2009.

[21] M. Potier and M. Trebak, "New developments in the signaling mechanisms of the store-operated calcium entry pathway," *Pflügers Archiv—European Journal of Physiology*, vol. 457, no. 2, pp. 405–415, 2008.

[22] J. T. Smyth, S. Y. Hwang, T. Tomita, W. I. DeHaven, J. C. Mercer, and J. W. Putney, "Activation and regulation of store-operated calcium entry," *Journal of Cellular and Molecular Medicine*, vol. 14, no. 10, pp. 2337–2349, 2010.

[23] Y. Sakaki, M. Sugioka, Y. Fukuda, and M. Yamashita, "Capacitative Ca^{2+} influx in the neural retina of chick embryo," *Journal of Neurobiology*, vol. 32, no. 1, pp. 62–68, 1997.

[24] J. Ichikawa, Y. Fukuda, and M. Yamashita, "In vitro changes in capacitative Ca^{2+} entry in neuroblastoma X glioma NG108-15 cells," *Neuroscience Letters*, vol. 246, no. 2, pp. 120–122, 1998.

[25] M. Yamashita and Y. Fukuda, "Calcium channels and GABA receptors in the early embryonic chick retina," *Journal of Neurobiology*, vol. 24, no. 12, pp. 1600–1614, 1993.

[26] J. J. LoTurco, D. F. Owens, M. J. S. Heath, M. B. E. Davis, and A. R. Kriegstein, "GABA and glutamate depolarize cortical progenitor cells and inhibit DNA synthesis," *Neuron*, vol. 15, no. 6, pp. 1287–1298, 1995.

[27] L. Nguyen, B. Malgrange, I. Breuskin et al., "Autocrine/paracrine activation of the $GABA_A$ receptor inhibits the proliferation of neurogenic polysialylated neural cell adhesion molecule-positive (PSA-$NCAM^+$) precursor cells from postnatal striatum," *Journal of Neuroscience*, vol. 23, no. 8, pp. 3278–3294, 2003.

[28] M. Andäng, J. Hjerling-Leffler, A. Moliner et al., "Histone H2AX-dependent $GABA_A$ receptor regulation of stem cell proliferation," *Nature*, vol. 451, no. 7177, pp. 460–464, 2008.

[29] H. Fujisawa, H. Morioka, K. Watanabe, and H. Nakamura, "A decay of gap junctions in association with cell differentiation of neural retina in chick embryonic development," *Journal of Cell Science*, vol. 22, no. 3, pp. 585–596, 1976.

[30] A. E. Warner, "The electrical properties of the ectoderm in the amphibian embryo during induction and early development of the nervous system," *Journal of Physiology*, vol. 235, no. 1, pp. 267–286, 1973.

[31] R. Shi and R. B. Borgens, "Embryonic neuroepithelial sodium transport, the resulting physiological potential, and cranial development," *Developmental Biology*, vol. 165, no. 1, pp. 105–116, 1994.

[32] J. L. Franklin and E. M. Johnson Jr., "Block of neuronal apoptosis by a sustained increase of steady-state free Ca^{2+} concentration," *Philosophical Transactions of the Royal Society of London. Series B*, vol. 345, no. 1313, pp. 251–256, 1994.

[33] O. V. Gerasimenko, J. V. Gerasimenko, A. V. Tepikin, and O. H. Petersen, "Calcium transport pathways in the nucleus," *Pflügers Archiv—European Journal of Physiology*, vol. 432, no. 1, pp. 1–6, 1996.

[34] O. H. Petersen, O. V. Gerasimenko, J. V. Gerasimenko, H. Mogami, and A. V. Tepikin, "The calcium store in the nuclear envelope," *Cell Calcium*, vol. 23, no. 2-3, pp. 87–90, 1998.

[35] G. K. Voeltz, M. M. Rolls, and T. A. Rapoport, "Structural organization of the endoplasmic reticulum," *EMBO Reports*, vol. 3, no. 10, pp. 944–950, 2002.

[36] M. Mazzanti, J. O. Bustamante, and H. Oberleithner, "Electrical dimension of the nuclear envelope," *Physiological Reviews*, vol. 81, no. 1, pp. 1–19, 2001.

[37] D. Burdakov, O. H. Petersen, and A. Verkhratsky, "Intraluminal calcium as a primary regulator of endoplasmic reticulum function," *Cell Calcium*, vol. 38, no. 3-4, pp. 303–310, 2005.

[38] M. Yamashita, "Fluctuations in nuclear envelope's potential mediate synchronization of early neural activity," *Biochemical and Biophysical Research Communications*, vol. 406, no. 1, pp. 107–111, 2011.

[39] M. Yazawa, C. Ferrante, J. Feng et al., "TRIC channels are essential for Ca^{2+} handling in intracellular stores," *Nature*, vol. 448, no. 7149, pp. 78–82, 2007.

[40] Y. Maruyama, H. Shimada, and J. Taniguchi, "Ca^{2+}-activated K^+-channels in the nuclear envelope isolated from single pancreatic acinar cells," *Pflügers Archiv—European Journal of Physiology*, vol. 430, no. 1, pp. 148–150, 1995.

[41] M. Yamashita, "'Quantal' Ca^{2+} release reassessed—a clue to oscillation and synchronization," *FEBS Letters*, vol. 580, no. 21, pp. 4979–4983, 2006.

[42] M. Yamashita, "Synchronization of Ca^{2+} oscillations: Is gap junctional coupling sufficient?" *The FEBS Journal*, vol. 277, no. 2, p. 277, 2010.

Hindawi Publishing Corporation
Stem Cells International
Volume 2012, Article ID 454180, 9 pages
doi:10.1155/2012/454180

Review Article

Large Pore Ion and Metabolite-Permeable Channel Regulation of Postnatal Ventricular Zone Neural Stem and Progenitor Cells: Interplay between Aquaporins, Connexins, and Pannexins?

Leigh E. Wicki-Stordeur[1] and Leigh Anne Swayne[1, 2, 3, 4]

[1] *Division of Medical Sciences, Island Medical Program, University of Victoria, Victoria, BC, Canada V8W 2Y2*
[2] *Department of Biology, University of Victoria, Victoria, BC, Canada V8W 3N5*
[3] *Department of Biochemistry and Microbiology, University of Victoria, Victoria, BC, Canada V8W 3P6*
[4] *Department of Cellular and Physiological Sciences, University of British Columbia, Vancouver, BC, Canada V6T 1Z3*

Correspondence should be addressed to Leigh Anne Swayne, lswayne@uvic.ca

Received 5 April 2012; Accepted 27 April 2012

Academic Editor: Stefan Liebau

The birth of new neurons from unspecialized neural stem and progenitor cells surrounding the lateral ventricles occurs throughout postnatal life. This process, termed neurogenesis, is complex and multistepped, encompassing several types of cellular behaviours, such as proliferation, differentiation, and migration. These behaviours are influenced by numerous factors present in the unique, permissive microenvironment. A major cellular mechanism for sensing the plethora of environmental cues directing this process is the presence of different channel forming proteins spanning the plasma membrane. So-called large pore membrane channels, which are selective for the passage of specific types of small molecules and ions, are emerging as an important subgroup of channel proteins. Here, we focus on the roles of three such large pore channels, aquaporin 4, connexin 43, and pannexin 1. We highlight both their independent functions as well as the accumulating evidence for crosstalk between them.

1. Introduction

New neurons are produced in the ventricular zone (VZ) of the lateral ventricles throughout postnatal life [1]. This is a remarkable developmental process, in which unspecialized neural stem and progenitor cells (NSC/NPCs) pass through a complex gauntlet of cell behaviours, such as proliferation, differentiation, and migration. It is now becoming increasingly clear that the highly controlled movement of several ions and small molecules trigger numerous, complex signaling pathways that underscore the regulation of these behaviours (recently reviewed in [2, 3]). As follows, there is a growing body of evidence implicating "large pore" channels in the control of postnatal VZ neurogenesis. In contrast to typical ion channels, which are selective for small ions, large pore channels can additionally (or exclusively) allow passage of small molecules (neutral or charged). Aquaporin 4 (AQP4) connexin 43 (Cx43), and pannexin 1 (Panx1) are three such large pore channels that are expressed in postnatal VZ. Perhaps not surprisingly the roles of these channels appear to be closely linked with one another and also with the functions of other ion channels in the regulation of postnatal VZ NSC/NPC biology.

2. AQP4

There are thirteen known types of AQPs in mammals (AQP0-12; recently reviewed in [4]). These are categorized into two primary subgroups based on function: those selective solely for water (AQP0, AQP1, AQP2, AQP4, AQP5), and those permeable to water as well as small nonpolar solutes such as glycerol and urea (AQP3, AQP7, AQP9, and AQP10). Additional types can conduct ions (AQP6, AQP8), while so-called "unorthodox" members (AQP11, AQP12) are more distantly related to the other aquaporins and are expressed on intracellular membranes [5]. In general, AQP proteins are comprised of about 300 amino acids with six transmembrane

α-helices arranged in a right-handed bundle with intracellular N- and the C-termini [6, 7]. AQP monomers oligomerize to form tetramers, generating four aqueous pores [8, 9]. Specific motifs within the interhelical loop regions form the water conduit and selectivity filter [10]. Slight variations in peptide sequence between different AQPs have generated variability in the size of the pore. This is part of the basis for water selectivity (small pore) versus simultaneous water and nonpolar solute permeability (larger pore) [8].

AQPs 1, 4, and 9 are present in the central nervous system (CNS), largely in epithelial cells, ependymal cells, and/or astroglia ([11–14], reviewed in [15, 16]), where they facilitate movement of water between blood and brain, and between brain and cerebrospinal fluid compartments. Dysregulation of cell volume in the brain underlies clinical conditions such as edema and hypoxia. Water balance also plays a crucial role in neurogenesis, as NSC/NPCs must move considerable amounts of water into or out of the cell to rapidly change their volume during proliferation, differentiation, and migration.

The major AQP found in brain, AQP4, is highly enriched in the neurogenic regions [11, 14, 17], particularly the VZ, and is the main isoform expressed in adult NSC/NPCs and ependymal cells [17, 18]. As described above, AQP4 is a member of the water-only permeable subgroup. Considerable AQP8 (water plus small nonpolar solutes) and AQP9 (water plus ions) have also been detected in NSC/NPCs in culture [18]. In contrast to AQP4, which is more ubiquitous in the VZ, AQP9 is mainly localized in NSC/NPCs in the dorsolateral corner [17]; however, its exact functional significance in NSC/NPC biology remains to be determined. AQP8 is detected primarily in the mitochondria-enriched fraction, although whether it is present in neurogenic regions *in situ* has not yet been reported [18].

Most of what is currently known about the role of AQPs in NSC/NPCs comes from recent work on AQP4 [19–21]. Using AQP4 knockout (KO) mice, Kong et al. [19] demonstrated that it controls proliferation, survival, migration, and neuronal differentiation of VZ NSC/NPCs. An observed impairment in neurosphere formation in AQP4 KO mice was attributed to both increased cell apoptosis and decreased cell proliferation due to cell cycle arrest in G2/M phase. Furthermore, upon neurosphere differentiation, the proportion of immature neurons in the AQP4 KO population was significantly lower than in the wildtype population, whereas there was no significant difference in the proportion of astrocytes. To help elucidate the underlying mechanism, the authors investigated the effects of AQP4 loss on Ca^{2+} oscillations. In NSC/NPCs, L-type Ca^{2+} channel mediated Ca^{2+} fluxes [22, 23] and purinergic receptor- (P2R-) dependent Ca^{2+} oscillations [24–27] play major roles in directing neurogenesis (recently reviewed in [2, 3]), in part through Ca^{2+}-dependent transcription [23]. Interestingly, these P2R-mediated Ca^{2+} oscillations can even occur spontaneously without exogenous stimulation in NSC/NPCs [25, 26]. AQP4 KO increased the frequency but decreased the amplitude of spontaneous Ca^{2+} oscillations and suppressed high K^+-induced Ca^{2+} influx. Given its demonstrated effects on intracellular Ca^{2+}, it is not surprising that AQP4 KO also affected the expression of other channels: the expression of both Cx43 and the L-type voltage-gated Ca^{2+} channel $Ca_v1.2$ subtype were reduced.

3. Cx43

Cxs are a family of vertebrate four-pass transmembrane proteins with intracellular N- and C-termini, that oligomerize into hexameric channels known as connexons (hemichannels), which, in turn, can connect neighboring cells across the extracellular space by formation of gap junctions [28]. These junctions provide a physical link between cells through which ions, metabolites, and other messengers of up to 1 kDa in size can diffuse, thereby mediating cell-cell communication through passage of signaling molecules such as ATP [29], IP_3, and Ca^{2+} ([30] reviewed in [31, 32]). Gap junction-independent functions of hemichannels have also recently been identified, in which similar exchanges between the cell and its extracellular environment are facilitated (reviewed in [33]). Furthermore, the variable C-terminal domains of individual Cxs can exert intrinsic functionality independent from channel activity (reviewed in [34]), that appears to be regulated by signaling/adaptor proteins like protein kinases, phosphatases, and structural proteins (reviewed in [35]). Cxs have been shown to widely influence physiological and pathological processes and are key in coordinating metabolic and electrical activities as well as cell growth and proliferation (reviewed in [36]), cytoskeletal dynamics [37], and transcriptional regulation [38–40].

Over twenty mammalian members of the Cx family have been identified, with each respective isoform originally named for its molecular weight (reviewed in [41]). Cx43 (gap-junction protein alpha-1, Gja1) is the most widely and highly expressed Cx in almost every tissue [42], and it is the predominant isoform within the CNS. Within the developing CNS, Cx43 is detected in several cell types including astrocytes, NSC/NPCs, cortical neurons, and dopaminergic neurons of the developing midbrain [43–49]. Cx43 is critical for proper CNS formation and organization, likely through its role in the neurogenic processes of NSC/NPC proliferation [50], differentiation [47, 51], and migration [52–54] during development. Interestingly, studies in human and murine embryonic stem cells have found transcriptional regulatory elements controlled by the NSC transcription factor SOX2 within the Cx43 gene region [55] and have identified Cx43 as necessary for both neuroectodermal specification [56] and stem cell proliferation [57].

In the postnatal and adult brain, Cx43 expression becomes much more highly restricted to astrocytes [58–60]. However, Cx43 remains present in cortical neurons [61], ependymal cells [44], NSC/NPCs, and migratory neuroblasts [62–65]. Within the neurogenic VZ and subsequent rostral migratory stream (RMS), a dramatic increase in Cx43 is noted between neonatal periods and adulthood [66] in the astrocytes, NSC/NPCs, and ependymal cells, all of which exhibit gap-junction-dependent coupling [63, 64, 67]. Within this stem cell environment, Cx43 is further thought to be involved in hemichannel mediated ATP uptake and release

[68, 69], contributing to propagation of Ca^{2+} waves from intracellular IP_3-dependent stores [70, 71]. This Ca^{2+} release regulates NSC/NPC cell cycle entry and thus proliferation [72]. Cx43 hemichannels are also permeable to Ca^{2+} and controlled by Ca^{2+} (for recent studies see [73, 74]).

The data on the role of Cx43 in postnatal VZ neurogenesis is somewhat conflicting, and studies have been hindered by the lethality of the full Cx43 knock-out due to severe neonatal heart defects [75]. Some lines of evidence point to a negative regulation of proliferation by Cx43. Within the subependymal layers and RMS, levels of Cx43 were inversely correlated with lower levels of DNA synthesis [66]. Intriguingly, this correlation was only mimicked in a primary cell culture model upon high levels of confluence, indicating a potential role for Cx43 in contact inhibition. Furthermore, *in vitro* studies in mouse Neuro2a neuroblastoma cells, a commonly used NPC model, demonstrated an increased doubling-time upon Cx43 overexpression under nongap junction forming conditions. Interestingly, only the C-terminal tail was required for this reduced proliferation, possibly through transcriptional regulatory mechanisms, as this domain contains a putative nuclear localization signal [76]. Additional work in Neuro2a cells identified Cx43 as a Ca^{2+}-dependent regulator of cell volume [77]. Murine PC12 cells, a well-studied pheochromocytoma-derived cell model for neurite outgrowth, exhibited enhanced NGF-induced neurite outgrowth when overexpressing Cx43. Interestingly, untransfected cells within the same dish as those overexpressing Cx43 also demonstrated enhanced neuritogenesis due to Cx43 hemi-channel-mediated ATP release [78]. Similarly, using murine embryonal carcinoma P19 cell line, Cx43 (and Gjb2) inhibition resulted in decreased astrocytic and neuronal differentiation of these cells [79]. In contrast to these results pointing to a role for Cx43 in negative regulation of proliferation, other studies suggest Cx43 is a positive regulator of proliferation. In developing and early postnatal hippocampus, conditional Cx43 knockout in radial glia and astrocytes causes severe inhibition of hippocampal NSC/NPC proliferation [80]. Moreover, embryonic cortical neurospheres were dependent on Cx43 gap junctional coupling to maintain cells in proliferative state [50], but whether this is conserved in the postnatal VZ is unknown.

Still, the functional relevance of Cx43 in NSC/NPCs of the postnatal VZ *in vivo* remains to be discovered. Currently, much is assumed from the previously mentioned cell culture experiments, as well as developmental and postnatal hippocampal studies. Together, it appears a role for Cx43 may be emerging in VZ NSC/NPC self-renewal, differentiation and migration, thereby contributing to the regulation of the postnatal process of neurogenesis.

4. Panx1

Panx1 is part of a three-membered family of proteins with homology to the invertebrate gap junction forming innexins [81]. However, little concrete evidence exists pointing towards gap junction functions for Panxs, which are instead widely considered single-membrane channels (reviewed in [82–84]). Panx1 monomers have a predicted four-pass transmembrane sequence, with a conserved intracellular N-terminus and much longer, variable intracellular C-terminus. These monomers oligomerize into large hexameric pores [85] that may be opened by depolarization [86, 87], increased extracellular K^+ (independent of depolarization) [88, 89], mechanical stimulation [90], NMDAR activation [91], intracellular Ca^{2+} [92], or low oxygen and glucose conditions [93, 94]. Recently, it has been demonstrated that the C-terminal domain of Panx1 is autoinhibitory, and can be removed by caspase-dependent cleavage, resulting in constitutive activation of this channel [95, 96]. Furthermore, Panx1 activation can be inhibited by dramatically increased extracellular ATP [97] or upon cytoplasmic acidification [92], as well as through mimetic peptides [98] and channel blockers [99, 100]. Once activated, the Panx1 pore may nonselectively pass ions, metabolites, and other signaling molecules up to 1 kDa in size (reviewed in [82–84]); however, recent evidence has pointed towards Panx1 as being selective for anions (e.g., Cl^-) and anionic small molecules [101]. These channels are involved in several physiological and pathological processes, largely by mediating ATP release in several cell types (reviewed in [82–84]).

Panx1 is found in a wide range of rodent tissues, with an expression profile similar to that of Cx43 [100]. It is abundantly expressed in the brain [102, 103]. Importantly, this relatively newly discovered large pore channel has recently been identified in postnatal VZ NSC/NPCs and their immature neuronal progeny [27]. Using Neuro2a murine neuroblastoma cells and primary postnatal VZ neurosphere cultures, Panx1 overexpression and inhibition dramatically increased and decreased NSC/NPC proliferation, respectively. Furthermore, this regulation was partly due to the ability of Panx1 to release ATP (reviewed in [82, 83, 100, 104]), a potent signalling metabolite, which is released in sporadic bursts from NSC/NPCs [25]. Released ATP triggers intracellular Ca^{2+} mobilization via activation of P2R signaling [24–27]. Ongoing studies will likely uncover additional regulatory roles of Panx1 in neurogenesis, as well as underlying mechanisms.

5. Crosstalk between "Large" Pore Channels and Convergence of Signaling Mechanisms

Figure 1 summarizes the roles of AQP4, Cx43 and Panx1 in postnatal VZ NSC/NPCs. Interestingly, there appears to be multiple levels of crosstalk between each of these large pore channels. Here, we outline three primary interconnected ways in which the regulation and function of these large pore channels converge: solute gradient regulation, cytoskeletal signaling related to cell volume changes, and nucleotide signaling.

5.1. Gradient Regulation. The movement of ions and metabolites is often dependent on the ability to tightly control concentration gradients. These gradients cannot be generated and/or maintained without concomitant control of water volume. The mechanism underlying the effects of

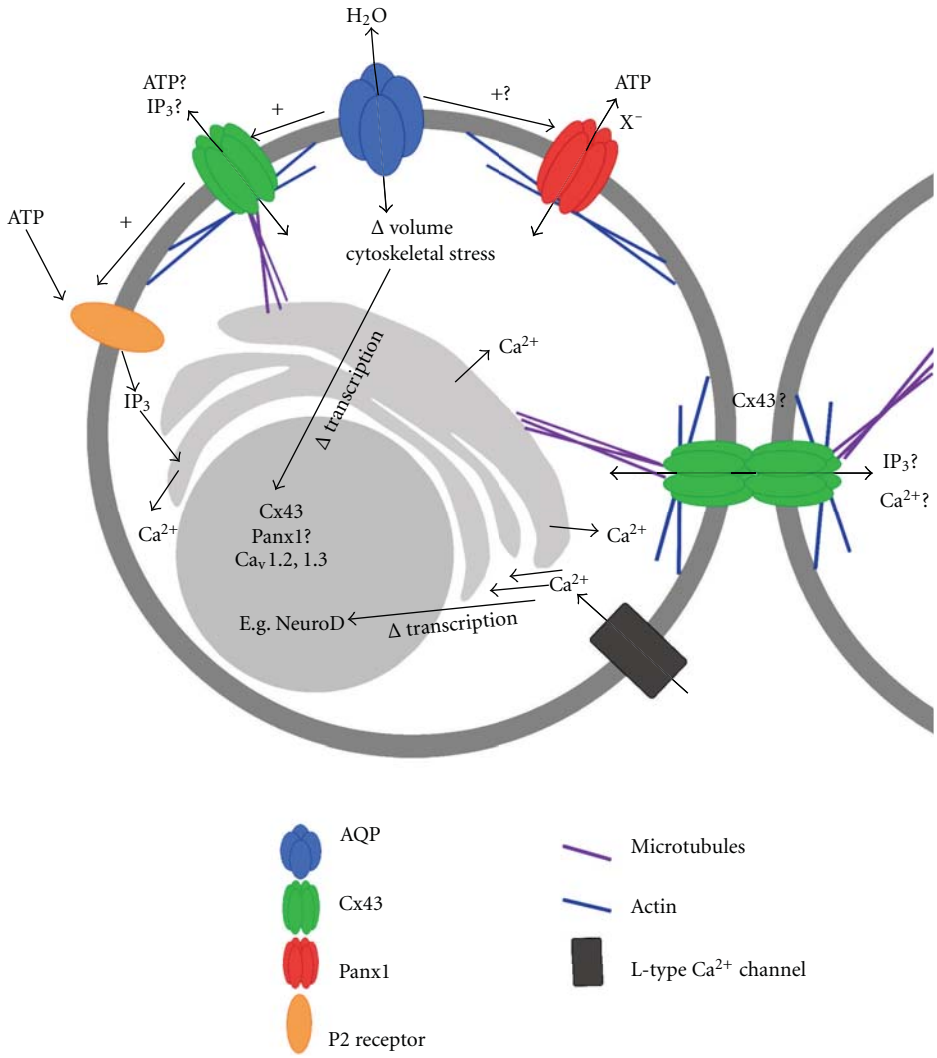

Figure 1: Schematic illustration of the interplay between AQP4, Cx43 and Panx1 large pore channels as they mediate cytoskeletal interactions, Ca^{2+} signaling, transcriptional regulation, ATP flux, and cell-cell communication between VZ NSC/NPCs.

AQP4 loss on Ca^{2+} oscillations and changes in L-type and Cx43 channel expression have not been fully elucidated; however, it is conceivable that these changes could result, in part, from alterations in ion concentration gradients. Cx43 has also been implicated in volume control (for review see [105]), perhaps through reciprocal relationships with AQP4, as described above. Thus, the ion fluxes through Cx43 and Panx1 are dependent on the capacity of AQP4 to regulate solute concentration gradients.

5.2. Cytoskeletal Signaling. Proliferating, differentiating and migrating NSC/NPCs and neuroblasts must make specific and substantial changes in cell volume and morphology that undoubtedly require the movement of water molecules. For example, cell proliferation required for neurosphere formation is inhibited by a hypertonic medium [106]—in glioma cells this results in sustained cell swelling following transient cell shrinkage [107, 108]. The precise details of volume-sensing signaling mechanisms triggered by AQP4-mediated water movement that are important for neurogenesis remain to be further elucidated. An early study in cultured astrocytes demonstrated that AQP4 knockdown also induced alterations of the actin cytoskeleton [109]. Therefore, AQP4-mediated changes in cell volume could directly regulate Cx43 and Panx1 signaling through stretch activation of the channels and/or the cytoskeletal-associated signaling pathways to which they are linked. Recent work has demonstrated that extracellular matrix stiffness modulates NSC behaviour [110] and that cytoskeletal-regulating Rho GTPases mediate the lineage commitment of hippocampal NSCs [111]. For many years, Cxs have been closely linked to the cytoskeleton in numerous cell types (e.g., see [37, 112–116], for reviews see [105, 117, 118] with actomyosin-mediated contractility actually inhibiting Cx43 hemichannel activity [118]).

As described above, we also now know that Panx1 regulates NSC/NPC proliferation [27] which adds another layer

of complexity. Previous work has shown that these channels can be activated by mechanical stress [90]. Further suggesting the potential for positive crosstalk between Panx1 and the actin cytoskeleton in NSC/NPCs, Panx1 has been demonstrated to interact with the actin cytoskeleton [119] and drive actin remodeling [120]. Moreover, nucleotide-dependent mechanisms (e.g., ATP flux, P2R signaling) are implicated in cytoskeletal remodeling in NSC/NPCs [121]. Interestingly, recent work has demonstrated that, in addition to regulating Cx43 and the actin cytoskeleton, AQP4 knockdown reduces a maxi volume-regulated anion current of unknown molecular identity [122]. Given the discovery of the anion selectivity of Panx1 [123], it is tempting to speculate that Panx1 is the molecular basis of this enigmatic maxi volume regulated anion channel—which, incidentally, also mediates ATP release [124].

5.3. Nulceotide Signaling. Purinergic signaling mechanisms also further link Cx43 and Panx1, albeit somewhat controversially. Prior to the discovery of Panx1, channel-mediated ATP release was mainly attributed to Cx43 hemichannels. Interestingly, Cx43 expression also regulates P2R expression [26] in embryonic VZ NSC/NPCs. Cx43 hemichannel-mediated ATP release was heavily studied in astrocytes (e.g., see [68, 125]), however, this role has recently been challenged in favour of Panx1 [126]. Importantly, while Cx43 did not appear to form hemichannels in *Xenopus* oocytes [127], numerous studies in mammalian cells have elucidated the intricacies of Cx43 hemichannel activity (e.g., see [73, 74]). Furthermore, the cross-inhibition of Cx hemichannels, Panxs, and volume-activated ion channels by certain pharmacological tools is now well known [98, 104, 128], adding further levels of complexity as several previously identified Cx channel blockers are now known to inhibit Panx1 with equal or greater efficacy. Whether Cx43 has hemichannel activity in postnatal VZ NSC/NPCs may thus be more of an open question than was previously thought and further work is clearly needed to elucidate its role. Given that we now know that Panx1 appears to play an important role in purinergic signaling in NSC/NPCs, likely in part through mediating ATP release [27], it will be important to determine if and how Panx1 and Cx43 functionally interact in the postnatal VZ. Might there be crosstalk between Cx43 and Panx1 in ATP release and downstream purinergic signaling in the postnatal VZ? Furthermore, what is the added value of having both types of channels? Distinctions between Cx43 and Panx1 signaling may potentially lie in differences in regulation by internal and external Ca^{2+} concentrations, ion selectivity, single channel conductance, and/or involvement in separate protein complexes and signaling pathways (for reviews, see [83, 84, 117, 118, 129] and also see recent developments [73]). These and other similar questions will undoubtedly be the focus of future work.

6. Conclusions and Perspectives

Here, we have reviewed literature on the roles of three large pore ion channels, AQP4, Cx43, and Panx1 in the regulation of postnatal VZ neurogenesis. A common thread that has emerged during this process is that the regulation and functions of these channels seem to intimately connected (Figure 1).

Acknowledgments

L. A. Swayne is supported by a Natural Sciences and Engineering Research Council of Canada Discovery grant, a Victoria Foundation Willa and Ella Dawson Fund grant, and a University of Victoria laboratory startup grant.

References

[1] G. L. Ming and H. Song, "Adult neurogenesis in the mammalian brain: significant answers and significant questions," *Neuron*, vol. 70, no. 4, pp. 687–702, 2011.

[2] L. A. Swayne and L. Wicki-Stordeur, "Ion channels in postnatal neurogenesis: potential targets for brain repair," *Channels*, vol. 6, no. 2, 2012.

[3] T. Yasuda and D. J. Adams, "Physiological roles of ion channels in adult neural stem cells and their progeny," *Journal of Neurochemistry*, vol. 114, no. 4, pp. 946–959, 2010.

[4] K. Ishibashi, S. Hara, and S. Kondo, "Aquaporin water channels in mammals," *Clinical and Experimental Nephrology*, vol. 13, no. 2, pp. 107–117, 2009.

[5] A. Rojek, J. Praetorius, J. Frøkiaer, S. Nielsen, and R. A. Fenton, "A current view of the mammalian aquaglyceroporins," *Annual Review of Physiology*, vol. 70, pp. 301–327, 2008.

[6] G. M. Preston and P. Agre, "Isolation of the cDNA for erythrocyte integral membrane protein of 28 kilodaltons: member of an ancient channel family," *Proceedings of the National Academy of Sciences of the United States of America*, vol. 88, no. 24, pp. 11110–11114, 1991.

[7] G. M. Preston, J. S. Jung, W. B. Guggino, and P. Agre, "Membrane topology of aquaporin CHIP. Analysis of functional epitope- scanning mutants by vectorial proteolysis," *The Journal of Biological Chemistry*, vol. 269, no. 3, pp. 1668–1673, 1994.

[8] T. Gonen and T. Walz, "The structure of aquaporins," *Quarterly Reviews of Biophysics*, vol. 39, no. 4, pp. 361–396, 2006.

[9] B. L. Smith and P. Agre, "Erythrocyte M(r) 28,000 transmembrane protein exists as a multisubunit oligomer similar to channel proteins," *The Journal of Biological Chemistry*, vol. 266, no. 10, pp. 6407–6415, 1991.

[10] J. S. Jung, G. M. Preston, B. L. Smith, W. B. Guggino, and P. Agre, "Molecular structure of the water channel through aquaporin CHIP. The hourglass model," *The Journal of Biological Chemistry*, vol. 269, no. 20, pp. 14648–14654, 1994.

[11] H. Hasegawa, T. Ma, W. Skach, M. A. Matthay, and A. S. Verkman, "Molecular cloning of a mercurial-insensitive water channel expressed in selected water-transporting tissues," *The Journal of Biological Chemistry*, vol. 269, no. 8, pp. 5497–5500, 1994.

[12] S. Nielsen, B. L. Smith, E. I. Christensen, and P. Agre, "Distribution of the aquaporin CHIP in secretory and resorptive epithelia and capillary endothelia," *Proceedings of the National Academy of Sciences of the United States of America*, vol. 90, no. 15, pp. 7275–7279, 1993.

[13] M. N. Mylonakou, P. H. Petersen, E. Rinvik et al., "Analysis of mice with targeted deletion of AQP9 gene provides conclusive evidence for expression of AQP9 in neurons,"

Journal of Neuroscience Research, vol. 87, no. 6, pp. 1310–1322, 2009.

[14] J. S. Jung, R. V. Bhat, G. M. Preston, W. B. Guggino, J. M. Baraban, and P. Agre, "Molecular characterization of an aquaporin cDNA from brain: candidate osmoreceptor and regulator of water balance," *Proceedings of the National Academy of Sciences of the United States of America*, vol. 91, no. 26, pp. 13052–13056, 1994.

[15] J. L. Venero, M. L. Vizuete, A. Machado, and J. Cano, "Aquaporins in the central nervous system," *Progress in Neurobiology*, vol. 63, no. 3, pp. 321–336, 2001.

[16] M. J. Tait, S. Saadoun, B. A. Bell, and M. C. Papadopoulos, "Water movements in the brain: role of aquaporins," *Trends in Neurosciences*, vol. 31, no. 1, pp. 37–43, 2008.

[17] C. Cavazzin, D. Ferrari, F. Facchetti et al., "Unique expression and localization of aquaporin-4 and aquaporin-9 in murine and human neural stem cells and in their glial progeny," *Glia*, vol. 53, no. 2, pp. 167–181, 2006.

[18] C. A. M. La Porta, P. Gena, A. Gritti, U. Fascio, M. Svelto, and G. Calamita, "Adult murine CNS stem cells express aquaporin channels," *Biology of the Cell*, vol. 98, no. 2, pp. 89–94, 2006.

[19] H. Kong, Y. Fan, J. Xie et al., "AQP4 knockout impairs proliferation, migration and neuronal differentiation of adult neural stem cells," *Journal of Cell Science*, vol. 121, no. 24, pp. 4029–4036, 2008.

[20] H. Kong, L. L. Sha, Y. Fan et al., "Requirement of AQP4 for antidepressive efficiency of fluoxetine: implication in adult hippocampal neurogenesis," *Neuropsychopharmacology*, vol. 34, no. 5, pp. 1263–1276, 2009.

[21] L. L. Xie, X. L. Sun, Y. Fan, H. Kong, J. H. Ding, and G. Hu, "Aquaporin 4 knockout resists negative regulation of neural cell proliferation by cocaine in mouse hippocampus," *International Journal of Neuropsychopharmacology*, vol. 12, no. 6, pp. 843–850, 2009.

[22] M. D'Ascenzo, R. Piacentini, P. Casalbore et al., "Role of L-type Ca^{2+} channels in neural stem/progenitor cell differentiation," *European Journal of Neuroscience*, vol. 23, no. 4, pp. 935–944, 2006.

[23] K. Deisseroth, S. Singla, H. Toda, M. Monje, T. D. Palmer, and R. C. Malenka, "Excitation-neurogenesis coupling in adult neural stem/progenitor cells," *Neuron*, vol. 42, no. 4, pp. 535–552, 2004.

[24] S. K. Mishra, N. Braun, V. Shukla et al., "Extracelluar nucleotide signaling in adult neural stem cells: synergism with growth factor-mediated cellular proliferation," *Development*, vol. 133, no. 4, pp. 675–684, 2006.

[25] J. H. C. Lin, T. Takano, G. Arcuino et al., "Purinergic signaling regulates neural progenitor cell expansion and neurogenesis," *Developmental Biology*, vol. 302, no. 1, pp. 356–366, 2007.

[26] E. Scemes, N. Duval, and P. Meda, "Reduced expression of P2Y1 receptors in connexin43-null mice alters calcium signaling and migration of neural progenitor cells," *Journal of Neuroscience*, vol. 23, no. 36, pp. 11444–11452, 2003.

[27] L. E. Wicki-Stordeur, A. D. Dzugalo, R. M. Swansburg, J. M. Suits, and L. A. Swayne, "Pannexin 1 regulates postnatal neural stem and progenitor cell proliferation," *Neural Development*, vol. 7, no. 1, article 11, 2012.

[28] D. A. Goodenough, "The structure and permeability of isolated hepatocyte gap junctions," *Cold Spring Harbor Symposia on Quantitative Biology*, vol. 40, pp. 37–43, 1976.

[29] G. S. Goldberg, A. P. Moreno, and P. D. Lampe, "Gap junctions between cells expressing connexin 43 or 32 show inverse permselectivity to adenosine and ATP," *The Journal of Biological Chemistry*, vol. 277, no. 39, pp. 36725–36730, 2002.

[30] J. C. Saez, J. A. Connor, D. C. Spray, and M. V. L. Bennett, "Hepatocyte gap junctions are permeable to the second messenger, inositol 1,4,5-trisphosphate, and to calcium ions," *Proceedings of the National Academy of Sciences of the United States of America*, vol. 86, no. 8, pp. 2708–2712, 1989.

[31] D. B. Alexander and G. S. Goldberg, "Transfer of biologically important molecules between cells through gap junction channels," *Current Medicinal Chemistry*, vol. 10, no. 19, pp. 2045–2058, 2003.

[32] H. A. Dbouk, R. M. Mroue, M. E. El-Sabban, and R. S. Talhouk, "Connexins: a myriad of functions extending beyond assembly of gap junction channels," *Cell Communication and Signaling*, vol. 7, article 4, 2009.

[33] D. C. Spray, Z. C. Ye, and B. R. Ransom, "Functional connexin "hemichannels": a critical appraisal," *Glia*, vol. 54, no. 7, pp. 758–773, 2006.

[34] J. X. Jiang and S. Gu, "Gap junction- and hemichannel-independent actions of connexins," *Biochimica et Biophysica Acta*, vol. 1711, no. 2, pp. 208–214, 2005.

[35] B. N. G. Giepmans, "Gap junctions and connexin-interacting proteins," *Cardiovascular Research*, vol. 62, no. 2, pp. 233–245, 2004.

[36] E. Kardami, X. Dang, D. A. Iacobas et al., "The role of connexins in controlling cell growth and gene expression," *Progress in Biophysics and Molecular Biology*, vol. 94, no. 1-2, pp. 245–264, 2007.

[37] S. Olk, A. Turchinovich, M. Grzendowski et al., "Proteomic analysis of astroglial connexin43 silencing uncovers a cytoskeletal platform involved in process formation and migration," *Glia*, vol. 58, no. 4, pp. 494–505, 2010.

[38] D. A. Iacobas, S. Iacobas, M. Urban-Maldonado, and D. C. Spray, "Sensitivity of the brain transcriptome to connexin ablation," *Biochimica et Biophysica Acta*, vol. 1711, no. 2, pp. 183–196, 2005.

[39] J. P. Stains, F. Lecanda, J. Screen, D. A. Towler, and R. Civitelli, "Gap junctional communication modulates gene transcription by altering the recruitment of Sp1 and Sp3 to connexin-response elements in osteoblast promoters," *The Journal of Biological Chemistry*, vol. 278, no. 27, pp. 24377–24387, 2003.

[40] J. P. Stains and R. Civitelli, "Gap junctions regulate extracellular signal-regulated kinase signaling to affect gene transcription," *Molecular Biology of the Cell*, vol. 16, no. 1, pp. 64–72, 2005.

[41] G. Söhl and K. Willecke, "An update on connexin genes and their nomenclature in mouse and man," *Cell Communication and Adhesion*, vol. 10, no. 4–6, pp. 173–180, 2003.

[42] E. C. Beyer, D. L. Paul, and D. A. Goodenough, "Connexin43: a protein from rat heart homologous to a gap junction protein from liver," *Journal of Cell Biology*, vol. 105, no. 6, pp. 2621–2629, 1987.

[43] D. S. Y. Leung, K. Unsicker, and B. Reuss, "Expression and developmental regulation of gap junction connexins cx26, cx32, cx43 and cx45 in the rat midbrain-floor," *International Journal of Developmental Neuroscience*, vol. 20, no. 1, pp. 63–75, 2002.

[44] R. Dermietzel, O. Traub, T. K. Hwang et al., "Differential expression of three gap junction proteins in developing and mature brain tissues," *Proceedings of the National Academy of Sciences of the United States of America*, vol. 86, no. 24, pp. 10148–10152, 1989.

[45] D. J. Belliveau and C. C. G. Naus, "Cellular localization of gap junction mRNAs in developing rat brain," *Developmental Neuroscience*, vol. 17, no. 2, pp. 81–96, 1995.

[46] R. Rozental, M. Morales, M. F. Mehler et al., "Changes in the properties of gap junctions during neuronal differentiation of hippocampal progenitor cells," *Journal of Neuroscience*, vol. 18, no. 5, pp. 1753–1762, 1998.

[47] N. Duval, D. Gomès, V. Calaora, A. Calabrese, P. Meda, and R. Bruzzone, "Cell coupling and Cx43 expression in embryonic mouse neural progenitor cells," *Journal of Cell Science*, vol. 115, no. 16, pp. 3241–3251, 2002.

[48] K. S. Bittman and J. J. LoTurco, "Differential regulation of connexin 26 and 43 in murine neocortical precursors," *Cerebral Cortex*, vol. 9, no. 2, pp. 188–195, 1999.

[49] B. Nadarajah, A. M. Jones, W. H. Evans, and J. G. Parnavelas, "Differential expression of connexins during neocortical development and neuronal circuit formation," *Journal of Neuroscience*, vol. 17, no. 9, pp. 3096–3111, 1997.

[50] A. Cheng, H. Tang, J. Cai et al., "Gap junctional communication is required to maintain mouse cortical neural progenitor cells in a proliferative state," *Developmental Biology*, vol. 272, no. 1, pp. 203–216, 2004.

[51] M. F. Santiago, P. Alcami, K. M. Striedinger, D. C. Spray, and E. Scemes, "The carboxyl-terminal domain of Connexin43 is a negative modulator of neuronal differentiation," *The Journal of Biological Chemistry*, vol. 285, no. 16, pp. 11836–11845, 2010.

[52] L. A. B. Elias, D. D. Wang, and A. R. Kriegstein, "Gap junction adhesion is necessary for radial migration in the neocortex," *Nature*, vol. 448, no. 7156, pp. 901–907, 2007.

[53] E. Scemes, N. Duval, and P. Meda, "Reduced Expression of P2Y1 Receptors in Connexin43-Null Mice Alters Calcium Signaling and Migration of Neural Progenitor Cells," *Journal of Neuroscience*, vol. 23, no. 36, pp. 11444–11452, 2003.

[54] M. Marins, A. L. R. Xavier, N. B. Viana, F. S. A. Fortes, M. M. Fróes, and J. R. L. Menezes, "Gap junctions are involved in cell migration in the early postnatal subventricular zone," *Developmental Neurobiology*, vol. 69, no. 11, pp. 715–730, 2009.

[55] L. A. Boyer, T. I. Lee, M. F. Cole et al., "Core transcriptional regulatory circuitry in human embryonic stem cells," *Cell*, vol. 122, no. 6, pp. 947–956, 2005.

[56] B. Parekkadan, Y. Berdichevsky, D. Irimia et al., "Cell-cell interaction modulates neuroectodermal specification of embryonic stem cells," *Neuroscience Letters*, vol. 438, no. 2, pp. 190–195, 2008.

[57] M. G. Todorova, B. Soria, and I. Quesada, "Gap junctional intercellular communication is required to maintain embryonic stem cells in a non-differentiated and proliferative state," *Journal of Cellular Physiology*, vol. 214, no. 2, pp. 354–362, 2008.

[58] J. E. Rash, T. Yasumura, K. G. V. Davidson, C. S. Furman, F. E. Dudek, and J. I. Nagy, "Identification of cells expressing Cx43, Cx30, Cx26, Cx32 and Cx36 in gap junctions of rat brain and spinal cord," *Cell Communication and Adhesion*, vol. 8, no. 4–6, pp. 315–320, 2001.

[59] M. Theis, G. Söhl, D. Speidel, R. Kühn, and K. Willecke, "Connexin43 is not expressed in principal cells of mouse cortex and hippocampus," *European Journal of Neuroscience*, vol. 18, no. 2, pp. 267–274, 2003.

[60] P. E. Micevych and L. Abelson, "Distribution of mRNAs coding for liver and heart gap junction proteins in the rat central nervous system," *Journal of Comparative Neurology*, vol. 305, no. 1, pp. 96–118, 1991.

[61] B. Nadarajah, D. Thomaidou, W. H. Evans, and J. G. Parnavelas, "Gap junctions in the adult cerebral cortex: regional differences in their distribution and cellular expression of connexins," *The Journal of Comparative Neurology*, vol. 376, no. 2, pp. 326–342, 1996.

[62] B. Lacar, S. Z. Young, J. C. Platel, and A. Bordey, "Gap junction-mediated calcium waves define communication networks among murine postnatal neural progenitor cells," *European Journal of Neuroscience*, vol. 34, no. 12, pp. 1895–1905, 2011.

[63] X. Liu, A. J. Bolteus, D. M. Balkin, O. Henschel, and A. Bordey, "GFAP-expressing cells in the postnatal subventricular zone display a unique glial phenotype intermediate between radial glia and astrocytes," *Glia*, vol. 54, no. 5, pp. 394–410, 2006.

[64] Z. Mirzadeh, F. T. Merkle, M. Soriano-Navarro, J. M. Garcia-Verdugo, and A. Alvarez-Buylla, "Neural stem cells confer unique pinwheel architecture to the ventricular surface in neurogenic regions of the adult brain," *Cell Stem Cell*, vol. 3, no. 3, pp. 265–278, 2008.

[65] A. S. Freitas, A. L. Xavier, C. M. Furtado et al., "Dye coupling and connexin expression by cortical radial glia in the early postnatal subventricular zone," *Developmental Neurobiology*. In press.

[66] F. Miragall, P. Albiez, H. Bartels, U. De Vries, and R. Dermietzel, "Expression of the gap junction protein connexin43 in the subependymal layer and the rostral migratory stream of the mouse: evidence for an inverse correlation between intensity of connexin43 expression and cell proliferation activity," *Cell and Tissue Research*, vol. 287, no. 2, pp. 243–253, 1997.

[67] X. Liu, Q. Wang, T. F. Haydar, and A. Bordey, "Nonsynaptic GABA signaling in postnatal subventricular zone controls proliferation of GFAP-expressing progenitors," *Nature Neuroscience*, vol. 8, no. 9, pp. 1179–1187, 2005.

[68] C. E. Stout, J. L. Costantin, C. C. G. Naus, and A. C. Charles, "Intercellular calcium signaling in astrocytes via ATP release through connexin hemichannels," *The Journal of Biological Chemistry*, vol. 277, no. 12, pp. 10482–10488, 2002.

[69] K. Braet, S. Aspeslagh, W. Vandamme et al., "Pharmacological sensitivity of ATP release triggered by photoliberation of inositol-1,4,5-trisphosphate and zero extracellular calcium in brain endothelial cells," *Journal of Cellular Physiology*, vol. 197, no. 2, pp. 205–213, 2003.

[70] N. Dale, "Dynamic ATP signalling and neural development," *Journal of Physiology*, vol. 586, no. 10, pp. 2429–2436, 2008.

[71] T. A. Weissman, P. A. Riquelme, L. Ivic, A. C. Flint, and A. R. Kriegstein, "Calcium waves propagate through radial glial cells and modulate proliferation in the developing neocortex," *Neuron*, vol. 43, no. 5, pp. 647–661, 2004.

[72] D. F. Owens and A. R. Kriegstein, "Patterns of intracellular calcium fluctuation in precursor cells of the neocortical ventricular zone," *Journal of Neuroscience*, vol. 18, no. 14, pp. 5374–5388, 1998.

[73] M. De Bock, N. Wang, M. Bol et al., "Connexin-43 hemichannels contribute to cytoplasmic Ca^{2+} oscillations by providing a bimodal Ca^{2+}-dependent Ca^{2+}-entry pathway," *The Journal of Biological Chemistry*, vol. 287, no. 15, pp. 12250–12266, 2012.

[74] E. De Vuyst, N. Wang, E. Decrock et al., "Ca^{2+} regulation of connexin 43 hemichannels in C6 glioma and glial cells," *Cell Calcium*, vol. 46, no. 3, pp. 176–187, 2009.

[75] A. G. Reaume, P. A. De Sousa, S. Kulkarni et al., "Cardiac malformation in neonatal mice lacking connexin43," *Science*, vol. 267, no. 5205, pp. 1831–1834, 1995.

[76] C. Moorby and M. Patel, "Dual functions for connexins: Cx43 regulates growth independently of gap junction formation," *Experimental Cell Research*, vol. 271, no. 2, pp. 238–248, 2001.

[77] A. P. Quist, S. K. Rhee, H. Lin, and R. Lal, "Physiological role of gap-junctional hemichannels: extracellular calcium-dependent isosmotic volume regulation," *Journal of Cell Biology*, vol. 148, no. 5, pp. 1063–1074, 2000.

[78] D. J. Belliveau, M. Bani-Yaghoub, B. McGirr, C. C. G. Naus, and W. J. Rushlow, "Enhanced neurite outgrowth in PC12 cells mediated by connexin hemichannels and ATP," *The Journal of Biological Chemistry*, vol. 281, no. 30, pp. 20920–20931, 2006.

[79] M. Bani-Yaghoub, T. M. Underhill, and C. C. G. Naus, "Gap junction blockage interferes with neuronal and astroglial differentiation of mouse p19 embryonal carcinoma cells," *Developmental Genetics*, vol. 24, no. 1-2, pp. 69–81, 1999.

[80] A. Kunze, M. R. Congreso, C. Hartmann et al., "Connexin expression by radial glia-like cells is required for neurogenesis in the adult dentate gyrus," *Proceedings of the National Academy of Sciences of the United States of America*, vol. 106, no. 27, pp. 11336–11341, 2009.

[81] Y. Panchina, I. Kelmanson, M. Matz, K. Lukyanov, N. Usman, and S. Lukyanov, "A ubiquitous family of putative gap junction molecules," *Current Biology*, vol. 10, no. 13, pp. R473–R474, 2000.

[82] G. E. Sosinsky, D. Boassa, R. Dermietzel et al., "Pannexin channels are not gap junction hemichannels," *Channels*, vol. 5, no. 3, pp. 193–197, 2011.

[83] B. A. MacVicar and R. J. Thompson, "Non-junction functions of pannexin-1 channels," *Trends in Neurosciences*, vol. 33, no. 2, pp. 93–102, 2010.

[84] S. Penuela, R. Gehi, and D. W. Laird, "The biochemistry and function of pannexin channels," *Biochimica et Biophysica Acta*. In press.

[85] C. Ambrosi, O. Gassmann, J. N. Pranskevich et al., "Pannexin1 and pannexin2 channels show quaternary similarities to connexons and different oligomerization numbers from each other," *The Journal of Biological Chemistry*, vol. 285, no. 32, pp. 24420–24431, 2010.

[86] R. Bruzzone, S. G. Hormuzdi, M. T. Barbe, A. Herb, and H. Monyer, "Pannexins, a family of gap junction proteins expressed in brain," *Proceedings of the National Academy of Sciences of the United States of America*, vol. 100, no. 23, pp. 13644–13649, 2003.

[87] W. Ma, H. Hui, P. Pelegrin, and A. Surprenant, "Pharmacological characterization of pannexin-1 currents expressed in mammalian cells," *Journal of Pharmacology and Experimental Therapeutics*, vol. 328, no. 2, pp. 409–418, 2009.

[88] M. F. Santiago, J. Veliskova, N. K. Patel et al., "Targeting pannexin1 improves seizure outcome," *PLoS ONE*, vol. 6, no. 9, article e25178, 2011.

[89] W. R. Silverman, J. P. de Rivero Vaccari, S. Locovei et al., "The pannexin 1 channel activates the inflammasome in neurons and astrocytes," *The Journal of Biological Chemistry*, vol. 284, no. 27, pp. 18143–18151, 2009.

[90] L. Bao, S. Locovei, and G. Dahl, "Pannexin membrane channels are mechanosensitive conduits for ATP," *FEBS Letters*, vol. 572, no. 1–3, pp. 65–68, 2004.

[91] R. J. Thompson, M. F. Jackson, M. E. Olah et al., "Activation of pannexin-1 hemichannels augments aberrant bursting in the hippocampus," *Science*, vol. 322, no. 5907, pp. 1555–1559, 2008.

[92] S. Locovei, J. Wang, and G. Dahl, "Activation of pannexin 1 channels by ATP through P2Y receptors and by cytoplasmic calcium," *FEBS Letters*, vol. 580, no. 1, pp. 239–244, 2006.

[93] R. J. Thompson, N. Zhou, and B. A. MacVicar, "Ischemia opens neuronal gap junction hemichannels," *Science*, vol. 312, no. 5775, pp. 924–927, 2006.

[94] P. Bargiotas, A. Krenz, S. G. Hormuzdi et al., "Pannexins in ischemia-induced neurodegeneration," *Proceedings of the National Academy of Sciences of the United States of America*, vol. 108, no. 51, pp. 20772–20777, 2011.

[95] F. B. Chekeni, M. R. Elliott, J. K. Sandilos et al., "Pannexin 1 channels mediate "find-me" signal release and membrane permeability during apoptosis," *Nature*, vol. 467, no. 7317, pp. 863–867, 2010.

[96] J. K. Sandilos, Y. H. Chiu, F. B. Chekeni et al., "Pannexin 1, an ATP release channel, is activated by caspase cleavage of its pore-associated C terminal autoinhibitory region," *The Journal of Biological Chemistry*. In press.

[97] F. Qiu and G. Dahl, "A permeant regulating its permeation pore: inhibition of pannexin 1 channels by ATP," *American Journal of Physiology*, vol. 296, no. 2, pp. C250–C255, 2009.

[98] J. Wang, M. Ma, S. Locovei, R. W. Keane, and G. Dahl, "Modulation of membrane channel currents by gap junction protein mimetic peptides: size matters," *American Journal of Physiology*, vol. 293, no. 3, pp. C1112–C1119, 2007.

[99] R. Dando and S. D. Roper, "Cell-to-cell communication in intact taste buds through ATP signalling from pannexin 1 gap junction hemichannels," *Journal of Physiology*, vol. 587, no. 24, pp. 5899–5906, 2009.

[100] M. T. Barbe, H. Monyer, and R. Bruzzone, "Cell-cell communication beyond connexins: the pannexin channels," *Physiology*, vol. 21, no. 2, pp. 103–114, 2006.

[101] W. Ma, V. Compan, W. Zheng et al., "Pannexin 1 forms an anion-selective channel," *Pflügers Archiv*, vol. 463, no. 4, pp. 585–592, 2012.

[102] A. Vogt, S. G. Hormuzdi, and H. Monyer, "Pannexin1 and Pannexin2 expression in the developing and mature rat brain," *Molecular Brain Research*, vol. 141, no. 1, pp. 113–120, 2005.

[103] A. Ray, G. Zoidl, S. Weickert, P. Wahle, and R. Dermietzel, "Site-specific and developmental expression of pannexin1 in the mouse nervous system," *European Journal of Neuroscience*, vol. 21, no. 12, pp. 3277–3290, 2005.

[104] R. Bruzzone, M. T. Barbe, N. J. Jakob, and H. Monyer, "Pharmacological properties of homomeric and heteromeric pannexin hemichannels expressed in Xenopus oocytes," *Journal of Neurochemistry*, vol. 92, no. 5, pp. 1033–1043, 2005.

[105] J. C. Sáez, V. M. Berthoud, M. C. Brañes, A. D. Martínez, and E. C. Beyer, "Plasma membrane channels formed by connexins: their regulation and functions," *Physiological Reviews*, vol. 83, no. 4, pp. 1359–1400, 2003.

[106] T. Yasuda, P. F. Bartlett, and D. J. Adams, "K_{ir} and K_v channels regulate electrical properties and proliferation of adult neural precursor cells," *Molecular and Cellular Neuroscience*, vol. 37, no. 2, pp. 284–297, 2008.

[107] J. M. Dubois and B. Rouzaire-Dubois, "The influence of cell volume changes on tumour cell proliferation," *European Biophysics Journal*, vol. 33, no. 3, pp. 227–232, 2004.

[108] B. Rouzaire-Dubois, M. Malo, J. B. Milandri, and J. M. Dubois, "Cell size-proliferation relationship in rat glioma cells," *Glia*, vol. 45, no. 3, pp. 249–257, 2004.

[109] G. P. Nicchia, M. Srinivas, W. Li, C. F. Brosnan, A. Frigeri, and D. C. Spray, "New possible roles for aquaporin-4 in astrocytes: cell cytoskeleton and functional relationship with connexin43," *FASEB Journal*, vol. 19, no. 12, pp. 1674–1676, 2005.

[110] K. Saha, A. J. Keung, E. F. Irwin et al., "Substrate modulus directs neural stem cell behavior," *Biophysical Journal*, vol. 95, no. 9, pp. 4426–4438, 2008.

[111] A. J. Keung, E. M. de Juan-Pardo, D. V. Schaffer, and S. Kumar, "Rho GTPases mediate the mechanosensitive lineage commitment of neural stem cells," *Stem Cells*, vol. 29, no. 11, pp. 1886–1897, 2011.

[112] S. Imbeault, L. G. Gauvin, H. D. Toeg et al., "The extracellular matrix controls gap junction protein expression and function in postnatal hippocampal neural progenitor cells," *BMC Neuroscience*, vol. 10, article 13, 2009.

[113] J. W. Smyth, J. M. Vogan, P. J. Buch et al., "Actin cytoskeleton rest stops regulate anterograde traffic of connexin 43 vesicles to the plasma membrane," *Circulation Research*, vol. 110, no. 7, pp. 978–989, 2012.

[114] R. Francis, X. Xu, H. Park et al., "Connexin43 modulates cell polarity and directional cell migration by regulating microtubule dynamics," *PLoS ONE*, vol. 6, no. 10, article e26379, 2011.

[115] S. Crespin, J. Bechberger, M. Mesnil, C. C. Naus, and W. C. Sin, "The carboxy-terminal tail of connexin43 gap junction protein is sufficient to mediate cytoskeleton changes in human glioma cells," *Journal of Cellular Biochemistry*, vol. 110, no. 3, pp. 589–597, 2010.

[116] T. Toyofuku, M. Yabuki, K. Otsu, T. Kuzuya, M. Hori, and M. Tada, "Direct association of the gap junction protein connexin-43 with ZO-1 in cardiac myocytes," *The Journal of Biological Chemistry*, vol. 273, no. 21, pp. 12725–12731, 1998.

[117] S. Olk, G. Zoidl, and R. Dermietzel, "Connexins, cell motility, and the cytoskeleton," *Cell Motility and the Cytoskeleton*, vol. 66, no. 11, pp. 1000–1016, 2009.

[118] R. Ponsaerts, N. Wang, B. Himpens, L. Leybaert, and G. Bultynck, "The contractile system as a negative regulator of the connexin 43 hemichannel," *Biology of the Cell*. In press.

[119] R. Bhalla-Gehi, S. Penuela, J. M. Churko, Q. Shao, and D. W. Laird, "Pannexin1 and pannexin3 delivery, cell surface dynamics, and cytoskeletal interactions," *The Journal of Biological Chemistry*, vol. 285, no. 12, pp. 9147–9160, 2010.

[120] B. A. Bao, C. P. Lai, C. C. Naus, and J. R. Morgan, "Pannexin1 drives multicellular aggregate compaction via a signaling cascade that remodels the actin cytoskeleton," *The Journal of Biological Chemistry*, vol. 287, no. 11, pp. 8407–8416, 2012.

[121] I. Grimm, S. N. Ullsperger, and H. Zimmermann, "Nucleotides and epidermal growth factor induce parallel cytoskeletal rearrangements and migration in cultured adult murine neural stem cells," *Acta Physiologica*, vol. 199, no. 2, pp. 181–189, 2010.

[122] V. Benfenati, G. P. Nicchia, M. Svelto, C. Rapisarda, A. Frigeri, and S. Ferroni, "Functional down-regulation of volume-regulated anion channels in AQP4 knockdown cultured rat cortical astrocytes," *Journal of Neurochemistry*, vol. 100, no. 1, pp. 87–104, 2007.

[123] W. Ma, V. Compan, W. Zheng et al., "Pannexin 1 forms an anion-selective channel," *Pflügers Archiv*, vol. 463, no. 4, pp. 585–592, 2012.

[124] R. Z. Sabirov and Y. Okada, "The maxi-anion channel: a classical channel playing novel roles through an unidentified molecular entity," *Journal of Physiological Sciences*, vol. 59, no. 1, pp. 3–21, 2009.

[125] J. Kang, N. Kang, D. Lovatt et al., "Connexin 43 hemichannels are permeable to ATP," *Journal of Neuroscience*, vol. 28, no. 18, pp. 4702–4711, 2008.

[126] R. Iglesias, G. Dahl, F. Qiu, D. C. Spray, and E. Scemes, "Pannexin 1: the molecular substrate of astrocyte "hemichannels"," *Journal of Neuroscience*, vol. 29, no. 21, pp. 7092–7097, 2009.

[127] Q. V. Hoang, H. Qian, and H. Ripps, "Functional analysis of hemichannels and gap-junctional channels formed by connexins 43 and 46," *Molecular Vision*, vol. 16, pp. 1343–1352, 2010.

[128] Z. C. Ye, N. Oberheim, H. Kettenmann, and B. R. Ransom, "Pharmacological "cross-inhibition" of connexin hemichannels and swelling activated anion channels," *Glia*, vol. 57, no. 3, pp. 258–269, 2009.

[129] J. C. Sáez, M. A. Retamal, D. Basilio, F. F. Bukauskas, and M. V. L. Bennett, "Connexin-based gap junction hemichannels: gating mechanisms," *Biochimica et Biophysica Acta*, vol. 1711, no. 2, pp. 215–224, 2005.